GENE PROFILING OF LUNG TOXICITY

Dominique Balharry

A thesis presented for the degree of Doctor of Philosophy

at

Cardiff University

May 2005

Cardiff School of Biosciences
Cardiff University
Museum Avenue
CARDIFF
CF10 3US

ProQuest LLC
789 East Eisenhower Parkway
P.O. Box 1346
Ann Arbor, MI 48106-1346

CONTENTS

ACKNOWLEDGEMENTS

Firstly I'd like to thank AstraZeneca for funding this research and making the whole project possible! Thanks also to Dr. Victor Oreffo for arranging everything at AZ and for being involved right from the start with all the planning! Your input was invaluable!

I'd like to say a huge thank you to Prof. Roy Richards for saving me from Bath, and restoring my faith in scientists!! I'm so glad I had the opportunity to work (and drink!) with you! Your support, guidance and wisdom over the last three years have made it an enjoyable experience that I'll never forget! To Dr. Kelly BéruBé for being a source of knowledge (and entertainment!) throughout my PhD, but especially for stepping in to take over at the last minute! You've been an absolute star!!

Everyone in W2.01 over the years, you know who you are! You're a great bunch, I couldn't have asked for better people to spend the last few years with! Leona, for being there right from the start and always keeping me company over a much needed drink! And I can't thank you enough for persuading me to talk to Roy in the first place!! To Helen for being my 'radioactive twin' and keeping me sane in our little windowless room! Massive thanks to Martina for a multitude of things! For some fantastic times in NZ, for taking me horse riding and for getting worse hangovers than me! Of course I can't forget Keith, who has been a constant source of knowledge (about everything from PCR to bleeding radiators!) and helped me out of many a sticky situation!! You're all great! Thanks!

Rich, I'm sure you know anyway, but thank you for everything!!

Finally I'd like to say an enormous thank you to my entire family! Especially to my mum and my sister Chloë (and not just for your editorial skills!). You've been there through thick and thin and I wouldn't be where I am today if it hadn't been for you both! Thank you!

PUBLICATIONS

Balharry, D., Oreffo, V. and Richards, R. J. (2005). Use of Toxicogenomics for Identifying Genetic Markers of Pulmonary Oedema. *Toxicology and Applied Pharmacology* **204**, 101-108.

Wise, H., Balharry, D., Reynolds, L J., Sexton, K. and Richards R J. (2004). Conventional and Toxicogenomic Assessment of the Acute Pulmonary Damage Induced by the Instillation of Cardiff PM_{10} into the Rat Lung. *Science of the Total Environment*, In Press

PUBLISHED ABSTRACTS

Balharry, D., Oreffo V. and Richards, R. J. (2004). Gene Expression Analysis of Lung Toxicity, *Abstracts of the British Association for Lung Research, Summer Meeting, 2003, Brighton, UK.* Experimental Lung Research **30(6)**, 503-534

Balharry, D., Oreffo V. and Richards, R. J. (2004). Bioinformatic Analysis of Genetic Expression during Mild Pulmonary Oedema. *Toxicology* **202 (1-2)**, 58

Balharry, D., Oreffo V. and Richards, R. J. (2003). Gene Profiling of Lung Toxicity, *Abstracts of the British Association for Lung Research, Summer Meeting, 2002, Dublin, Ireland,* Experimental Lung Research **29(6),** 413-444

COMMUNICATIONS

Gene Profiling of Lung Toxicity *AstraZeneca Science Day, Alderley Park, UK*, **2005**

mRNA Expression Profiling of Mild and Severe Pulmonary Oedema. *3rd Annual International Conference on Bioinformatics, Auckland, NZ,* **2004**

Gene Expression Analysis of Lung Toxicity, *AstraZeneca Science Day, Alderley Park, UK*, **2004**

Gene Expression Analysis of the Early and Peak Phase of Pulmonary Oedema, *British Association for Lung Research, Summer Meeting, Leicester, UK*, **2004**

ABBREVIATIONS

1°	Primary antibody
2D SDS PAGE	Two dimensional sodium dodecyl sulphate polyacrylamide gel electrophoresis
Ach	Acetylcholine
AQP	Aquaporin
BAL	Broncho-alveolar lavage
BCIP	5-bromo-4-chloro-3-indolyl phosphate
bFGF	Basic fibroblast growth factor
BM	Basement membrane
bp	Base pairs
BrdU	5-Bromo-2-deoxy-uridine
BSA	Bovine serum albumin
CaMK	Calcium/calmodulin dependent kinase
cAMP	Cyclic adenosine monophosphate
CART	Cocaine/amphetamine-induced rat transcript
CC	Cocoacrisp
CDC	Cell division control
cDNA	Complementary DNA
CDS	Complementary DNA sequence
Ci	Curies
conc.	Concentration
cpm	Counts per minute
CRISP	Cysteine-rich secreted protein
Ct	Cycle threshold
dATP	Deoxyadenosine triphosphate
dCTP	Deoxycytidine triphosphate
dGTP	Deoxyguanosine triphosphate
DNA	Deoxyribonucleic acid
DNase	Deoxyribonuclease
dNTP	Deoxynucleotide triphosphate
DTT	Dithiothreitol
dTTP	Deoxythymidine triphosphate
ECM	Extracellular matrix
E.coli	*Escherichia coli*
EDTA	Ethylenediaminetetracetic acid
EPO	Erythropoietin
FGF	Fibroblast growth factor
G_1 phase	Gap 1 phase (of cell cycle)
G_2 phase	Gap 2 phase (of cell cycle)
GABA	Gamma aminobutyric acid
GCS-F	Granulocyte colony stimulating factor
gDNA	Genomic DNA
GDNF	Glial cell line-derived neurotrophic factor

GFs	Growth factors
GLUR	Glutamate receptor
GM-CSF	Granulocyte-macrophage colony-stimulating factor
GNRP	Guanine nucleotide release/exchange factor
GP	Glycoprotein
GPCR	G-protein-coupled receptor
GRP-R	Gastrin releasing peptide receptor
GTP	Guanosine triphosphate
GTPase	Guanosine triphosphatase
H & E	Haematoxylin and eosin
IA	Image analysis
IFN	Interferon
IL	Interleukin
INF	Intrinsic factor
IP	Intraperitoneal
IPTG	Isopropylthiogalactoside
IT	Intratracheal
IV	Intravenous
JNK	c-Jun-N-terminal-kinase
kb	Kilo bases
kDa	Kilo Daltons
keV	Kilo electron-volts
KRP	Krebs ringer phosphate
L:B ratio	Lung parenchyma:body weight ratio
LB	Luria broth
LCCL domain	Domain-family first discovered in Limulus factor C, Coch-5b2 and Lgl1
LFC	Lavage free cells
Lgl	Late gestation lung protein
LM	Light microscopy
LP	Lung parenchyma
LPS	Lipopolysaccharide
M phase	Mitotic phase (of cell cycle)
MCT	Monocarboxylate transporter
MMLV-RT	Moloney murine leukaemia virus reverse transcriptase
MR	Mineralocorticoid Receptor
mRNA	Messenger ribonucleic acid
n	Number of replicates
NBT	Nitroblue tetrazolium
NCBI	National Centre for Biotechnology Information
NGF	Nerve growth factor
NK	Natural killer
NM	Neuromedin
NMR	Nuclear magnetic resonance
P2Y	Purinoceptor 2Y
PBS	Phosphate buffered saline

PCR	Polymerase chain reaction
PKC	Protein kinase C
PLA	Phospholipase A
Prl	Preprolactin
PYY	Peptide YY
Q-PCR	Quantitative PCR
RAD	Ras associated with diabetes
RBC	Red blood cell
Rn	Reporter number
RNA	Ribonucleic acid
RNase	Ribonuclease
RT	Reverse transcription
RT-PCR	Reverse transcription PCR
RTU	Ready to use
rxn	Reaction
S phase	DNA synthesis phase (of cell cycle)
SC	Subcutaneous
SCP	Secretory component
sd	Standard deviation
SDS	Sodium dodecyl sulphate
SEM	Scanning electron microscopy
Sg	Secretogranin
SKR	Substance K receptor
SP-A	Surfactant protein-A
SP-B	Surfactant protein-B
SP-C	Surfactant protein-C
SP-D	Surfactant protein-D
SSC	Saline-sodium citrate buffer
STX2	Syntaxin 2
SV	Synaptic vesicle
SVAT	Synaptic vesicle amine transporter
SYT	Synaptotagmin
TBE	Tris-borate-ethylenediaminetetracetic acid
TBS	Tris buffered saline
TEM	Transmission electron microscopy
TIFF	Tag image file format
TM	Tubular myelin
TNF	Tumour necrosis factor
UV	Ultraviolet
v/v	Volume to volume
VEGF	Vascular endothelial growth factor
VIP	Vasoactive intestinal polypeptide
VIP-R	Vasoactive intestinal polypeptide receptor
w/v	Weight to volume
X-Gal	5-bromo-4-chloro-3-indolyl-b-D-galactosidase

ABSTRACT

Bleomycin is a potent anti-tumour compound used in the treatment of squamous cell carcinomas. An unfortunate side effect of this drug is pulmonary toxicity. The onset of this damage manifests as mild oedema and inflammation which eventually develops into pulmonary fibrosis. The ability to correctly identify patients showing early signs of lung injury could significantly reduce the morbidity associated with bleomycin treatment. As such, this study was undertaken to identify genetic markers of early oedema and inflammation.

A model of mild pulmonary injury was induced by bleomycin. Conventional quantitative analysis of broncho-alveolar lavage was used to indicate the severity of the oedematous response, whilst morphological changes were identified by histology and electron microscopy. Macroarrays were used to measure the expression of multiple genes during mild, progressive and severe oedema. Following normalisation and statistical analysis, gene expression patterns were compared from saline- and bleomycin-treated rats. A variety of genes were differentially expressed during each model, with the number increasing with the severity of the oedema. A cluster and two individual genes were consistently expressed across two of the models of oedema. The magnitude of the changes in gene expression were quantified and confirmed by quantitative PCR.

In summary, complete toxicological and histological characterisation of the bleomycin-induced model of pulmonary injury successfully identified specific endpoints of injury. This model proved to be ideal for studying differential gene expression in response to drug-induced pulmonary oedema. A cluster of ion channels and trafficking genes has the potential to act as a biomarker. Two specific genetic markers (Na+/Cl- betaine/GABA transporter, glucocorticoid receptor), and a protein marker (cocoacrisp) have been identified for the oedema. In addition to these genes and protein being potential biomarkers of injury, they are also prospective targets for clinical treatment.

CHAPTER 1:

INTRODUCTION

1.1 THE RESPIRATORY SYSTEM

1.1.1 OVERVIEW

The term "respiration" is used to describe two related processes: (1) cellular respiration and (2) mechanical respiration. Energy production by the metabolism of organic molecules is known as cellular respiration. This process requires oxygen, which is obtained via mechanical respiration. Mechanical respiration is carried out by the respiratory system. The primary function of the respiratory system is to remove excess carbon dioxide that is generated as a metabolic waste product from blood, as well as providing molecular oxygen for cellular oxidation.

The respiratory system is comprised of proximal conducting airways and a distal respiratory region (Harkema *et al.*, 1991). The conducting system transports inspired and expired air to and from the lungs. The respiratory portion acts as an interface for passive exchange of gases between the atmosphere and the blood. The complete system is divided anatomically into two parts, the upper and lower respiratory tracts, which are separated by the pharynx (Figure 1.1).

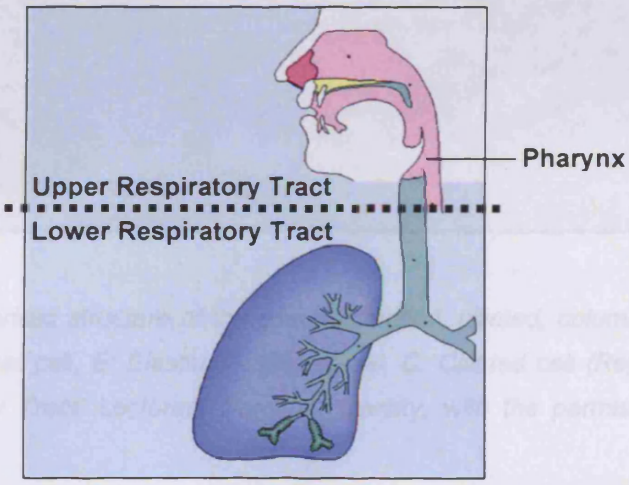

Figure 1.1 *The structure of the respiratory system indicating the separation between the lower and upper respiratory tract (Reproduced with permission of Dr. K BéruBé).*

The upper respiratory tract is made up of a series of interconnected spaces: the nasal cavity, the paranasal sinuses and the nasopharynx. Its primary function is filtering, humidifying and adjusting the temperature of inspired air. It is also involved in detoxification of harmful gases, and entrapment of potentially harmful bacteria and viruses. The majority of these functions are achieved by the respiratory mucous membrane or respiratory mucosa. The respiratory mucosa consists of a pseudostratified, columnar epithelium containing numerous goblet cells, supported on a loose collagenous layer, the lamina propria (Figure 1.2).

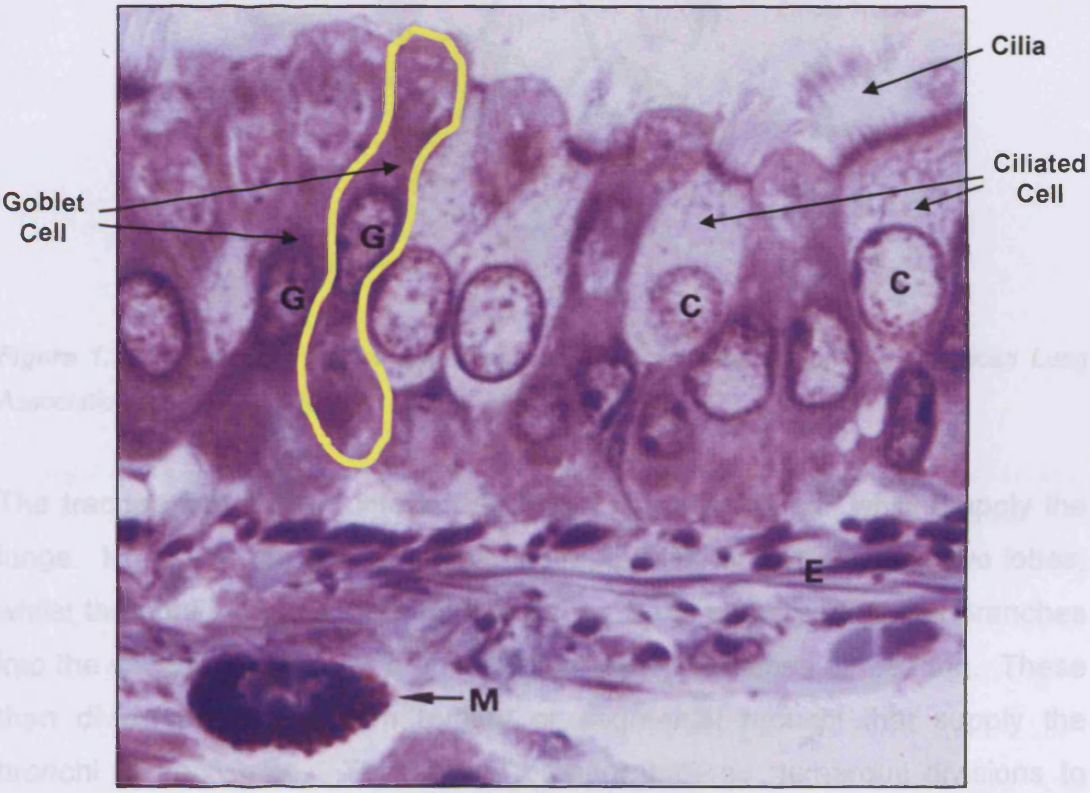

Figure 1.2 *The characteristic structure of the pseudostratified, ciliated, columnar respiratory epithelium lining. M: Mast cell, E: Elastin, G: Goblet cell, C: Ciliated cell (Reproduced from 'Histology of Respiratory Tract' Lectures, Cardiff University, with the permission of Dr. K. BéruBé,).*

The lower respiratory tract begins at the larynx and continues into the thorax as the trachea. The trachea then divides repeatedly into smaller and smaller airways to reach the alveoli (Figure 1.3).

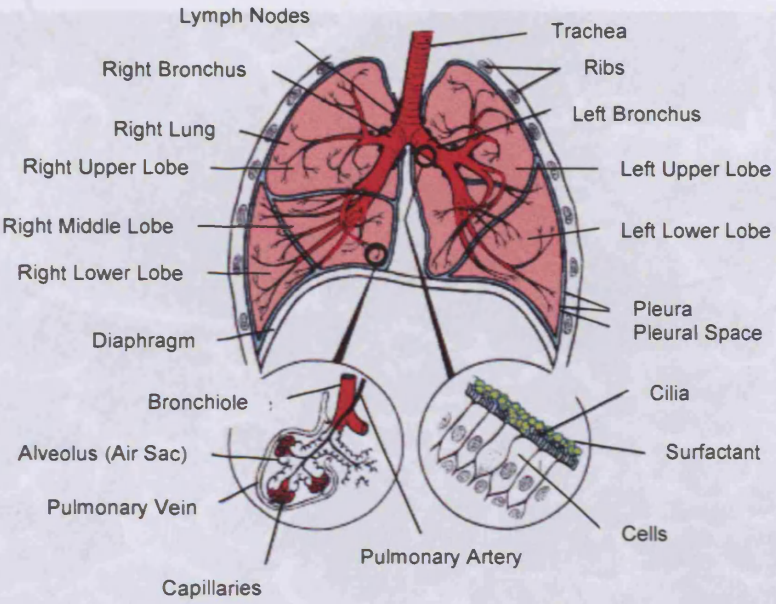

Figure 1.3 *The structure of the lower respiratory tract (Adapted from the American Lung Association Website, 2002).*

The trachea first divides into left and right primary bronchi, which supply the lungs. Human lungs consist of five lobes; the left lung is split into two lobes, whilst the right lung is separated into three. Each primary bronchus branches into the secondary or lobar bronchi which supply the lobes of the lung. These then divide further to form tertiary or segmental bronchi that supply the bronchi of each lobe. The tertiary bronchi undergo numerous divisions to produce bronchioles, the smallest of which are called terminal bronchioles. The terminal bronchioles mark the end of the purely conducting portion of the tract.

The gaseous exchange region is derived from further branching of the terminal bronchioles. This results in a series of transitional airways, the respiratory bronchioles and alveolar ducts. These airways end in dilated spaces called alveolar sacs, which open into the alveoli (Figure 1.4). The unit

of lung structure consisting of a terminal bronchiole and its respiratory bronchioles and alveoli is sometimes called the acinus (Young and Heath, 2000).

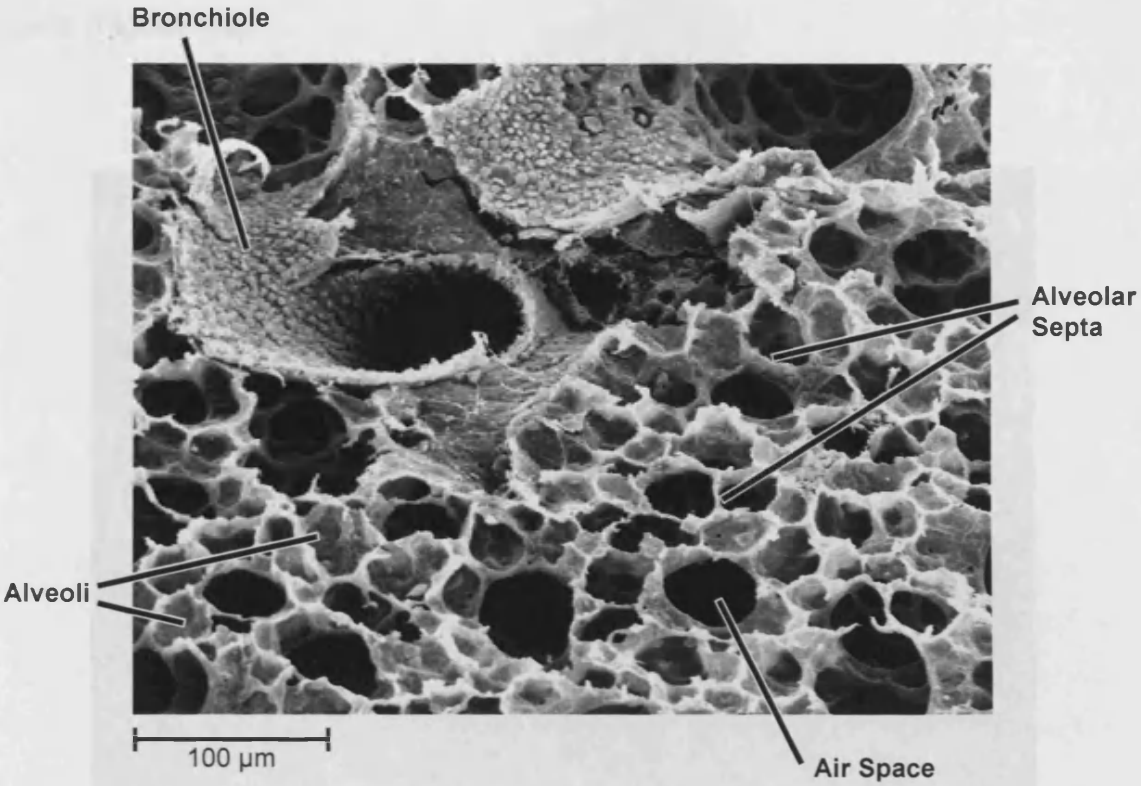

Figure 1.4 *Scanning electron micrograph of the distal respiratory region from normal rat lung (Lung sample donated by Dr. K BéruBé, image taken by D. Balharry and M. Hicks, 2004).*

The structural characteristics of each type of airway are distinct from each other, but there is a gradual transition from one type to the next. The lining of the trachea and bronchi consists of a pseudostratified, columnar epithelium containing ciliated cells and goblet (mucous secreting) cells (Breeze and Wheeldon, 1977). This progresses to a simple, cuboidal, non-ciliated form in the smallest airways.

1.1.2 Structure and Function of the Respiratory Bronchioles

The terminal bronchioles are the smallest passages of the conducting portion of the respiratory tree, and are not significantly involved in gaseous exchange. These terminal bronchioles divide to form short, thinner-walled branches

called respiratory bronchioles. The respiratory bronchioles contain a small number of single alveoli in their walls. The epithelium of the respiratory bronchioles is totally lacking in goblet cells, and instead largely consists of ciliated, cuboidal cells and smaller numbers of non-ciliated cells called Clara cells (Figure 1.5).

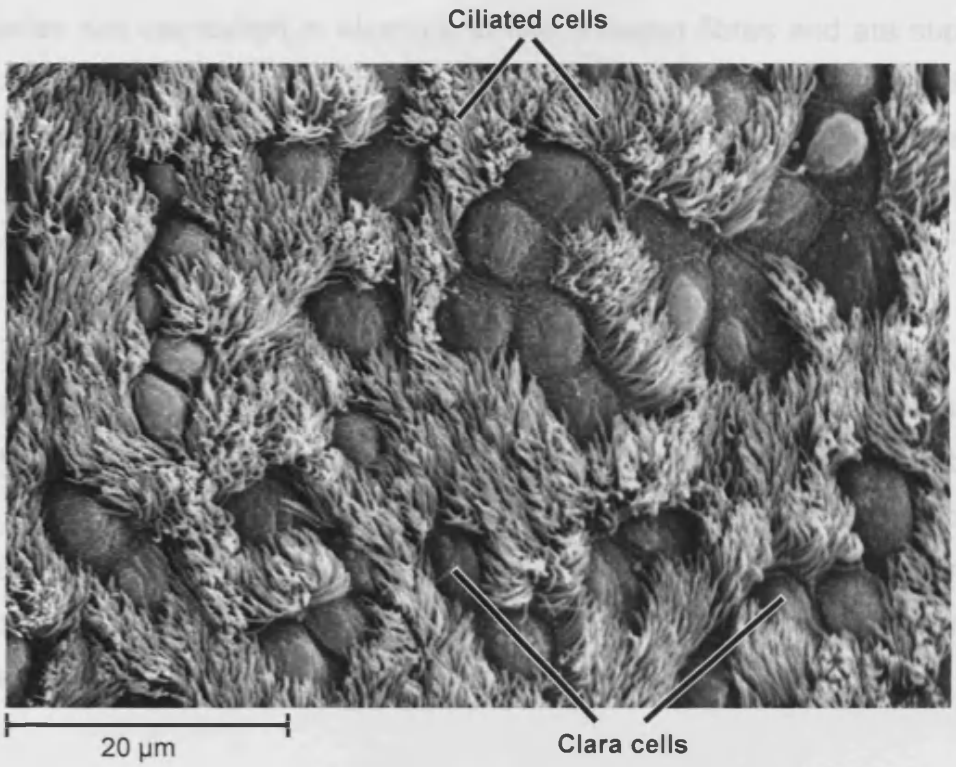

Figure 1.5 *Scanning electron micrograph of the surface of a respiratory bronchiole from normal rat lung. Shows ciliated cells interspersed with Clara cells (Lung sample donated by Dr. K BéruBé, image taken by D. Balharry and M. Hicks, 2004).*

In the furthest areas of the respiratory bronchioles, Clara cells are the predominant cell type. Clara cells produce some of the protein components of surfactant (Walker *et al.*, 1986) and are enriched with phase I and phase II biotransformation enzyme systems, which can detoxify noxious substances (Baron *et al.*, 1988). They can also act as progenitor cells, in that they are able to divide, differentiate and replace other damaged cell types (Evans *et al.*, 1976). Each respiratory bronchiole divides further into several alveolar ducts, which have numerous alveoli opening along their length. Each alveolar duct ends in an alveolar sac, which in turn opens into several alveoli.

1.1.3 *Structure and Function of the Alveoli*

Respiratory alveoli are the structures in which molecular oxygen and carbon dioxide are exchanged in the lung. Each alveolus consists of a pocket which is lined by flattened epithelial cells and opens at one side. Most of the alveolar wall is comprised of a network of pulmonary capillaries. The capillaries are enmeshed in elastin and fine collagen fibres and are supplied by pulmonary vessels that follow the airways. The collagen and elastin fibres supporting the capillaries condense around the opening of each alveolus. They join with those around the openings of adjacent alveoli to form a three-dimensional supporting network for the whole lung parenchyma.

The alveolar wall has two basement membranes, one associated with endothelial cells and one with epithelial cells. Where the wall becomes very thin these two basement membranes fuse into a single basement membrane (BM). At this point the wall is composed only of a type I pneumocyte cell, a single fused basement membrane, and a single endothelial cell. This thin wall facilitates gas exchange between the channel of blood and the alveolar spaces (Figure 1.6).

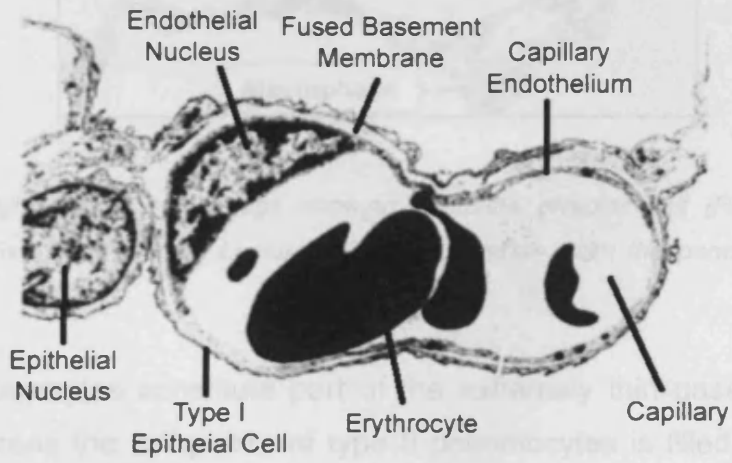

Figure 1.6 *Transmission electron micrograph of an alveolar wall. It shows a capillary with erythrocytes that is separated from the alveolar space by a layer of tissue consisting of type I epithelium, endothelium and interstitial space (Image from West, 1992).*

The alveolar walls contain small openings about 8μm in diameter, called alveolar pores or pores of Kohn. These allow pressure equalisation between alveoli, and provide air circulation should a bronchiole become obstructed.

In addition to the blood vessels and supporting tissue, the alveolar wall also consists of surface epithelial cells. The epithelium provides a continuous lining to each alveolus and consists mainly of two cell types (Figure 1.7). Most of the alveolar surface is covered by large squamous cells called type I epithelial cells. The second type of epithelial cell makes up 60% of cells in the lining epithelium. It is known as the type II, or granular pneumocyte and is rounded in shape. Consequently, type II cells occupy a much smaller proportion (about 5%) of the alveolar surface area. The alveolar interstitium also contains other cells such as fibroblasts and lymphoid cells.

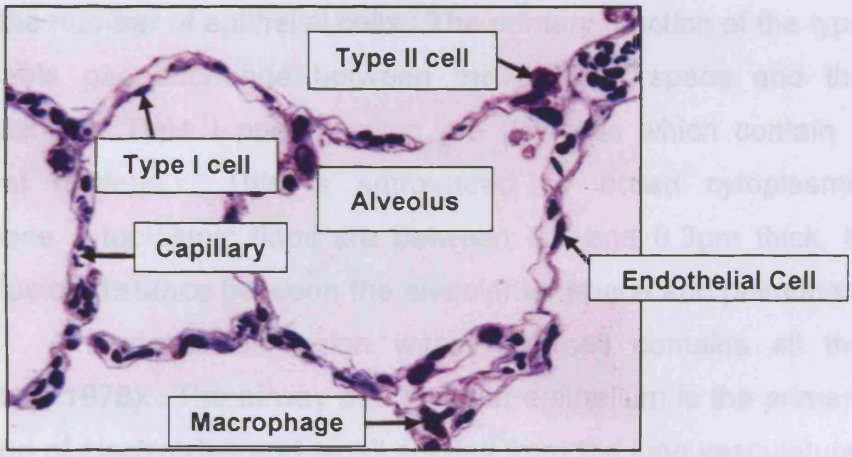

Figure 1.7 *Light microscopic image showing complete alveolar unit (Reproduced from 'Histology of Respiratory Tract' Lectures, Cardiff University, with the permission of Dr. K. BéruBé,).*

Type I pneumocytes constitute part of the extremely thin gaseous diffusion barrier, whereas the cytoplasm of type II pneumocytes is filled with vesicles containing phospholipid in the form of lamellar bodies. These bodies are discharged into the alveolar space where they contribute to the surfactant layer. Surfactant reduces the surface tension within the alveoli, preventing alveolar collapse during expiration.

The extremely high levels of differentiation of type I pneumocytes suggest that these cells are incapable of division and cannot change their phenotype (Williams, 2003). Type II pneumocytes retain the capacity for cell division and therefore function as stem cells for type I cells in response to damage to the alveolar lining (Miller and Hook, 1990).

Although the upper airways filter most particulate matter from inspired air, small particles such as carbon can reach the alveoli. Here they are engulfed by large phagocytic cells (macrophages) found in the alveolar wall or free in the alveolar space.

1.1.3.1 TYPE I (MEMBRANOUS) PNEUMOCYTE

This cell type covers 95% of the surface area of the alveolar wall but accounts for only 40% of the number of epithelial cells. The primary function of the type I cell is to enable gas exchange between the alveolar space and the pulmonary capillaries. Type I pneumocytes are flat cells which contain a flattened, central nucleus. This is surrounded by broad cytoplasmic extensions. These cytoplasmic flaps are between 0.1 and 0.3µm thick, to minimise the diffusion distance between the alveolar air space and pulmonary capillary blood. A perivascular region within the cell contains all the organelles (Weibel, 1978). The airway and alveolar epithelium is the primary barrier to diffusion of electrolytes and small solutes from the lung vasculature. Proteins and fluids can be actively transported across type I epithelium to maintain normal functioning of the lung (Johnson *et al.*, 2002; Kreda *et al.*, 2001).

Whilst the highly specialised structure of the type I cell is ideal for the function of gas exchange, it also makes the cell more susceptible to injury. Damage to these cells can lead to exudation of fluid and proteins which then collects in air spaces (Godwin, 1995). Type I cells have no mitotic potential and cannot regenerate; therefore, another mechanism is required for repair of damage caused to the lung surface.

1.1.3.2 *Type II (granular) Pneumocyte*

Type II cells are spherical pneumocytes most commonly located at a branching point of the alveolar septum (Figure 1.8). The main identifying characteristics of these cells are the numerous lamellar inclusion bodies and many microvilli on their free surface (Telford and Bridgman, 1995). The Golgi apparatus is extremely well developed, so that segments of it appear in all parts of the cell. The endoplasmic reticulum is predominantly granular, and extends through the cell and occupying space between the other organelles and the lamellar bodies. The cytoplasm is filled with small vacuoles representing the characteristic lamellar bodies. These are membrane-bound and the lamellae within them are composed mainly of phospholipids.

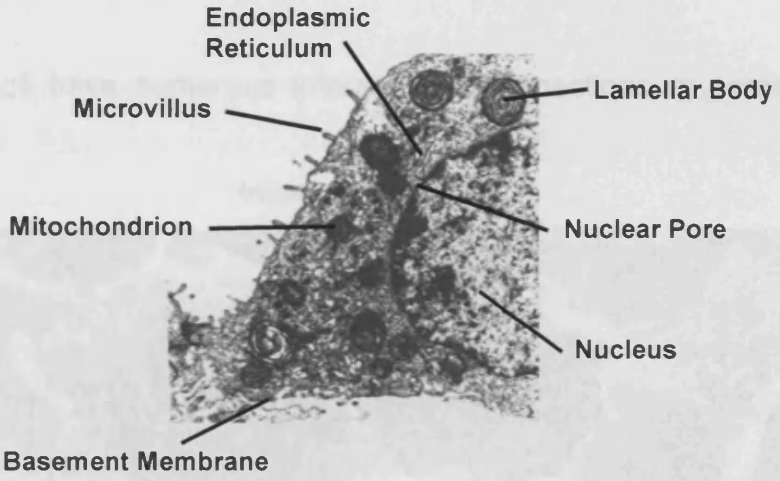

Figure 1.8 *A type II pneumocyte from human lung. Cytoplasmic organelles can be seen (Image from Scarpelli, 1988).*

Type II cells have had four major functions attributed to them: 1) synthesis and secretion of surfactant; 2) xenobiotic metabolism; 3) transepithelial movement of water; and 4) regeneration of the alveolar epithelium following lung injury (Castranova *et al.*, 1988).

Production of surfactant is facilitated by the exocytotic release of phospholipid stored as lamellar bodies. On the alveolar surface it combines with other carbohydrate- and protein-containing secretory products (some of which are

derived from Clara cells) to form a tubular lattice of lipoprotein known as tubular myelin (Gil and Reiss, 1973). Type II cells are also related to the bronchiolar Clara cell in that they contain biotransformation enzymes enabling breakdown of chemicals reaching the alveolar surface (Devereux *et al.,* 1989). The movement of water molecules is regulated by type II cells, primarily by the active transport of sodium (Goodman *et al.*, 1983) but also by the presence of aquaporins (Kreda *et al.*, 2001). When type I cells are damaged, type II cells divide, migrate and spread along the denuded basement membrane. The epithelium is reformed by proliferation of these cells, and subsequent differentiation into either normal type II or squamous type I cells (Bishop, 2004).

1.1.3.3 Pores of Kohn (Interalveolar Pores)

Adjacent alveoli have numerous interalveolar connections or pores (Figure 1.9).

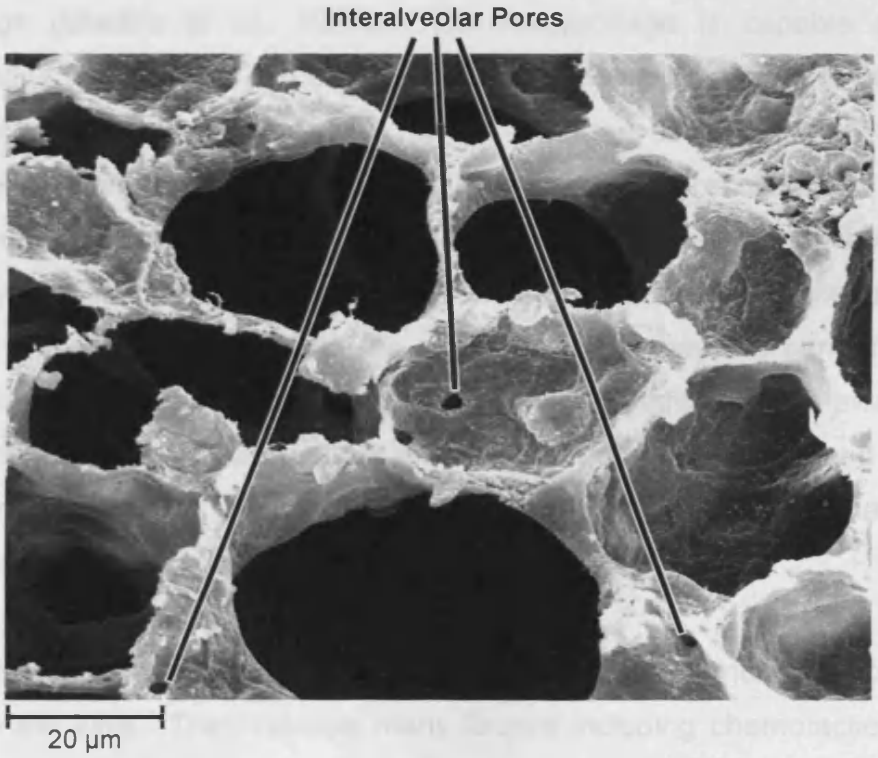

Figure 1.9 *Scanning electron micrograph showing pores of Kohn in alveoli from normal rat lung (Lung sample donated by Dr. K BéruBé, image taken by D. Balharry and M. Hicks, 2004).*

These allow ventilation of a partially deflated lung to occur to some extent. The pores allow passage of other materials such as fluid, bacteria and inflammatory cells. Fluid can spread rapidly to adjacent alveoli through these pores (Godwin, 1995).

1.1.3.4 ALVEOLAR MACROPHAGE

Alveolar macrophages constitute only a small percentage of the cells in the alveoli, but they represent the main cellular host defence mechanism in the alveolar space (Bowden, 1984). They are responsible for the phagocytosis of microorganisms and other particulate matter that has reached the alveoli. They can be found on the surface of alveolar lining cells as well as in the supporting tissue of the alveolar septa.

The macrophage population is derived primarily from blood monocytes, although some arise from mitotic division of macrophages already resident in the lungs (Shellito *et al.,* 1987). The macrophage is capable of rapid proliferation and release into the airways, in response to a number of natural and experimental stimuli (Bowden, 1976). They are large cells, 10-12µm in diameter (Telford and Bridgman, 1995) and are usually recognisable by their numerous pseudopodia. The pseudopodia are used for macrophage movement and for phagocytosis. After the engulfment of material, the majority appear to migrate into the airways, where they are carried up the mucociliary escalator and disposed of by coughing and swallowing (Langenback *et al.*, 1990). Others may pass into the interstitium and exit via the blood vessels or lymphatics, often accumulating in the regional lymph nodes (Lehnert *et al.*, 1986).

Macrophages have also been shown to be involved in immune responses to insult to the lung. They release many factors including chemotactic factors and cytokines. Some of these cytokines can recruit neutrophils and inflammatory proteins, whilst others can interact with T lymphocytes for cell-mediated immune response (Lohmann-Matthes *et al.*, 1994).

1.1.3.5 PULMONARY SURFACTANT

The entire alveolar surface is lined with a thin fluid known as pulmonary surfactant. The principal function of surfactant is the maintenance of low surface tension at the air-liquid interface and prevention of alveolar collapse. Pulmonary surfactant overcomes the effect of surface tension in the lung that would otherwise cause two alveolar surfaces to adhere, and stabilises alveoli for efficient gas exchange.

Surfactant consists of approximately 90% lipid and 10% protein, with small amounts of carbohydrate (Lynn *et al.*, 1974). Surfactant phospholipids are stored in lamellar bodies within the type II cell, and secreted by exocytosis. After the lamellar bodies have been released into the alveolar space, they unravel into a characteristic cross-hatched structure termed tubular myelin (Figure 1.10). The organisation of tubular myelin (TM) is carried out by several of the proteins in surfactant (SP-A, SP-B and SP-C) (Daniels and Orgeig, 2003). The protein component of pulmonary surfactant is made up of four surfactant proteins (SP-A, SP-B, SP-C and SP-D). These proteins are synthesised in alveolar type II cells (Yano *et al.*, 2000). Surfactant proteins SP-A and SP-D can also bind and activate alveolar macrophages, influencing a number of events such as chemotaxis and secretion of inflammatory cytokines (Wright and Youmans, 1993).

After the transition into TM, the lipid and protein components separate as the lipid is inserted into the monolayer at the air-liquid interface. It is this lipid structure that provides the surface film which regulates the surface tension of the liquid lining of the lung (Rooney *et al.*, 1994).

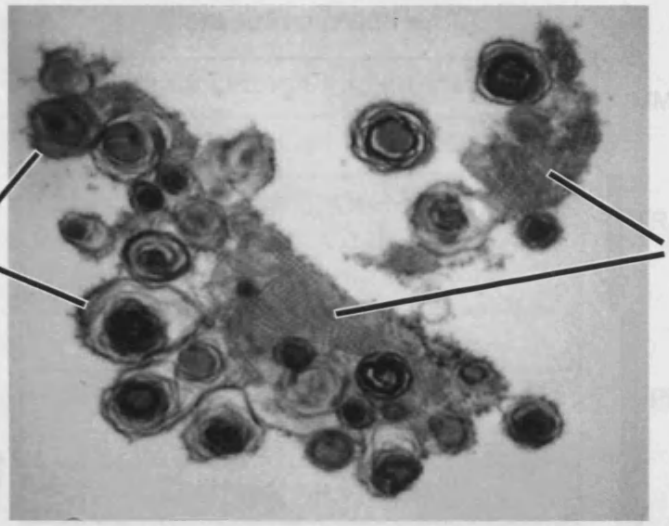

Figure 1.10 *Transmission electron micrograph showing lamellar bodies unravelling to form tubular myelin in rat lung (Image taken by D. Balharry and M. Hicks, 2004).*

Surfactant is subsequently broken down into small aggregate vesicles through mechanical or biological actions. Inactivated surfactant is cleared from the alveolar space by removal of these small aggregate particles (Veldhuizen, 1997). Seventy to eighty percent of surfactant is taken up and reused by type II cells, whilst the remaining surfactant is phagocytosed by alveolar macrophages. (Trapnell and Whitsett, 2002).

1.1.4 THE PATHWAYS OF LUNG INJURY

Injury to the lung parenchyma elicits a typical sequential pattern of response (Figure 1.11). The first response is at the alveolar surface. This may become altered by abnormal leakage of fluid into the alveoli (oedema) or by breakdown of the mechanisms designed to remove the liquid and particulate matter from the alveolar lumen (clearance failure) (Lewis *et al.*, 1987). This may be followed by an inflammatory response leading to microscopic changes in vascular calibre and blood flow. Chronic inflammation responses may lead to excessive or abnormal tissue remodelling (hyperplasia, metaplasia).

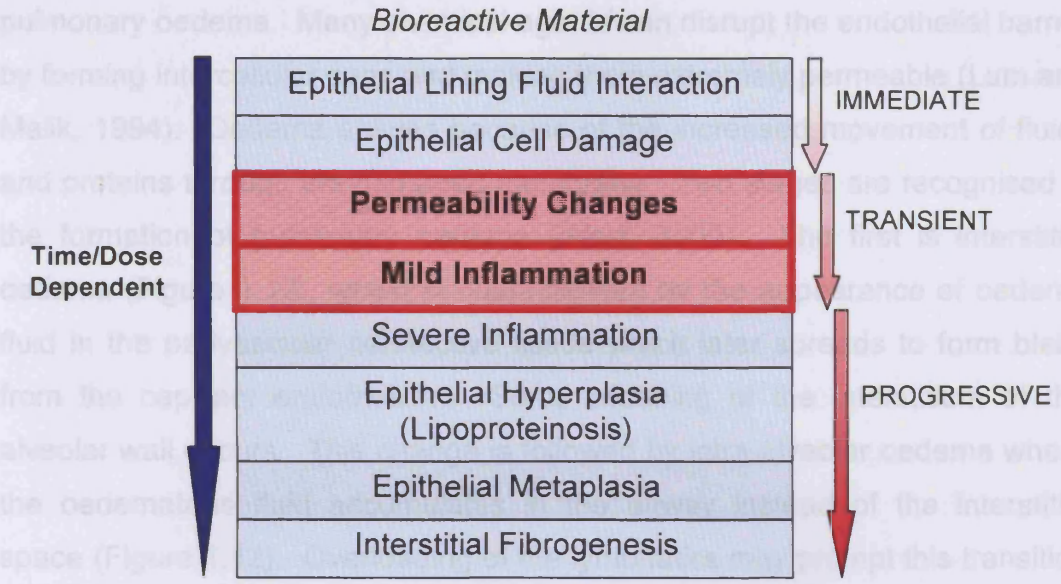

Figure 1.11 *Response endpoints of damaged respiratory tissue. Sections highlighted in red are the areas investigated in this study.*

If the toxicant leading to lung injury is not removed, a common response is the formation of too much collagenous material on the interstitial tissue (pulmonary fibrosis) or a loss and redistribution of tissue elements (emphysema).

1.1.4.1 OEDEMA

The maintenance of lung fluid balance and the correct hydration state of the interstitium is essential for normal functioning of the lung. As such, the integrity of both the capillary endothelial and the alveolar epithelial barriers is very important. The capillary endothelium is highly permeable to water and many solutes, including small molecules and ions, however the alveolar epithelium is not (Taylor and Gaar, 1970). Consequently, any fluid or protein which has leaked onto the lung is actively pumped from the alveolar surface to the interstitial space (Al-Bazzaz, 1986). In normal lungs, the tissue fluid is then removed through the alveolar interstitium into the pulmonary lymphatic channels (Mehta *et al.*, 2004).

Capillary damage is the most important factor in the development of pulmonary oedema. Many chemical agents can disrupt the endothelial barrier by forming intercellular gaps and making them extremely permeable (Lum and Malik, 1994). Oedema ensues because of the increased movement of fluids and proteins through the damaged membrane. Two stages are recognised in the formation of pulmonary oedema (West, 2000). The first is interstitial oedema (Figure 1.12), which is characterised by the appearance of oedema fluid in the perivascular connective tissue which later spreads to form blebs from the capillary endothelium. Some widening of the interstitium of the alveolar wall occurs. This change is followed by intra-alveolar oedema where the oedematous fluid accumulates in the airway instead of the interstitial space (Figure 1.12). Overloading of the lymphatics may prompt this transition from interstitial to alveolar oedema. The pressure in the interstitial space is increased so much that fluid spills over into the alveoli (West, 2000).

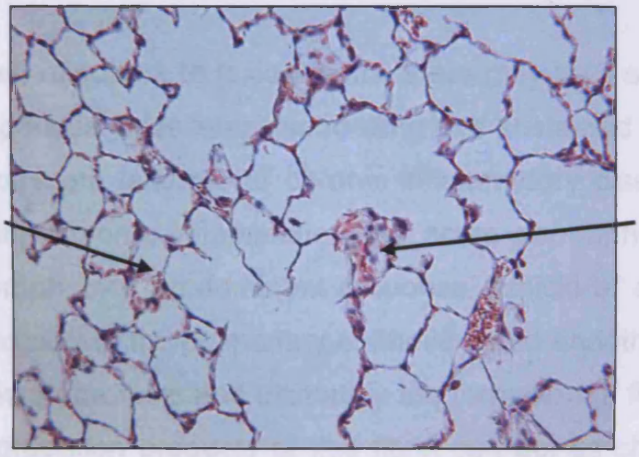

Figure 1.12 *Haematoxylin and eosin stained lung section(x160 magnification) (image taken by D. Balharry, 2002). Tissue has interstitial oedema and some intra-alveolar oedema, where the oedematous fluid containing plasma proteins, cell debris and macrophages accumulates in the airway instead of the interstitial space.*

The fluid containing plasma proteins, fibrin and disintegrated cell organelles moves across the alveoli as they are filled one by one. Macrophages cover the sites of alveolar epithelial cell destruction.

1.1.4.2 INFLAMMATION

Inflammation is the tissue response to injury. Its purpose is to repair, restore and, if necessary, remodel the injured tissue. Lung injury triggers an inflammatory response that includes migration and activation of both resident and circulating inflammatory cells, and production of cytokines and growth factors. This inflammatory cascade results in microscopic alterations that include changes in vascular calibre and blood flow, tissue oedema and leukocyte emigration (Swaisgood *et al.*, 2000). Initial recruitment of inflammatory cells into the alveolar spaces is brought about by chemoattractant agents derived from the injured lung tissue. If the damage is acute, the inflammatory cell infiltrate is predominantly made up of polymorphonuclear cells (mainly neutrophils) (Grattendick *et al.*, 2002). The duration of the response to injury is short, leading to resolution, healing and repair.

If there is repeated exposure to toxic agents, there may be a switch to chronic inflammation responses. Vascular remodelling and sustained leukocyte influx are the most prominent features of chronic inflammatory diseases (Ezaki *et al.*, 2001). During chronic inflammation the acute neutrophilic response is replaced by a lymphocyte predominant response (Izbicki *et al.*, 2002). The increased permeability of the pulmonary epithelium and endothelium results in movement of plasma proteins and ultimately the formation of fibrin clots in the alveoli. The degradation products of this fibrin can act as chemoattractants for leukocytes (Richardson *et al.*, 1976). In this instance, the inflammatory response could be augmented by the recruitment of new inflammatory cells. In a similar manner, the adherence of lymphocytes to the endothelium can lead to further induction of cytokines, which may also increase leukocyte traffic and recruitment of phagocytic cells during inflammation (Berman *et al.*, 1990). Neutrophils, macrophages and lymphocytes are well documented as sources of endothelial cell mitogens (Ezaki *et al.*, 2001). The increased number of these inflammatory cells could lead to endothelial cell proliferation resulting in enlargement of the airway vasculature. These changes to the cell structure could be a further stimulus leading to the sustained influx of

leukocytes which initiates tissue remodelling (Murphy *et al.*, 1999). This may then lead to an abnormal tissue restoration (hyperplasia, metaplasia) resulting in altered function or failure to function normally, as in fibrosis or emphysema (Jeffery, 2000).

1.1.4.3 Alveolar Proteinosis

Phospholipidosis (alveolar lipoproteinosis or alveolar proteinosis) is a form of response to a variety of noxious agents. The condition is characterised by a build-up of large amounts of phospholipid and protein in the alveoli (Hook, 1991). The accumulated material is rich in tubular myelin, membranous vesicles and lamellated structures resembling lamellar bodies. This suggests that the disease state results from aberrant accumulation of pulmonary surfactant (Onodera *et al.*, 1983). An accompanying intense hyperplasia of type II pneumocytes in alveolar walls has been found by some investigators (Witschi, 1976). The hyperplasia alone does not account for the increase in extracellular surfactant, although a large number of hypertrophic type II cells have also been identified. These hypertrophic cells have been shown to produce phospholipids and SP-A at an elevated rate (Miller and Hook, 1988). Respiratory bronchioles and alveolar walls are usually of normal thickness but may be slightly thickened due to a lymphocytic infiltration. In addition, intracellular lipid, identified as cholesterol or cholesterol ester, is also found in the alveolar walls (Spencer, 1985).

One of the indicators of lipoproteinosis is the massive accumulation of foam cells in the alveoli of the lung (Gonzalez-Rothi and Harris, 1986). These cells, which are alveolar macrophages, contain large amounts of phospholipids and other lipids which have been engulfed from the extracellular spaces (Figure 1.13). The build up of phospholipids in alveolar macrophages has been shown to severely impair phagocytic activity (Gonzalez-Rothi and Harris, 1986). This can lead to reduced alveolar clearance and decreased resistance to infection. Extracellular accumulation of this surfactant-like material also interferes with normal cellular functions and impairs gas exchange (Hook, 1991).

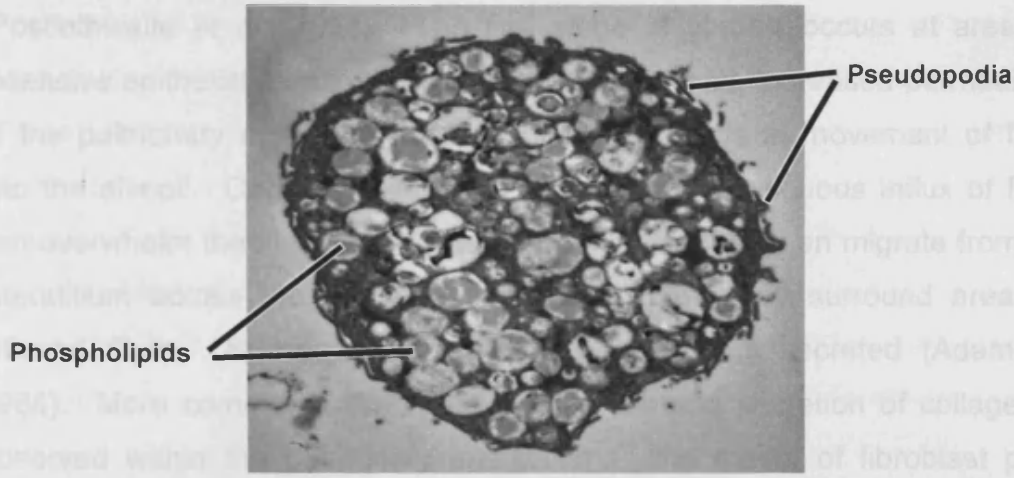

Figure 1.13 *Transmission electron micrograph showing a foamy macrophage in rat lung. (Image taken by D. Balharry and M Hicks, 2004)*

Under normal conditions in the lung, the rate at which phospholipids are synthesised is equal to the rate at which they are used, which in turn is equal to the rate at which they are cleared from the lung (Hook, 1991). During pulmonary alveolar phospholipidosis the rates of biosynthesis, secretion and clearance of phospholipids have been shown to be elevated by varying amounts (Dethloff *et al.*, 1989). The imbalance between synthesis, secretion and clearance leads to increases in the levels of phospholipids in the lung. This only helps to potentiate the effects of the disease.

1.1.4.4 PULMONARY FIBROSIS

Pulmonary fibrosis is most likely to ensue if the cause of the initial lung damage persists. Fibrosis is a serious, debilitating disease. A number of drugs are known to induce pulmonary fibrosis in humans. These include bleomycin, busulfan and mitomycin. Fibrosis is usually signified by a significant increase in total lung collagen. Primary damage to the lung leads to oedema and inflammation as previously described. This includes an increase in the number of macrophages. These macrophages can secrete a variety of potentially fibrogenic cytokines (Richards *et al.*, 1991). Lymphocytes have also been shown to generate fibroblast chemotactic

factors, and influence both fibroblast proliferation and collagen synthesis (Postlethwaite *et al.*, 1984). The first stage of fibrosis occurs at areas of extensive epithelial damage. As previously described, increased permeability of the pulmonary epithelium and endothelium results in movement of fibrin into the alveoli. Continuing injury to the lung and continuous influx of fibrin can overwhelm the fibrinolytic system. Fibroblasts may then migrate from the interstitium across the denuded epithelium where they surround areas of influxed fibrin. Subsequently, additional collagen is secreted (Adamson, 1984). More commonly, fibroblast proliferation and secretion of collagen is observed within the pulmonary interstitium. The extent of fibroblast post-translational modification may determine the ratio and types of collagen produced. Finally, cross-linking enzymes bring about the maturation of the collagen (Richards *et al.*, 1991). Associated with these extensive areas of interstitial fibrosis is the appearance of proliferated, cuboidal type II cells (Adamson, 1984).

1.2 BLEOMYCIN

1.2.1 STRUCTURE AND MECHANISMS OF TOXICITY

Bleomycins are a family of compounds produced by *Streptomyces verticillis*. Bleomycins show antibiotic and potent anti-tumour effects which have given them an important place in cancer chemotherapy. They are used extensively in the management of squamous cell carcinomas, malignant lymphomas and testicular teratomas, usually as part of a combination of drugs (NetDoctor.co.uk, 2001). They are cell cycle specific in their anti-tumour effect, acting predominantly in the G_2 and M phases of the cell cycle (Barranco *et al.*, 1973). Unfortunately, the use of bleomycin in the treatment of these diseases is limited by its toxic effects, the most serious being pulmonary injury. This is thought to be primarily due to the lack of a specific bleomycin metabolising enzyme known as bleomycin hydrolase in the lung (Lazo and Humphreys, 1983).

All bleomycins have the same bleomycinic acid background (Figure 1.14). The bleomycin molecule is made up of a bithiazole component which partially intercalates into the deoxyribonucleic acid (DNA) helix, parting the strands, and pyrimidine and imidazole structures, which bind iron and oxygen forming an activated complex. This complex is capable of releasing damaging oxidants in close proximity to the polynucleotide chains of DNA (Dorr, 1992). This may lead to chain scission or structural modifications leading to release of free bases or their propenal derivatives (Wu *et al.*, 1983). Some of the DNA strand damage may repair, but usually the cell cycle is affected, often leading to cell death.

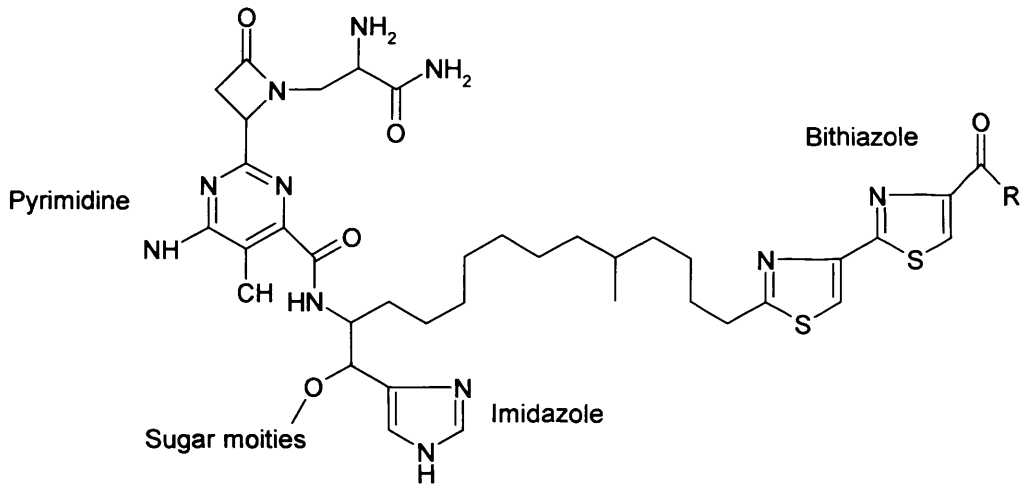

Figure 1.14 *Simplified model of bleomycin showing active sites. The bithiazole ring intercalates with DNA, whilst the pyrimidine and imidazole structures bind iron and oxygen.*

Bleomycin can also cause cell damage independent of its effect on DNA by inducing lipid peroxidation (Ekimoto *et al.*, 1985). This may be particularly important in the lung, and in part account for its ability to cause alveolar cell damage and subsequent pulmonary inflammation. Bleomycin has also been shown to inhibit the entry of cells into mitosis (Vig and Lewis, 1978).

Bleomycin is thought to exert its cytotoxic effect by cleaving DNA in an oxygen and metal ion-dependent process. Bleomycin binds to a variety of metals, including copper, manganese, vanadium, iron and cobalt. The iron complex is probably the most important *in vivo*, but DNA can be cleaved by the vanadium and manganese complexes. The complex of bleomycin with

iron has been most extensively investigated. Bleomycin simultaneously binds DNA and Fe(II) (Stubbe and Kozarich, 1987). In the presence of molecular oxygen, hydroxyl radicals are released. Following this, DNA damage and oxidation of Fe(II) occurs. This oxygen-ligated, ferric-bleomycin complex is termed 'activated bleomycin', and is thought to be the DNA-attacking species. The bleomycin metabolising enzyme, bleomycin hydrolase, is a cytosolic aminopeptidase which is thought to react with bleomycins. The resulting metabolite is unable to bind metals such as iron, rendering it inactive (Doelman and Bast, 1990).

Activated bleomycin is formed in two distinct steps. A transient oxygen-iron-bleomycin complex is formed. This yields a further species (activated bleomycin) by a single electron reduction. The reduction of the oxygen-iron-bleomycin complex to activated bleomycin is thought to be brought about by ferric-bleomycin. However, in the absence of DNA, the oxygenation of ferric-bleomycin results in the formation of a self-inactivating complex.

The two functional components of the bleomycin molecule necessary for its DNA damaging effects are two thiazole rings at one end of the molecule and a pyrimidine-imidazole moiety at the other. The two thiazole rings and the NH_2-terminal residues contribute to DNA binding, whilst the pyrimidine and imidazole moieties are responsible for dioxygen activation and iron chelation. The positively charged bithiazole moiety interacts with the negatively charged polynucleotide chain of DNA. This delivers the 'active' iron-oxygen components to appropriate DNA, and creates the subsequent damage (Duncan, 1989). DNA damage includes deoxyribose modification and the release of free bases without scission. However, single and double strand scission does occur at the C3′-C4′ bond of the sugar residue. This occurs at a limited number of sites, with preferential cleavage at G-C and G-T sequences.

Other mechanisms of toxicity have been suggested. Fe(III)-bleomycin has been shown to initiate decomposition of long chain unsaturated fatty acids (present in cell membranes) releasing a powerful oxidising agent, singlet

oxygen. Enhanced lipid peroxidation by complexes of bleomycin with Fe(II) and Fe(III) has been observed (Ekimoto *et al.,* 1985).

In order to damage DNA, bleomycin must enter cells, penetrate the nucleus and become activated in close proximity to DNA. Bleomycin has been shown to enter cells and the amidification of the C-terminal carboxyl group appeared to be important for this.

Peak pulmonary levels of bleomycin occur 45-60 minutes after subcutaneous injection. However, this represents less than 1% of the injected dose. Following intratracheal instillation of the drug, 95% of the administered dose can be detected, but this falls to 1% by 24 hours (Hay *et al.,* 1991).

1.2.2 THE EVOLUTION OF BLEOMYCIN-INDUCED LUNG INJURY

The pathological changes in the lung parenchyma following intratracheal instillation of bleomycin include cellular infiltration, pulmonary oedema, changes to type II pneumocytes and interstitial fibrosis (Brown *et al.,* 1988).

The initial morphological damage seen after treatment with bleomycin appears as damage to the pulmonary endothelial cells. This occurs in the form of endothelial cell swelling and blebbing (Aso *et al.*, 1976). Subsequently, there is loss of the type I epithelium. This destruction of the type I cells is the most critical event following bleomycin administration. As this barrier is broken down oedema fluid is allowed access to the interstitium, and the permeability of the vascular endothelium is altered (Adamson, 1984). As such, the lung injury that develops in the initial 48 hours following intratracheal bleomycin is characterised histologically by perivascular oedema, capillary congestion and alveolar wall thickening. The oedema is predominantly interstitial, with only minimal intra-alveolar oedema. There is an inflammatory cell infiltrate in the alveolar walls and spaces, together with intra-alveolar haemorrhage. The influx of cells includes a 10-fold increase in the number of macrophages and monocytes, lymphocytes, polymorphonuclear leukocytes and occasional plasma cells (Hay *et al.,* 1991).

They are found mainly in the perivascular, peribronchiolar and alveolar interstitium, and only occasionally in the intra-alveolar space. Another indicator of the acute phase of bleomycin-induced lung injury is a measure of the vascular permeability using radiolabelled markers such as ^{125}I-albumin. This provides a sensitive index of oedema (Hay *et al.,* 1987). Some areas of alveoli are entirely denuded of epithelium. Necrosis of capillary endothelium is also observed. Despite the severity of lung injury, the process is patchy, with some normal areas of lung interspersed. At this early stage, there is no sign of fibrosis.

Following the early response induced by intratracheal bleomycin instillation, extracellular matrix glycoprotein tenascin and collagen, messenger ribonucleic acids (mRNA) are induced (Zhao *et al.,* 1998). Tenascin is principally induced following the increased influx of activated inflammatory cells, during the early inflammatory stage. Tenascin is induced only in areas of tissue inflammation in the alveolar septal walls and secondary septal tips. The induction of tenascin could ensure the reparative phase is initiated, by providing invading cells with migratory pathways. Tenascin may participate in tissue inflammation and remodelling by modulation of cell migration and proliferation, and by mediating cell adhesion. This then regulates mesenchymal-epithelial interactions. Tenascin is a unique, early-response extracellular matrix component to bleomycin-induced pulmonary injury. The development of fibrosis is associated with a decrease in tenascin but an increase in collagen (Zhao *et al.,* 1998).

A common but not inevitable consequence of early phase oedema and inflammation is marked alveolar and bronchiolar epithelial cell proliferation (Miller and Hook, 1990). The type II cells undergo atypical structural changes and pneumocyte proliferation (hyperplasia). These cells are found either attached to the alveolar wall or free within the alveolar spaces. The alveolar epithelium undergoes squamous metaplasia and becomes cuboidalised (Richards *et al.*, 1991; Folkesson *et al.*, 1998; Figure 1.15).

Figure 1.15 *TEM image showing alveolar epithelium lined by cuboidal, hyperplastic type II cells after bleomycin treatment. Enlarged lamellar bodies are indicated by arrows (Image reproduced from Folkesson et al., 1998, with permission).*

A minimal collapse of the alveoli can occur. Alveolar obliteration takes place when the alveolar space becomes obstructed with inflammatory cells or atypical type II cells. Metaplasia is accompanied by lymphocyte infiltration, focal areas of interstitial fibrosis and minimal intra-alveolar fibrosis (Brown *et al.,* 1988). The fibrotic lesions show the typical thickening of the alveolar wall. This is characterised by the presence of abnormal production and deposition of collagen, and other matrix components in the interstitium (Swaisgood *et al.,* 2000). The excessive amount of fibrous tissue that is laid down in the interstitium consists of a variety of components. It is chiefly comprised of proteins and glycoproteins, of which the most abundant are collagens. Collagen synthesis and deposition usually occurs within seven days of bleomycin administration. There is no change in the proportion of collagen types I and III, suggesting a proportional increase in both (Hay *et al.,* 1991).

The peribronchial areas of fibrotic lungs contain an additional network of blood vessels. The architecture of the alveolar capillaries is modified by the occurrence of interstitial fibrosis of the alveolar wall (Peão *et al.,* 1994). This

leads to oedema of the capillary endothelium, resulting in fibroblasts and lymphocytes accumulating around areas of fibrosis. In response to bleomycin, alveolar macrophages secrete a fibroblast growth factor. These fibroblasts or their secreted collagen fibres can influence epithelial cell growth and differentiation. Epithelial cells secrete a product which has a fibroblast inhibitory effect on normal cells (Young and Adamson, 1993). This product is not secreted in a fibrotic lung in which excess fibroblast growth occurs. In a reciprocal interaction, epithelial cell proliferation is promoted by exposure to a product of lung fibroblasts. This indicates that a fibroblast-derived factor is capable of stimulating epithelial growth and so may accelerate repair (Young and Adamson, 1993). Fibroblasts could be exposed to numbers of mediators released by resident cells, or those entering tissues from the circulation.

1.2.3 Animal Models of Bleomycin-Induced Lung Injury

A large amount of the information gathered about the *in vivo* effects of bleomycin has been acquired using animal models. Interstitial fibrosis after repeated bleomycin administration has been reported in many different species, including humans, pigs (Balazs *et al.*, 1994), rabbits (Catravas *et al.*, 1983), hamsters (Starcher *et al.*, 1978), rats (Thrall *et al.*, 1979) and mice (Aso *et al.*, 1976). The overall fibrotic response is morphologically very similar between different species (Lazo *et al.*, 1990). This ability to reproducibly cause a similar condition in different experimental animals has led to bleomycin becoming one of the most commonly used agents to study the pathogenesis of pulmonary fibrosis. Despite the consistent development of pulmonary fibrosis, there appear to be some differences in sensitivity to bleomycin treatment. For example, the pulmonary fibrotic response in rabbits is less than that seen in mice with approximately equal doses (Lazo *et al.*, 1981). The age of the experimental animal may also be important. Bleomycin does not show pulmonary toxicity to young mice (Umezawa, 1979), and when bleomycin is administered to newborn lambs there is no evidence of pulmonary fibrosis (Pitt *et al.*, 1991). Although the basis for this unresponsiveness is unclear, it is well known that antioxidant defence mechanisms are enhanced in the neonate (Frank, 1985). Furthermore,

bleomycin hydrolase activity is greater in the lungs of newborn mice in comparison to mature mice (Umezawa, 1979). The varying susceptibility of animal models to bleomycin can be thought of as advantageous, in that it allows a fuller depiction of the various stages and levels of a toxic response (Kaminski *et al.*, 2000a). Genetically modified animals can be used to alter the response to insult, to gain an even better understanding of the disease processes (e.g. Kaminski *et al.*, 2000b, Swaisgood *et al.*, 2000).

Interstitial pulmonary fibrosis has been reported after multiple intravenous (IV), subcutaneous (SC), intraperitoneal (IP) or intratracheal (IT) doses (Lazo *et al.*, 1990). The relationship between the route of bleomycin administration and the development of fibrosis has been best studied in mice. With both IV and IP administration, large amounts of bleomycin are required to generate a reproducible, measurable fibrotic response (Lazo *et al.*, 1990). Repeated SC injections of bleomycin will produce interstitial pulmonary fibrosis, but again this requires a high dose (Filderman *et al.*, 1988). The IT route of administration requires a relatively small dose to produce a rapidly progressing fibrotic response (Bakowska and Adamson, 1998). Measurable fibrosis occurs much sooner using IT administration, than seen with systemic routes of administration.

Further well-characterised models use a single IT instillation of bleomycin to generate pulmonary injury. This model initially induces lung inflammation that is followed by oedema and the progressive destruction of normal lung architecture (e.g. Kaminski *et al.*, 2000a). However, this model rarely progresses to the fibrotic state.

1.3 TOXICOGENOMICS AND GENE EXPRESSION STUDIES

Genomics is the structural, functional and comparative analysis of genomes and gene products from a wide variety of organisms. The purpose of genomics is not to simply identify the component parts, but to understand how these components work together to comprise functioning cells and organisms.

The characterisation of the genetic responses of cells and tissues to a variety of toxicant and chemical insults is known as toxicogenomics. An important step in the pursuit of this is defining gene expression profiles. This compares patterns of expression in different tissues and developmental stages, in normal and diseased states, or in distinct *in vitro* conditions. This can be accomplished using reverse transcription polymerase chain reaction (RT-PCR), RNase protection assays, or Northern blot analysis, but these methods focus on only a few genes at a time. A more recent approach for analysing multiple genes simultaneously is the hybridisation of entire complementary DNA (cDNA) populations to nucleic acid arrays. The arrays are most commonly used to simultaneously measure levels of expression (mRNA abundance) for thousands of genes. For the majority of genes, changes in mRNA abundance are related to changes in protein concentration (Lockhart and Winzeler, 2000). The degree of mRNA expression is very informative about the state of a cell and the activity of genes. The transcription of genomic DNA (gDNA) to produce mRNA is the first step in protein synthesis, therefore the expression profile of a collection of genes is a major determinant of cellular phenotype and function. The differences in gene expression are indicative of both morphological and phenotypic differences, as well as of cellular responses to environmental stimuli. In terms of understanding the function of genes, knowing when, where, and to what extent a gene is expressed is key to understanding the activity and biological roles of its encoded protein. In addition, changes in the expression patterns can provide information about regulatory mechanisms and broader cellular functions and biochemical pathways (Lockhart and Winzeler, 2000).

The construction of microarrays and macroarrays is based on immobilising DNA sequences (which may be oligonucleotides or polymerase chain reaction (PCR) amplified cDNA) at specific locations on a solid support. A labelled cDNA copy of an RNA probe is hybridised to the DNA molecules attached to the array (Figure 1.16). This method exploits the specificity and affinity of complementary base pairing.

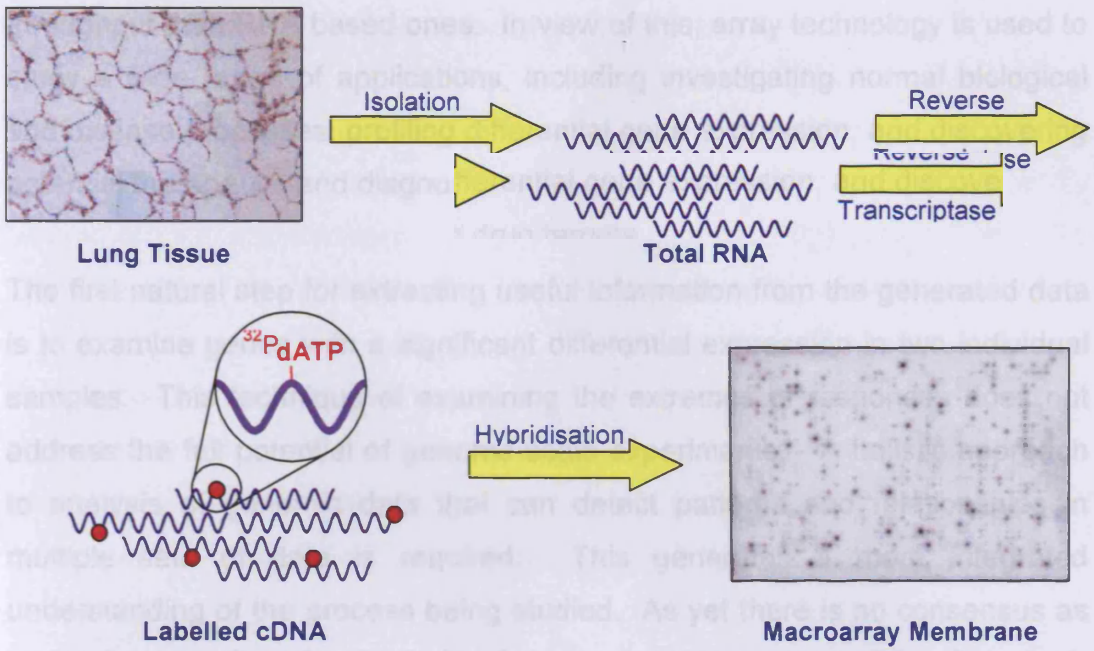

Figure 1.16 *A summary of the array technique. Total cellular RNA is isolated from the sample. Reverse transcription generates a radiolabelled probe prior to hybridisation to the array membrane. Hybridisation is visualised and quantified using a phosphorimager screen. For details, see Chapter 4.*

Following quantification, the extent of differential hybridisation to each individual sequence on the array can be determined by phosphorimager analysis (or similar techniques). The relative abundance of each of the gene sequences in two or more biological samples can be compared (Brown and Botstein, 1999). Arrays can contain sequences selected to investigate specific endpoints or pathways, or include genes representing a wide range of biological processes. A number of 'housekeeping genes' are included to aid in normalisation of data. The expression of housekeeping genes is expected to be stable under a wide range of conditions.

Arrays can only measure changes at the mRNA level and therefore cannot confirm changes in levels of the functional protein encoded by the gene. In addition, post-translational protein modifications such as phosphorylation, which may have profound influence on protein function, will not be directly measured by array analysis (Pennie, 2000). However, protein-based approaches are generally more difficult, less sensitive and have a lower

throughput than RNA based ones. In view of this, array technology is used to study a wide range of applications, including investigating normal biological and disease processes, profiling differential gene expression, and discovering potential therapeutic and diagnostic drug targets

The first natural step for extracting useful information from the generated data is to examine genes with a significant differential expression in two individual samples. This technique of examining the extremes of responses does not address the full potential of genome-scale experiments. A holistic approach to analysis of genomic data that can detect patterns and relationships in multiple sets of data is required. This generates a more integrated understanding of the process being studied. As yet there is no consensus as to the best method for analysis of micro and macroarrays (Mocellin *et al.*, 2004). However, the visualisation of large sets of array data is a popular method of analysis. This includes principal component analysis, singular value decomposition, multidimensional scaling and various clustering techniques (Slonim, 2002). Clustering applies to a wide range of methods used for organising multivariate data into groups with roughly similar patterns of expression (pairwise average linkage cluster analysis: Eisen, 1998; hierarchical clustering: Brown and Botstein, 1999; K-means clustering: Katsuma *et al.*, 2001). A number of techniques for analysis of arrays have been emerging but often these require the involvement of a specialist statistician (Cunningham *et al.*, 2000; Lee *et al.*, 2000; Nadon and Shoemaker, 2002).

In 2001, availability of a comparatively inexpensive conventional product for worldwide use in laboratories became available. This relatively simple technique for analysis of macroarray data used the AtlasImage™ 1.0 software for analysis directly from the phosphorimage. Preliminary work with this product demonstrated that by combining a series of analysis techniques with this software, significant genetic responses could be detected (Reynolds and Richards, 2001).

1.4 *AIMS AND OBJECTIVES OF THE STUDY*

The aim of this study was to develop a better understanding of the mechanisms of early bleomycin-induced lung injury, and specifically to identify biomarkers for pulmonary oedema, inflammation and epithelial repair. To accomplish this, an animal model of bleomycin-induced injury was employed.

Conventional toxicological and histological approaches were used to characterise the model and obtain different endpoints of injury. Once these had been established the new gene array technique was utilised to evaluate global gene expression patterns of the various stages of pulmonary damage and repair.

In detail, the sequential steps of this study were as follows:

- Identification of the progressive stages of oedema/inflammation and repair using pulmonary lavage techniques, cellular counting methods and assays for alveolar surface proteins and cellular proliferation (Chapter 2).

- Use of histological analysis to confirm the morphological changes occurring during oedema, inflammation and cellular repair following bleomycin-induced damage. Study of the detailed cellular changes occurring to the microstructure of the lung using transmission electron microscopy (TEM). Determination of the location and cell types involved in cellular repair by optimisation of the procedure for labelling replicating cells (Chapter 3).

- Use of the toxicology and histology information (Chapters 2 and 3) to characterise the progressive severity of the bleomycin-induced model of pulmonary injury (Chapter 3).

- Optimisation of mRNA extraction from lung tissue and the macroarray procedure (Chapter 4).

- Global expression analysis of multiple samples of saline lung tissue for comparison with mild bleomycin-induced damage (Chapter 4).

- Development of bioinformatic systems for analysing data generated by the array process (Chapter 4).

- Confirmation of the gene expression studies and bioinformatic analysis using quantitative RT-PCR (Chapter 4).

- Application of gene expression studies and bioinformatic analysis to progressive and severe pulmonary oedema (Chapter 5).

- Identification of genetic markers, individual genes or gene clusters, for mild, progressive and severe oedema (Chapters 4 and 5).

- Use of immunohistochemistry to evaluate the potential of a novel lung protein to act as a biomarker for pulmonary oedema (Chapter 6).

CHAPTER 2:

TOXICOLOGICAL IDENTIFICATION OF OEDEMA, INFLAMMATION AND REPAIR

2.1 INTRODUCTION

Bleomycin is known to cause pulmonary toxicity and was therefore used to induce sequential lung damage in rats. This model of lung injury was utilised to obtain global gene expression profiles of specific events during pulmonary injury, such as oedema and inflammation followed by subsequent repair.

Prior to gene profiling (Chapter 4), toxicological identification of oedema, inflammation and repair mechanisms needed to be established. To this end, rats were instilled with bleomycin and the extent of pulmonary injury was monitored over three weeks. From this preliminary study, three and seven days post-dosing were chosen for further investigation. Previous studies (outlined below) have indicated that significant oedema occurred at these time points, and that repair mechanisms were elevated by day seven.

In response to pulmonary damage, an initial oedema reaction caused by damage to type I cells is observed. Increased permeability of the epithelium allows oedema and inflammatory cell infiltrate to enter the alveoli (i.e. neutrophils, macrophages and lymphocytes). The maximum level of cellular infiltrate has been reported to occur three days post-bleomycin instillation (Adamson and Bakowska, 1999). Another study used the accumulation of albumin in the interstitial tissues as a measure of vascular permeability. This resulted in an increase in the interstitial space, which peaked at three days (Hay *et al.,* 1987). In agreement with these studies, Savani *et al.*, 2000, used hyaluronan content, macrophage numbers and motility as markers for injury, which showed significant increases two to seven days after bleomycin instillation. In a separate investigation, Savani *et al.,* 2001, state that maximum respiratory distress (monitored by measuring respiratory rate) occurred seven days post-instillation. This was verified by increased surface tension of broncho-alveolar lavage (BAL) and a significant drop in surfactant proteins. Jang *et al.,* 2004, also used respiration rate as a measure of lung injury in bleomycin-treated rats, and observed maximal damage at four and seven days. A further study in rats measured the extent of pulmonary injury

using nuclear magnetic resonance (NMR). The lung water content was shown to be significantly increased one week post-bleomycin instillation (Cutillo *et al.,* 2002). Collectively, these experiments indicate that oedema consistently occurs between three and seven days after bleomycin-induced pulmonary injury.

The subsequent repair phase following oedema and inflammation is marked by alveolar and bronchiolar epithelial cell proliferation. After type I cell injury the type II cells proliferate and differentiate to restore normal lung architecture. In an earlier study by Smith and Wyatt (1981), diamine putrescine was shown to be actively accumulated in lung tissue slices, as well as in epithelial cells *in vivo* (Wyatt *et al.*, 1988). Putrescine is believed to be important in the control of cell proliferation and differentiation, and therefore acts as a marker for type II hyperplasia/epithelial repair. Seven days after bleomycin-induced injury in the rat lung, putrescine accumulation was noted to be significantly increased above saline-treated controls (Housley and Richards, 1996). This indicated that the repair phase was under way seven days after the onset of pulmonary injury.

Once the model of lung injury was established using instillation of bleomycin, toxicology techniques were used to assess the level of oedema and inflammation. In conjunction with these techniques, a method for determining the level of cellular repair was also required. This was achieved by utilising cell proliferation as a marker for repair.

During the S phase of the cell cycle, a cell will undergo DNA synthesis to replicate its genome. By using DNA replication as an indicator for proliferation, it is possible to label cells as they enter the S phase. If labelled DNA precursors are present as cells undergo DNA synthesis, the labelled nucleotide is incorporated into the daughter cell DNA. Traditionally, ^{3}H-thymidine (Kuo *et al.*, 2001) incorporation assays have been used to measure cellular proliferation, and the subsequent accumulation of this compound within the tissue is detected by liquid scintillation counting.

In summary, the primary objectives of the studies described in this chapter were to optimise the thymidine assay for monitoring lung cell proliferation and to link this with conventional toxicological measurements of bleomycin-induced lung damage.

2.2 MATERIALS AND STOCK SOLUTIONS

2.2.1 ANIMALS AND MATERIALS

Supplier:	Material:
Charles River Ltd, Kent	Male *Sprague Dawley* Rats (pathogen free, 200-250g)
Rhone Merieux, Essex	Euthatal Halothane
Kyowa Hakko (UK) Ltd, Slough	Bleomycin (PL no. 12196/0005)
Sigma-Aldrich, Dorset	Bradford Reagent (B6916)
Amersham, Buckinghamshire	Methyl-^{3}H-Thymidine in 2% Ethanol (1 mCi/ml)
Packard BioScience, Groningen, Holland	Soluene-350 Opti-Fluor-Scintillation Fluid

2.2.2 STOCK SOLUTIONS

Bleomycin solution	One Ampoule in 0.15M Saline (1unit/1ml Saline)
Bovine Serum Albumin (20 mg/ml)	Dilute to Range 0-10 µg/ml
Krebs Ringer Phosphate solution	130 mM Saline 5.2 mM Potassium Chloride 10 mM Sodium Hydrogen Phosphate (Anhydrous) 11 mM Glucose 1.9 mM Calcium Chloride (Dihydrate) 1.29 mM Magnesium Sulphate (Heptahydrate) pH 7.4

2.3 METHODS

2.3.1 EXPERIMENTAL MODELS OF PULMONARY INJURY AND REPAIR

Preliminary studies utilised a single dose of bleomycin sulphate (Section 2.3.2) to induce mild pulmonary oedema. The progress of the injury was monitored using lung parenchyma:body weight ratio (Section 2.3.4) over 22 days. This time course was used to determine the most appropriate point for further studies. Initially, three days post-dosing was chosen as a suitable time to study early phase injury (n=9). To investigate more severe pulmonary injury, and potentially some repair processes, seven days post-dosing was also studied (n=6). In a further study, severe injury, possibly leading to lipoproteinosis and fibrogenesis, was generated utilising a double dose of bleomycin (Brown *et al.*, 1988). The second dose was administered seven days after the first. Studies were carried out three (n=6) and seven days (n=6) after the second dose. A final investigation was carried out three weeks (n=6) after the second dose, in the anticipation that some resolution of the disease might have occurred.

2.3.2 ADMINISTRATION OF BLEOMYCIN

Animals were treated with 0.5 units of bleomycin sulphate suspended in 0.5ml 0.15M saline. Sham controls received only 0.15M saline (0.5ml). Prior to treatment with either bleomycin or saline, rats were lightly anaesthetised with Halothane. The dose was administered via non-invasive intratracheal instillation (Reynolds and Richards, 2001). This ensured that every animal received the same quantity of drug directly to the target tissue. In agreement with the Local Ethical Committee and the Home Office Project Licence the recovery time of the rats was monitored before returning them to their cage. Animals were also closely monitored every two hours for six hours, and twice a day thereafter, using a post-procedure pain and distress score sheet (Wolfensohn and Lloyd, 1998).

2.3.3 *HARVESTING OF EXPERIMENTAL ANIMALS*

Sham and bleomycin-treated rats (200-250g) were anaesthetised with Halothane and then administered a lethal intraperitoneal injection (1-2ml) of Euthatal. The rats were subsequently weighed and cardio-respiratory death confirmed prior to dissection.

2.3.4 *DISSECTION OF EXPERIMENTAL ANIMALS*

The fur on the abdominal cavity of harvested experimental rats was washed with ethanol (70% v/v) and the ventral surface skin removed. The peritoneal cavity was opened by midline incision and the major dorsal blood vessels cut. A tracheotomy was performed and a Luer Cannula, attached to a 20ml syringe, securely tied into place in the trachea. The diaphragm was then opened and the ventral portion of the rib cage and thymus removed.

A Luer cannula attached to a gravity feed of sterile saline was then fed into the pulmonary artery and the right atrium was cut upon expansion to allow fluid to exit. The lungs were perfused via artificial ventilation with 8-10ml of air by means of the syringe attached to the Luer Cannula of the trachea. Ventilations (usually 8-10) were continued until the pulmonary circulation was clear of all blood, to produce white parenchymal lung tissue.

The heart was removed and the lungs and trachea dissected free from the carcass. The oesophagus and any fatty tissue were dissected from the lungs and trachea. Any mucoidal material or blood clots on the exterior of the tissue were removed by means of absorbent tissue. The lung parenchyma was weighed to calculate the L:B ratio. An increased L:B ratio was used as an early indicator of lung damage.

2.3.5 *LUNG LAVAGE*

The lungs were lavaged (five to eight times) by means of a Luer cannula attached to the trachea (Figure 2.1) with 6-8mls of 0.15M saline, and the BAL

fluid pooled in a centrifuge tube and maintained on ice. Following infection or inflammation, the number of large free cells within the lavage will usually increase. The free cell count was obtained by counting a sample of the BAL using a standard haemocytometer (Section 2.3.6).

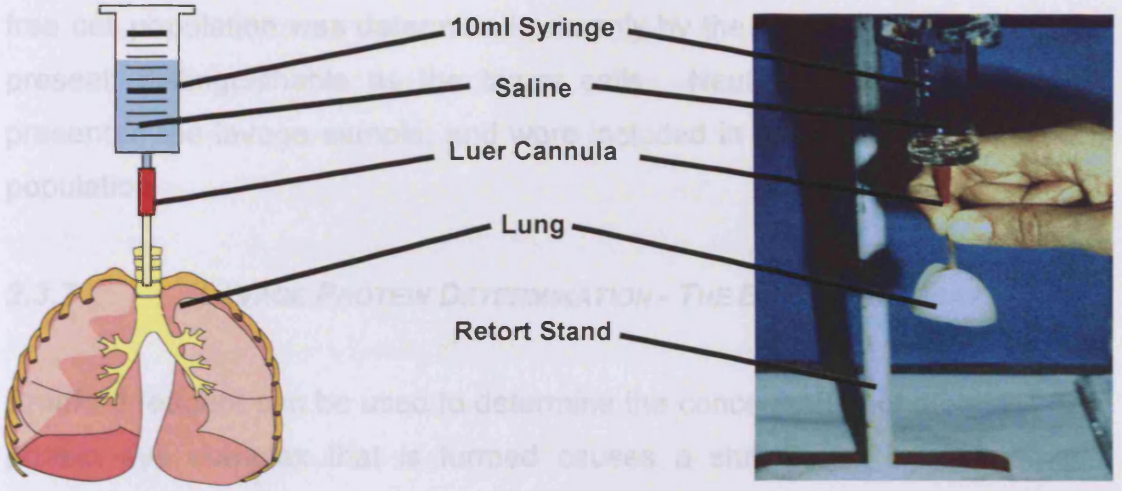

Figure 2.1 *Demonstration of saline lavage technique. A syringe full of saline is attached via a Luer cannula to the trachea. Saline is gravity fed into the lung until fully inflated. The saline is then poured off via the cannula into a collecting tube.*

During oedema the cellular membranes breakdown or become compromised. This leads to an influx or increased transport of plasma proteins to the lung surface. The concentration of these proteins was determined by the Bradford assay (Section 2.3.7). The number of macrophages and the concentration of protein within the lavage serve as an assessment of the respiratory health of the animal. The intact cells and surface proteins were collected then separated from the BAL fluid by centrifugation (at 300 x *g*) and stored (-80°C) for use in later experiments. After lavaging, the five lobes of the lungs were separated, flash frozen in liquid nitrogen and stored at -80°C for use in gene profiling studies.

2.3.6 DETERMINATION OF FREE CELL NUMBERS

A standard haemocytometer was used for counting cells. Phase contrast microscopy was used to aid cell identification. Contaminating red blood cells

were recognisable by their characteristic biconcave disc morphology and small size. These cells were sometimes found in lavage samples but comprised a small proportion of the total cell population and were not included in any subsequent cell counts. Damaged cells and debris were identified as grey or black outlines and were not included during any cell counts. The large free cell population was determined primarily by the number of macrophages present, distinguishable as the larger cells. Neutrophils were sometimes present in the lavage sample, and were included in the count of the free cell population.

2.3.7 LAVAGE PROTEIN DETERMINATION - THE BRADFORD ASSAY

Bradford reagent can be used to determine the concentration of proteins. The protein dye complex that is formed causes a shift in the dye absorption maximum from 465nm to 595nm. The change in absorption at 595nm is therefore proportional to the protein concentration (Bradford, 1976).

A set of standards were made up using bovine serum albumin (BSA) ranging from 0 to 10µg/ml. BAL (supernatant from 300 x *g* centrifugation) was diluted 10 or 20-fold in saline, and 200µl added to each well of a 96-well plate. Fifty microlitres of Bradford reagent was then added to each sample. The absorbance was read at 590nm using a plate reader. Assays were performed in triplicate for each animal and the mean value recorded.

2.3.8 CELL PROLIFERATION ASSAY - TRITIATED THYMIDINE UPTAKE

The occurrence of cellular repair in the lung was monitored *ex vivo*. This was achieved by measuring the level of cellular proliferation and differentiation by the use of a labelled nucleoside (tritiated thymidine). Thymidine is involved in DNA synthesis and therefore acts as a suitable marker for epithelial repair. Each sample was carried out in triplicate, and saline-instilled animals were used as a comparison.

After the lungs were excised, the largest lobe was manually cut into 500µm slices. Krebs Ringer Phosphate solution (KRP, 500µl) was added to each well of a 24-well plate, and a tissue slice placed into the well. Control wells were included which contained no tissue. The wet weight of tissue in each well was recorded and was usually between 20-40mg. A further 495µl KRP was added. The tissue samples were allowed to equilibrate at 37°C for 10 minutes. After the 10 minute incubation, 5µl tritiated thymidine (50µCi/ml) was added to a final concentration of 0.25µCi. The addition of the tritiated thymidine made a total volume of 1ml per well. The samples were then incubated at 37°C for a further 30 minutes. An equivalent 24-well plate with 500µl KRP in each well was prepared and stored on ice. After 30 minutes the incubated tissue was transferred to the chilled plate and washed copiously with KRP solution. The washed samples were then transferred into a vial containing 1ml soluene (tissue solubiliser) and placed in a boiling water bath for 30 minutes. Once cooled, 10ml of scintillant was added and well mixed. At the same time, 500µl was removed from control samples (containing no tissue) and added to a vial containing 10ml scintillant. All samples were counted in a scintillation counter 24 hours after addition of scintillant. Thymidine uptake was calculated as the number of nanomoles incorporated per lung in 30 minutes.

$$\text{Thymidine uptake} = \left(\frac{\text{cpm (tissue) x conc. (nmol)}}{\text{slice wt (g) x cpm (medium)}} \right) \text{x total LP weight (g)}$$

2.3.9 STATISTICAL ANALYSIS

The statistical difference between data points was determined using a two-tailed Student's t-test.

2.4 RESULTS

2.4.1 ASSESSMENT OF OEDEMA AND INFLAMMATORY RESPONSE

A preliminary study was carried out over three weeks to identify the peak of early phase oedema. Lung parenchyma:body weight ratio (L:B ratio) was measured at regular intervals over three weeks after a single bleomycin/saline instillation (Figure 2.2). The L:B ratio is used as an indication of lung health. During infection, injury or inflammation, an influx of cells and protein together with tissue retention of excess water will cause an increase in the lung weight, reflected in an elevated ratio (Richards and Curtis, 1984).

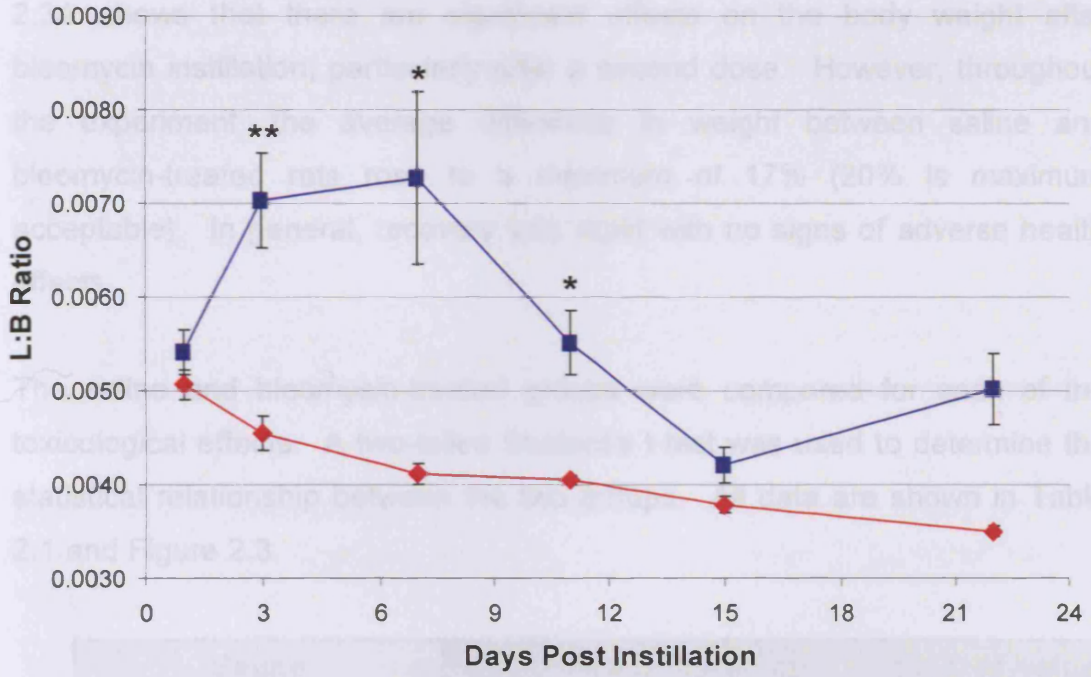

Figure 2.2 *Comparison between L:B ratios of saline (◆) and bleomycin (■) instilled rats over a three week time course. Days 1, 11, 15 and 22: n=3; Days 3 and 7: n=9. Error bars indicate one standard deviation. * Significant (p≤ 0.05) ** Significant (p≤ 0.001)*

The most significant differences from control was observed at three (p=0.0004) and seven (p=0.0086) days post-bleomycin instillation. This corresponds with the predicted peak of injury as reported in previous studies (Adamson and Bakowska, 1999; Hay *et al.*, 1987; Savani *et al.*, 2001; Jang *et*

al., 2004). Subsequent studies were carried out at three and seven days post-single or double instillation. A final time point was also carried out three weeks after a second bleomycin instillation to monitor possible resolution of the injury.

The following parameters were recorded for each rat; body weight, L:B ratio, total surface protein concentration, and the lavage free cell (LFC) count from the lavage sample. The body weight was carefully monitored, as a failure to gain weight is evidence of damage to the overall health of the rat. The Home Office project licence regulations permit a failure to gain weight of up to 20% before termination of the experiment is considered. The weight of all the rats prior to instillation with bleomycin or saline was approximately 200g. Figure 2.3A shows that there are significant effects on the body weight after bleomycin instillation, particularly after a second dose. However, throughout the experiment, the average difference in weight between saline and bleomycin-treated rats rose to a maximum of 17% (20% is maximum acceptable). In general, recovery was rapid with no signs of adverse health effects.

The saline and bleomycin-treated groups were compared for each of the toxicological effects. A two-tailed Student's t-test was used to determine the statistical relationship between the two groups. All data are shown in Table 2.1 and Figure 2.3.

	Saline			Bleomycin			t-test (p-value)		
Days post instillation	L:B ratio	LFC ($x10^6$)	Protein (mg/rat)	L:B ratio	LFC ($x10^6$)	Protein (mg/rat)	L:B ratio	LFC ($x10^6$)	Protein (mg/rat)
3	0.0046	5.92	2.35	0.0071	7.93	3.55	0.003	0.03	0.003
7	0.0041	5.14	1.27	0.0068	11.55	13.29	0.0001	0.016	0.0001
10 (*3)	0.0041	7.31	1.65	0.0076	13.81	14.11	0.0000003	0.010	0.0003
15 (*8)	0.0037	5.13	1.72	0.0085	3.73	13.58	0.0011	0.002	0.000002
29 (*22)	0.0034	3.51	1.63	0.0053	6.03	8.07	0.0025	0.038	0.0031

Table 2.1 *Comparison of the toxicological data between the saline and bleomycin-instilled lung; n=6 (except day 3: n=9). * Days post-second instillation.*

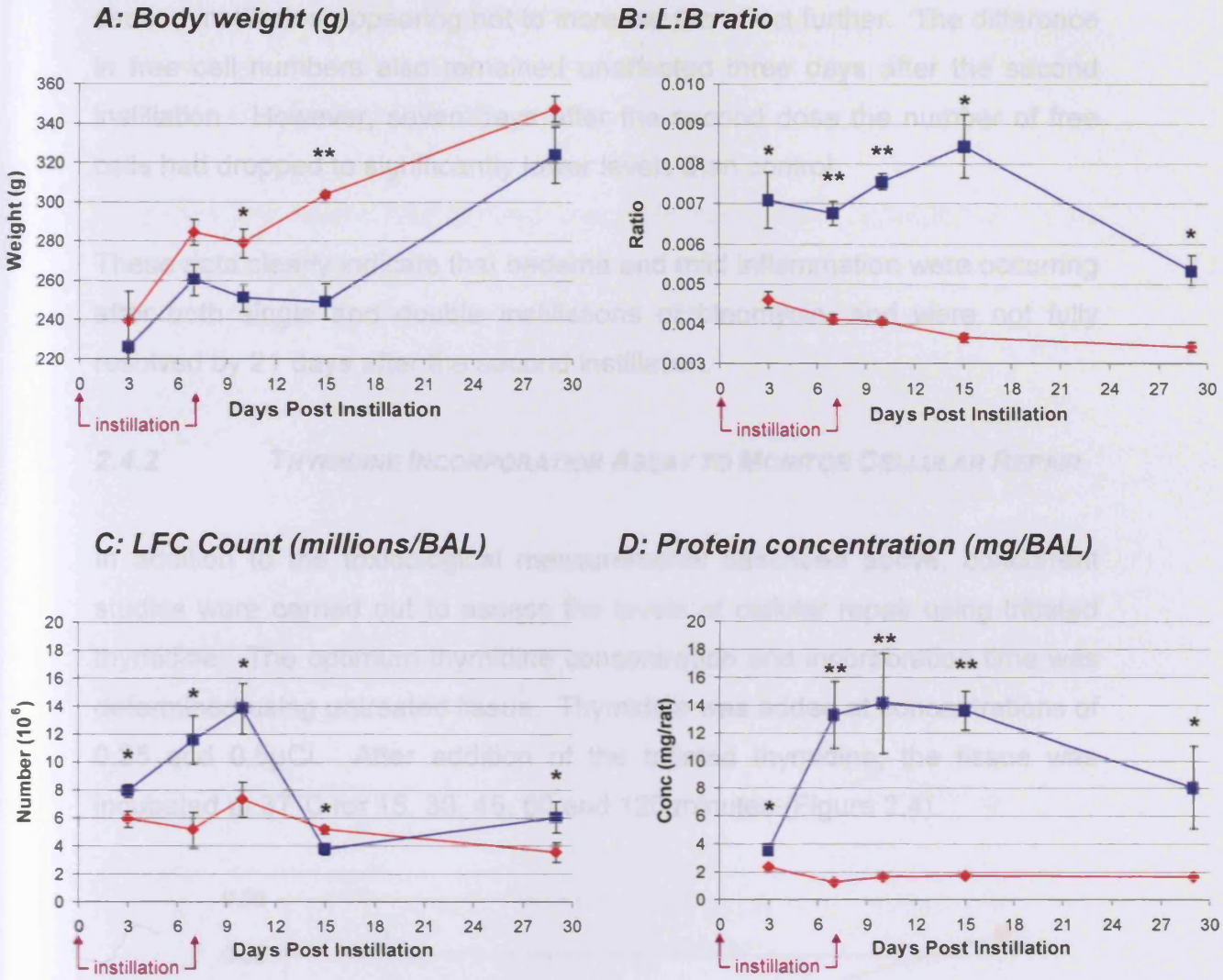

Figure 2.3 *Comparison between the saline (◆) and bleomycin (■) instilled lung. n=6 (except day 3: n=9). Error bars indicate one standard deviation. * Significant: p≤ 0.05, ** Significant: p≤ 0.001.*

At all time points measured, for all toxicological markers of injury, the bleomycin-treated tissue was significantly different from the controls. After the single dose of bleomycin, the difference in L:B ratio between saline and bleomycin-treated samples remained constant. However, after the second instillation the difference had increased, and continued to rise up to seven days after dosing. For both protein concentration and free cell counts the difference between control and bleomycin-treated samples was relatively low three days after the first instillation, but greatly increased by seven days. The protein levels remained fairly constant from seven days onwards, with the

second instillation appearing not to increase the effect further. The difference in free cell numbers also remained unaffected three days after the second instillation. However, seven days after the second dose the number of free cells had dropped to significantly lower levels than control.

These data clearly indicate that oedema and mild inflammation were occurring after both single and double instillations of bleomycin, and were not fully resolved by 21 days after the second instillation.

2.4.2 *Thymidine Incorporation Assay to Monitor Cellular Repair*

In addition to the toxicological measurements described above, concurrent studies were carried out to assess the levels of cellular repair using tritiated thymidine. The optimum thymidine concentration and incorporation time was determined using untreated tissue. Thymidine was added at concentrations of 0.25 and 0.5µCi. After addition of the tritiated thymidine, the tissue was incubated at 37°C for 15, 30, 45, 60 and 120 minutes (Figure 2.4).

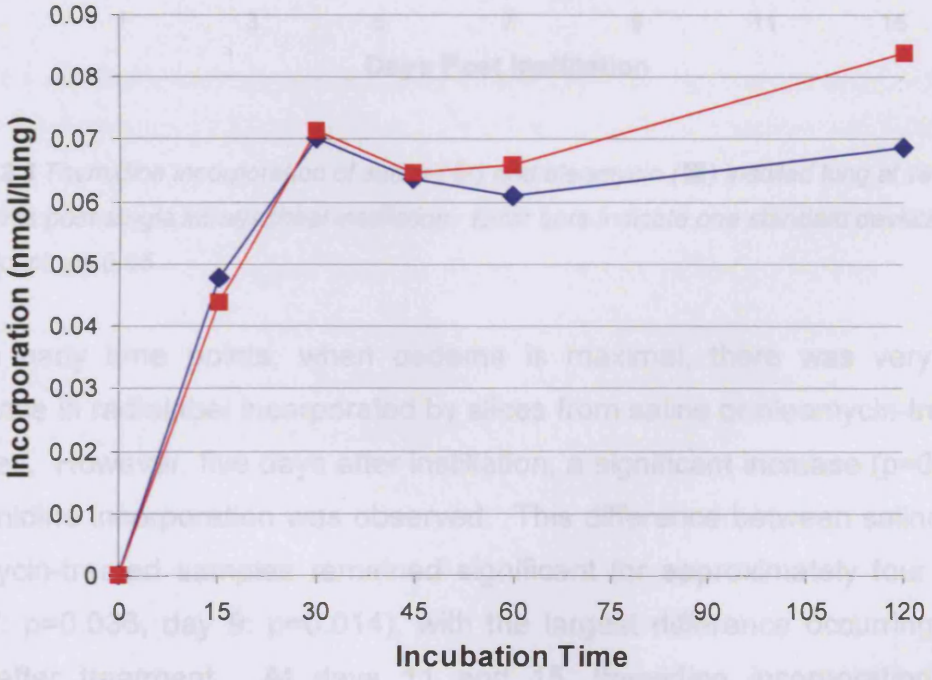

Figure 2.4 *Incorporation of 0.25µCi (◆) tritiated thymidine and 0.5µCi (■) tritiated thymidine by lung slices over differing incubation periods.*

There was no significant difference between the incorporation of either concentration, so further experiments were carried out using 0.25 µCi tritiated thymidine and incubated for 30 minutes.

A preliminary assay was carried out over two weeks following a single bleomycin instillation (Figure 2.5). Three biological replicates were taken at each time point, and each of these was assayed in triplicate (n=9).

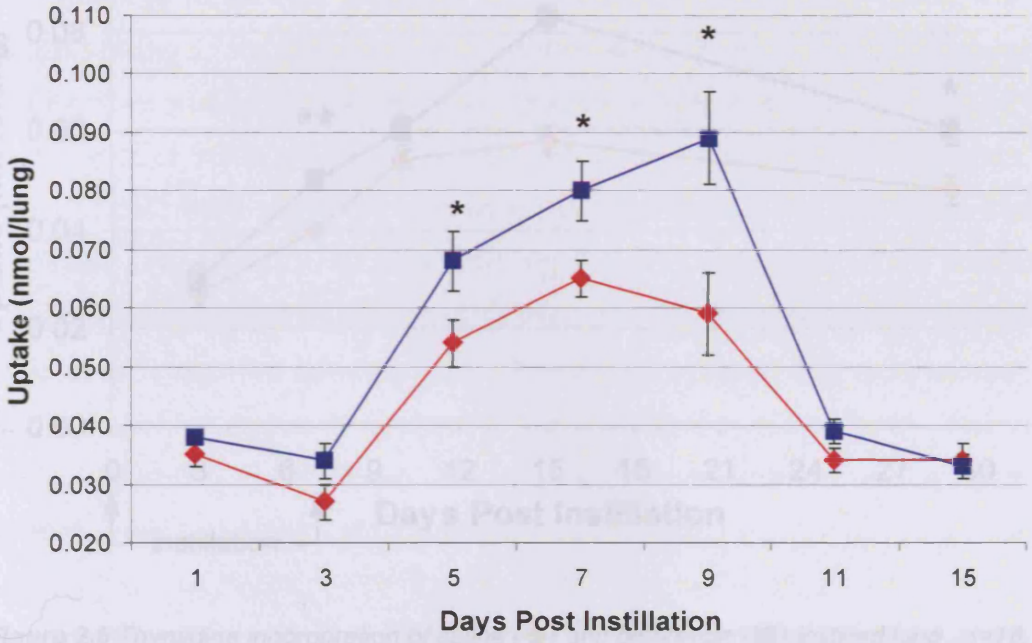

Figure 2.5 *Thymidine incorporation of saline (◆) and bleomycin (■) instilled lung at various time points post-single intratracheal instillation. Error bars indicate one standard deviation.*
** Significant: p≤ 0.05*

At the early time points, when oedema is maximal, there was very little difference in radiolabel incorporated by slices from saline or bleomycin-treated samples. However, five days after instillation, a significant increase (p=0.045) in thymidine incorporation was observed. This difference between saline and bleomycin-treated samples remained significant for approximately four days (day 7: p=0.036, day 9: p=0.014), with the largest difference occurring nine days after treatment. At days 11 and 15, thymidine incorporation was identical in both saline and bleomycin-treated lung slices.

A further radiolabelling experiment was carried out in parallel with the above toxicology studies. Lung slices were prepared three and seven days after a single instillation. A second dose was instilled at seven days, and more samples measured at three, eight and 22 days post-second instillation. The results from this experiment are shown in Figure 2.6.

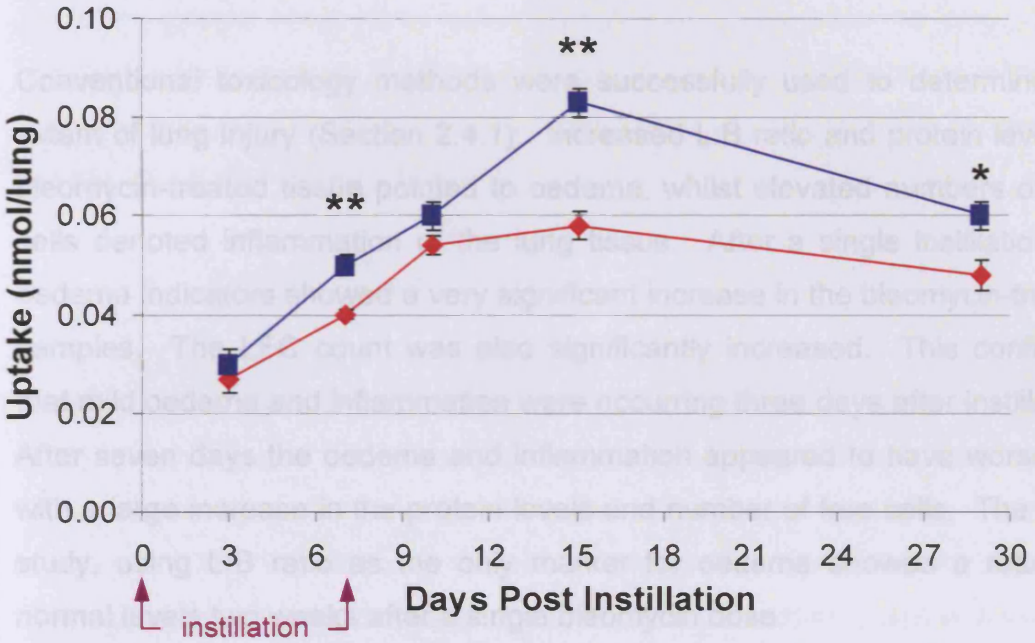

Figure 2.6 *Thymidine incorporation of saline (◆) and bleomycin (■) instilled lung. n=18. Error bars indicate one standard deviation. * Significant: p≤ 0.05, ** Significant: p≤ 0.001.*

Seven days after a single dosing, total thymidine uptake in bleomycin-treated lung was significantly higher than in saline controls (p=0.001). The greatest change was observed eight days (day 15) after the second bleomycin dose (p=0.000002). By day 29 (three weeks after second instillation) thymidine uptake was still significantly raised (p=0.007).

Conventional toxicology methods were successfully used to determin extent of lung injury (Section 2.4.1). Increased L:B ratio and protein lev bleomycin-treated tissue pointed to oedema, whilst elevated numbers o cells denoted inflammation of the lung tissue. After a single instillatio oedema indicators showed a very significant increase in the bleomycin-tr samples. The LFC count was also significantly increased. This confi that mild oedema and inflammation were occurring three days after instill After seven days the oedema and inflammation appeared to have worse with a large increase in the protein levels and number of free cells. The study, using L:B ratio as the only marker for oedema showed a retu normal levels two weeks after a single bleomycin dose.

After a second bleomycin instillation the L:B ratio had increased by three and peaked after seven days. The protein concentration and free numbers remained significantly raised, but did not differ greatly from the seven (single dose) levels. However, unlike the single dose model which returned to normal by day 15, the oedema markers were still signific elevated three weeks after the double-bleomycin instillation.

Initial thymidine incorporation assays after a single bleomycin instill showed a significant increase in cellular proliferation from day five contir to day nine. This had returned to control levels by day 11, confirming transient nature of the single dose model.

A similar trend was observed after a double dose of bleomycin. Seven after the second instillation, thymidine uptake was significantly increase

bleomycin-treated tissue. Contrary to the initial study, there was no evidence of the thymidine uptake returning to control levels by day 11; uptake was still significantly different three weeks after the second instillation. These data confirm that cellular proliferation was induced seven days after dosing (acute repair), and that these repair processes were still functioning three weeks (chronic) after a double bleomycin dose. To improve the accuracy of the thymidine uptake assay, a microtome could be used to slice the lung. It has previously been shown that the method of slicing the tissue, manually or mechanically, greatly affects the accumulation of radiolabelled compounds (Smith, Wyatt and Cohen, 1982).

2.6 *CONCLUSIONS*

These studies are in agreement with the previously reported findings described in Section 2.1. The toxicology studies showed that after a single bleomycin dose, oedema and mild inflammation were occurring three and seven days after instillation. Cellular proliferation reached maximum levels nine days post-dosing, but was fully repaired by 11 days (transient oedema model). After a double dose, the oedema observed was far more severe, and again peaked at seven and three days. Whilst significant levels of cellular repair were observed eight days post-dosing, the injury was not resolved by 22 days after the second dose (persistent oedema model). Thus, the distinction between the models of bleomycin-induced lung damage was successfully achieved.

Before proceeding with the genomic expression analysis of the tissue (Chapter 4), lung samples from parallel experiments to those reported in this chapter were processed for histology and electron microscopic analysis (Chapter 3).

CHAPTER 3:

HISTOCHEMICAL AND ELECTRON MICROSCOPIC IDENTIFICATION OF OEDEMA, INFLAMMATION AND REPAIR

3.1 INTRODUCTION

A model of pulmonary injury was established using instillation of bleomycin, and partially quantified using conventional toxicology (Chapter 2). These quantitative biochemical investigations primarily utilised broncho-alveolar lavage (BAL) techniques. Data gathered in this way reflects the changes at the lung surface, which may not always represent the overall changes to the lung. Under certain circumstances, for example when lipoprotein accumulation and interstitial wall thickening are very severe, the alveoli may not be washed out efficiently. In addition, lavage techniques provide little information on the cellular or interstitial changes occurring throughout the disease processes.

Histological analysis was used to complement the previous studies (Chapter 2) and increase understanding of the progression of injury. In this manner, morphological changes in the lung were detected. To study the detailed cellular changes occurring to the microstructure of the lung, transmission electron microscopy (TEM) was employed. In conjunction with these techniques, a method for determining the location and cell types involved in cellular repair was also required. This was again achieved by utilising cell proliferation as a marker for repair.

Experiments have shown that the thymidine analogue 5-bromo-2-deoxy-uridine (BrdU) is incorporated into newly formed cellular DNA in a similar manner to the incorporation of thymidine (Roche, 2000). The incorporated BrdU can then be detected by a quantitative cellular enzyme immunoassay using monoclonal antibodies directed against BrdU. This allows identification and semi-quantification of the cells undergoing replication in the tissue.

A number of authors (Quinlan *et al.,* 1995; BéruBé *et al.,* 1996; Gallagher and Gottleib, 2001) have reported the successful use of BrdU labelling in lung tissue. However, preliminary investigations of the available literature indicated that no simple, standardised technique for successful and efficient *in*

vivo labelling of tissue was available. Consequently, a series of experiments were undertaken in an attempt to optimise the BrdU technique in bleomycin-treated rats, and implement a set protocol for all subsequent studies.

The primary objectives of the studies described in this chapter were to identify the type of lung injury generated by the bleomycin model and to optimise the BrdU incorporation assay to monitor the repair mechanisms. By investigating the morphological changes in the lung, in combination with the toxicology data, the aim was to obtain clear differentiation between models of injury and cellular repair for use in later genomic investigations.

3.2 MATERIALS AND STOCK SOLUTIONS

3.2.1 MATERIALS AND SUPPLIERS

Raymond A Lamb, Sussex	1% Aqueous Eosin (LAMB/100-D)
Roche Diagnostics Ltd, Sussex	5-Bromo-2-Deoxy-Uridine Labelling and Detection Kit II (1 299 964)
Sigma-Aldrich, Dorset	5-Bromo-2-Deoxy-Uridine (B5002) Poly-L-Lysine Coated Glass Slides (P0425) Mayer's Haematoxylin (51275)
Fisher Scientific, Leicestershire	Toluidine Blue (34860-0050)
BDH Laboratory Supplies, Dorset	Aquamount (362262H) DPX Mountant (36029)
Agar Scientific, Essex	Sodium Cacodylate (R1102) 25% Glutaraldehyde (R1010) Osmium Tetroxide (R1015) Propylene Oxide (R1080) Araldite CY212 (R1040) 200-mesh, 3.05mm Copper Grids (G246) 2% Uranyl Acetate (R1260) Reynold's Lead Citrate (R1210)

3.2.2 STOCK SOLUTIONS

10% Neutral buffered formalin

EM fixative (pH 7.4)	3% Glutaraldehyde 0.1M Cacodylate 3mM Calcium Chloride

3.3 METHODS

3.3.1 EXPERIMENTAL MODELS OF PULMONARY INJURY AND REPAIR

Concurrent studies were carried out with those described in Sections 2.3.1-2.3.4. Bleomycin was instilled intratracheally to induce pulmonary damage. Samples were taken three and seven days after a single bleomycin dose for all the studies described in this chapter. Samples were also collected three, seven and twenty one days after a double instillation of bleomycin for TEM and haematoxylin and eosin (H and E) staining.

3.3.2 5-BROMO-2-DEOXY-URIDINE INCORPORATION

As a cell is about to divide it undergoes DNA synthesis and replicates its genome. If a labelled DNA precursor is present it will be incorporated into the new cellular DNA. The integrated precursor can then be detected by a quantitative enzyme immunoassay. This facilitates visualisation of proliferating cells at an isolated time point. The precursor used in this case was 5-bromo-2-deoxy-uridine (BrdU).

Two approaches were adopted, one of which involved *in vivo* labelling of lung cells. This was achieved either by directly injecting BrdU into the intraperitoneal (IP) cavity as described by Quinlan *et al* (1995), or using a new approach by intratracheally (IT) instilling the compound into the lung. A second *ex vivo* method was tried whereby the treated lung was removed from the rat and subsequently inflated and instilled with BrdU.

3.3.2.1 IN VIVO INCORPORATION

BrdU was administered via intraperitoneal injection or intratracheal instillation. This was done at three and seven days post-instillation of bleomycin. The animals were injected intraperitoneally with 100mg/kg body weight (Quinlan *et*

al., 1995), the equivalent to 26mg/rat, or instilled intratracheally with 300µg/rat. The BrdU was then incorporated *in vivo* into proliferating cells.

The length of time for maximum incorporation of BrdU *in vivo* was uncertain, so two time points were chosen for initial investigation. Incorporation of BrdU for one hour was recommended for *in vitro* studies (Roche, 1999, pack insert). As the present experiments were *in vivo*, it was considered five hours should allow sufficient time for the BrdU to enter the lungs from the peritoneal cavity. Twenty-four hours was also chosen as a time point (Quinlan *et al.,* 1995). After this time the lungs were excised and stored as described in Section 3.3.3.1.

3.3.2.2 Ex Vivo Incorporation

The animals were sacrificed seven days after bleomycin treatment. The lungs were excised as detailed in Section 2.3.4. BrdU was diluted in cell culture medium to a concentration of 10µmol/l. The intact lung was then filled with BrdU solution via a syringe and cannula. The lung was tied off to prevent the BrdU leaking out, and incubated for 60 minutes at 37°C in a saline bath. After this time the BrdU solution was poured off via the cannula and replaced with 10% neutral buffered formalin (Section 3.3.3.1).

3.3.3 Processing Tissue for Light Microscopy

3.3.3.1 Fixation of Lung Tissue

The lungs were excised as detailed in Section 2.3.4. Lung tissue was treated *in vivo* or *ex vivo* with BrdU as described in Section 3.3.2. All tissue to be processed for light microscopy (LM) was left untreated. The intact lung was filled with 10% neutral buffered formalin via a syringe and cannula (Figure 3.1). The inflated lung was then immersed in 10% neutral buffered formalin at 4°C for at least 24 hours in preparation for tissue processing (Section 3.3.3.2).

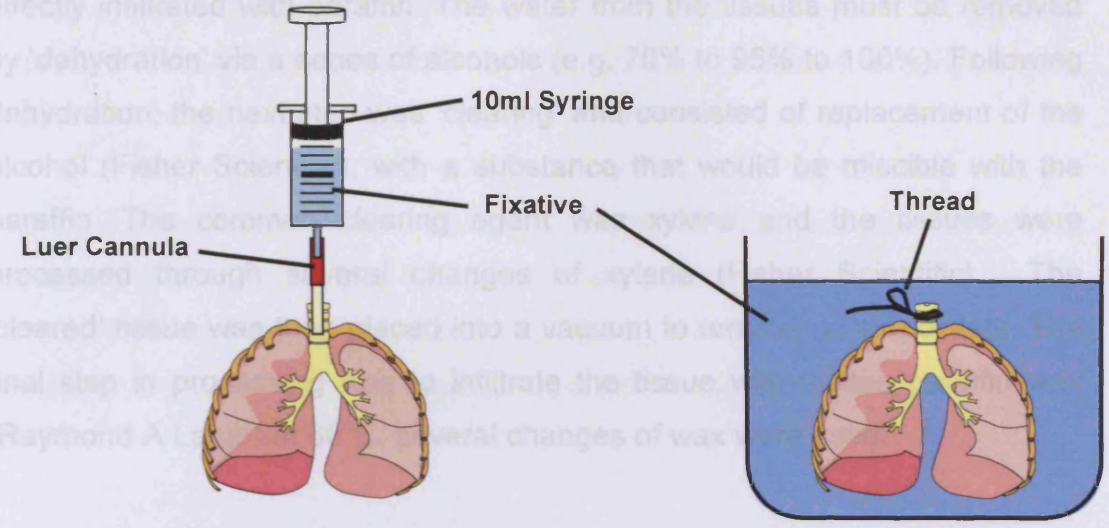

Figure 3.1 *Inflation of lung with fixative. Fixative is forced into the lung via a syringe and cannula to the trachea. Trachea is then tied off with thread and immersed in more fixative.*

Tissue processing, sectioning and staining for LM was carried out by a histotechnologist, Mr Derek Scarborough, at the School of Biosciences, Cardiff University. A brief overview of these procedures has been outlined below in Sections 3.3.3.2 to 3.3.3.4.

3.3.3.2 TISSUE PROCESSING

Once the tissue has been fixed (Section 3.3.3.1), it must be processed into a form in which it can be made into thin microscope sections. This was achieved by embedding tissues in paraffin, which is similar in density to tissue and can be sectioned at anywhere from 3 to 10 microns. The main steps in this process are 'dehydration', 'clearing' and 'paraffin infiltration'. Prior to tissue processing, the fixed tissues were placed into processing cassettes that were used to carry the tissues through the various stages of dehydration, clearing and paraffin infiltration. The cassettes were then loaded into a basket which was placed inside a fully enclosed Vacuum Tissue Processor (Leica TP1050, Leica UK). Automation consisted of the movement of the tissues through the various agents on a preset time scale.

Wet-fixed tissues, such as the lung samples from this study, cannot be directly infiltrated with paraffin. The water from the tissues must be removed by 'dehydration' via a series of alcohols (e.g. 70% to 95% to 100%). Following dehydration, the next step was 'clearing' and consisted of replacement of the alcohol (Fisher Scientific), with a substance that would be miscible with the paraffin. The common clearing agent was xylene and the tissues were processed through several changes of xylene (Fisher Scientific). The 'cleared' tissue was then placed into a vacuum to remove all air pockets. The final step in processing was to infiltrate the tissue with molten paraffin wax (Raymond A Lamb) at 60°C; several changes of wax were used.

3.3.3.3 PARAFFIN EMBEDDING

It was important for the tissue to be fully supported by paraffin wax to prevent the tissue shredding during sectioning. To achieve this, the lung tissue was placed into a plastic 'embedding mould', and a Leica EG1140 Embedding Centre (Leica UK) was used to surround the tissue in warm paraffin wax. After allowing the wax to set (30 minutes on a cold plate), the tissue was removed from the embedding mould and the sample was ready for sectioning.

3.3.3.4 SECTIONING

Following tissue processing and paraffin embedding, the lung tissue had to be cut into sections that could be placed on a glass slide for the purpose of LM. Sectioning was achieved using a Leica RM2135 microtome (i.e. a knife with a mechanism for advancing a paraffin block standard distances across it). The embedded lung tissue samples were placed on ice to ensure uniform sections were obtained. The ice hardens the wax and softens the tissue so the entire sample is of the same consistency for sectioning. The tissue was then cut into 5µm sections using the microtome.

Once the sections were cut, they were floated on a warm water bath (40-50°C) that facilitated the removal of wrinkles and air bubbles produced during sectioning. The paraffin embedded sections of lung tissue were then collected

onto a glass microscope slide (Raymond A Lamb). The slides used were coated in poly-L-lysine to improve adhesion of sections. The samples were then left to bind to the slides on a hot plate for 15-30 minutes, then in an oven at 37-45°C for a minimum of 24 hours.

In order to allow water soluble dyes to penetrate the sections, the embedding process must be reversed to remove the paraffin wax from the tissue. Therefore, before any staining could be done, the slides were 'dewaxed' by running them through xylene followed by a series of graded alcohols (100% to 70%).

3.3.4 HAEMATOXYLIN AND EOSIN STAIN

To evaluate the lung architecture by LM the tissue sections were stained with Haematoxylin and Eosin (H and E), a routine stain chosen for its ability to stain various cellular components of tissue. Haematoxylin is a basic dye that stains nuclear heterochromatin and cytoplasm rich in ribonucleoprotein blue. Eosin is an acid dye that stains cytoplasm, muscle and connective tissue various shades of pink.

The dewaxed tissue sections were stained with Mayer's haematoxylin (Raymond A Lamb) for 1.5 minutes. Sections were washed in running tap water for five minutes, and then stained with 1% aqueous eosin (Raymond A Lamb) for 10 minutes. This was followed by a final 20 second wash in running tap water.

The stained section on each slide was covered with a glass cover-slip (Fisher Scientific) to protect the tissue from being scratched. This also provided better optical quality for viewing under the LM and preserved the tissue section for archival purposes. The stained slides were dehydrated by reversing the dewaxing step (i.e. series of graded alcohol to xylene), at which time permanent mountant DPX (Fisher Scientific) was placed over the sections followed by a coverslip. The stained sections were then ready to view by LM.

3.3.5 *BROMODEOXYURIDINE DETECTION*

The dehydrated and dewaxed sections which had not been stained with H and E were rehydrated by washing with wash buffer (phosphate buffered saline [PBS]). The sections were then covered with an anti-BrdU primary antibody and incubated in a humidity chamber for 30 minutes at 37°C. The humidity chamber was used for all further incubations to prevent drying of the tissue samples. After further washing in PBS, the slides were incubated with an alkaline phosphatase-linked secondary antibody for 30 minutes at 37°C. The sections were washed once more (PBS) and then incubated with colour substrate solution (nitroblue tetrazolium [NBT] and 5-bromo-4-chloro-3-indolyl phosphate [BCIP]) for 1-10 minutes at room temperature. After a final wash with PBS the stained sections were mounted in Aquamount (BDH laboratory supplies), a water based fixative. The samples were then viewed via light microscopy (LM). Cells stained a blue/black colour due to alkaline phosphatase dependant precipitation of NBT/BCIP were identified as having incorporated BrdU.

3.3.6 *PROCESSING TISSUE FOR TRANSMISSION ELECTRON MICROSCOPY*

3.3.6.1 *FIXATION OF LUNG TISSUE*

The lungs were excised as detailed in Section 2.3.4. The upper right lobe of the lung was selected for examination by transmission electron microscopy (TEM). This region of the lung was chosen as it is the first lobe to be challenged by inhaled xenobiotics. The lobe was tied off from the rest of the lung and rapidly instilled with cold (4°C) glutaraldehyde (3%) fixative (Section 3.2.2). The lobe was then removed and immersed in fresh fixative for 1 hour at 4°C. This method of fixation preserves the cellular structure of the tissue by cross-linking proteins via their amine groups. The glutaraldehyde fixative was replaced with phosphate buffer and washed overnight.

Tissue processing, sectioning and staining for TEM was carried out by an electron microscopist, Mr Mike Turner, at the School of Biosciences, Cardiff University. A brief overview of these procedures has been outlined below in Sections 3.3.6.2 to 3.3.6.4.

3.3.6.2 TISSUE PROCESSING

Once the tissue had been fixed (Section 3.3.6.1), it had to be processed into a form that was suitable for TEM. This was achieved by embedding the fixed lung tissue in a resin (Araldite) that acts as a support matrix for the lung tissue. This permitted ultra-thin (e.g. 60 to 90nm) sections to be cut.

Prior to tissue processing, a piece of fixed lung tissue was excised from the lobe and cut into 1mm cubed pieces. The tissue cubes were placed into a squat glass sample vial that was used to carry the tissues through the various stages of post-fixation, dehydration and resin infiltration. The sample vials were kept on a rotating wheel inside a fume cupboard.

Post-fixation was carried out by osmicating (1% osmium tetroxide [Agar Scientific] in phosphate buffer) for 60 minutes at 4°C. The tissue was then passed through a series of graded alcohols, (30%-90%: 15 minutes in each, then 2 x 100%: 30 minutes each). Once dehydrated, the lung tissue samples were placed into new sample vials and immersed in propylene oxide (Agar scientific) for 30 minutes. This was followed by overnight rotation in a fume cupboard in a 50/50 mix of propylene oxide and Araldite CY212 (Agar Scientific). During this time the propylene oxide dissipated leaving only the Araldite. The following day the tissue was infiltrated with Araldite for eight hours.

Finally, the tissue samples were embedded in Araldite. This process involved placing one cube of tissue into a plastic embedding capsule and topping up the capsule with fresh Araldite. The capsule was then placed into a resin oven and polymerised at 60°C for 48 hours.

3.3.6.3 *SECTIONING*

Following resin polymerisation, the capsule was cut away from the resin/tissue block using a razor blade. Excess resin was trimmed from the blocks until the tissue was exposed. Semi-thin survey sections (2µm) were taken using a glass knife and mounted onto glass slides (Sigma-Aldrich), and the tissue stained with toluidine blue (Fisher Scientific). This stain helps to reveal cellular architecture. Appropriate areas for ultra-thin sectioning were identified from the semi-thin sections and the blocks trimmed accordingly. The resin blocks were sectioned to 60-90nm on an LKB 3 Ultramicrotome using a diamond knife. Sections were expanded on the water trough and collected onto clean 200-mesh, 3.05mm copper grids (Agar Scientific).

3.3.6.4 *COUNTER STAINING*

Prior to visualisation of the tissue sections via TEM, heavy metal staining or 'counter staining' was required to help resolve the ultrastructure of the lung tissue. Counter staining was achieved by using Reynold's lead citrate and 2% aqueous uranyl acetate. These heavy metal stains are general purpose and not very specific. Uranyl acetate stains membranous structures and structures containing nucleic acids. The lead in lead citrate binds to RNA-containing structures and hydroxyl groups of carbohydrates.

Droplets of each stain were placed in rows on the sterile side of parafilm and the grids were floated section side down on a given drop. Sections were stained for 10 minutes with uranyl acetate, followed by staining with Reynolds lead citrate for five minutes. Finally, the grids were washed by transferring over three drops of filtered de-ionised water. The grids were allowed to air dry at room temperature in filter paper-lined Petri dishes prior to viewing in the TEM. The sections were imaged using a JEOL 1210 TEM at an acceleration voltage of 80 keV.

3.4 RESULTS

3.4.1 BROMODEOXYURIDINE DETECTION OF CELL PROLIFERATION

Proliferating cells labelled with bromodeoxyuridine (BrdU) were identified as having a dark blue/black colouration. These labelled cells were counted manually under a light microscope. The difference in number, location and type of proliferating cells was studied three and seven days after exposure to bleomycin. These were compared to appropriately treated saline-instilled tissue from control animals.

The initial optimisation studies were carried out using the *in vivo* treated sections. The colour differential between the labelled and unlabelled cells was greatly affected by the length of incubation with the colour substrate. The recommended length of time was 15 to 30 minutes exposure. To get an indication of how rapidly the samples would take up the stain, an initial incubation of 20 minutes was carried out. This proved to be too long, and the tissue was over stained. A series of time points were covered in the second study including one, two, five, seven and ten minutes (results not shown). Up to five minutes exposure to the colour substrate resulted in under staining. Incubation for seven and ten minutes generated the clearest results, with ten minutes fractionally better. Only those exposed for ten minutes are shown in Figure 3.2.

As well as monitoring the level of cellular proliferation, these preliminary *in vivo* studies also investigated the effectiveness of the different modes of BrdU administration. The length of time after intratracheal administration of BrdU had a large effect on the amount of BrdU signal that was observed. The amount of BrdU detected was lower in the samples that were sacrificed after 24 hours (results not shown). The tissue sections shown in Figure 3.2 were sacrificed five hours after BrdU instillation and 24 hours after intraperitoneal injection.

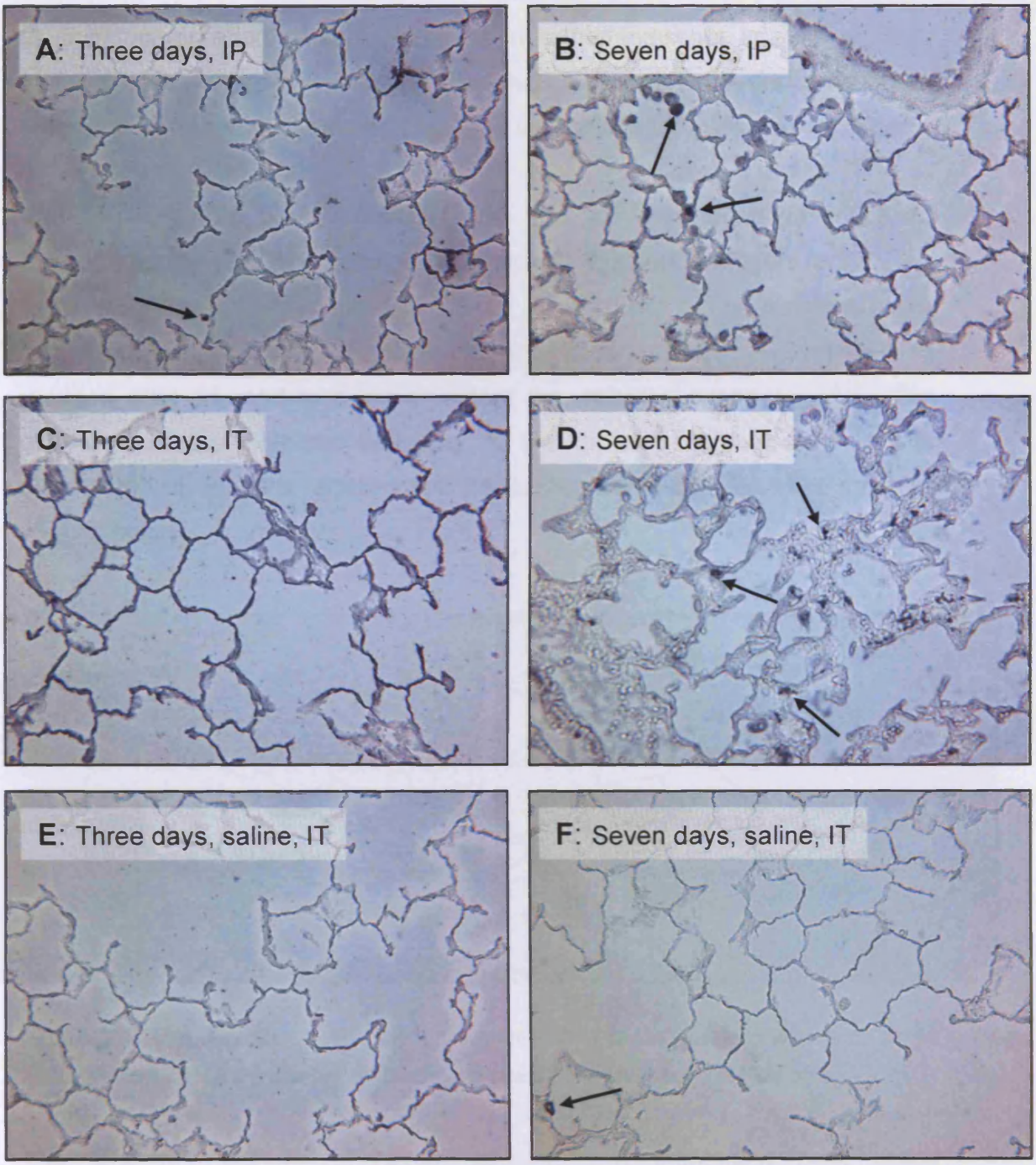

Figure 3.2 *Lung sections treated with saline or bleomycin. Labelled in vivo with BrdU (x160 magnification). A: three days after bleomycin treatment, BrdU administered intraperitoneally (IP); B: seven days after bleomycin treatment, BrdU administered via IP; C: three days after bleomycin treatment, BrdU administered intratracheally (IT); D: seven days after bleomycin treatment, BrdU administered via IT; E: three days after saline treatment, BrdU administered via IT; F: seven days after saline treatment, BrdU administered via IT. Arrows show labelled cells.*

In vivo incorporation of BrdU resulted in rather indistinct images of BrdU labelled cells. Despite incubating with the colour substrate for a variety of times, the differentiation between labelled and unlabelled cells was not clear.

The *in vivo* data was compared with the *ex vivo* technique of BrdU incorporation seven days after treatment with bleomycin (Figure 3.3). The initial study was carried out with three time points. The sections were incubated with the stain for five, ten and fifteen minutes. Over-staining resulted after 15, and to a lesser extent ten, minutes exposure. After five minutes exposure clearer definition of the labelled cells is seen. The distinction between the labelled and unlabelled cells was clearer with the *ex vivo* technique.

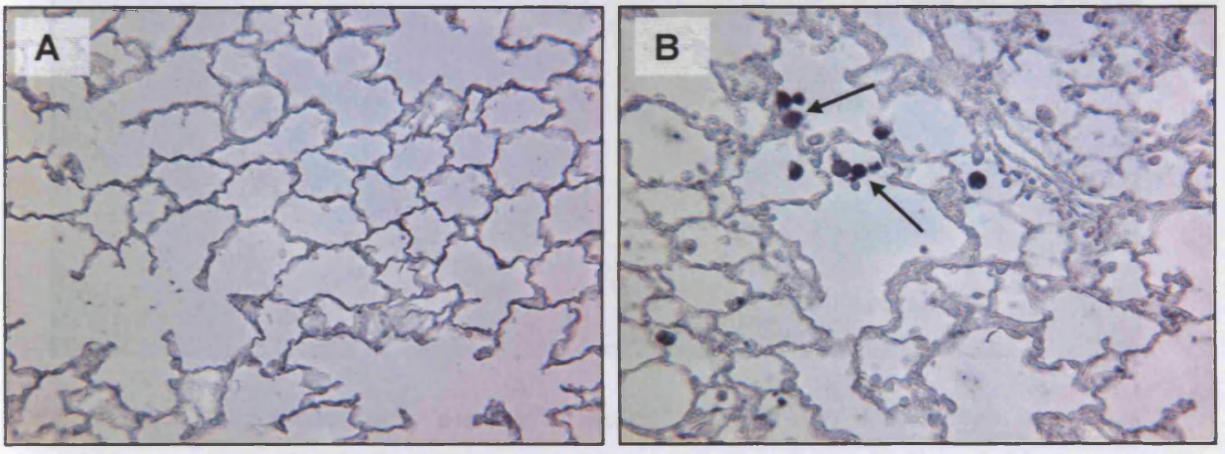

Figure 3.3 *Lung sections seven days post-treatment. Labelled ex vivo with BrdU (x160 magnification). A: Saline treated; B: Bleomycin treated. Arrows show labelled cells.*

The lack of distinction between labelled and unlabelled cells made quantification of the data very difficult. However, it appeared that seven days after bleomycin-treatment there were approximately four times more labelled cells than in saline-treated tissue. It should also be noted that a number of free cells located in the airspaces seemed to be incorporating BrdU.

3.4.2 HAEMATOXYLIN AND EOSIN VISUALISATION OF TISSUE

Haematoxylin and eosin staining was carried out on tissue sections from every time point. This was done as visual confirmation to the basic toxicology described in Chapter 2. The results are shown in Figure 3.4 and 3.5.

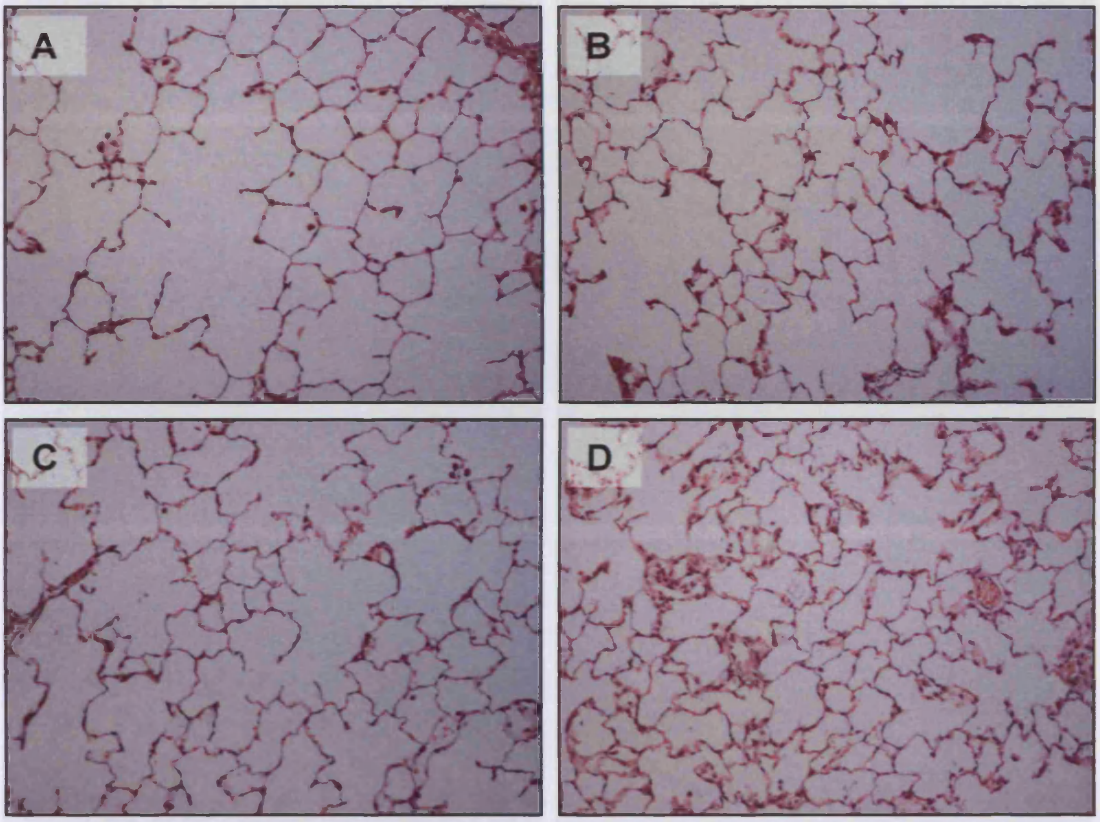

Figure 3.4 *Lung sections after a single instillation. Stained with Haematoxylin and Eosin (x100 magnification). A: three days post-saline instillation; B: three days post-bleomycin instillation; C: seven days post-saline instillation; D: seven days post-bleomycin instillation.*

After a single instillation the alveolar structure was normal in both the control samples. There was no evidence of interstitial thickening or septal swelling and the airspaces were all clear. However, by day three after a single bleomycin dose (Figure 3.4 B) there was widespread thickening of the interstitium and some swelling of the septa. By day seven (Figure 3.4 D) this damage was more extensive and there was also evidence of some cellular infiltrate and inflammatory cells.

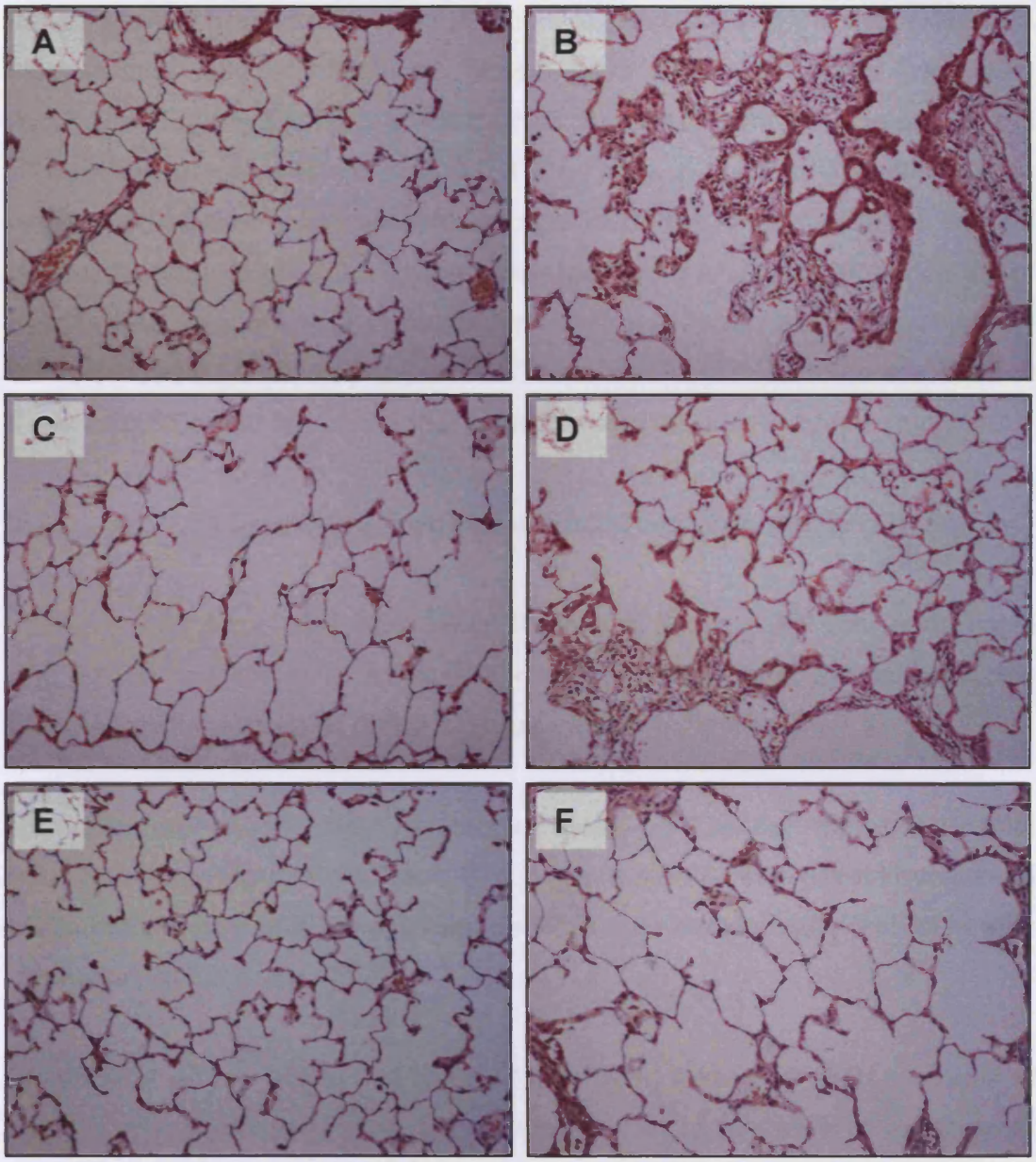

Figure 3.5 *Lung sections after a double instillation. Stained with Haematoxylin and Eosin (x100 magnification). A: three days after second saline instillation; B: three days after second bleomycin instillation; C: seven days after second saline instillation; D: seven days after second bleomycin instillation; E: 21 days after second saline instillation; F: 21 days after second bleomycin instillation.*

After a double saline instillation (Figures 3.5 A, C, E) there were small areas of interstitial and septal thickening, but generally the alveolar structure was normal. However, three days after a double bleomycin dose (Figure 3.5 B) there were huge changes to the tissue. The alveolar interstitium was greatly thickened and the septa were swollen. Large amounts of cellular infiltrate and

debris were in the airspaces. In addition, large regions of the tissue showed disorganised lung architecture. Seven days after the second bleomycin instillation (Figure 3.5 D) the effects had lessened, although there was still widespread damage to the tissue. There were a number of focal regions where the tissue structure was still disorganised. By 21 days after the second bleomycin dose (Figure 3.5 F) the tissue was still showing some evidence of injury. The interstitium and septa remained swollen in several areas, and some cellular infiltrate was observed. There also continued to be evidence of a few small focal areas where the tissue showed disorganised structure.

3.4.3 Transmission Electron Microscopic Analysis of Tissue

Tissue sections for TEM were taken three and seven days after both single and double instillations of bleomycin and three weeks after the double dose. Representative examples of the data are shown in Figures 3.6-3.8.

Parenchymal tissue after a single dose of saline showed normal microstructure (Figures 3.6 A and B, 3.7 A and 3.8 A). There were occasional blebs in the type I cells (intracellular oedema) and some small areas of fibrous deposition in the septa.

Three days after a single instillation of bleomycin there was clear evidence of cytoplasmic blebbing (Figure 3.6 C) resulting in focal areas of intracellular oedema. The capillary endothelium and type I cells showed regions containing elevated numbers of caveolae (plasmalemmal vesicles) (Figure 3.6 C). There were also focal areas where some build-up of fibres could be seen. The septa all showed signs of damage, with thickening of the interstitium and fibrous deposition at the ends (Figure 3.7 B). After seven days the damage was more widespread. There were larger areas where fibres had accumulated, and the continuing presence of membrane blebbing and caveolae. Some macrophages (Figure 3.7 C) and inflammatory cells were present in the alveolar airspaces. At both time points a number of flattened type II cells were observed (Figure 3.8 B).

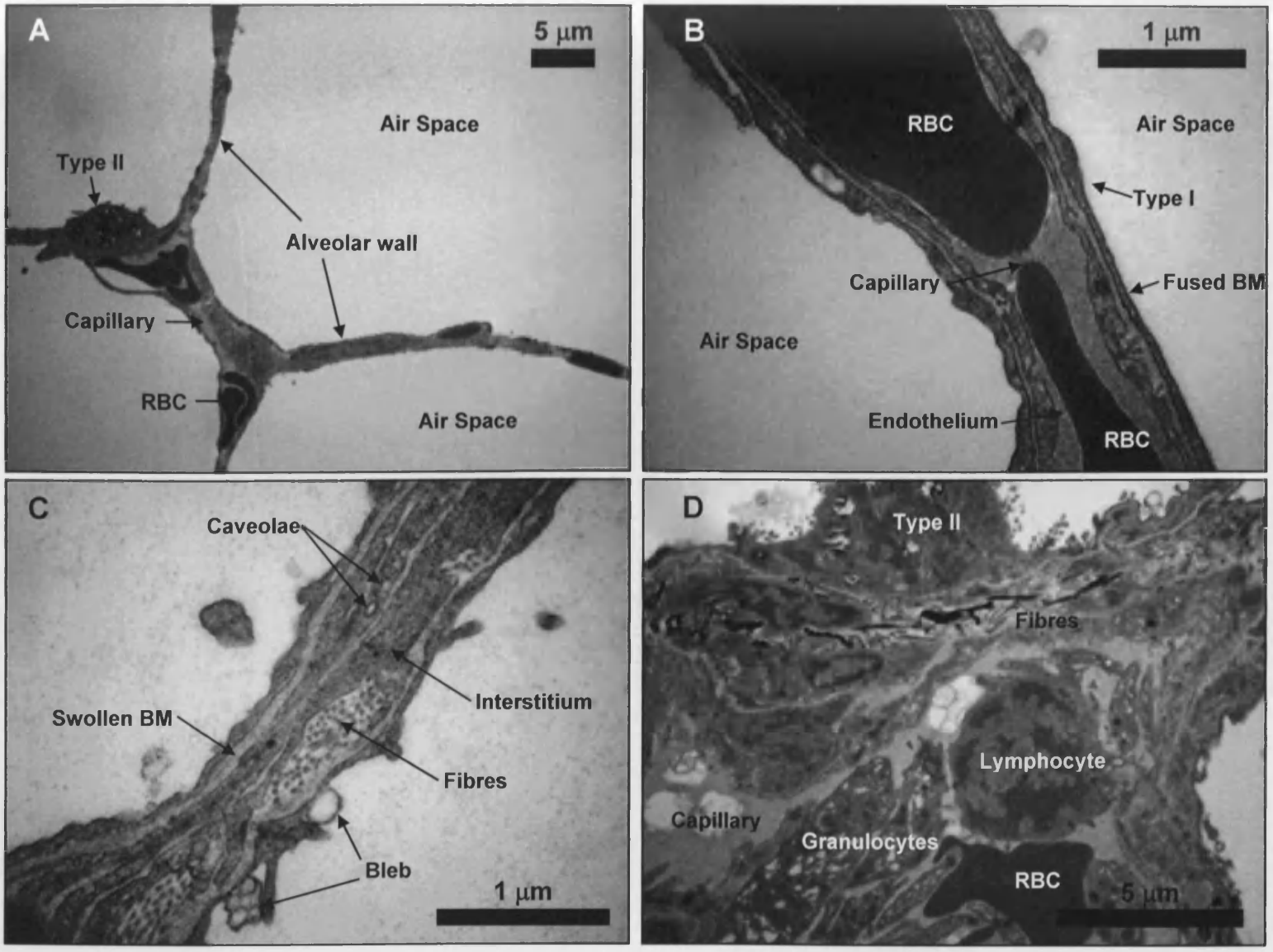

Figure 3.6 *TEM images showing normal (A & B) and damaged (C & D) tissue. A: Alveoli showing thin walls and clear airspaces; B: Alveolar wall showing normal epithelium and endothelium, and a fused basement membrane; C: Alveolar wall showing signs of early damage including thickened interstitium, blebbing and caveolae; D: Alveolar wall showing signs of severe damage including accumulation of fibres, cellular influx and disorganised architecture.*

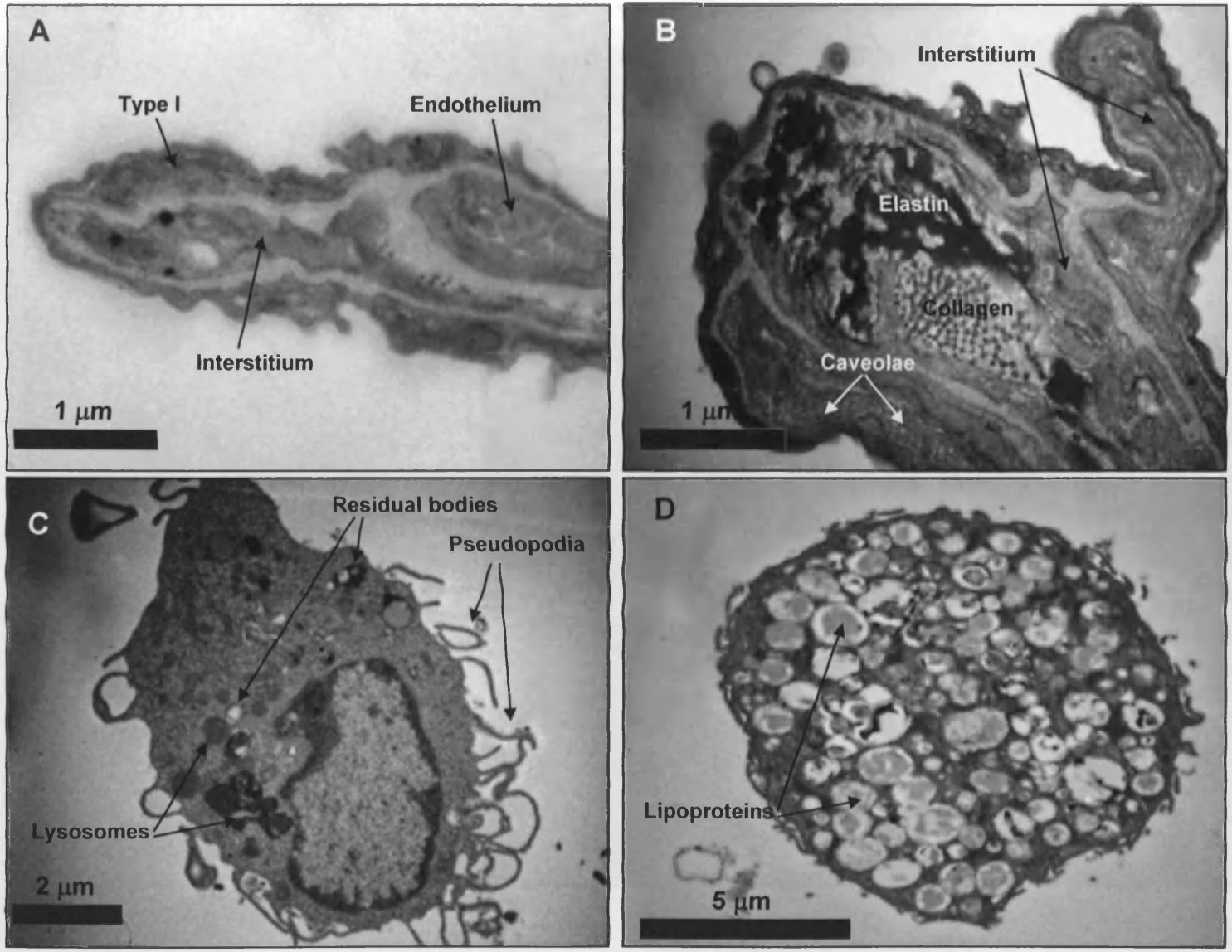

Figure 3.7 *TEM images showing A: Normal septa; B: Damaged septa showing thickened interstitium, fibrous deposits and caveolae; C: Normal macrophage; and D: Foamy macrophage.*

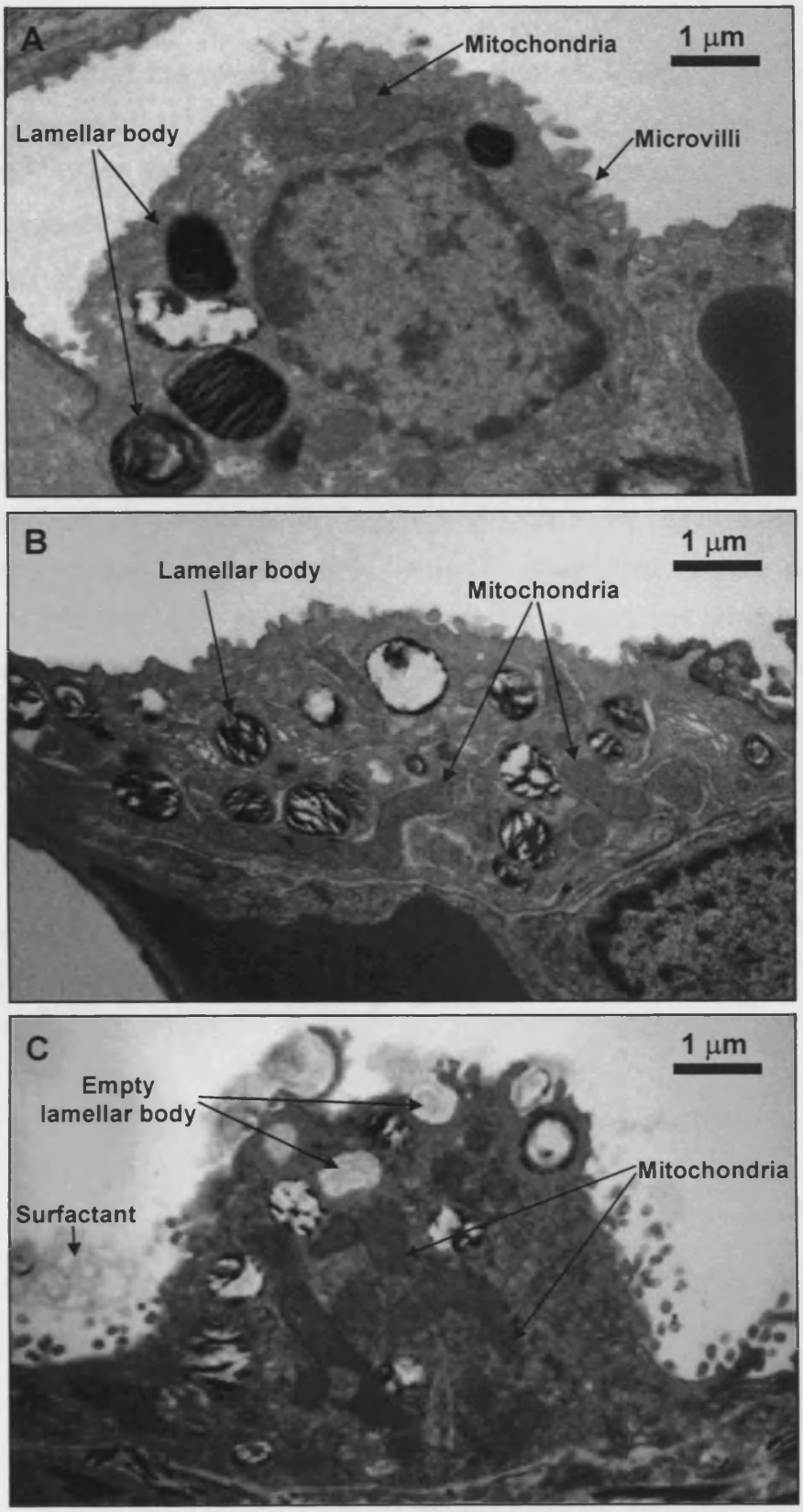

Figure 3.8 *Type II pneumocytes at different stages of repair. A: Normal type II after saline instillation; B: Flattened type II after bleomycin instillation; C: Cuboidal type II after bleomycin instillation.*

After the second bleomycin instillation, heightened blebbing and caveolae activity was noted. Three days after the second dose, widespread thickening of the interstitium and increased fibre deposition had occurred. Large regions of the tissue showed completely disorganised architecture, as well as an influx of inflammatory cells (Figure 3.6 D). There was also the appearance of several cuboidal type II cells (Figure 3.8 C) and a number of flattened type II cells with empty lamellar bodies (Figure 3.8 B). By seven days this level of injury had reduced, but a great deal of disorganisation and inflammatory cells still persisted. At this time point the first foamy macrophages were observed (Figure 3.7 D). A number of flattened type II cells could still be seen, with an increasing number of cuboidal cells. After 21 days (post second instillation) the injury had markedly reduced. However, there were still large areas with thickened interstitium and accumulation of fibres. Debris could be seen in the airspaces along with a number of foamy macrophages. Cuboidal and flattened type II cells were regularly observed.

3.5 DISCUSSION

Histological examination was employed to investigate morphological or structural changes in the lung, induced by bleomycin. In conjunction with this, immunohistochemical assays were carried out to assess the re-epithelialisation of the tissue in response to injury. Both light and electron microscopy were used during this investigation.

Immunohistochemical analysis of tissue sections was carried out to determine the number and type of cells involved in repopulating the damaged tissue. The techniques required to obtain consistent uptake and identification of BrdU-labelled cells were optimised. This was partially successful, although clearer images may have been achieved by counter staining the sections with haematoxylin (Quinlan *et al.,* 1995). After the initial *in vivo* studies, it was considered that perhaps the BrdU was not reaching the target cells. A second possibility was that the cells were successfully targeted, but the period of time allowed for BrdU incorporation was too great. This would result in dispersion of the BrdU as the cells continued to replicate. To overcome these possibilities an *ex vivo* labelling technique (Section 3.3.2.2) was applied. In this way, the BrdU was delivered directly onto the tissue to be studied, ensuring the target cells were reached. This enabled a shorter incubation period, which reduced the opportunity for continued proliferation resulting in dissipation of BrdU. *Ex vivo* was also preferable as it removed the need to give a second treatment to the rat.

An objective analysis of BrdU incorporation showed that there were approximately four times more proliferating cells in bleomycin treated lungs in comparison to saline treated lungs after seven days (Section 3.4.1). However, after three days of exposure to bleomycin no difference was observed. This is in agreement with the thymidine uptake assay (Section 2.4.2) and supports the premise that, although some repair of the damaged tissue was occurring after one week, at three days the repair process had not yet begun. A number of free cells also appeared to be labelled. This could be

due to their recent recruitment into the lung, and continued differentiation into their final cellular structure.

The information gained from these experiments was difficult to obtain, and the images were not sufficiently clear for the studies to be continued on the remaining time points.

The toxicology results (Chapter 2) were supported by the histological data. Three days after a single bleomycin instillation the lung tissue was showing signs of focal damage. Injury progressively worsened up to seven days after dosing, with more widespread damage and some cellular infiltrate and oedematous fluid in the alveolar airspaces. This clearly represented interstitial damage progressing onto focal areas of intra-alveolar oedema after a single bleomycin instillation. However, unlike the toxicology data, which showed no marked increase in the levels of protein or free cells, following the second dose of bleomycin the effect on the lung pathology was markedly worse. This disparity between the toxicology data and the information observed here could be due to the failure of the lungs to lavage properly before toxicological analysis. Three days after the second instillation, cellular infiltrate, oedema fluid and interstitial and septal swelling was observed throughout the tissue. There were also large areas of the sections which showed complete destruction of the normal architecture of the lung. These effects were reduced seven days after treatment, but there were still focal areas of disorganised tissue architecture. These features indicated that severe interstitial and intra-alveolar oedema was occurring. Three weeks after the second bleomycin dose the tissue was still showing evidence of injury. There continued to be some interstitial and septal swelling, although the cellular infiltrate was no longer apparent. There also remained some very small regions of tissue where the disorganised structure had not been fully restored. This confirmed the toxicology data, that after 21 days, the tissue was still not fully repaired, and had not returned to its normal state.

To study the ultrastructure of the damaged tissue, TEM was used. The resulting images clearly demonstrated that oedema and inflammation was

occurring in the bleomycin treated tissue. Evidence of repair and re-epithelialisation was also observed.

The earliest indicator for increased permeability in the lung was the formation of membrane blebs in the plasma membrane of type I epithelial cells. These blebs filled with intracellular fluid which was eventually released onto the lung surface. This corresponded with an increased number of caveolae (pinocytotic vesicles) in the endothelium and type I cells. This produced rapid transfer of plasma products and fluid to the alveolar surface. It also led to deposition of fibres (collagen and elastin) in the interstitium as injury progressed. One of the more severe indicators of oedema was the disruption of normal tissue architecture. There was a lack of recognisable features, with the tissue being filled with the debris of dead cells, plasma products and inflammatory cells, making it difficult to identify the types of cell within the interstitium.

The TEM observations suggested that during the early stages of repair in the lung, the damaged type I epithelium were replaced by cells from the type II population. The type II cells became flattened and gradually lost their lamellar bodies. These cells appeared to develop into type I-like cells to restore the normal lung architecture. During persistent injury (as seen with the double dose model) re-epithelialisation was extensive. This resulted in the formation of cuboidal type II cells which produced a thickened epithelial layer. These cells actively made surfactant by releasing the lamellar bodies onto the surface of the lung. This led to lipoproteinosis, as surfactant accumulated in the alveolar airspaces. A good indicator of lipoproteinosis was the presence of 'foamy' macrophages in the airspaces.

There were numerous flattened type II cells in all bleomycin treated samples. A small number were also detected after saline treatment, from seven days onwards. Several cuboidal cells and foamy macrophages were observed seven and 21 days after bleomycin treatment. This signified that both acute and chronic repair mechanisms were functioning.

3.6 CONCLUSIONS

This information on the pathology of the lung increased understanding of the oedema model, and combined with the toxicological data, enabled the progressive severity of injury at each time point to be determined (Figure 3.9).

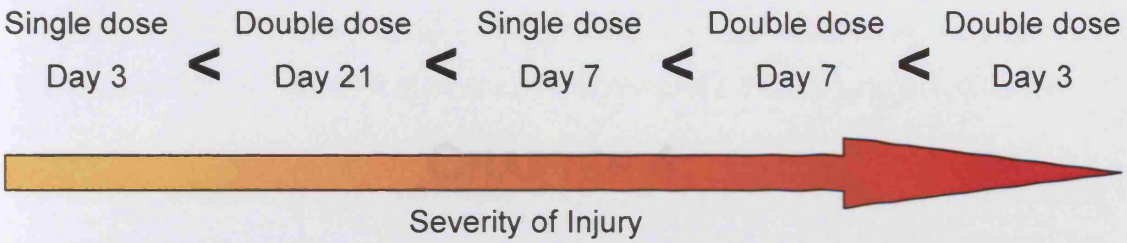

Figure 3.9 *The progressive levels of injury within the bleomycin model as determined by conventional toxicology, histology and TEM.*

One of the main objectives of this study was to identify early genetic markers for oedema. As such, three and seven days after a single bleomycin dose were chosen for genetic analysis. These samples provided the opportunity to study both the development of injury and mild oedema whilst allowing some insight into the repair mechanisms. Moreover, a comparison between mild (early) and severe oedema could aid the understanding of the mechanisms behind the onset of oedema, so three days after a second bleomycin dose was also selected (Chapter 4).

CHAPTER 4:

ANALYSIS OF TRANSCRIPTIONAL CHANGES IN EARLY OEDEMA AND INFLAMMATION

4.1 INTRODUCTION

The primary objective of this study was to investigate differential gene expression at the transcriptional level during the development of pulmonary oedema and inflammation. A model for bleomycin-induced injury to rat lung was previously characterised using conventional toxicology (Chapter 2) and histology (Chapter 3). Experiments were designed to identify early molecular markers for events in pulmonary injury. As such, this initial study was carried out in tissue taken at the first time point, three days after a single instillation.

In order to examine global gene expression in lung tissue, macroarray technology was applied. This allows the expression of multiple mRNAs to be examined. Clontech Atlas rat cDNA expression macroarrays were used for this study. This system was chosen because it is readily available and offers reproducibility to a range of laboratories at relatively low cost. It had also proven successful in previous investigations of toxicant effects in the lung (Reynolds and Richards, 2001). The Clontech arrays are composed of hundreds of cDNAs spotted onto a positively charged nylon membrane. Plasmid and bacteriophage DNAs are included as negative controls and to confirm hybridisation specificity. Several housekeeping genes are also incorporated as positive controls. Atlas arrays specifically include genes that are known to play key roles in many biological functions. Targeted primers specific to each type of array are used to generate radiolabelled cDNA. The probes are hybridised to the oligonucleotides on the array and detected by phosphorimager screens.

Optimisation of the macroarray procedure for lung tissue was undertaken. The validity of information obtained from an array is dictated by the yield and purity of isolated RNA. Techniques for isolation of RNA were refined and developed to meet these requirements. Purification of the labelled probe and hybridisation of this probe to the membrane was also investigated. Finally, the differential gene expression detected by these new macroarray techniques was confirmed by quantitative polymerase chain reaction (Q-PCR)

for a selection of genes. The optimised procedures were applied to oedematous lung tissue isolated from rats three days after bleomycin treatment versus saline controls.

There are currently no well established techniques for bioinformatic analysis of macroarray data (Mocellin *et al.*, 2004). One of the main objectives of this study was to develop a simplistic method for interpreting the large volume of data generated by macroarrays.

4.2 MATERIALS

4.2.1 MATERIALS AND SUPPLIERS

Supplier:	Materials:
Qiagen, West Sussex	RNeasy Mini Kit (74104) (containing all appropriate buffers and solutions) QIAshredders (79654) RNase-Free DNase Set (79254) (containing DNase I and appropriate buffer) QuantiTect SYBR Green PCR Kit (204143)
BDH, Dorset	β-Mercaptoethanol (436022 A)
Clontech, Oxford	Atlas™ Rat 1.2 Array System (7854-1) (containing all required solutions and preparations) Advantage 2 PCR Kit (30 rxns) (639207)
Sigma-Aldrich, Dorset	Agarose (Type 1A)(A0169) 10x TBE* (T4415) Ethidium Bromide (10 mg/ml) (E1510) Loading Dye (G2526) **Diluted to 1x TBE in distilled water, prior to use* Tri-reagent™ (T9424) Salmon Testes DNA (9.5 mg/ml) (D7656) GenElute™ Agarose Spin Columns
Amersham, Buckinghamshire	[α-^{32}P]dATP (10 µCi/mmol) (PB 10204) Storage Phosphor Screen (63-0034-89)
Invitrogen, Paisley	Random Primers (48190-011)

Supplier:	**Materials:**
Promega, Southampton	MMLV-RT
	5x Reaction Buffer (M1701)
	dNTPs (U120-123)
	RNase Inhibitor (RNasin, N251)
	E.coli JM109 Competent Cells, >10^8cfu/µg (L2001)
	pGEM®-T Vector System I (A3600)
	Wizard® *Plus* SV Minipreps DNA Purification System (A1340)
ABgene, Surrey	Thermo-fast® 96 Detection Plates (AB-1100)
	Ultra Clear Cap Strips (AB-0866)
Sigma-Genosys, Suffolk	Primer Sequences for PCR:

Primer name		Primer sequence		Fragment length
D50497	Forward	TGGCAGACGCTCTTGGGCGAGAG	23 (bases)	227
	Reverse	CACCACCGGAAAGCCGCTGTACG	23 (bases)	
Z11690	Forward	CGCCGCTCGCGCCTCATGATC	21 (bases)	190
	Reverse	CGAAGACACCGCTGGTCATCCAG	23 (bases)	
L31622	Forward	GAAGTTTCGCTCATGGACCTACGAC	25 (bases)	192
	Reverse	AGTGGTTTGCGACGAATGATGAAGTC	26 (bases)	
X15467	Forward	TGAGAACATCTTACTCAGCACTCTTGAG	28 (bases)	264
	Reverse	CGATCAATGGCGTTCACATCAGTCAAG	27 (bases)	
U37101	Forward	AGCTGCTGCTGTGGCACAGTGCAC	24 (bases)	297
	Reverse	GCAGTTGGCTCAGGCACTTTGTCTG	25 (bases)	
V01217	Forward	CCCTCTGAACCCTAAGGCCAACCG	24 (bases)	285
	Reverse	GTGGTGGTGAAGCTGTAGCCACGC	24 (bases)	

Table 4.1 *Oligonucleotide (desalted) primer sequences for PCR*

Supplier:	**Software:**
Clontech, Oxford	AtlasImage 2.0 Atlas Navigator™ 1.0 (Silicon Genetics)
Microsoft, USA	Excel 2003
Minitab Ltd, Coventry	Minitab (version 13.32)
Spotfire AB, Göteborg, Sweden	Spotfire Pro 3 for Windows (version 3.3.4)

4.2.2 STOCK SOLUTIONS

4.2.2.1 MACROARRAY

10x denaturing solution	1 M Sodium Hydroxide 10 mM EDTA
2x neutralising solution	1 M Sodium Hydrogen Phosphate (pH 7.0) (Store at room temperature)
Wash Solution 1	2x SSC 1% SDS (Store at room temperature)
Wash Solution 2	0.1x SSC 0.5% SDS (Store at room temperature)

Array Master Mix:

	1 reaction (rxn)	Double rxn*
5x Reaction Buffer *(250 mM Tris-HCl [pH 8.3], 375 mM KCl, 15 mM $MgCl_2$)*	2.0	4.0
10x dNTP Mix *(5 mM each dCTP, dGTP, dTTP)*	1.0	2.0
^{32}P dATP	3.5	5.0
DTT (Dithiothreitol) (100mM)	0.5	1.0
Total Volume(µl):	7.0	12.0
Total required per array (inc. MMLV-RT**) (µl)	8.0	13.0

Table 4.2 *Preparation of Master Mix solution (macroarray procedure detailed in Section 4.3.2). All volumes in µl.*

**Double rxn mix is prepared if 2 µg isolated RNA is in a volume of water greater than 2 µl.*

***1 µl Moloney Murine Leukaemia Virus Reverse Transcriptase (MMLV-RT) added per reaction after incubation.*

4.2.2.2 QUANTITATIVE PCR

Reverse Transcription (RT) reaction mix:

	1 rxn
MMLV-RT (200 units/µl)	2.0
5x Reaction Buffer	6.0
Random Hexamer (100 pmol/µl)	0.5
dNTPs (10mM)	1.5
RNase Inhibitor (RNasin, 40 units/µl)	1.0
Total	11.0

Table 4.3 *Preparation for the reaction mix (RT procedure carried out in Section 4.3.9.1). One reaction generates 30µl cDNA. All volumes in µl.*

PCR reaction mix:

	50 µl rxn	20 µl rxn
cDNA	2	0.8
10x Reaction Buffer	5	2.0
dNTPs (50x)	1	0.4
Primer 1	1	0.4
Primer 2	1	0.4
Polymerase Mix (Taq, $MgCl_2$)	1	0.4
PCR Grade Water	39	15.6
Total	50	20.0

Table 4.4 *Preparation for the PCR mix used in Section 4.3.9.1. All volumes in µl.*

Ligation master mix:

	1 rxn
PCR Product	3
2x Ligation Buffer	5
pGEM-T Vector (50ng)	1
T4 DNA Ligase	1
Total	10

Table 4.5 *Preparation for the ligation mix used in Section 4.3.9.2. All volumes in µl.*

SYBR Green PCR master mix

	50 µl rxn	20 µl rxn
Plasmid DNA	1	0.4
2x SYBR Green PCR Master Mix	25	10.0
Primer 1	1	0.4
Primer 2	1	0.4
PCR Grade Water	22	8.8
Total	50	20.0

Table 4.6 *Preparation for the SYBR green PCR master mix used in Section 4.3.9.7. All volumes in µl.*

4.3 METHODS

4.3.1 RNA EXTRACTION AND PREPARATION

4.3.1.1 RNA ISOLATION USING TRI-REAGENT™ PROTOCOL

RNA from whole lung tissue was isolated using Tri-reagent™ (Sigma-Aldrich) as outlined in the Sigma Technical Bulletin (Sigma-molecular-biology, 1994). This is a single step, liquid phase separation procedure, which allows the simultaneous extraction of RNA, DNA and protein. The technique is based on an extraction outlined by Chomczynski and Sacchi (1987) and works well on large or small amounts of starting material.

Briefly, whole lung tissue isolated from the rat was snap frozen in liquid nitrogen and ground to a fine powder using a pestle and mortar. The cells were then lysed in Tri-reagent™, a mono-phase solution of guanidine thiocyanate and phenol, by mixing thoroughly with a pipette to form a homogenous lysate. All insoluble material and high molecular weight DNA was removed by centrifugation (12,000 x *g*). After the addition of chloroform, the solution was mixed thoroughly and then centrifuged (12,000 x *g*). This resulted in the separation of the solution into three layers, a red organic phase (protein), an interphase (DNA) and colourless upper aqueous phase (RNA). The aqueous layer was carefully removed and an equal volume of isopropanol added. After centrifugation (12,000 x *g*) the RNA precipitate formed a pellet. The pellet was washed in ethanol, then reformed by centrifugation (12,000 x *g*). The pellet was air dried to remove all residual ethanol before being resuspended in RNase/DNase-free water (20-30µl).

4.3.1.2 RNA ISOLATION USING RNEASY KIT

The RNeasy Mini kit (Qiagen) was used to isolate total cellular RNA from rat lung tissue. Under high salt conditions, long RNA molecules are bound to a silica gel based membrane. Once bound, the RNA was washed and eluted utilising microspin technology. The purified RNA could then be used in a

number of molecular biology techniques (RNeasy manual, 2001). This technique can be applied to extract RNA from a small amount of starting material. All the buffers used (Buffer RLT, RPE and RW-1) were supplied in the kit.

The lung tissue from saline and bleomycin-treated rats was snap frozen in liquid nitrogen and stored at -80°C to prevent any initial degradation of the RNA. The frozen tissue sample was powdered in liquid nitrogen with a pestle and mortar, and then lysed in RLT Buffer (contains guanidine isothiocyanate). The sample was homogenised by passing the lysate (several times) through a 20-gauge needle fitted to a syringe, followed by centrifugation (>8,000 x *g*, two minutes) in a QIAshredder column. This reduces the viscosity of the lysates, increasing the efficiency of RNA for binding to the RNeasy membrane. Ethanol was added to promote selective binding of the RNA to the membrane. The entire sample was loaded in successive aliquots onto the RNeasy mini column and centrifuged in a bench top centrifuge (>8,000 x *g*, 15 seconds, room temperature). The eluant was discarded and the column washed with wash buffers provided in the kit, (RW-1 and RPE buffer) in order to remove all contaminants. The column was centrifuged in a fresh collecting tube to eliminate any residual traces of ethanol from the RPE buffer, which would contaminate the purified RNA. The RNA was eluted from the RNeasy column into a sterile eppendorf with RNase/DNase-free water (30µl).

4.3.1.3 DNase Treatment of the RNA

The RNase-Free DNase Set (Qiagen) was used to treat the RNA to ensure there were no DNA contaminants in the sample. The kit provides on-column digestion of DNA during RNA purification. RNA is treated with DNase I while bound to the silica-gel membrane. The DNase is then removed in subsequent wash steps. The removal of contaminants from the RNA is particularly important for obtaining reproducible results with the Atlas macroarrays. Poor quality RNA can result in a high background on the membrane, and/or an inaccurate hybridisation pattern. The procedure is detailed in the RNeasy Mini Handbook (Qiagen, 2001).

The lysis, homogenisation and loading into the RNeasy mini column were carried out as indicated in Section 4.3.1.2. DNase I was diluted in Buffer RDD (both provided in the kit) and mixed gently to avoid denaturation of the DNase. After washing the column with a reduced volume of RW1 buffer, DNase I solution was applied to the column and incubated for 25 minutes. The DNase I was then removed by a second wash with Buffer RW1. Washing with RPE buffer and elution was then performed as described in Section 4.3.1.2.

4.3.1.4 Quantifying the RNA Isolate

The purity and yield of all RNA samples were assessed regardless of extraction procedure using the GeneQuant™ (Pharmacia). Purity was established by measuring the 260:280nm absorption ratio. A ratio of 2.0 was indicative of a very pure RNA sample (GeneQuant RNA/DNA Calculator User Manual). However, a ratio of over 1.8 was considered acceptable for subsequent gene analysis. Lower ratios can indicate contamination in the sample. The yield of the sample was deduced from the absorbency of the sample at a wavelength of 260nm.

4.3.1.5 Checking Integrity of RNA: Running an Agarose Gel

A sample of the RNA (1-2µg) was run on a 1% Agarose gel (0.5g in 50ml 1x TBE with 3µl of 10mg/ml Ethidium bromide). Each well was loaded with 1-2µg RNA, 2µl loading dye, and made up to a total of 10µl in high purity RNase/DNase free water. The gel was electrophoresed (approximately 40 minutes, 90 volts) and viewed under UV using the Syngene™ Gel doc System.

4.3.2 MACROARRAYS

4.3.2.1 PREPARATION OF THE MEMBRANES

The macroarray membranes (Clontech) were washed with deionised water and placed in individual hybaid bottles. Hybridisation solution (minimum 5ml per membrane) was pre-warmed to 68°C and added to the hybaid bottles containing the membranes. Heat denatured salmon testes DNA (0.5mg/membrane) was added to the hybridisation solution in the hybaid bottles and the membranes were left to prehybridise. Prehybridisation took place at 68°C for at least 30 minutes, with rotation to ensure the solution was evenly distributed across the membrane.

4.3.2.2 PREPARATION OF ^{32}P-LABELLED FIRST STRAND cDNA PROBE

Isolated RNA (2µg), free from genomic contamination, was mixed with 10x CDS primer mix (1µl). The master mix stock (Table 4.2) and the RNA/primers were heated to 70°C. The solutions were cooled to 48°C and MMLV reverse transcriptase was added to the master mix (MMLV-RT is denatured above 48°C). The master mix containing MMLV-RT was added to each RNA sample and then immediately heated at 48°C for 25 minutes to allow cDNA synthesis. The reaction was terminated using 10x termination mix and placed on ice.

Labelled cDNA probe was purified from unincorporated ^{32}P-labelled nuclides and small cDNA fragments by column chromatography. The Atlas NucleoSpin® Extraction Kit was used for purification. This kit incorporates small-scale column chromatography and centrifugation to give quick, reproducible separation of labelled probe from contaminants. The probe was eluted in a low-salt buffer and the radioactivity checked with a Geiger counter. Denaturing solution (10x) was added and the solution placed at 68°C for 20 minutes to allow full denaturation of the cDNA probe. C_0t-1 DNA and 2x neutralisation solution were added and placed at 68°C for a further 10 minutes.

4.3.2.3 *Hybridisation of the Probe to the Array*

The denatured, radiolabelled probe was added into the prehybridisation solution to avoid getting concentrated probe on the membrane. The membrane was then hybridised overnight (68°C) with continuous agitation. The membranes were subsequently washed until the radioactive counts dropped to 10-20 counts per minute (cpm). Wash solution 2 (Section 4.2.2.1) was used for a very stringent wash, or wash solution 1 for a less stringent wash. Wash solution 1 was used initially to determine the level of washing required. Then wash solution 1 or 2 was used as necessary. The membrane was removed, wrapped well to prevent drying, and placed under a phosphorimager screen (Amersham) within a cassette and left (room temperature) for two to seven days depending on the final radioactivity on the membrane.

4.3.2.4 *Processing the Phosphorimager Screen*

The exposed phosphorimager screen was scanned (50 micrometer resolution) and the resultant image analysed using the AtlasImage 2.0 (Clontech) computer software. This generated a report that was saved as a Microsoft Excel file and used for further analysis.

4.3.2.5 *Stripping the Membranes*

The cDNA probe was stripped from the membrane prior to storage at -20°C. The membranes were boiled vigorously in 0.5% SDS solution (5-10 minutes) and rinsed in wash solution 1. The membrane was checked for radioactivity (cpm<5) before sealing in a bag for storage at -20°C. The phosphorimager screen was cleaned by exposure to bright light (15 minutes) and stored at room temperature until required.

4.3.3 *Expression Analysis of Whole Lung Tissue*

RNA was isolated, using the RNeasy Mini kit (Qiagen) (Section 4.3.1.2) from whole lung tissue. Rat lung tissue was obtained from animals sacrificed three days post intratracheal instillation. On day 0, sham control animals received 0.5ml of 0.15M saline, and experimental animals received 0.5 units bleomycin (Bleo-kyowa) in 0.5ml saline. Animals (n=9) were assessed by conventional toxicology for oedema (Chapter 2) and used for genetic analysis. Saline treated animals (n=9) were studied for comparison.

4.3.4 *Data Normalisation*

The information on all 18 rats (n=9 saline and n=9 bleomycin treated) generated by the AtlasImage 2.0 software was imported into Excel. An adjusted intensity value was calculated by subtracting the background intensity from the spot intensity. The adjusted intensity was taken to be a quantitative measure of gene expression. This adjusted intensity value was used for all further calculations.

Numerous statistical techniques were available to make comparisons between groups of data. However, to obtain meaningful results from most of these tests, the distribution of the data must be known. Preliminary statistical analysis in Minitab™ 13.32 (Minitab Ltd) indicated that the data were not normally distributed across the arrays. This was determined by the Anderson-Darling normality test. An example of this for one gene is shown in Figure 4.1.

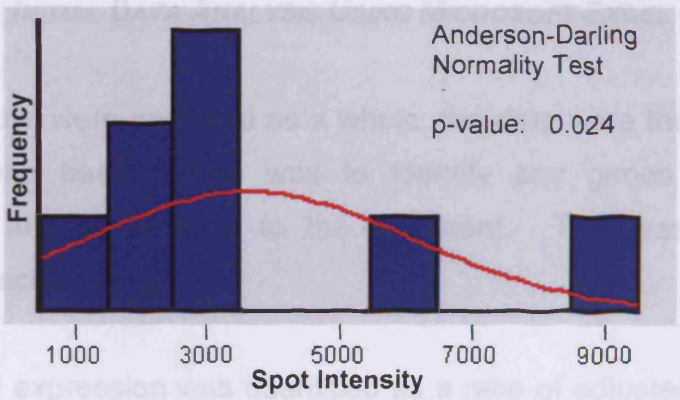

Figure 4.1 *Normality test for one gene applied to raw array data. This was carried out for a representative selection of genes from the array. For normally distributed data p≥ 0.05.*

This led to the initial component of the analysis, which was to normalise the data. The aim of normalisation was to eliminate the variability occurring from experimental differences such as the age of the radioisotope label, or the length of time the membrane was exposed to the phosphorimage screen.

Firstly, a log10 transformation (Nadon and Shoemaker, 2002) reduced the skewness of the data. Global normalisation was then carried out by dividing the spot intensity of each gene by the median spot intensity of the whole array (Balharry *et al.*, 2005). This resulted in data where each gene was comparable across all replicates, and could be used for further analysis. This is illustrated in Figure 4.2.

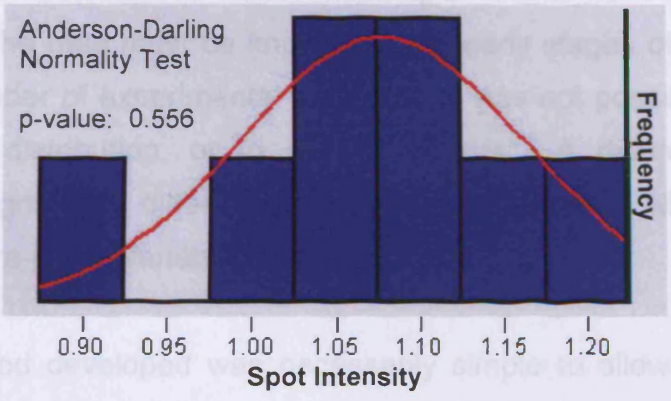

Figure 4.2 *Normality test for one gene applied to log10 transformed, normalised array data. This was carried out for a representative selection of genes from the array. For normally distributed data p≥ 0.05.*

4.3.5 *Initial Data Analysis Using Microsoft Excel*

After the arrays were analysed as a whole, the data were then analysed on a gene by gene basis. This was to identify any genes that responded consistently and significantly to the treatment. This was carried out as detailed in Section 4.3.5.

Altered gene expression was quantified as a ratio of adjusted intensities as a further method of quantifying altered gene expression. Ratio was calculated for up-regulated genes by dividing bleomycin gene intensity by saline gene intensity. For down-regulated genes, saline was divided by bleomycin intensity, and a minus sign was placed in front of the resulting ratio. This generated a figure that was representative of fold change in expression. The positive or negative sign indicated up or down-regulation of the gene. Previous experiments have shown that over 75% of genes with a ratio change of 1.5 or more can be confirmed by reverse transcription polymerase chain reaction (RT-PCR) (Treadwell and Singh, 2004; deVos *et al.,* 2003). The lower threshold for identifying relevant genes was therefore set at a ratio of 1.5.

4.3.5.1 *Range: Low Number of Sample Replicates*

Numerous statistical techniques are available to make comparisons between groups of data. However, to obtain meaningful results from these tests, the distribution of the data must be known. In the early stages of these studies, with a low number of experimental replicates, it was not possible to establish the shape of distribution, or to identify outliers. A different method of determining significant differences in gene expression, which took into account the intra-group variability, was required.

This first method developed was necessarily simple to allow for the limited sample size. For each gene, the normalised intensity values from each of the three saline arrays were plotted on a single graph. The three data points from the bleomycin arrays were plotted alongside these on the same graph. If

there was a clear separation between the range of the bleomycin array points and the range of the saline points, the gene was considered relevant for further study (Figure 4.3).

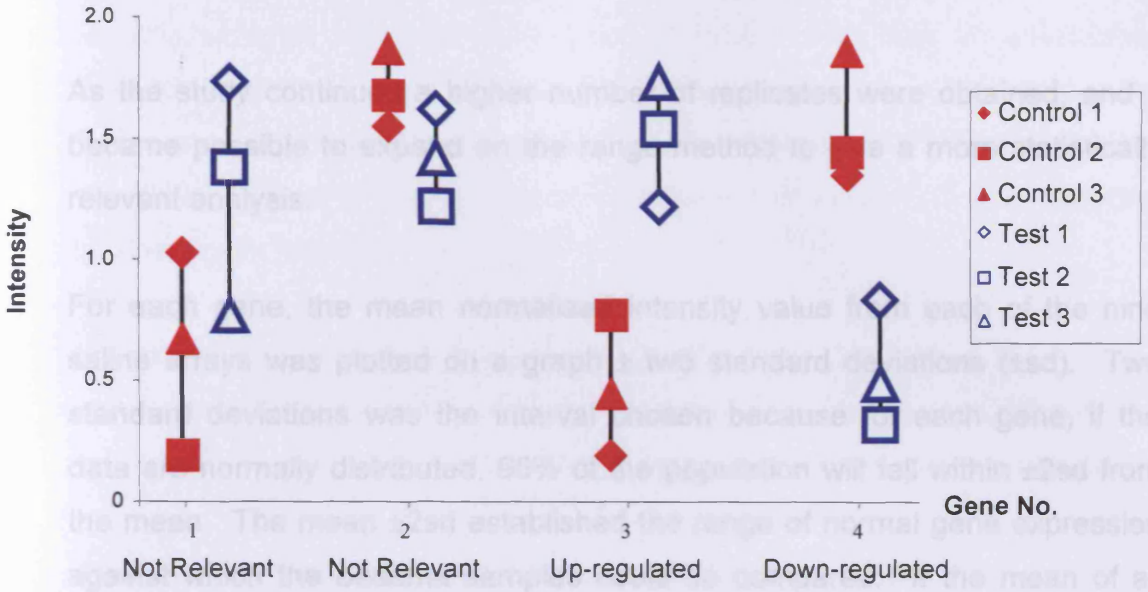

Figure 4.3 *The 'range' method of gene selection. Genes 3 and 4 show a clear difference between the groups, indicating these genes are relevant for further study. Data is for illustrative purposes only and not taken from experimental data.*

Of the genes selected by this method, several criteria were used to identify which genes were most appropriate for use as markers in further studies.

- Large separation between the two groups made it unlikely that experimental error could cause a false overlap
- A narrow range of measured intensities suggested low variability in expression between samples
- A high ratio between the saline and bleomycin groups suggested the effect of treatment was large (the mean values of adjusted intensity were used to calculate expression ratios)
- Groups of functionally related genes exhibiting similar behaviour suggested the results were less likely to be anomalous.

As well as considering the above criteria, it was important to take into account the biological significance of the genes.

4.3.5.2 *Two Standard Deviation: High Number of Sample Replicates*

As the study continued a higher number of replicates were obtained, and it became possible to expand on the range method to give a more statistically relevant analysis.

For each gene, the mean normalised intensity value from each of the nine saline arrays was plotted on a graph ± two standard deviations (±sd). Two standard deviations was the interval chosen because for each gene, if the data are normally distributed, 95% of the population will fall within ±2sd from the mean. The mean ±2sd established the range of normal gene expression against which the oedema samples could be compared. If the mean of all nine of the oedema samples fell outside the two standard deviations limits, the gene was considered relevant for further study (Figure 4.4) (Balharry *et al.*, 2005).

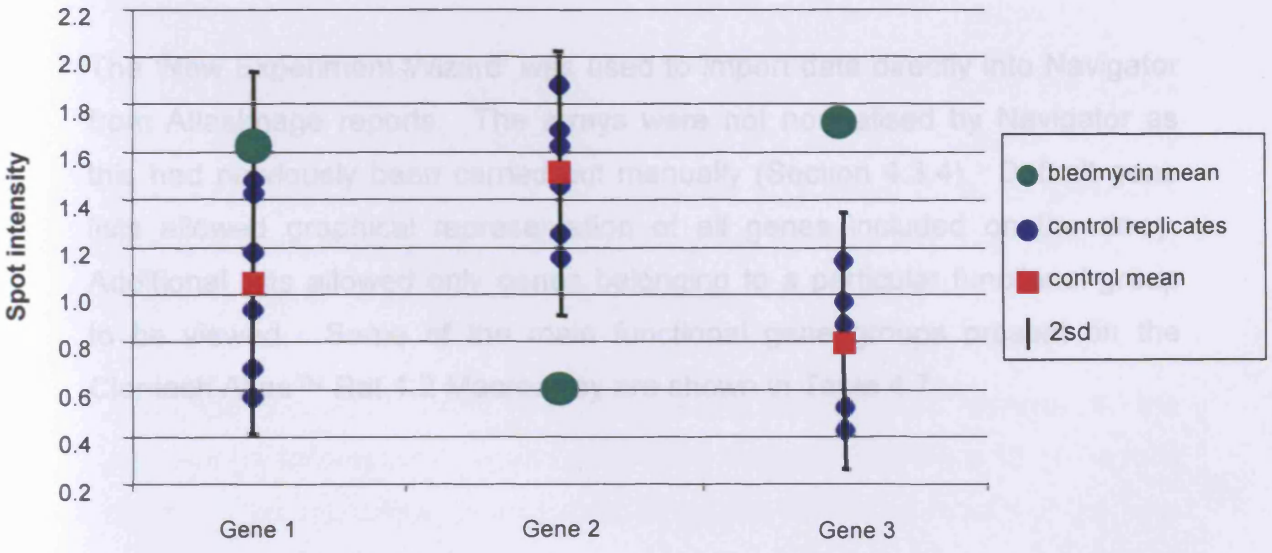

Figure 4.4 *The 2sd method of gene selection. Gene 1 is not significantly altered by bleomycin treatment, genes 2 and 3 are relevant for further study. Gene 2 is down-regulated, and gene 3 is up-regulated. Data is for illustrative purposes only and not taken from experimental data.*

4.3.5.3 *T-TEST: LOW OR HIGH NUMBER OF SAMPLE REPLICATES*

A third method for determining significant differences between the control and oedema samples was also carried out in Excel. This was an established statistical technique, the two-tailed Student's t-test, which is frequently used during array analysis (Dong *et al.*, 2002; Katsuma *et al.*, 2001; Bartosiewicz *et al.*, 2000). Genes with a p-value of less than or equal to 0.05 were selected as statistically relevant.

Of the genes selected by these methods (Section 4.3.5), those with a gene expression ratio of over 1.5 fold were accepted to be the most significant (the mean values of adjusted intensity were used to calculate expression ratios).

4.3.6 *FURTHER ANALYSIS WITH ATLAS NAVIGATOR™ 1.0*

Atlas Navigator (Clontech) was designed specifically for analysis of Clontech Atlas macroarrays. It provided a convenient method for visualisation of the complex expression data generated by AtlasImage.

The 'New Experiment Wizard' was used to import data directly into Navigator from AtlasImage reports. The arrays were not normalised by Navigator as this had previously been carried out manually (Section 4.3.4). Default gene lists allowed graphical representation of all genes included on the array. Additional lists allowed only genes belonging to a particular functional group to be viewed. Some of the main functional gene groups present on the Clontech Atlas™ Rat 1.2 Macroarray are shown in Table 4.7.

Rat 1.2 Macroarray (7854-1)
Apoptosis associated proteins
Cell adhesion receptors
Cell cycle
Cell receptors (by activities)
Cell receptors (by ligands)
Cell signalling, extracellular communication
Cytoskeleton-motility proteins
DNA binding and chromatin proteins
Extracellular transport-carrier proteins
Intracellular transducers-effectors-modulators
Membrane channels and transporters
Metabolism
Post translational modification-protein folding
Protein turnover
Trafficking-targeting proteins
Translation
DNA synthesis, recombination and repair
Functionally unclassified
Immune system proteins
Oncogenes and tumour suppressers
Stress response proteins
Transcription
Housekeeping genes

Table 4.7 *Summary of the main functional gene classes on the Atlas™ Rat 1.2 macroarray*

A new gene list was created to include only the genes identified as relevant using the strategies outlined in Section 4.3.5.

The genes were plotted on a graph with bleomycin dose along the x-axis (control dose=0, bleomycin dose=0.5 units/0.5ml saline). Relative intensity (ratio) was plotted on the y-axis. Relative intensity (ratio) for each gene was defined as the normalised adjusted intensity divided by the normalised adjusted intensity of an arbitrarily selected array.

Each gene was represented as a line, the gradient of which represented the ratio change between saline and bleomycin samples (Figure 4.13 in Results section). This technique was used to study the combined results of the nine saline arrays with the nine bleomycin arrays.

To study the genetic response to different levels of oedema, each set of arrays was separated according to their pathology. The L:B ratio (Chapter 2)

was chosen as a single indicator of oedema. The difference in gene expression at these various levels of oedema was compared (Figure 4.14 in Results section).

4.3.7 *Visual Data Mining with Spotfire Pro 3*

Spotfire Pro was developed to visually explore large data sets. The layout of the display facilitated identification of trends within the data, including clusters and anomalies. The information was formatted in Excel and exported into Spotfire. The data were coloured according to any of the discrete variables, i.e. each functional classification is a different colour (Figure 4.15). Discrete variables were also allocated a check box, so each category could be viewed separately. For example, it is possible to view only those genes associated with apoptosis. Any of the variables (gene code, gene name, ratio, intensity difference, etc.) could be chosen for either of the axes. Genes were allocated to the x-axis, with either intensity difference or ratio on the y-axis. Data were filtered into three categories using the Bin Wizard. The limits were defined according to ratios: less than -1.5, between -1.5 and 1.5, and greater than 1.5. This meant that it was possible to view all the data in any format, without the presence of genes with ratio changes of less than 1.5 (Figure 4.5).

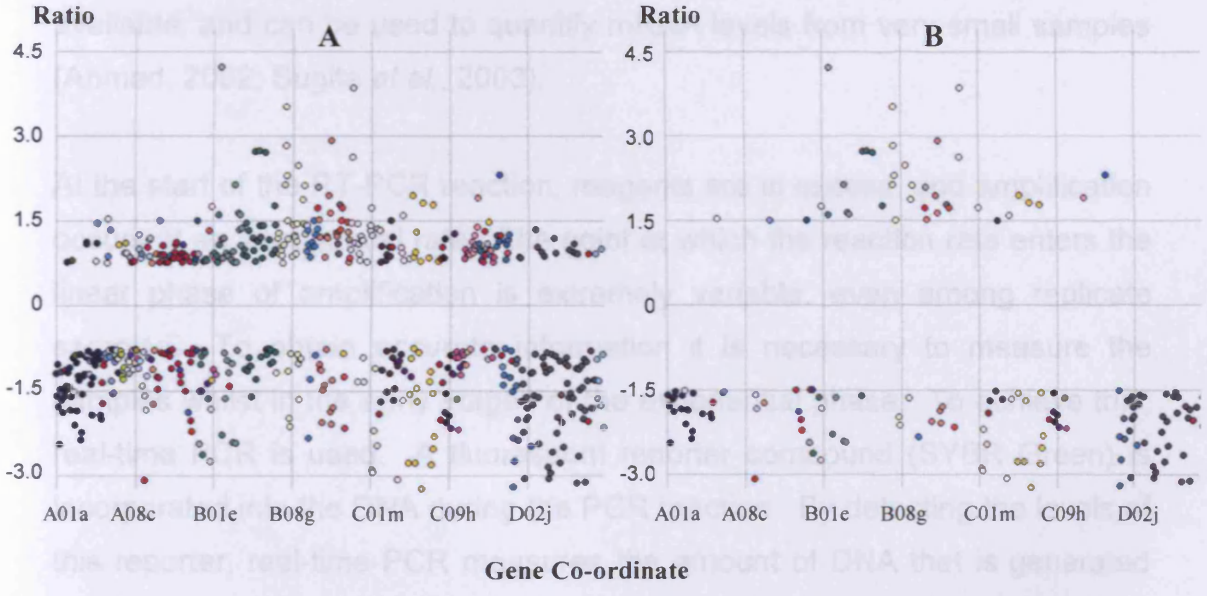

Figure 4.5 *Spotfire data. A: Raw data; B: Data which has been filtered to remove genes with less than a 1.5 ratio change.*

4.3.8 *PHYLOGENIC TREE - GENE CLUSTERING*

In order to identify clustering of the genes, and to represent this graphically, the data were analysed using a phylogenic tree predictor (Tree Top). The sequence data for all the genes previously determined as relevant were formatted in Microsoft Word and inserted into 'Tree Top' (Genebee, 2001). The protein sequence of each gene was determined using NCBI (National Centre for Biotechnology Information), and imported into Word with no spaces. This information was copied directly into the website. Analysis was carried out using the cluster algorithm. The output graph was shown in slanted format. Tree top organises the genes according to the similarity between the sequences and produces a simple graphical representation (dendogram) as illustrated by Figure 4.19 in the Results section. More complex versions of this are available (phylogenic trees), but were not necessary in this instance, as only simplistic clustering according to functionality was required.

4.3.9 *Q-PCR TO CONFIRM ALTERED EXPRESSION OF IMPORTANT GENES*

Q-PCR makes use of the RT-PCR technique. This is one of the most sensitive techniques for mRNA detection and quantification currently available, and can be used to quantify mRNA levels from very small samples (Ahmed, 2002; Sugita *et al.*, 2003).

At the start of the RT-PCR reaction, reagents are in excess, and amplification occurs at an exponential rate. The point at which the reaction rate enters the linear phase of amplification is extremely variable, even among replicate samples. To obtain accurate information it is necessary to measure the samples whilst in the early stages of the exponential phase. To achieve this, real-time PCR is used. A fluorescent reporter compound (SYBR Green) is incorporated into the DNA during the PCR reaction. By detecting the levels of this reporter, real-time PCR measures the amount of DNA that is generated during every cycle of the PCR reaction (Figure 4.6). From this it is possible to

determine the point at which the samples increase significantly above a predetermined baseline level (Ct).

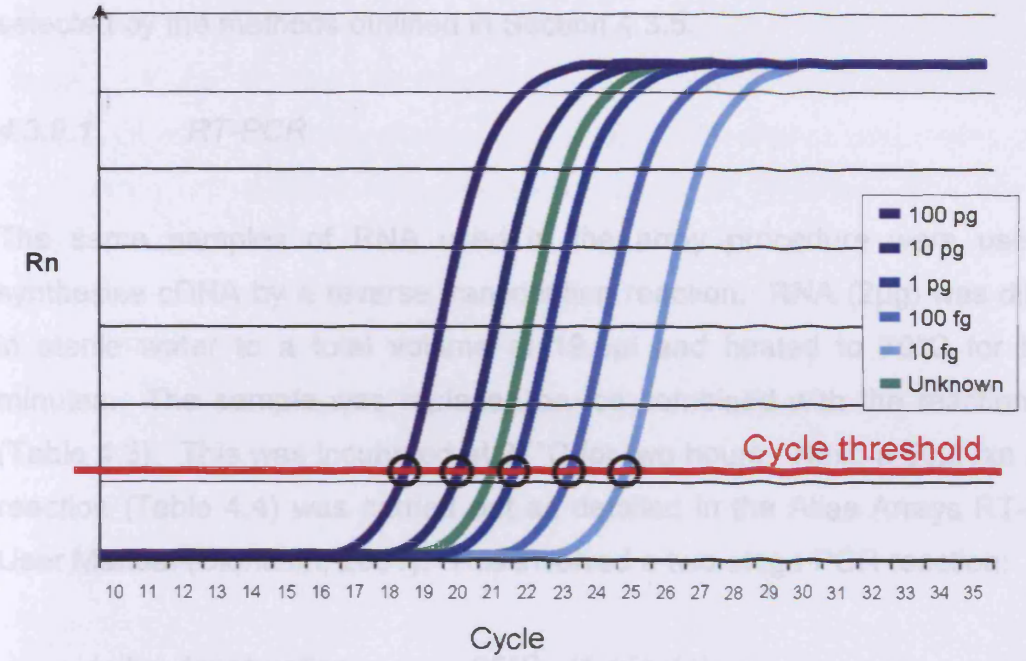

Figure 4.6 *Example data for real-time RT-PCR. Shows an exponential increase in the amount of cDNA present in each sample (Rn, Reporter number).*

Firstly, a standard curve was constructed from RNA extracted from untreated lung tissue (Figure 4.7). The samples were of known concentrations (10fg-100pg), and were plotted against their Ct values.

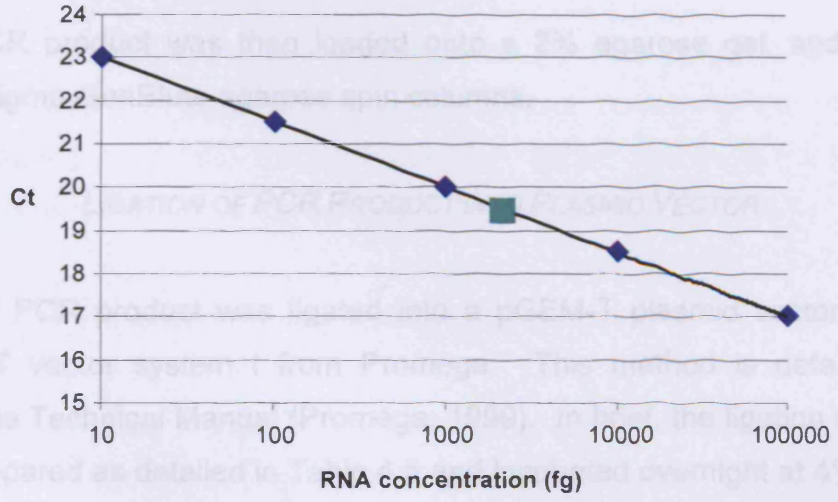

Figure 4.7 *Standard curve resulting from data in Figure 4.6. Standards (◆), Unknown (■).*

This was used as a reference for interpolating information for RNA of unknown concentrations. This technique was carried out on five of the genes selected by the methods outlined in Section 4.3.5.

4.3.9.1 RT-PCR

The same samples of RNA used in the array procedure were used to synthesise cDNA by a reverse transcription reaction. RNA (2µg) was diluted in sterile water to a total volume of 19.5µl and heated to 70°C for three minutes. The sample was replaced on ice combined with the reaction mix (Table 4.3). This was incubated at 37°C for two hours. Next, a 50µl rxn PCR reaction (Table 4.4) was carried out as detailed in the Atlas Arrays RT-PCR User Manual (Clontech, 2001). This involved a two-stage PCR reaction:

Initial denaturation	95°C	(1 minute)
↓		
Denature	95°C	(30 seconds) ←
↓		x 30 cycles
Anneal and extend	68°C	(1 minute) ←
↓		
Final extension	68°C	(1 minute)

The PCR product was then loaded onto a 2% agarose gel, and extracted using Sigma GenElute agarose spin columns.

4.3.9.2 LIGATION OF PCR PRODUCT INTO PLASMID VECTOR

Purified PCR product was ligated into a pGEM-T plasmid vector using the pGEM-T vector system I from Promega. This method is detailed in the Promega Technical Manual (Promega, 1999). In brief, the ligation master mix was prepared as detailed in Table 4.5 and incubated overnight at 4°C.

4.3.9.3 TRANSFORMATION INTO E.COLI

The tubes containing the ligation reaction were centrifuged and 2µl was transferred to a fresh tube. Frozen *E.coli* JM109 competent cells were thawed on ice for five minutes and gently mixed by flicking. Thawed competent cells (50µl) were added to the ligation reactions and mixed gently by pipetting. The tubes were placed on ice for 20 minutes. The samples were heat shocked for 45-50 seconds at 42°C then returned to ice for two minutes. Luria broth (LB) (950µl) was added to each tube, and incubated with shaking for 1.5 hours at 37°C. The transformed *E.coli* (100µl and 200µl respectively) was plated on to pre-prepared LB/ampicillin/IPTG/X-Gal agar plates. The remaining media was centrifuged and the pellet resuspended in 100µl of LB. This was also plated out, and all three plates were cultured overnight at 37°C.

4.3.9.4 SCREENING TRANSFORMANTS FOR INSERTS

Successful cloning of an insert into the pGEM-T vector interrupts the coding sequence of β-galactosidase. This results in a colour change between clones which contain PCR product, and those that do not. Recombinant clones can therefore be identified by a white colouring, compared to uncloned vectors which remain blue.

LB (10ml) containing 1mg/ml ampicillin was inoculated with a white colony, and incubated overnight at 37°C. The culture containing the recombinant clones was plated onto LB agar/ampicillin plates and sent for sequencing whilst the remainder was stored as a 20% glycerol stock.

4.3.9.5 PLASMID DNA PURIFICATION

Purification of plasmid DNA from the bacterial cells was undertaken using the Wizard *Plus* SV Minipreps DNA Purification System. LB containing the recombinant *E.coli* (1.5 ml) was centrifuged (10000 x *g*) for five minutes. The

resulting pellet was resuspended in 250µl resuspension buffer and vortexed. Cell lysis solution (250µl) was added and mixed by inverting. The sample was incubated at room temperature until the cell suspension had cleared (maximum of five minutes). Alkaline protease solution (10µl) was added and mixed by inverting, then incubated at room temperature for five minutes. After incubation, 350µl neutralisation solution was added and immediately mixed by inversion. The sample was then centrifuged at maximum speed for 10 minutes, and the cleared lysate decanted into a prepared spin column. This was centrifuged at maximum speed for one minute. The columns were then washed with 750µl column wash solution and centrifuged for a further one minute. A final wash was carried out by adding 250µl column wash solution to the column and centrifuging for two minutes. To elute the plasmid, 50µl nuclease-free water was added to the column, and centrifuged for one minute. The concentration of DNA in the resultant eluant was measured using a GeneQuant™ (Pharmacia).

4.3.9.6 Serial Dilution of Standards

When the sequence of the insert was confirmed, standards were created for each gene. The GeneQuant measurement of the eluted DNA (Section 4.3.1.4) was used to calculate the dilution factor necessary to obtain a concentration of 1ng/µl. Serial dilutions were then carried out to obtain a series of standards ranging from 10fg/µl to 100pg/µl.

4.3.9.7 Q-PCR of Experimental Genes

RNA was isolated from experimental lung as described in Section 4.3.1.2, and cDNA was synthesised from this, by a reverse transcription reaction (Section 4.3.9.1). Samples and standards were prepared for Q-PCR using the QuantiTect SYBR Green PCR Kit. The PCR reactions were set up as shown in Table 4.6. Each sample and standard was loaded in triplicate (20µl per well) into a Thermofast 96 well PCR detection plate. The plate was analysed on an Applied Biosystems ABI PRISM 7700 Sequence Detection System.

4.4 RESULTS

4.4.1 ISOLATION AND PREPARATION OF RNA

RNA preparations from Tri-reagent™ (Sigma-Aldrich) and the RNeasy Mini kit (Qiagen) were compared (n=3) using the GeneQuant (Pharmacia) (Table 4.8).

Isolation Technique	Absorbance (260nm)	RNA concentration (µg/ml)	Ratio A_{260}/A_{280}
Tri-reagent™	1.020	771.9	1.87
Tri-reagent™	1.787	1421.9	1.51
Tri-reagent™	1.105	950.7	1.39
Mean	1.304	1048.2	1.59
RNeasy Mini kit	1.021	996.6	2.04
RNeasy Mini kit	0.479	383.3	1.99
RNeasy Mini kit	0.647	532.4	2.03
Mean	0.716	637.4	2.02

Table 4.8 *Comparative data from the two RNA isolation techniques generated by the GeneQuant RNA/DNA Calculator. RNA was isolated from the same section of lung tissue each time.*

The isolated RNA was run on an agarose gel and viewed under UV (Syngene™ gel doc System) to check the integrity and highlight any genomic contamination. The presence of DNA was detected as a third band (Figure 4.8). Smeared bands would indicate RNA degradation.

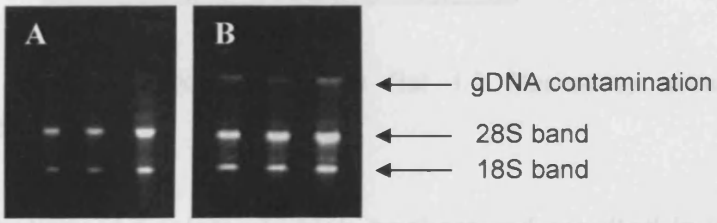

Figure 4.8 *Agarose gel of total RNA isolated from lung tissue. A: Isolated using the RNeasy Mini kit, followed by DNase treatment; B: Isolated using Tri-reagent™.*

Preparation with Tri-reagent™ resulted in almost double the RNA yield, however, the RNeasy isolation contained fewer contaminants. This can be seen from the gel pictures (Figure 4.8) and the high absorbance ratios calculated by the GeneQuant (Table 4.8). RNA preparations of greater purity were isolated following DNase treatment (Section 4.3.1.3).

Before using the isolated RNA in the array procedure, the GeneQuant (Pharmacia) was used to confirm the purity and yield of the samples. Sham-control samples and bleomycin-treated samples were used as outlined in Chapter 2. Samples with a ratio of over 1.8 were chosen, as this value indicated that there was little or no DNA contamination. The RNA purity was confirmed by checking against the agarose gel images.

4.4.2 MACROARRAY

4.4.2.1 MACROARRAY OPTIMISATION

Initial array studies were ineffective due in part to poor RNA isolations. However, even after optimisation of RNA isolation procedures (Section 4.3.1), some arrays were still not providing adequate gene expression images (Figure 4.9).

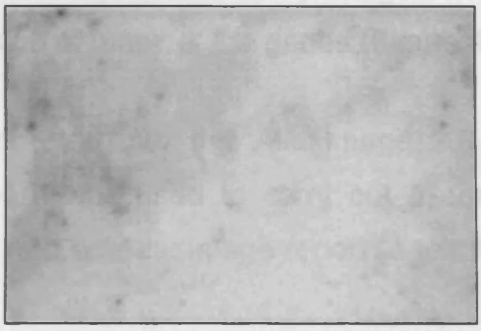

Figure 4.9 *Scanned phosphorimage of Clontech Rat 1.2 Macroarray showing poor hybridisation and high background.*

The lack of hybridisation and relatively high background resulted in indistinct separation on the arrays. The two possible causes of this were problems with the hybridisation solution, or inadequate separation of the labelled probe. The

hybridisation solution was probably ineffective due to repeated heating to 60°C. To remedy these problems, a new batch of hybridisation solution, designed specifically for use on the Atlas Rat 1.2 macroarrays (7854-1) was purchased. The solution was separated into aliquots to avoid repeated heating. The technique used to purify the labelled probe was updated from a large scale gravity-fed column purification method (procedure not shown), to the method described in Section 4.3.2.2 (spin-column chromatography). Subsequent arrays showed clear hybridisation, and a relatively low background (Figure 4.10).

4.4.2.2 MACROARRAY ANALYSES

The array procedure was designed to find genes that were consistently significantly up or down-regulated by 1.5-fold or greater in the oedematous lung. The first stages of oedema in the rat lung occurred three days post-bleomycin instillation, as confirmed by the biochemical analysis detailed in Chapters 2 and 3. Consequently, lung tissue from this time point was taken for genetic analysis. Saline-treated and bleomycin-treated samples were used in conjunction with the Atlas™ Rat 1.2 Macroarray (7854-1) and the resultant array images analysed with the AtlasImage 2.0 (Clontech) computer software. Visual examination of the array images showed a great deal of change in the expression of many of the genes (Figure 4.10).

The images were imported into the AtlasImage 2.0 (Clontech) computer program. This software was used to carry out a comparative quantitative analysis of the arrays and an AtlasImage report (a text file) was generated for each of the arrays.

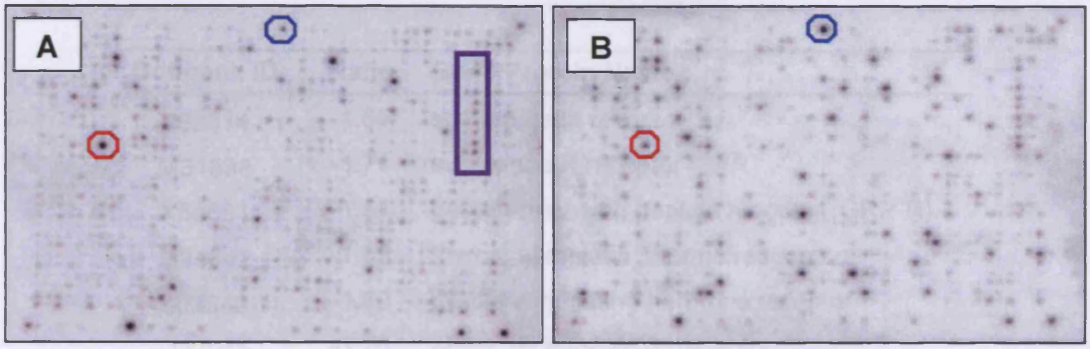

Figure 4.10 *Scanned phosphorimage of Clontech Rat 1.2 Macroarrays, three days after treatment. A: Saline; B: Bleomycin. Examples of two genes altered by bleomycin treatment are indicated: ○, Down-regulated; ○, Up-regulated; □, Cluster/family of genes.*

4.4.3 EXCEL ANALYSIS

4.4.3.1 STANDARD DEVIATION METHOD

The quantitative data generated for each of the arrays by AtlasImage 2.0 were exported to an Excel file. The genes with a consistent change in expression were identified (as described in Section 4.3.5.2) and limited to genes with a ratio change of over 1.5. A total of 23 genes were identified (Figure 4.11 and Table 4.9).

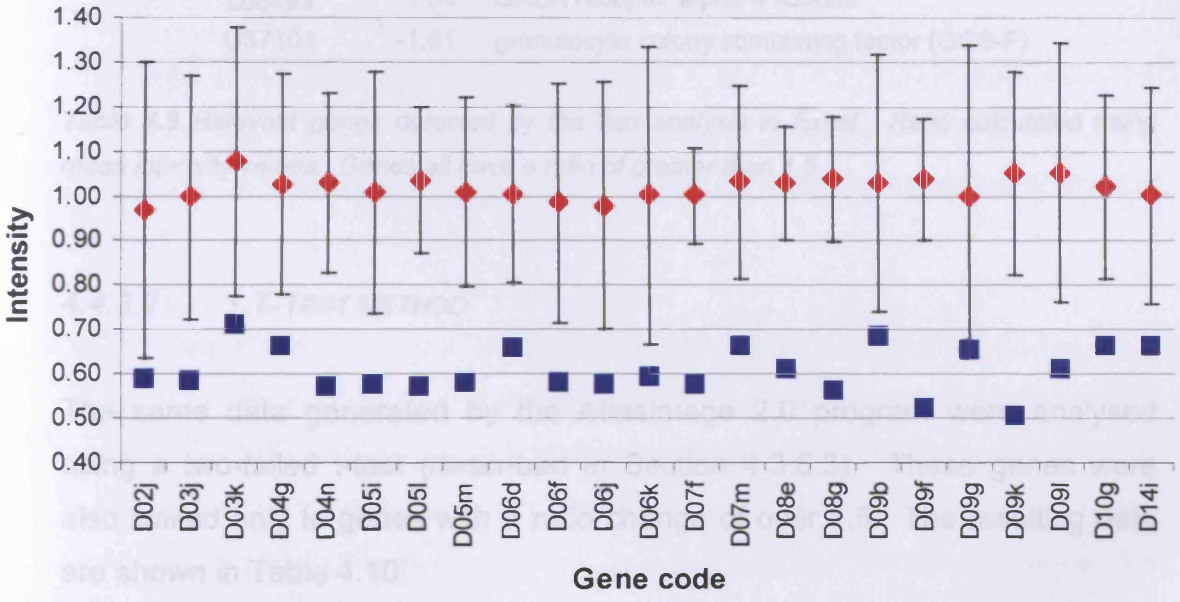

Figure 4.11 *Analysis of saline (n=9) and bleomycin (n=9) arrays by the standard deviation method in Excel. Mean saline intensity (◆), mean bleomycin intensity (■), ± 2sd (I).*

Genbank ID	Ratio	Gene/Protein Name
X62314	-1.65	somatostatin receptor 1
M31838	-1.71	substance K receptor (SKR)
X56661	-1.51	gastrin-releasing peptide receptor (GRP-R)
M34842	-1.55	thyroid stimulating hormone receptor
L02842	-1.80	follicle stimulating hormone receptor
D32045	-1.76	alpha 1B adrenergic receptor
L05596	-1.81	Serotonin receptor 1F
L10072	-1.74	serotonin receptor 5A
M88096	-1.53	cholecystokinin receptor
M93273	-1.70	somatostatin receptor 2
U37058	-1.70	neuromedin B receptor
U40395	-1.70	cannabinoid receptor 1
L10073	-1.74	serotonin receptor 5B
X63574	-1.55	somatostatin receptor 3
J03933	-1.69	thyroid hormone beta receptor
M14053	-1.84	glucocorticoid receptor
X95579	-1.51	GABA-A receptor rho-1 subunit precursor
L31622	-1.99	neuronal ACh receptor beta 2 subunit
M85035	-1.53	glutamate receptor 2 precursor
X15467	-2.08	GABA-A receptor beta-2 subunit precursor
L08497	-1.72	GABA-A receptor gamma-2 subunit
L08493	-1.54	GABA receptor alpha 4 subunit
U37101	-1.51	granulocyte colony stimulating factor (GCS-F)

Table 4.9 *Relevant genes detected by the 2sd analysis in Excel. Ratio calculated using mean intensity values. Genes all have a ratio of greater than 1.5.*

4.4.3.2 T-TEST METHOD

The same data generated by the AtlasImage 2.0 program were analysed using a two-tailed t-test (described in Section 4.3.5.3). These genes were also limited only to genes with a ratio change of over 1.5. The resulting data are shown in Table 4.10.

Genbank ID	Ratio	p-value	Gene/Protein Name
D50497	2.12	0.038	chloride channel protein
U15098	1.66	0.032	glutamate transporter
U28927	1.69	0.032	Na+/Cl- betaine/GABA transporter
U10096	2.15	0.021	sodium-potassium-chloride cotransporter
L10362	1.83	0.018	synaptic vesicle protein 2B
L02842	-1.80	0.037	follicle stimulating hormone receptor
D32045	-1.76	0.045	alpha 1B adrenergic receptor
L05596	-1.81	0.034	Serotonin receptor 1F
L10072	-1.74	0.049	serotonin receptor 5A
Z11690	-2.10	0.038	vasopressin/arginine receptor
L10073	-1.74	0.049	serotonin receptor 5B
J03933	-1.69	0.028	thyroid hormone beta receptor
M36074	-2.14	0.034	mineralocorticoid receptor (MR)
M14053	-1.84	0.029	glucocorticoid receptor
Z11716	-2.16	0.031	glutamate receptor 7 (GLUR7)
L31622	-1.99	0.015	neuronal ACh receptor β 2 subunit
X15467	-2.08	0.016	GABA-A receptor beta-2 subunit precursor

Table 4.10 *Relevant genes detected by the t-test analysis in Excel. Ratio calculated using mean intensity values. Genes have a p-value ≤ 0.05 and a ratio difference greater than 1.5.*

4.4.3.3 STANDARD DEVIATION / T-TEST COMPARISON

The gene lists generated in Sections 4.4.3.1 and 4.4.3.2 were compared for consistencies. These genes were considered particularly relevant. A list combining genes from both analysis techniques was compiled, as shown in Table 4.11.

As well as considering the statistical relevance as determined above, it is important to take into account the biological significance and clustering of the genes. Of the five up-regulated genes, four are involved in active transport of molecules across membranes and the fifth is a chloride channel. Many of the remaining significantly altered genes belonged to two functional groups, the neurotransmitter receptors (seven genes) and hormone receptors (fifteen genes).

Genbank ID	Ratio	Gene/Protein Name	Classification
D50497	2.12	chloride channel protein	Ion channels & trafficking proteins
U15098	1.66	glutamate transporter	Ion channels & trafficking proteins
U28927	1.69	Na+/Cl- betaine/GABA transporter	Ion channels & trafficking proteins
U10096	2.15	Na-K-Cl cotransporter	Ion channels & trafficking proteins
L10362	-1.83	synaptic vesicle protein 2B	Ion channels & trafficking proteins
X62314	-1.65	somatostatin receptor 1	Hormone receptors
M31838	-1.71	substance K receptor (SKR)	Hormone receptors
X56661	-1.51	gastrin-releasing peptide receptor	Hormone receptors
M34842	-1.55	thyroid stimulating hormone receptor	Hormone receptors
L02842	**-1.80**	**follicle stimulating hormone receptor**	**Hormone receptors**
D32045	**-1.76**	**alpha 1B adrenergic receptor**	**Hormone receptors**
L05596	**-1.81**	**Serotonin receptor 1F**	**Hormone receptors**
L10072	**-1.74**	**serotonin receptor 5A**	**Hormone receptors**
M88096	-1.53	cholecystokinin receptor	Hormone receptors
M93273	-1.70	somatostatin receptor 2	Hormone receptors
U37058	-1.70	neuromedin B receptor	Hormone receptors
U40395	-1.70	cannabinoid receptor 1	Hormone receptors
Z11690	-2.10	vasopressin/arginine receptor	Hormone receptors
L10073	**-1.74**	**serotonin receptor 5B**	**Hormone receptors**
X63574	-1.55	somatostatin receptor 3	Hormone receptors
J03933	**-1.69**	**thyroid hormone beta receptor**	**Nuclear receptors**
M36074	-2.14	mineralocorticoid receptor (MR)	Nuclear receptors
M14053	**-1.84**	**glucocorticoid receptor**	**Nuclear receptors**
X95579	-1.51	GABA-A receptor rho-1 subunit	Neurotransmitter receptors
Z11716	-2.16	glutamate receptor 7 (GLUR7)	Neurotransmitter receptors
L31622	**-1.99**	**neuronal ACh receptor β–2 subunit**	**Neurotransmitter receptors**
M85035	-1.53	glutamate receptor 2 precursor	Neurotransmitter receptors
X15467	**-2.08**	**GABA-A receptor β-2 subunit**	**Neurotransmitter receptors**
L08497	-1.72	GABA-A receptor gamma-2 subunit	Neurotransmitter receptors
L08493	-1.54	GABA receptor α–4 subunit	Neurotransmitter receptors
U37101	-1.51	granulocyte colony stimulating factor	GFs, Cytokines & Chemokines

Table 4.11 *Relevant genes detected by the 2sd analysis combined with the t-test analysis. Ratio calculated using mean intensity values. Genes all have a ratio change greater than 1.5. Genes in blue were identified only by the t-test. Genes in black were identified only by the 2sd method. Genes in bold were identified by both techniques*

4.4.3.4 *RANGE / STANDARD DEVIATION COMPARISON*

A comparison was carried out between the range method developed initially, and the statistical method derived from it. From the 18 arrays carried out, three saline and three bleomycin arrays were chosen randomly. These six arrays were then analysed by the 'range' method as described in Section 4.3.5.1. The resulting data were compared to the data generated by the analysis of all 18 arrays by the 2sd method described in Section 4.3.5.2.

The range method highlighted 56 genes that were altered by greater than 1.5-fold. Of these genes, 23 were up-regulated, eight of which were altered by greater than two-fold. The remaining 33 genes were down-regulated, 20 of which had greater than two-fold changes. The standard deviation method selected 23 genes, all of which were down-regulated by greater than 1.5-fold, as shown in Table 4.9. The genes which were consistent throughout both these analysis methods are shown in Table 4.12.

Genbank ID	Ratio (range)	Ratio (sd)	Gene/Protein Name	Classification
X62314	-2.56	-1.65	somatostatin receptor 1	Hormone receptors
M31838	-2.78	-1.71	substance K receptor (SKR)	Hormone receptors
M34842	-1.96	-1.55	thyroid stimulating hormone receptor	Hormone receptors
D32045	-2.72	-1.76	alpha 1B adrenergic receptor	Hormone receptors
M93273	-2.80	-1.70	somatostatin receptor 2	Hormone receptors
U37058	-2.61	-1.70	neuromedin B receptor	Hormone receptors
U40395	-2.85	-1.70	cannabinoid receptor 1	Hormone receptors
L10073	-3.00	-1.74	serotonin receptor 5B	Hormone receptors
X63574	-1.76	-1.55	somatostatin receptor 3	Hormone receptors
J03933	-3.21	-1.69	thyroid hormone beta receptor	Nuclear receptors
M14053	-3.00	-1.84	glucocorticoid receptor	Nuclear receptors
X95579	-2.83	-1.51	GABA-A receptor rho-1 subunit	Neurotransmitter receptors
L31622	-3.03	-1.99	neuronal ACh receptor β-2 subunit	Neurotransmitter receptors
X15467	-1.81	-2.08	GABA-A receptor β-2 subunit	Neurotransmitter receptors
U37101	-2.09	-1.51	granulocyte colony stimulating factor	GFs, Cytokines & Chemokines

Table 4.12 *Genes common in both the 2sd analysis and the range analysis. Ratio change calculated using mean intensity values. Genes all have a ratio of greater than 1.5.*

There was a relatively high level of correlation between the two methods, with 15 of the 23 genes identified by the standard deviation method also being picked up by the range method. Although a larger number of genes were highlighted using the range method, this may be indicative of more false positives.

4.4.4 NAVIGATOR ANALYSIS

The data generated by AtlasImage were imported into Navigator as described in Section 4.3.6. This produced a graphical representation of the global gene expression patterns generated by the Atlas 1.2 Rat macroarray (Figure 4.12).

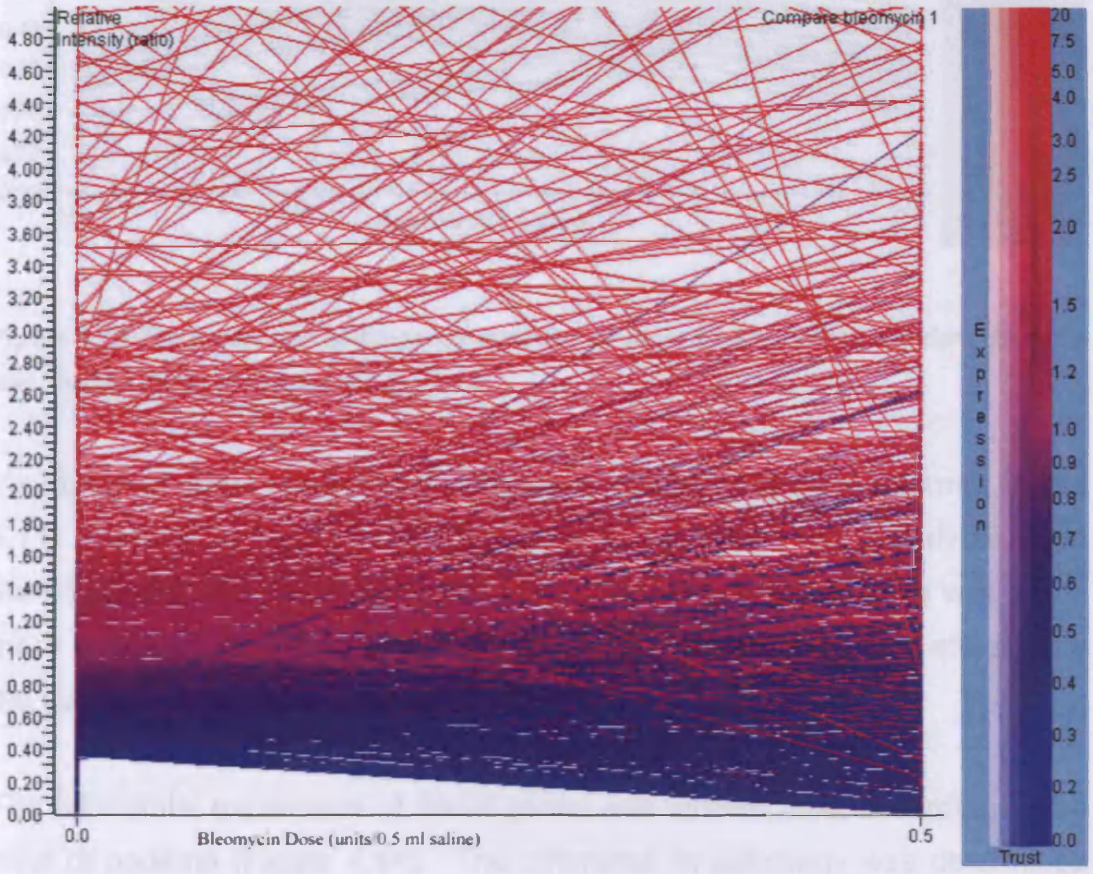

Figure 4.12 *The altered expression of all the genes on the Atlas Rat 1.2 macroarray.*

The entire array illustrated on one graph was not particularly beneficial (Figure 4.12). The large number of genes masked any extreme effects that may have

been visible with fewer genes present on the graph. Examination of functional groups individually, or genes that were previously determined as relevant, was found to be much more effective (Figure 4.13).

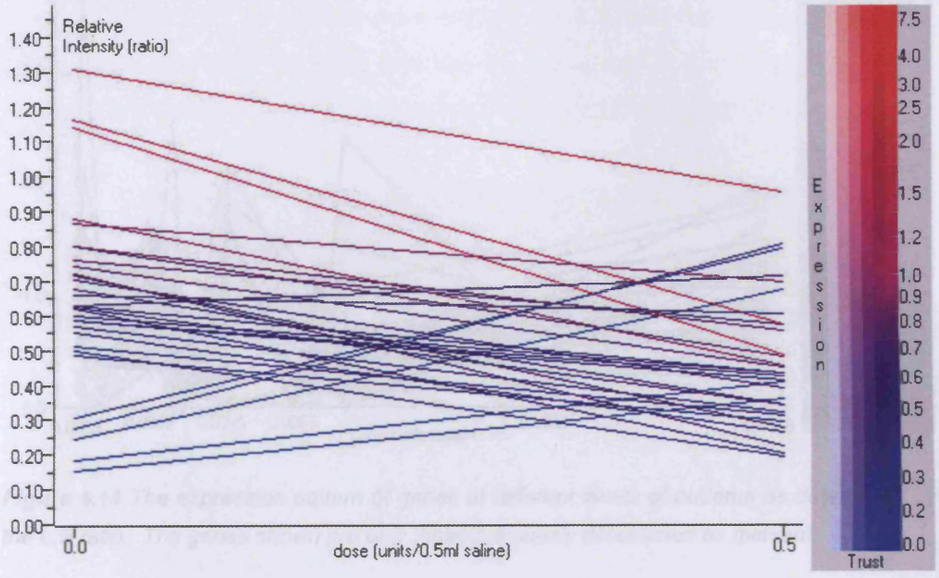

Figure 4.13 *The expression of the genes identified by a combination of the standard deviation and t-test methods (Section 4.4.3.3).*

Visualisation of the relevant data previously displayed in tabular format (Table 4.11) is shown in Figure 4.13. The effect of bleomycin was clearly seen on the 31 identified genes. A general trend towards down-regulation was much more noticeable and identification of those genes that were most affected by the treatment was made easier.

The differential expression of these genes was studied next, according to the level of oedema (Figure 4.14). The difference in pathology was determined by the L:B ratio.

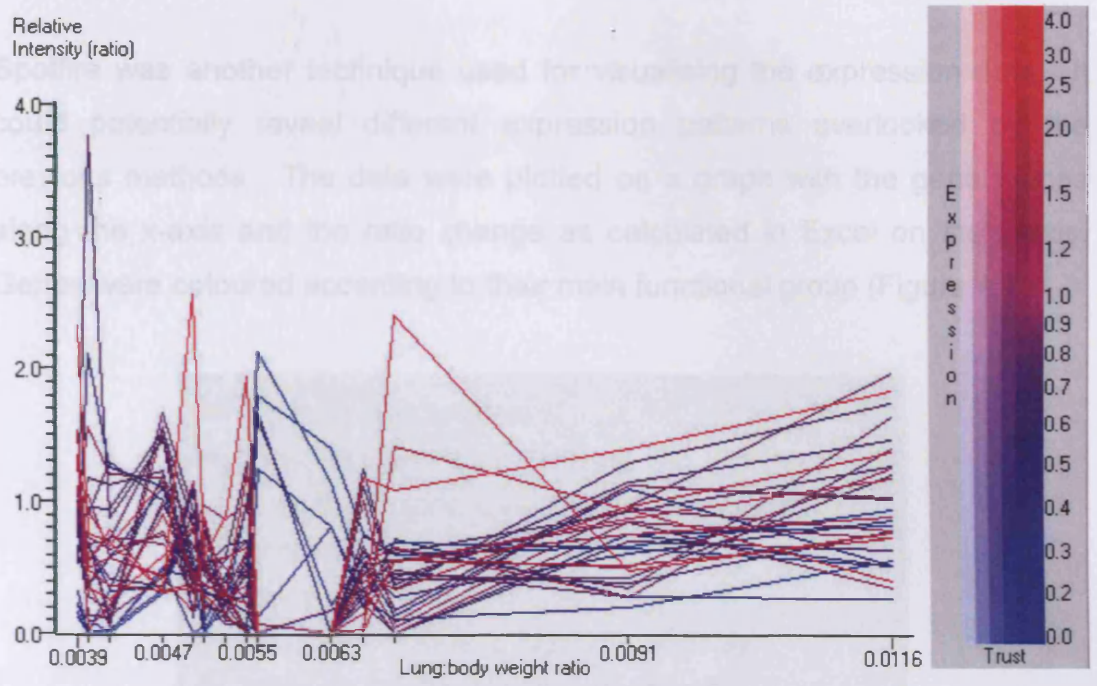

Figure 4.14 *The expression pattern of genes at different levels of oedema as determined by the L:B ratio. The genes shown are only those previously determined as relevant.*

This gives a more detailed picture of the expression patterns at progressing levels of oedema. The lowest L:B ratios were generated from the saline-instilled animals (e.g. L:B= 0.0039-0.0053). In undamaged tissue, normal gene expression fluctuations were occurring that resulted in large variations between samples. The greater the level of oedema (i.e. the greater the change from normal) the more the behaviour of the genes appeared to synchronise (e.g. L:B= 0.0063-0.0116).

One of the restrictions of this method of analysis is the lack of exact duplicates of the data. This means the level of confidence in these data is limited.

4.4.5 SPOTFIRE ANALYSIS

Spotfire was another technique used for visualising the expression data. It could potentially reveal different expression patterns overlooked by the previous methods. The data were plotted on a graph with the gene names along the x-axis and the ratio change as calculated in Excel on the y-axis. Genes were coloured according to their main functional group (Figure 4.15).

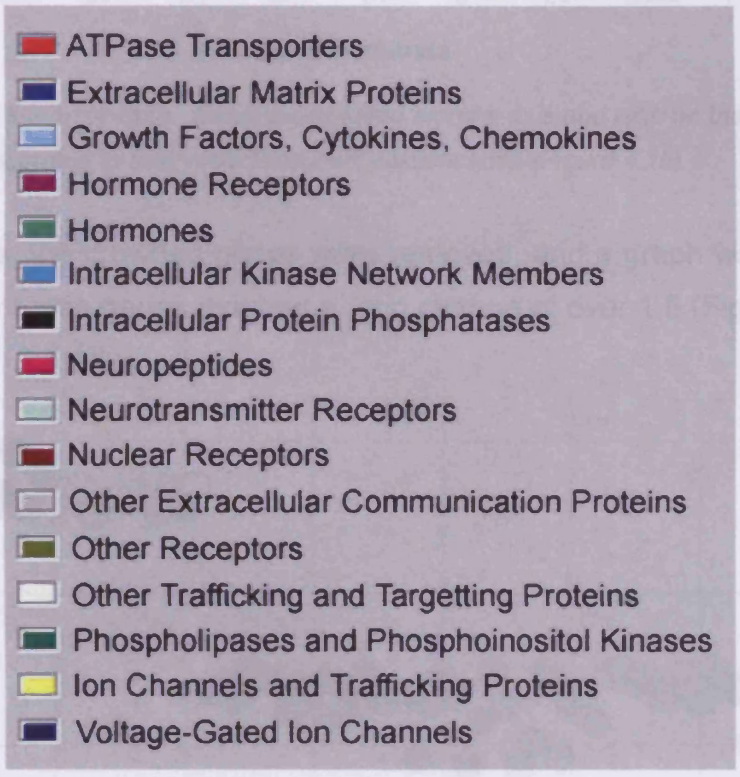

Figure 4.15 *Legend for the Spotfire analysis, showing the colour coding of the functional classification of the genes on the Atlas Rat 1.2 macroarray.*

The data for all the genes are shown in Figure 4.16. The information presented in this graph was unclear as a result of the clustering of data around the horizontal axis.

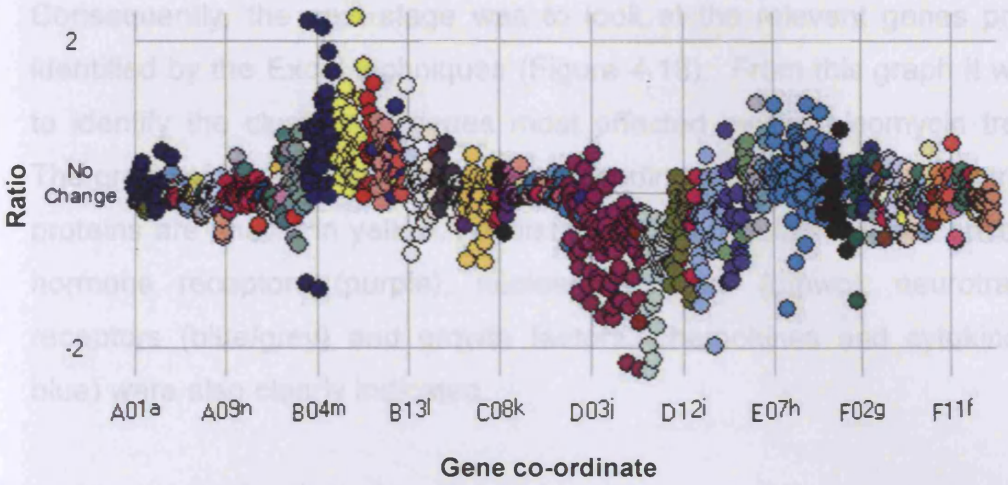

Figure 4.16 *All the array data. Gene codes listed along x-axis and ratio on the y-axis. Genes are coloured according to their main functional classification (Figure 4.15).*

To clarify this, the crowded genes were removed, and a graph was generated showing only those genes that had a ratio change of over 1.5 (Figure 4.17).

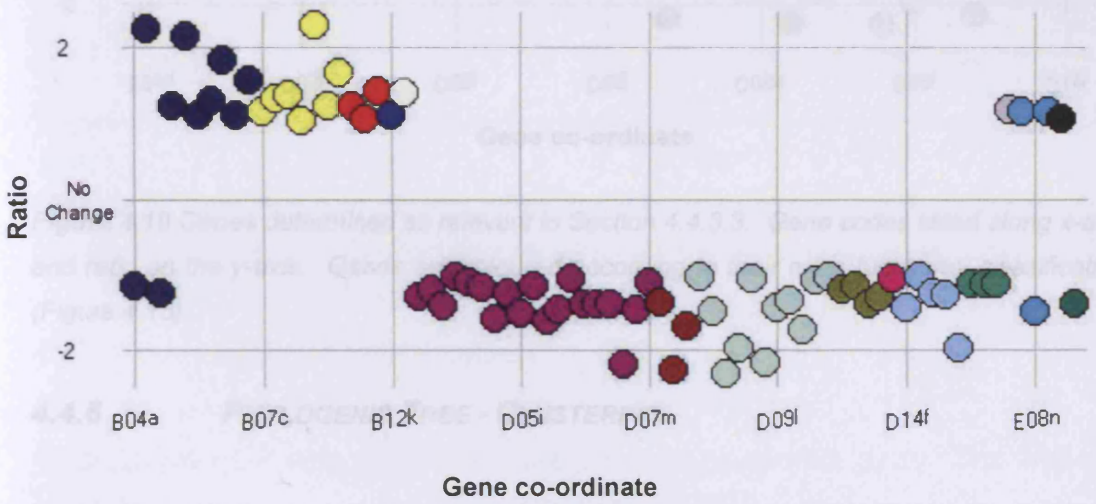

Figure 4.17 *Macroarray data excluding genes which have a ratio of less than 1.5. Gene codes listed along x-axis and the ratio on the y-axis. Genes are coloured according to their main functional classification (Figure 4.15).*

The grouping of families of genes on the array could clearly be seen. The genes with extreme responses to bleomycin in terms of ratio change were also easily identified.

Consequently, the next stage was to look at the relevant genes previously identified by the Excel techniques (Figure 4.18). From this graph it was easy to identify the clusters of genes most affected by the bleomycin treatment. The group of five up-regulated genes encoding for ion channels and trafficking proteins are shown in yellow. Whilst the down-regulated genes encoding for hormone receptors (purple), nuclear receptors (brown), neurotransmitter receptors (blue/grey) and growth factors, chemokines and cytokines (pale blue) were also clearly indicated.

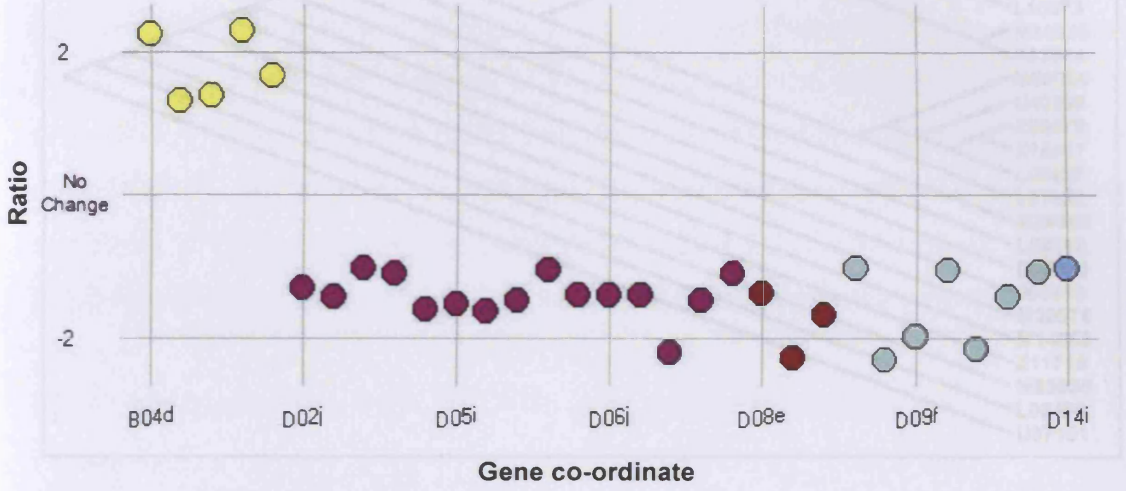

Figure 4.18 *Genes determined as relevant in Section 4.4.3.3. Gene codes listed along x-axis and ratio on the y-axis. Genes are coloured according to their main functional classification (Figure 4.15).*

4.4.6 PHYLOGENIC TREE - CLUSTERING

Tree top was used to cluster the genes previously identified as relevant (Table 4.11). The sequence homology between the protein products of the significant genes was used as the basis for clustering. The more related the protein sequences were to each other, the shorter the 'branches' were. The resultant dendogram is depicted in Figure 4.19. The relationship between the genes was clearly represented. For example, each cluster of either green, blue or purple coloured gene codes were loosely related to each other. However, the shorter branches on the tree (indicated by three different shades of blue) were more closely associated. By the same standard, longer

branches signified genes that showed no structural similarities, indicated by the brown colour.

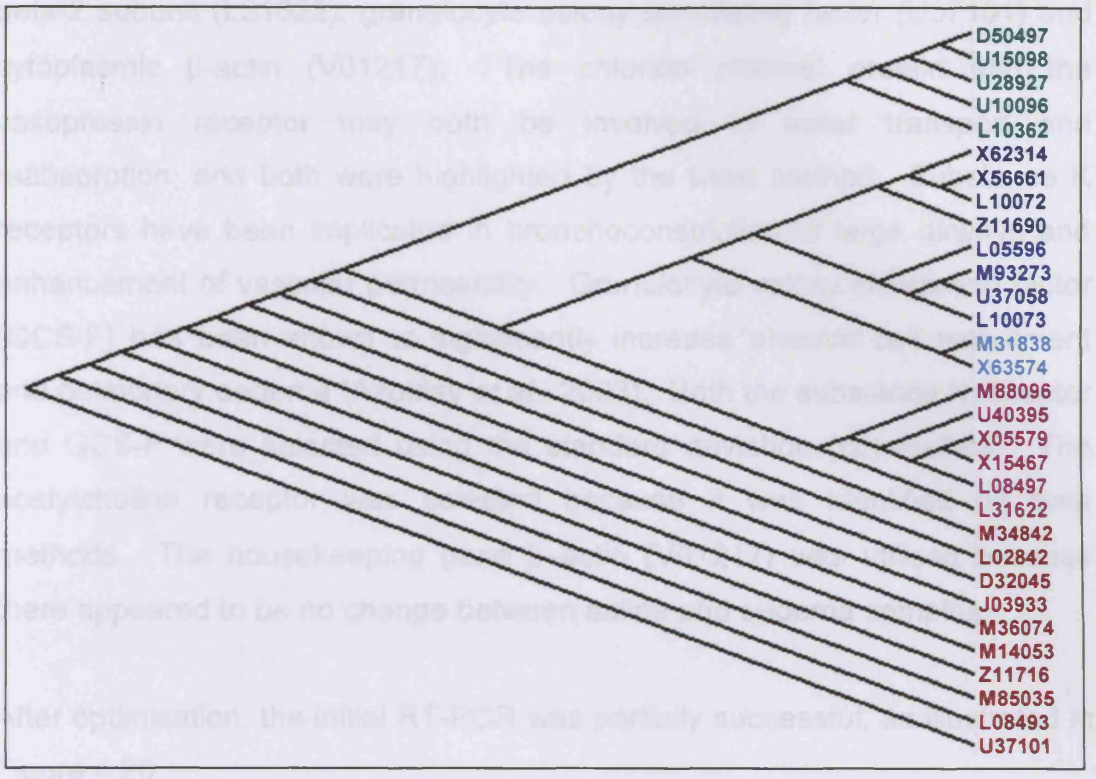

Figure 4.19 *Phylogenic tree showing the relationship between genes. The shorter branches indicate close similarity, whilst the longer branches (brown genes) indicate less similarity.*

4.4.7 QUANTITATIVE PCR

Quantitative PCR was carried out to achieve two separate aims. The first and most important reason was to determine whether the changes in gene expression predicted by the array were accurate. Secondly, this technique was used to determine whether the 2sd method or the t-test method of analysis (Sections 4.3.5.2 and 4.3.5.3) was better at highlighting relevant gene changes.

Q-PCR was carried out on five of the relevant genes shown in Table 4.11, and one housekeeping gene. The genes were chosen according to their potential biological significance, as well as the method by which they were highlighted.

The genes were: a chloride channel protein (D50497), substance K receptor (M31838), vasopressin receptor (Z11690), neuronal acetylcholine receptor beta-2 subunit (L31622), granulocyte colony stimulating factor (U37101) and cytoplasmic β-actin (V01217). The chloride channel protein and the vasopressin receptor may both be involved in water transport and reabsorption, and both were highlighted by the t-test method. Substance K receptors have been implicated in bronchoconstriction of large airways and enhancement of vascular permeability. Granulocyte colony stimulating factor (GCS-F) has been shown to significantly increase alveolar cell recruitment and pulmonary oedema (Azoulay *et al.*, 2003). Both the substance K receptor and GCS-F were selected using the standard deviation (sd) method. The acetylcholine receptor was selected because it was identified by both methods. The housekeeping gene β–actin (V01217) was utilised because there appeared to be no change between saline and oedema samples.

After optimisation, the initial RT-PCR was partially successful, as illustrated in Figure 4.20.

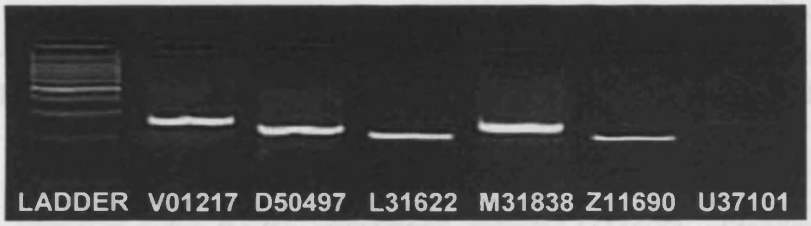

Figure 4.20 *Agarose gel containing all the PCR product (50µl) of the six genes named above. Ladder: 1kb made up of 100 bp graduations.*

Of the six genes, five were entirely successful and were immediately processed to generate standards for Q-PCR. The faint band visible for GCS-F was eluted using Sigma GenElute agarose spin columns, and re-run through the PCR reaction. This resulted in a clear band, and was used to produce standards for Q-PCR.

DNA sequencing confirmed that the recombinant clones contained the correct insert. These were then used to make up a series of standards for each gene. The standards were made to concentrations of 10fg, 100fg, 1pg, 10pg, and 100pg. The standards and unknown samples for each gene were analysed on an Applied Biosystems ABI PRISM 7700 Sequence Detection System.

The PCR reactions for all genes were successful. The standard curves were of a high calibre (e.g. Figure 4.21), with the lowest R^2 value equal to 0.92.

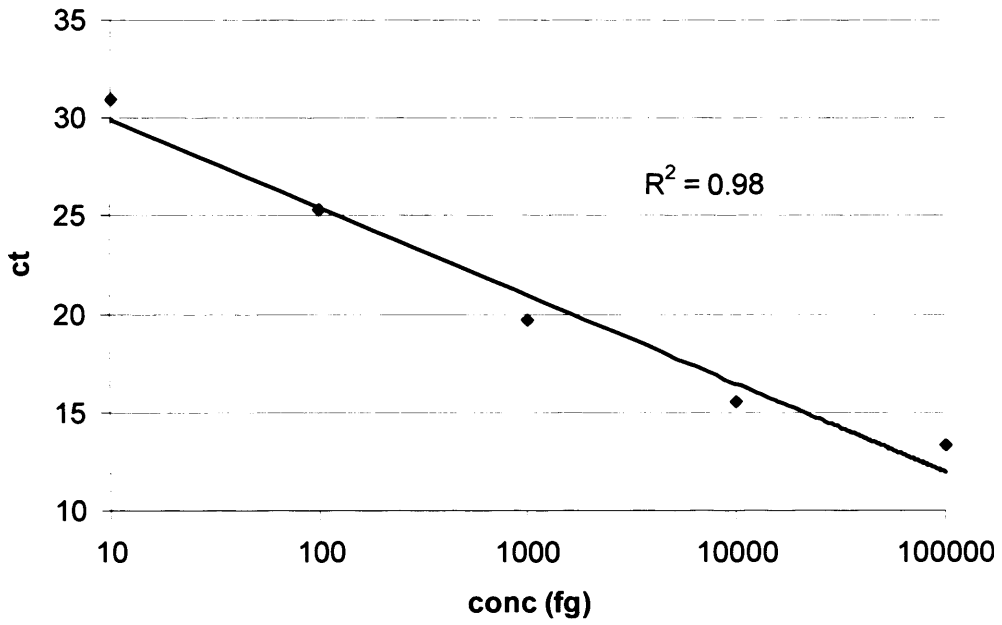

Figure 4.21 *Standard curve for the vasopressin receptor (Z11690). Standards for other genes are not shown.*

The concentration of each gene in the samples was determined from the standard curves. The average concentration of the saline controls and the average concentration of the bleomycin treated samples were used to calculate a ratio change for each gene. The results are shown in Table 4.13 and Figure 4.22.

The correlation between the macroarray and Q-PCR predicted ratio change was generally very high. This was especially true for genes M31838 and U37101, both of which were highlighted by the standard deviation method.

Genbank ID	Gene	Array ratio	Q-PCR ratio
D50497	Chloride channel protein	2.12	**1.56**
M31838	Substance K receptor	- 1.71	**- 1.64**
Z11690	Vasopressin receptor	- 2.10	**- 1.13**
L31622	Acetylcholine receptor	- 1.99	**- 1.87**
U37101	GCS-F	- 1.51	**- 1.51**
V01217	β-actin	1.01	**1.20**

Table 4.13 *Comparison between ratio predicted by the macroarray, and the ratio calculated from the Q-PCR data.*

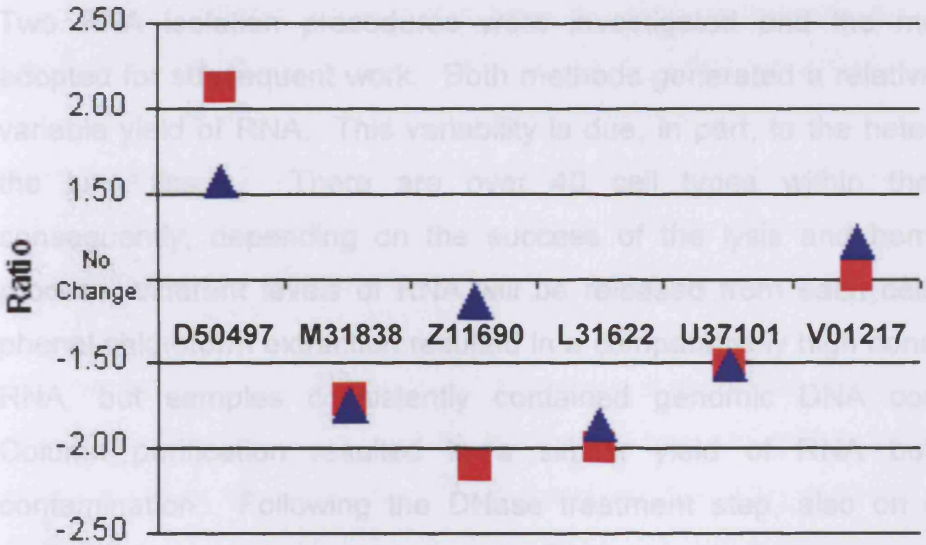

Figure 4.22 *Comparison between ratio change predicted by the macroarray (■) and ratio change determined by the Q-PCR (▲).*

4.5 DISCUSSION

4.5.1 MACROARRAY OPTIMISATION

Optimisation of the macroarray procedure was successfully achieved by paying particular attention to the hybridisation solution and probe purification, but primarily by ensuring high quality RNA.

An essential requirement for any gene expression study is the production of good RNA samples. The ability to obtain conclusive and reproducible results from an array is limited by the purity of the starting material. This chapter has reviewed the development of the most suitable method for isolation of RNA from lung tissue, and the optimisation of the macroarray procedure.

Two RNA isolation procedures were investigated and the most suitable adopted for subsequent work. Both methods generated a relatively high, yet variable yield of RNA. This variability is due, in part, to the heterogeneity of the lung tissue. There are over 40 cell types within the lung and consequently, depending on the success of the lysis and homogenisation process, different levels of RNA will be released from each cell type. The phenol chloroform extraction resulted in a comparatively high concentration of RNA, but samples consistently contained genomic DNA contamination. Column purification resulted in a similar yield of RNA but with less contamination. Following the DNase treatment step, also on column, the purity of the sample was increased. These conclusions were supported by both agarose gel electrophoresis and GeneQuant analysis. These findings dictate that column purification of RNA, with additional DNase treatment, should be implemented in all subsequent research.

After the macroarray procedure was optimised, the consistency and quality of the array images was greatly improved.

4.5.2 *DATA NORMALISATION AND ANALYSIS*

To gain a more comprehensive understanding of the oedematous reaction in the lung, 18 rats were used for genetic analysis. This approach was chosen in preference to using replicate samples from one tissue source. Obtaining replicates from different biological samples results in increased random error, but the findings have better external validity and broader applicability (Nadon and Shoemaker, 2002). The variation in genetic expression may be due to inherent differences in animal response to treatment and day-to-day experimental variations. Initial normalisation of the data was performed to overcome these experimental differences. Biological variation was addressed by the number of sample replicates and the design of the normalisation and data analysis methods.

The range method of analysis was a good technique for determining significant genes from a limited number of samples. A small modification of this method may improve the robustness of the analysis. The mean of the three data points may not be the best value for calculating the ratios since one extreme value could skew the data. For further experimental analysis using a small number of replicates, the median or mid-range value should be used.

The range method was developed to include a statistical element, in the form of the standard deviation method. However, this was only appropriate with a larger number of replicates. The standard deviation method was a very stringent analysis method, where any gene that fell outside the two standard deviation limit was considered to be altered by the treatment to the 0.05 significance level. Therefore, when the mean of all nine genes fell outside this control range, the gene was considered to be a reliable marker for oedema. Once the control data set had been established, individual samples could easily be assessed against it. As such, this approach had a good potential for clinical use, for example, screening of patients receiving bleomycin treatment.

The t-test was used to generate more statistical evidence of altered gene expression. This technique is appropriate for use on both small and large

sample sets, but cannot be used to compare one individual sample against a control data set.

Navigator was a useful tool for visualising the global expression patterns by displaying the information in a graphical form. The data was shown according to the relative intensity ratio which resulted in all down-regulated genes being compressed to a region between one and zero (whereas up-regulated genes ranged from one to infinity). However, different representations can be utilised. A logarithmic scale could be used to plot the ratios and remove this imbalance. Navigator is most useful when studying the gene expression separated according to pathology. The biological effect of the oedema becomes more noticeable. The problem with this method was the limited number of exact duplicates these data produce, which reduces confidence in the data.

Spotfire provided a good visual interpretation of the array data, but no additional information was supplied. Some of the genes identified by a combination of these analysis methods are discussed below.

4.5.3 Gene Changes Occurring in Mild Oedema

A group of five up-regulated ion channels and trafficking proteins were identified as significant following bleomycin-treatment. Of these genes, three were chloride channels. These genes may be involved in movement of water molecules by active transport. Up-regulation could result in increased movement of water, an event which is likely to occur during oedema. In contrast, a vasopressin receptor (Z11690), which is involved in water reabsorption, was down-regulated by over two-fold. Vasopressin controls the resorption of water and regulates the osmotic content of blood. In the kidney it acts on the renal collecting ducts, increasing the permeability to water (Nielsen *et al.,* 1995). Therefore, in the lung, down-regulation of this gene may reduce cellular permeability. This could lead to increased water on the alveolar surface, which is known to occur during oedema. Mineralocorticoid receptors (M36074) are also involved in regulation of water balance via an

effect on ion transport in the epithelium of the renal tubules. If a similar response occurs in the lung, down-regulation of this gene may lead to reduced movement of water away from the lung surface. This could again result in water accumulation in the alveolar spaces.

All of the remaining genes were down-regulated. Several of the hormone receptors appeared to be involved in the physiological response to oedema. The substance K receptor (M31838) and gastrin-releasing peptide receptor (X56661) affect smooth muscle constriction (Haley *et al.*, 2001; Lach *et al.*, 1993). Down-regulation could affect dilation of the conducting airways of the lung, which should increase the flow of air to the lungs. This would seem appropriate as the air spaces are covered by the oedematous fluid reducing the level of oxygen exchange. More direct links to oedema were unclear. Granulocyte colony stimulating factor (U37101) mediates the inflammatory response and is involved in the enhancement of vascular permeability (Sedgwick *et al.*, 2002). Gastrin-releasing peptide receptor (X56661) is implicated in vasodilation (Clive *et al.*, 2001). Conversely, the serotonin receptors (L05596, L10072, L10073), are involved in pulmonary vascular and airway constriction (Selig *et al.*, 1988); effects often observed during the inflammatory process. Alpha 1B adrenergic receptor (D32045) is also implicated in venule constriction (Leech and Faber, 1996). Glucocorticoid receptors (M14053) are thought to be involved with anti-inflammatory responses (Walsh *et al.*, 2003). Down-regulation could result in increased inflammatory responses, indicated by the elevated number of free cells in BAL.

4.5.4 GENE CLUSTERING

Clusters of genes are more reliable as markers for a pathological reaction, as a single anomaly should not effect the successful identification of oedema. Of the 31 significant genes identified, five belonged to the ion channels and trafficking proteins family, all of which are up-regulated. The 25 genes classified as receptors included three genes encoding nuclear receptors (J03933, M36074, M14053) which were closely associated. Although it is not

clear how these genes are related to oedema, as a cluster they were worth considering further.

The Phylogenic tree predictor (Tree Top) was used to determine the relationship between the genes. The genes were clustered in functionally-related families. A large group containing a number of hormone receptors and neurotransmitter receptors was identified. This contained several more tightly clustered groups. A number of specific hormone receptors were grouped into two clusters containing four genes each. A group of six genes encoding for four GABA-A receptors and two other hormone receptors was also identified. The substance K receptor and serotonin receptor were also clustered together, indicating a similar structure and function. However, the separation between these clusters was small and all these genes act in a similar manner to each other. The largest separation identified by Tree top was the group of genes encoding for the ion channels and trafficking proteins. As these genes behave in a different way to the majority of the altered genes (all up-regulated by approximately two-fold), this cluster of genes have potential as markers for early oedema.

4.5.5 Q-PCR

The changes in gene expression predicted by the macroarray were confirmed by Q-PCR. All of the genes tested showed an extremely high level of correlation, with the exception of the vasopressin receptor (Z11690). However, even in this case, the genetic response was shown to be down-regulated, which was in agreement with the change predicted by the array. The closest correlation was for the substance K receptor (M31838) and GCS-F (U37101) both of which were identified using the 2sd method. The gene encoding for the acetylcholine receptor (L31622) which was identified using both methods was also accurately predicted. This indicated that the 2sd method may be the best technique for identifying significant changes in genetic expression. Nevertheless, the t-test was also appropriate for selecting relevant genes, and may pick up some genes falsely discarded by

the very stringent 2sd method. The most effective approach may be to combine these two techniques (Balharry *et al.*, 2005).

4.6 CONCLUSIONS

In conclusion, the preliminary macroarray analysis has provided new transcriptional data on the mechanisms of the early events leading to pulmonary oedema following bleomycin treatment. High numbers of replicates (n=9) implies a good level of trust in the resulting data, and has been confirmed by Q-PCR. New methods have been developed for successful analysis of macroarray data. The t-test is a well established conventional method with recognised statistical significance. The standard deviation method is good for analysing groups of data. It can also be used to compare individual unknown samples against an established control range, which may be more practical in industrial/medical scenarios. The range method is a suitable alternative to the 2sd method for studies where obtaining a large number of replicates is not practicable.

CHAPTER 5:

ANALYSIS OF TRANSCRIPTIONAL CHANGES IN PERSISTENT AND SEVERE OEDEMA

5.1 INTRODUCTION

The toxicological effect of bleomycin instillation into the rat lung has been studied using biochemical analysis of BAL fluid (Chapter 2) and histology (Chapter 3). These investigations showed that bleomycin produced different biological endpoints relating to both dose (single or double) and time post-instillation.

A transient model of mild oedema resulted from a single bleomycin instillation. Utilising this model, the changes in mRNA expression during the onset of mild oedema (three days post-single instillation) have been identified (Chapter 4). The oedema persisted until seven days after instillation, whereupon the lung repair mechanisms began. After this time, the lung tissue rapidly returned to its normal state. In order to study this more persistent form of oedema, and some repair mechanisms, gene expression analysis was carried out on tissue seven days after a single bleomycin instillation.

Following a double bleomycin instillation, a model of severe oedema developed (Chapter 3). By using both toxicology and histology as tools for identifying oedema, the most significantly damaged tissue was identified at day three after the second instillation. As such, this time point was selected to profile gene expression changes during severe oedema.

Successful optimisation of the macroarray procedure and subsequent analysis (Chapter 4) resulted in clearly defined procedures which generate high levels of confidence in the gene expression data (Balharry *et al.,* 2005). This facilitated the objective of this study, which was to investigate altered gene expression in oedematous tissue in order to gain a better understanding of the genetic mechanisms underlying the disease state.

5.2 MATERIALS AND METHODS

5.2.1 MATERIALS AND SUPPLIERS

All materials and suppliers are detailed in Section 4.2.1. A brief summary of the materials needed for RNA extraction and the array procedure are outlined below.

Supplier:	Materials:
Qiagen, West Sussex	RNeasy Mini kit (74104), QIAshredders (79654), RNase-Free DNase Set (79254)
Clontech, Oxford	Atlas™ Rat 1.2 Macroarray (7854-1)
Amersham, Buckinghamshire	[α-^{32}P]dATP (10 µCi/mmol) (PB 10204)
Sigma-Aldrich, Dorset	Salmon Testes DNA (9.5 mg/ml) (D7656)
Amersham, Buckinghamshire	Storage Phosphor Screen (63-0034-89)
Clontech, Oxford	AtlasImage 2.0

The stock solutions required to carry out the array procedure are detailed in Section 4.2.2.1.

5.2.2 METHODS

RNA was isolated (Sections 4.3.1.2 and 4.3.1.3) from lung tissue collected seven days after a single bleomycin instillation, and three days after a double bleomycin instillation. The array procedure was carried out as described in Section 4.3.2. The resulting data was normalised (Section 4.3.4), and analysed utilising the standard deviation method (Section 4.3.5.2) and a Student's t-test (Section 4.3.5.3). Further analysis was carried out using phylogenic tree clustering (Section 4.3.8).

5.3 RESULTS

5.3.1 RELEVANT GENES IDENTIFIED DURING PROGRESSIVE OEDEMA

5.3.1.1 STANDARD DEVIATION AND T-TEST ANALYSIS

The quantitative data generated for each of the arrays by AtlasImage 2.0 was analysed using the standard deviation method and a two-tailed t-test (Sections 4.3.5.2 and 4.3.5.3). Genes with a consistent change in expression were identified and limited to genes with a ratio change of over 1.5. The resulting list of relevant genes for persistent oedema (day seven, single instillation) is shown in Table 5.1.

Progressive oedema was studied using lung tissue taken seven days after a single intratracheal bleomycin instillation. In comparison to saline-treated tissue, 53 genes were identified as significantly altered in bleomycin-treated lung. With the exception of one gene, all genes were down-regulated. The candidate genes were assigned into five major functional groups (Figure 5.1), which included ion channel and trafficking proteins, kinases, metabolism proteins, hormones and growth factors, cytokines and chemokines. The main significant gene changes are outlined below:

- A group of ten genes encoding for ion channels and trafficking proteins (J03145, X74834, L77929, L39018, AF013598, M26643, M86621, X83580, X83583, L25264) were down-regulated by 1.6-fold on average. Ion channels have been shown to modulate the transport of fluid to and from the lung.

- A synapsin (M27925) and syntaxin (L20823) were both down-regulated by 1.6-fold. Synapsins encode for proteins involved in trafficking of molecules.

Genbank ID	Gene/Protein Name		Ratio
J03145	Glucose transporter protein	■	-1.51
X74834	Serotonin receptor 3	■	-1.53
L77929	G-protein activated K^+ inward rectifier	■	-1.52
L39018	Sodium channel protein 6	■	-1.66
AF013598	Proton gated cation channel drasic	■	-1.66
M26643	Skeletal muscle Na^+ channel protein α subunit	■	-1.54
M86621	Calcium channel, -type, α 2 subunit	■	-1.57
X83580	K^+ channel, inward rectifier 11	■	-2.11
X83583	K^+ channel-like protein, β cell	■	-1.59
L25264	G-protein activated inward rectifier K^+ channel 1	■	-1.51
M27925	Synapsin 2A		-1.60
L20823	Syntaxin 2 (STX2)		-1.60
J03577	Intrinsic factor precursor (INF)		-1.50
X54080	Cytochrome c oxidase, subunit VIIa	◇	-1.56
L09216	Secretory glycoprotein-3 (GP-3)	◇	-1.53
M33986	Cytochrome P-450 19	◇	-1.53
U60063	Aldehyde dehydrogenase 2	◇	-1.56
M14053	Glucocorticoid receptor		-1.95
M96377	Non-processed neurexin II-beta major		-1.51
L35767	Very low-density lipoprotein receptor precursor		-1.71
X13722	Low-density lipoprotein receptor precursor		-1.90
X66539	Tumour necrosis factor α precursor (TNF-α)	●	-1.57
M36589	β-nerve growth factor precursor (β-NGF)	●	-1.55
D64085	Fibroblast growth factor 5 (FGF5)	●	-1.66
Z25868	Bone morphogenic protein 2	●	-1.51
U25651	Phosphofructokinase 1	□	-1.63
U25684	Thymosin β-like protein	□	6.31

Genbank ID	Gene/Protein Name		Ratio
M17523	Peptide YY precursor (PYY)	□	-1.77
AF010466	Interferon gamma precursor (IFN-gamma)		-1.65
U69272	Interleukin 15 (IL-15)		-1.53
M64711	Endothelial 1 precursor	□	-1.52
M69055	Insulin-like growth factor-binding protein		-1.67
M88469	F-spondin precursor		-1.51
U03628	Arrestin C		-3.63
X58631	Tyrosine-protein kinase	▲	-1.58
U13396	Jak 2 tyrosine-protein kinase	▲	-1.69
L27112	c-jun N-terminal kinase 2 (JNK2)	▲	-1.55
L27128	c-jun N-terminal kinase 3 (JNK3)	▲	-1.63
M90661	Insulin receptor-related receptor-α	▲	-1.64
U22296	Casein kinase 1	▲	-1.74
M16112	Calcium/calmodulin-dependent protein kinase	▲	-1.60
D26178	Serine/threonine kinase	▲	-1.56
U23443	PAK-α serine/threonine kinase	▲	-1.99
X60767	Cell division control protein 2 homolog (CDC2)	▲	-2.26
D31838	Wee1 tyrosine kinase	▲	-1.67
D89863	Ras-related protein m-ras		-1.54
U12187	Ras associated with diabetes (RAD1)		-1.53
M17527	Adenylate cyclase-inhibiting G α protein		-1.54
Y14019	Rab-3b ras-related protein	■	-1.51
M75153	Rab-11A	■	-1.69
M95780	G protein, gamma 5 subunit	■	-1.74
U18771	Rab26, ras reated GTPase	■	-2.22
X78605	Rab4B, ras related GTPase	■	-1.55

Table 5.1 *Relevant genes (seven days, post single dose) highlighted using a combination of the 2sd method and a t-test. The major functional groupings are indicated:* ■ *Ion channels and trafficking proteins,* ▲ *Kinases,* ◇ *Metabolism proteins,* ● *Growth factors, cytokines and chemokines,* □ *Hormones*

- A group of four genes encoding for metabolism proteins (X54080, L09216, M33986, U60063) were altered by ratios of between -1.53 and -1.56.

- The only gene to be significantly altered at both three and seven days after a singe bleomycin instillation was encoding for a glucocorticoid receptor (M14053). Glucocorticoids have been shown to modulate anti-inflammatory responses. At both time points this gene was down-regulated by approximately two-fold.

- Four genes classified as growth factors, cytokines and chemokines (X66539, M36589, D64085, Z25868) were down-regulated by approximately 1.6-fold. These genes have potential roles in the regulation of epithelial and endothelial cell proliferation.

- Peptide YY (M17523) plays an important role in regulating the secretion of fluids. This gene was down-regulated by 1.8-fold.

- Interferon gamma (AF010466) is a pro-inflammatory, pro-apoptotic protein, which was down-regulated by 1.7-fold.

- Interleukin 15 (U69272) was down-regulated by approximately 1.5-fold and is one of a large number of cytokines involved in the innate immune response.

- Endothelial 1 (M64711) is involved in vasoconstriction and was altered by -1.5-fold.

- The most down-regulated gene was encoding for arrestin C (U03628), which was altered by approximately four-fold. Arrestins mediate signal transduction.

- The largest group of genes at this time point consisted of 11 genes encoding for kinases (X58631, U13396, L27112, L27128, M90661, U22296, M16112, D26178, U23443, X60767, D31838). These genes are involved in a number of signalling pathways including intracellular signalling, immune responses and cell cycle. On average, the kinases were down-regulated by approximately 1.7-fold.

- Six genes were identified that encode for ras-related proteins (D89863, U12187, Y14019, M75153, U18771, X78605). Ras proteins are involved in intracellular signal transduction and were down-regulated by approximately 1.6-fold.

- Only one gene was up-regulated in bleomycin-treated tissue. This gene was encoding for thymosin β-like protein (U25684) and was altered by 6.3-fold; the largest change observed at this time point. Thymosin proteins have been shown to have a stimulatory effect on immune responses.

5.3.1.2 PHYLOGENIC TREE CLUSTERING

Tree Top was used to cluster genes according to the homology between the gene sequences. This identified clusters of related genes which have similar sequence and function. The information was represented as a dendogram. The data for persistent oedema (day seven, single instillation) are shown in Figure 5.1.

There were several genes which were associated in pairs (Figure 5.1, clusters 4, 6 and 7), but there were three large groups. The first cluster of eight genes (Figure 5.1, cluster 1) were encoding for six trafficking genes and two genes involved in metabolism. The second group of eight genes (Figure 5.1, cluster 2) consisted of three potassium channels, four kinases and the intrinsic factor gene. The third main cluster (Figure 5.1, cluster 7) was made up of two

growth factors and all five of the ras-related proteins. All the groups behaved in a similar manner, being down-regulated by approximately 1.6-fold.

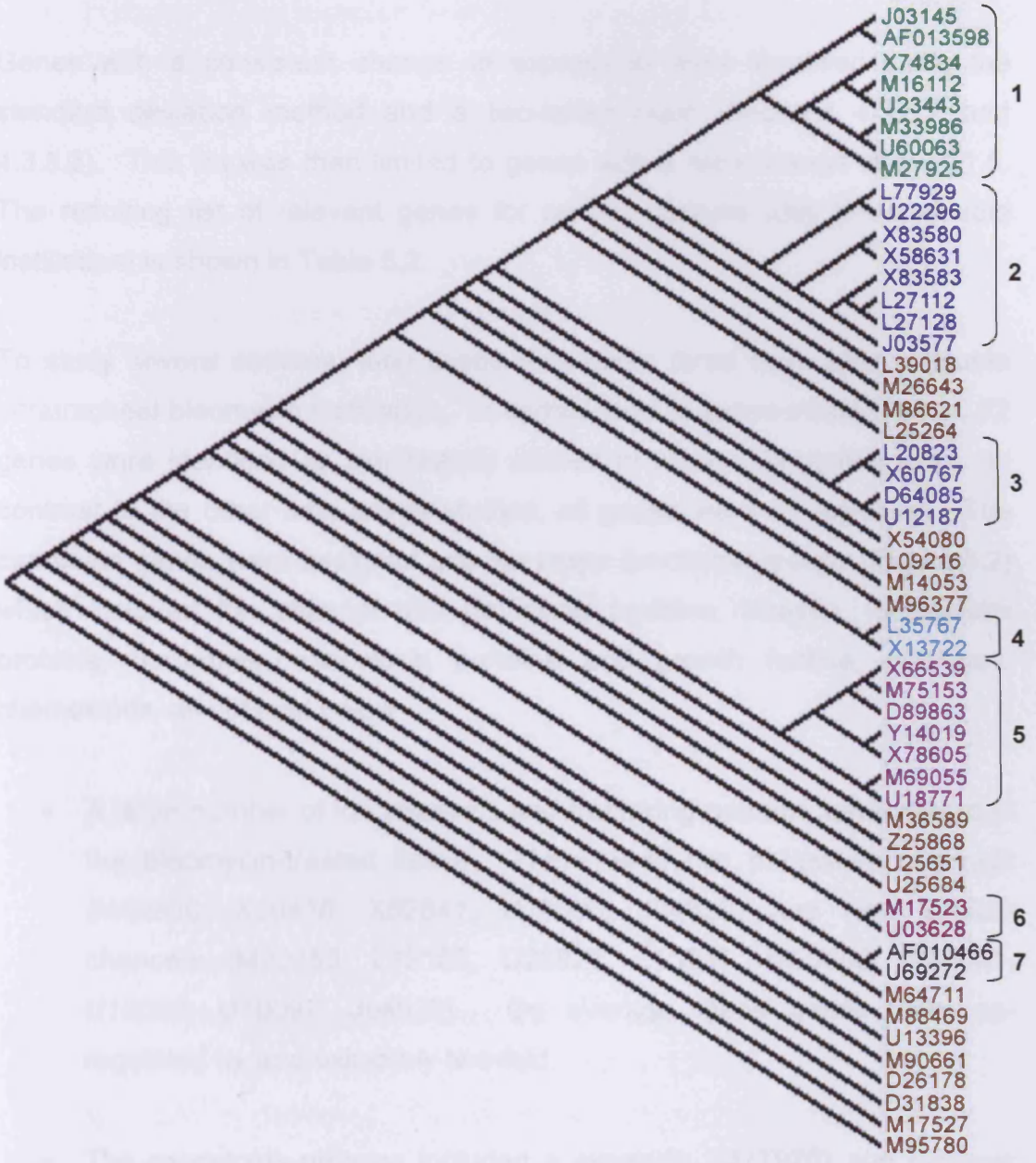

Figure 5.1 *Phylogenic tree clustering of relevant genes from seven days after a single bleomycin instillation.*

5.3.2 *Relevant Genes Identified During Severe Oedema*

5.3.2.1 *Standard Deviation and T-test Analysis*

Genes with a consistent change in expression were identified using the standard deviation method and a two-tailed t-test (Sections 4.3.5.2 and 4.3.5.3). This list was then limited to genes with a ratio change of over 1.5. The resulting list of relevant genes for severe oedema (day three, double instillation) is shown in Table 5.2.

To study severe oedema, lung tissue was taken three days after a double intratracheal bleomycin instillation. In comparison to saline-treated tissue, 72 genes were identified as significantly altered in bleomycin-treated lung. In contrast to the other time points studied, all genes were up-regulated. The candidate genes were assigned into six major functional groups (Figure 5.2) which included ion channel and trafficking proteins, kinases, metabolism proteins, hormones, exocytosis proteins and growth factors, cytokines, chemokines, as outlined below:

- A large number of ion channels and trafficking proteins were altered in the bleomycin-treated tissue. There were five potassium channels (M59980, X16476, X62841, U10096, J04629) and nine sodium channels (M22253, L19102, U28927, L13257, M85300, M85301, U10096, U10097, J04629). On average these genes were up-regulated by approximately two-fold.

- The exocytosis proteins included a synapsin (M27925) and syntaxin (L20823) which were altered by two-fold.

- Also included in this group of genes were two synaptotagmins (AF000423, L38247). Two similarly related genes were the genes encoding for the secretogranins (M93669, U02983) which were up-

regulated by over 2.5-fold. These four genes are involved in the formation and release of synaptic vesicles.

- Included in the receptor family were two P2Y purinoceptors (U22830, D63665) which were up-regulated by approximately two-fold. These proteins may modulate the function of ion channels.

- This group of receptor genes also includes a heat-stable enterotoxin receptor (M55636). This gene is thought to regulate salt and water transport and was altered by approximately two-fold.

- A group of ten growth factors, cytokines and chemokines (M32748, L15305, M60525, U00620, D32207, AF014827, D10763, D64085, M22427, X55183) were all significantly altered in bleomycin-treated tissue. These genes are thought to affect a number of epithelial and endothelial alterations. On average, the growth factors, cytokines and chemokines were up-regulated by approximately three-fold.

- The group of five genes encoding for hormones included peptide YY (M17523) and preprolactin (AF022935). These genes were up-regulated by approximately 2.5-fold and are thought to have an effect on osmoregulation.

- Also in the group of hormones was the gene encoding for vasoactive intestinal peptide (X02341). The receptor for this hormone (U09631) was also up-regulated. These genes are thought to have an effect on immune responses.

- Interleukin 1 (M98820) affects a pro-inflammatory response and was altered by 2.5-fold.

Genbank ID	Gene/Protein Name		Ratio
M34097	natural killer (NK) cell protease 1		1.84
M22253	sodium channel I	■	1.56
M59980	voltage-gated K+ channel protein	■	2.03
X16476	potassium channel drk1, delayed rectifier	■	2.23
X62841	potassium channel	■	1.96
X61394	calcium channel, beta subunit, brain	■	2.31
D63834	monocarboxylate transporter MCT1	■	2.45
L19102	sodium dependent sulfate transporter	■	2.86
U28927	Na+/Cl- betaine/GABA transporter	■	1.58
L13257	sodium/phosphate cotransporter 2	■	2.24
M85300	sodium/hydrogen exchange protein 3	■	1.66
M85301	sodium/hydrogen exchange protein 4	■	2.19
M95762	gamma-aminobutyric acid (GABA) transporter 2	■	3.13
U10096	sodium-potassium-chloride cotransporter	■	2.24
U10097	sodium/chloride cotransporter	■	2.43
J04629	sodium/potassium-transporting ATPase beta 2 subunit	■	1.57
U08344	ATPase, copper-transporting, Menkes protein	■	1.94
L05435	synaptic vesicle protein 2 (SV2)	■	1.93
M97381	synaptic vesicle amine transporter (SVAT)	■	2.07
AF007775	aquaporin (AQP 8)	■	1.61
U77971	urea transporter	■	1.61
U89529	fatty acid transport protein	■	2.36
L19031	organic anion transporter	■	2.07
U67958	urate transporter/channel	■	2.29
M27925	synapsin 2A	◇	1.92
L20823	syntaxin 2 (STX2)	◇	2.79
AF000423	synaptotagmin XI; membrane trafficking protein	◇	1.53
AF007836	Rab3 effector in synaptic-vesicle fusion	◇	1.57
L38247	synaptotagmin IV (SYT4)	■	1.86
M93669	secretogranin II precursor (Sg2)	■	2.60
M35991	fatty acid-binding protein		1.96
U09631	vasoactive intestinal polypeptide receptor 2 precursor (VIP-R-2)	▲	1.93
X57514	GABA-A receptor, gamma 1 subunit	■	2.88
L08491	GABA receptor alpha 2 subunit precursor	■	2.50
M61099	metabotropic glutamate receptor 1 precursor	▲	3.24
M92076	glutamate receptor, metabotropic 3	▲	1.88
U22830	P2Y purinoceptor	▲	1.91

Table 5.2 *Relevant genes (three days post double dose) highlighted using a combination of the 2sd method and a t-test. The major functional groupings are indicated:*

■ *Ion channels and trafficking proteins,* ▲ *Kinases,* ◇ *Exocytosis proteins,*

● *Growth factors, cytokines and chemokines,* □ *Hormones,* ▲ *Receptors*

Genbank ID	Gene/Protein Name		Ratio
D63665	P2Y purinoceptor 6	▲	2.19
M55636	heat-stable enterotoxin receptor precursor	▲	2.29
M94555	neuromedin U-23 precursor (NMU-23)		2.26
M32748	leukemia inhibitory/cholinergic neuronal differentiation factor	●	2.36
L15305	glial cell line-derived neurotrophic factor precursor	●	2.99
M60525	VGF8A protein precursor	●	2.64
U00620	granulocyte-macrophage colony-stimulating factor (GM-CSF)	●	3.08
D32207	trombopoietin	●	3.22
AF014827	vascular endothelial growth factor D (VEGF-D)	●	2.34
D10763	erythropoietin precursor (EPO)	●	2.19
D64085	fibroblast growth factor 5 (FGF5)	●	2.22
M22427	basic fibroblast growth factor (bFGF)	●	4.06
X55183	growth factor, schwannoma-derived	●	3.16
M36804	follicle stimulating hormone beta-subunit	□	2.54
M17523	peptide YY precursor (PYY)	□	2.35
X02341	vasoactive intestinal peptide	□	2.72
AF022935	preprolactin (Prl)	□	2.80
M54987	corticotropin-releasing hormone	□	3.16
M98820	interleukin 1, beta		2.52
U10071	cocaine/amphetamine-induced rat transcript (CART)		2.39
X58023	corticotropin-releasing factor binding protein		1.71
U02983	secretogranin 3 (Sg3)	■	2.91
X57986	cAMP-dependent protein kinase catalytic subunit	▲	2.01
L29281	Initiation factor-2 kinase	▲	3.36
L27128	c-Jun N-terminal kinase 3 (JNK3)	▲	1.84
X07286	protein kinase C alpha type (PKC-alpha)	▲	1.87
X07287	protein kinase C gamma type (PKC-gamma)	▲	1.99
X07320	phosphorylase kinase, gamma subunit	▲	2.07
U63971	rhodopsin kinase	▲	2.31
AB005541	serine/threonine kinase PCTAIRE3	▲	2.43
U28356	protein-tyrosine phosphatase	▲	1.91
X06889	Rab-3a ras-related protein	■	1.67
X06890	Rab-4a ras-related protein	■	8.20
X67241	guanine nucleotide release/exchange factor (GNRP)		2.27
U07798	14-kDa phospholipase A2 precursor (PLA2)	▲	2.21

***Table 5.2** continued:*

■ *Ion channels and trafficking proteins,* ▲ *Kinases,* ◇ *Exocytosis proteins,*

● *Growth factors, cytokines and chemokines,* □ *Hormones,* ▲ *Receptors*

- Kinases were altered in the bleomycin-treated tissue by approximately two-fold. These genes have been implicated in the control of cell-cycle and apoptosis.

- Two ras-related genes (X06889, X06890) were up-regulated at this time point. Rab3a (X06889) had an over eight-fold increase in expression, making it the most altered gene at all of the time points. These genes have an effect on endocytosis and exocytosis.

- Phospholipase A2 (U07798) precursor was shown to be altered in bleomycin-treated tissue by two-fold. This protein is involved in regulating inflammatory reactions.

5.3.2.2 PHYLOGENIC TREE CLUSTERING

The Phylogenic tree predictor (Tree Top) was used to determine the relationship between the genes. The genes were clustered in functionally related groups. The information for severe oedema (day three, double instillation) is represented as a dendogram shown in Figure 5.2. There were a large number of genes which were associated in small groups (Figure 5.2, clusters 3, 4, 5, 6, 7, 8, 10, 11 and 12), but there were four main groups (Figure 5.2, clusters 1, 2, 9 and 13). Of these groups, two appeared to be more significant. The first cluster consisted of eight genes (Figure 5.2, cluster 1), six of which were encoding for ion channels and trafficking proteins. The second group of six genes (Figure 5.2, cluster 2) was made up of a growth factor and five ion channels and trafficking proteins. These groups were considered to be potentially more significant than the other clusters because they could be related to changes occurring in the early oedema model (three days after a single bleomycin instillation).

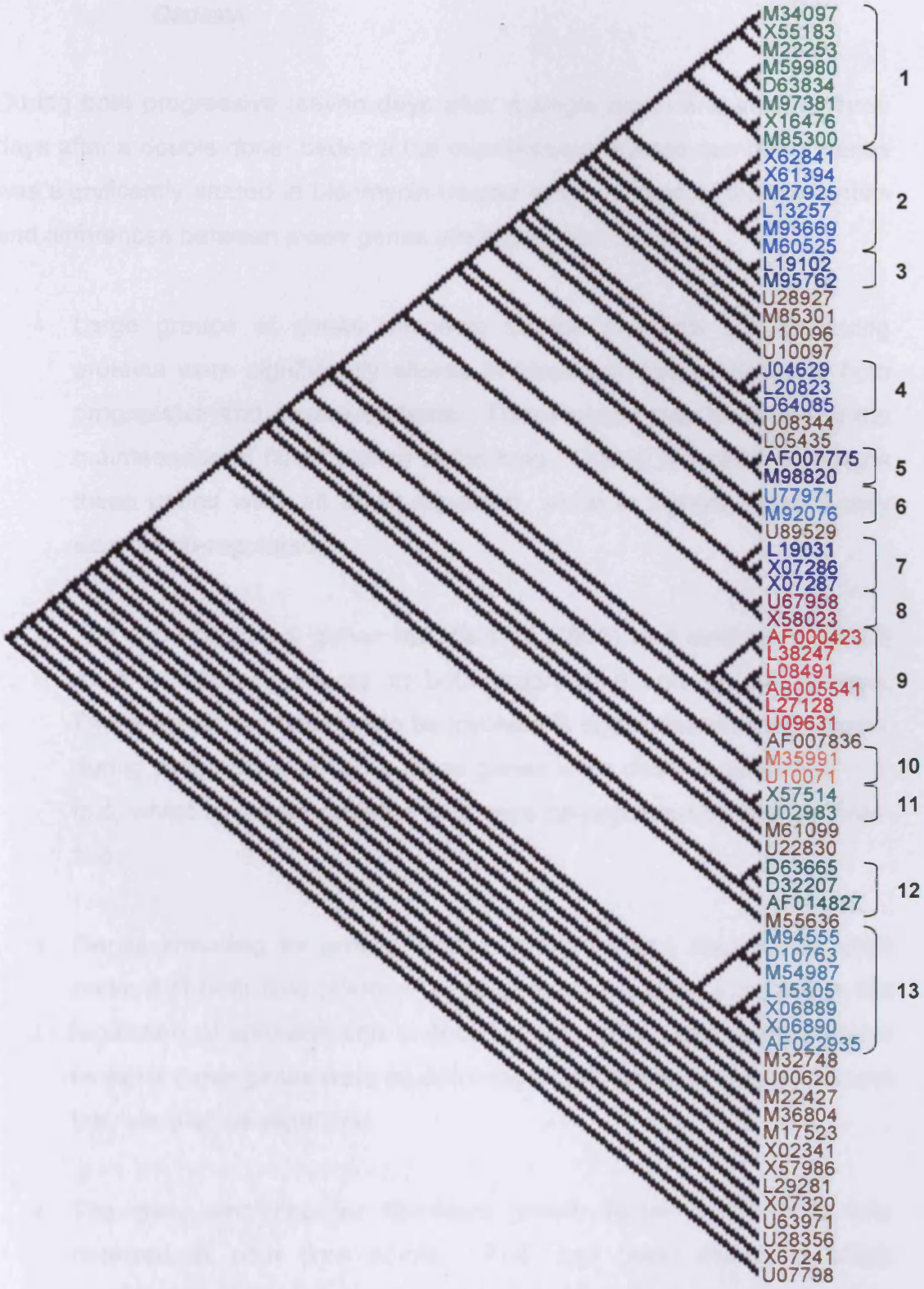

Figure 5.2 *Phylogenic tree clustering of relevant genes from three days after a double bleomycin instillation.*

5.3.3 *Comparison of Gene Changes in Progressive versus Severe Oedema*

During both progressive (seven days after a single dose) and severe (three days after a double dose) oedema the expression of a large number of genes was significantly altered in bleomycin-treated tissue. Some of the similarities and differences between these genes are highlighted below.

- Large groups of genes encoding for ion channels and trafficking proteins were significantly altered in bleomycin-treated tissue of both progressive and severe oedema. These genes may be linked to the maintenance of fluid balance in the lung. During progressive oedema these genes were all down-regulated, whilst in severe oedema they were all up-regulated.

- The two exocytosis genes synapsin (M27925) and syntaxin (L20823) were significantly altered in both progressive and severe oedema. These genes are believed to be involved in signal transduction. Again, during progressive oedema these genes were down-regulated by 1.6-fold, whilst in severe oedema they were up-regulated by two- to three-fold.

- Genes encoding for growth factors, cytokines and chemokines were present at both time points. These genes have been indicated in the regulation of epithelial and endothelial cell cycle. During progressive oedema these genes were all down-regulated, whilst in severe oedema they were all up-regulated.

- The gene encoding for fibroblast growth factor 5 (D64085) was detected at both time points. FGF has been shown to affect proliferation of epithelial and endothelial cells. As seen with the other growth factors, this gene was down-regulated by 1.7-fold during

persistent oedema, but was up-regulated by four-fold in severe oedema.

- Peptide YY (M17523) was found to be down-regulated in bleomycin-treated tissue taken seven days after a single instillation. In contrast, it was up-regulated in bleomycin-treated tissue from three days after a double dose. Peptide YY may be involved in osmoregulation.

- During progressive oedema, interleukin-15 (U69272), which is a pro-inflammatory cytokine, was down-regulated by 1.5-fold. Conversely, in severe oedema, interleukin-1, which is also pro-inflammatory, was found to be up-regulated by 2.5-fold.

- At both time points, ten genes encoding for various kinases were significantly altered. Kinases are involved in a large number of signalling mechanisms. Unlike the kinases which were down-regulated seven days after a single instillation, the kinases at three days after a double dose were all up-regulated.

- The gene encoding for C-jun N-terminal kinase 3 (L27128) was detected at both time points. This kinase is involved in pro-apoptotic responses. This gene was down-regulated seven days after a single bleomycin dose, but up-regulated three days after a double dose.

- During progressive oedema, six ras-related genes (D89863, U12187, Y14019, M75153, U18771, X78605) were down-regulated by roughly 1.5-fold. However, in severe oedema two different ras-related genes (X06889, X06890) were up-regulated by 1.7-fold and over eight-fold. These proteins have been implicated in trafficking of small molecules.

5.3.4 *Comparison of Gene Changes in Mild versus Progressive and Severe Oedema*

There were few similarities between the families of genes that were altered during all three stages of oedema. However, there appeared to be several specific genes which were consistent:

- At all three time points a number of ion channels and trafficking proteins were altered. In both mild and severe oedema (three days after a single or double dose of bleomycin) these genes were consistently up-regulated by approximately two-fold.

- The gene encoding for a Na+/Cl- betaine/GABA transporter (U28927) was up-regulated by approximately 1.6-fold in both mild and severe oedema.

- The gene encoding for a glucocorticoid receptor (M14053) was consistently down-regulated by approximately 1.9-fold in both mild and progressive oedema.

5.4 DISCUSSION

Following successful optimisation of the macroarray procedure, protocols for a simplistic analysis of the arrays were established (Chapter 4). These techniques were applied to two sample groups from the model of bleomycin-induced pulmonary oedema: seven days after the single instillation, which represented progressive injury, and three days after the double instillation which represented severe injury.

5.4.1 PROGRESSIVE OEDEMA

The large group of genes encoding for ion channels and trafficking proteins contained a number of potassium channels (L77929, X83580, X83583, L25264). Potassium channels in the epithelium play an essential role in electrolyte and fluid transport by regulating fluid clearance from the lung (O'Grady and Lee, 2003). Similarly, the two sodium channels (L39018, M26643) are involved in movement of sodium ions across the alveolar epithelium. This creates an osmotic force leading to re-absorption of alveolar fluid (Matalon *et al.*, 2002). Down-regulation of these six genes could result in increased fluid in the alveolar space, an event which is likely to occur during oedema. However, a previous study has shown that fluid clearance was increased despite down-regulation of alveolar sodium channels (Folkesson *et al.*, 1998).

Closely related to the trafficking proteins are a synapsin (M27925) and syntaxin (L20823). Synapsins encode for proteins involved in the regulation of neurotransmitter release. These phosphoproteins are widely distributed in nerve terminals and coat synaptic vesicles which can then bind to the cytoskeleton (Südhof *et al.*, 1989). Similarly, the syntaxins affect the docking of synaptic vesicles with the presynaptic membrane by acting as receptors (Bennett *et al.*, 1993). The alteration in expression of these genes may affect signal transduction.

The group of four genes encoding for metabolism proteins included Cytochrome c oxidase, which is one of the key functional and regulatory sites of energy metabolism. Subunit VIIa (X54080) is nuclearly encoded and involved in the assembly and regulation of this enzyme (Kadenbach *et al.*, 1991). This implies that reduced expression of the VIIa gene could result in reduced cytochrome c oxidase activity. In a previous *in vitro* study, partial inactivation of cytochrome c oxidase has been implicated in increased apoptosis (Das *et al.*, 2001). This may be occurring in the damaged lung tissue; as evidenced by the destruction of alveolar architecture revealed by the TEM images (Chapter 3). The cytochrome P450 (M33986) family are involved in metabolism of a large number of compounds, including foreign compounds, xenobiotics and other toxicants. Cytochrome P450 oxidises the xenobiotic, converting it into a more water-soluble derivative that is easier to excrete (Gonzalez, 2005). Down-regulation of this gene could potentiate the effect of the damage being caused by the bleomycin. Not only would bleomycin remain active, but any toxicants entering the alveoli due to the damage at the lung surface may not be effectively excreted.

The small family of growth factors, cytokines and chemokines included a gene encoding for tumour necrosis factor alpha (TNF-α). TNF-α (X66539) is a cytokine which plays a significant role in inflammation and the immune response (Grunfeld and Palladino, 1990). It is also involved in a number of cellular activities including differentiation and apoptosis (Leong and Karsan, 2000). The influence of TNF-α can be either pro- or anti-apoptotic, dependant on the nature of the stimulus (Sanlioglu *et al.*, 2004). Therefore, it is not possible to establish the effects of this gene in the bleomycin-treated tissue without further study.

TNF-α has also been linked to increased vascular permeability by either altering endothelial cell morphology, or by enhancing neutrophil-mediated cytotoxicity (Turnage *et al.*, 2002). Down-regulation of this gene may result in decreased vascular permeability, which is a potential candidate for a repair mechanism. Two growth factors, beta-nerve growth factor (β-NGF) and

fibroblast growth factor (FGF) were within this group of four genes. NGF (M36589) has been shown to promote epithelial cell proliferation in the eye (You *et al.*, 2000). Similarly, FGF (D64085) affects proliferation and differentiation of epithelial and endothelial cells (Warburton and Bellusci, 2004). The fourth gene in this group encodes for bone morphogenic protein (Z25868). This protein has been shown to induce the formation of epithelial cells (Zeisberg *et al.*, 2005). It was considered that if the effects of growth factors and bone morphogenic protein were consistent in lung tissue, then perhaps this would decrease levels of lung epithelial proliferation.

The hormone peptide YY (M17523) plays an important role in regulating gastrointestinal secretion of fluids (El-Salhy *et al.*, 2002). This protein inhibits the secretion of fluid and electrolytes, whist stimulating their absorption in the intestine (Mannon and Taylor, 1994). If a similar effect occurs within the lung, inhibited expression may result in increased secretion of fluids and reduced absorption. This in turn could increase the levels of fluid in the lung, as observed during oedema.

Interferon gamma (AF010466) has an inhibitory effect on cellular proliferation, and has been shown to induce apoptosis (Dai *et al.*, 1998). The effect of down-regulation of this gene may be to increase cellular proliferation and reduce apoptosis; mechanisms that could be linked to repair of the lung tissue. Interleukin 15 (U69272) is one of a large number of cytokines involved in the innate immune response. It stimulates natural killer (NK) cells, T- and B-cell proliferation and cytokine secretion (Yoshikai and Nishimura, 2000). Down-regulation of this gene could result in reduced inflammatory responses; although throughout the progressive oedema model, inflammatory responses appeared to be increased. Endothelial 1 (M64711) is secreted by endothelial cells and is involved in vasoconstriction (Yanagisawa *et al.*, 1988). Constriction of pulmonary vasculature is often observed during the inflammatory process. Down-regulation of Endothelial 1 could potentially combat this effect.

Arrestin C (U03628) was the second most highly altered gene at this time point. Arrestins mediate signal transduction by regulating G-protein-coupled receptor (GPCR) signalling. These proteins bind with most activated GPCRs, and prevent G-protein/receptor interaction, resulting in uncoupling of the receptor. One of the strongest associations is between arrestin and vasopressin receptors (Stalheim *et al.*, 2005). Reduction in the levels of arrestin may increase vasopressin activity, leading to reabsorption of water (Nielsen *et al.*, 1995). This would represent another step towards reinstating normal lung function.

The large group of kinases included two tyrosine-protein kinases (X58631, U13396), which are involved in a number of pathways including intracellular signalling (Foster, 1993), immune responses (Mustelin and Burn, 1993) and cell cycle. These kinases are involved in pathways which promote progression through the cell cycle and inhibit apoptosis (Tallett *et al.*, 1996). Down-regulation of these genes may cause damage to the epithelium, as observed at this time point, by reducing cell proliferation and inducing apoptosis. C-jun N-terminal kinases 2 and 3 (JNK2, JNK3) are involved in the transcription of pro-apoptotic genes (Gelderblom *et al.*, 2004) and induction of programmed cell death (Kanda and Miura, 2004). Down-regulation of JNK2 and JNK3 (L27112, L27128) could result in reduced cell death. This may be a defence mechanism in response to the destruction of the lung tissue due to bleomycin treatment. Casein kinases (U22296) are involved in many cellular processes. These include membrane transport and DNA repair pathways, induction of cell division and delaying apoptosis (Knippschild *et al.*, 2005). Cell proliferation is mediated by a number of proteins, including calcium/calmodulin-dependant kinases (CaMK) and cell division control protein 2 (CDC2). Progression through G_1 and from G_2 to M phase of the cell cycle is dependant on CaMK (M16112) (Kahl and Means, 2003). The transition from the G_2 to M phase can also be activated by a CDC2 (X60767)/cyclin complex (Black, 2000). Reduced expression of the casein kinase, CaMK and CDC2 genes might result in reduced cellular proliferation and increased apoptosis. There is a possibility that these mechanisms were occurring in the bleomycin-treated tissue, as indicated by the destruction of

the normal lung architecture. Conversely, Wee1 kinase (D31838) delays entry into mitosis (Kellogg, 2003); therefore down-regulation of this gene may promote cellular proliferation. This could be yet another feature of the repair mechanisms.

A small group of ras-related proteins (D89863, U12187, Y14019, M75153, U18771, X78605) was also identified. Ras proteins are small regulatory GTP-binding molecules involved in intracellular signal transduction (Hall, 1990). The ras-related proteins (D89863, U12187) play an essential role in regulating some of the physical exchanges between a cell and its environment, including endocytosis and exocytosis (Chardin, 1988). In particular, ras-related rab proteins (Y14019, M75153, U18771, X78605) have been implicated in intracellular trafficking of vesicles (Rosenfeld *et al.*, 2002).

The most altered gene expression during progressive oedema was encoding for thymosin β-like protein (U25684). Thymosin proteins have a stimulatory effect on immune responses by modulating the activity of cytokines and chemokines (Goldstein and Badamchian, 2004). In this instance, up-regulation could result in increased immune responses; an event which appeared to be confirmed by the influx of inflammatory cells to the lung (Section 2.4.1). There was also evidence that cells showing increased expression of thymosin β4 have a greater resistance to apoptosis (Iguchi *et al.*, 1999). This may be a response to the injury and represent another possible step toward repair.

The glucocorticoid receptor (M14053) was the only gene to be significantly altered during both mild (Chapter 4) and progressive oedema. Down-regulation of this gene may result in increased inflammatory responses similar to those observed in this study (Section 2.4.1).

Using the phylogenic tree predictor (Tree Top), three large groups of genes were detected. All the groups behaved in a similar manner, and as such, any one of these gene clusters could act as potential markers for progressive

pulmonary oedema. Unfortunately, at this stage, none of the clusters appeared to correlate with the clusters found at the early stages of oedema, i.e. three days after a single dose. This might be due to the increased level of repair-related gene changes. The only consistent gene was encoding for a glucocorticoid receptor which was down-regulated by about 1.9-fold at both three and seven days after a single bleomycin dose.

5.4.2 SEVERE OEDEMA

Similar to both mild and progressive oedema, a large number of ion channels and trafficking proteins were altered in the bleomycin-treated tissue. As previously discussed, these ion channels play a role in fluid reabsorption, therefore their up-regulation may result in increased fluid clearance from the lung; an event which is likely to occur in response to oedema. One of these genes encoded for a Na+/Cl- betaine/GABA transporter (U28927), which was also up-regulated three days after a single bleomycin dose (mild oedema). Betaine is an osmolyte used by plants, invertebrates and vertebrates to compensate for hypertonic stress (Petty and Lucero, 1999). The up-regulation of this gene could possibly be a response to the increased fluid on the lung, as observed during oedema. An aquaporin was also altered in bleomycin-treated tissue. In a similar manner to the other ion channels, the up-regulation of this gene might result in increased movement of water, in an attempt to equilibrate the osmotic pressure (Verkman and Mitra, 2000).

Closely related to the ion channel and trafficking proteins are the exocytosis proteins. These include a synapsin (M27925) and syntaxin (L20823) which were also significantly altered in the progressive oedema model (seven days after a singe dose). The effects of changes in expression of these genes have been discussed in Section 5.4.1. Also included in this group of genes are two synaptotagmins (AF000423, L38247). These proteins are involved in signal transduction by stimulating the release of synaptic vesicles (Südhof, 2004). Two similarly related genes are those encoding for the secretogranins (M93669, U02983). Secretogranins contribute to the formation of secretory vesicles and also have the ability to form ion channels (Taupenot *et al.*, 2003).

In a similar fashion to the synapsin and syntaxin, alteration in expression of synaptotagmins and secretogranins could effect signal transduction.

A number of receptors showed increased gene expression in bleomycin-treated tissue. These included two P2Y purinoceptors which belong to a family of G-protein-coupled receptors. These proteins may modulate the function of ion channels (Lee and O'Grady, 2003). P2Y purinoceptors have been shown to affect an increase in epithelial fluid (Leipziger, 2003), as observed during oedema. The heat-stable enterotoxin receptor (M55636) is believed to regulate salt and water transport in the intestine (Vaandranger, 2002). Should the same effect occur in the lung, up-regulation may lead to an increase in fluid on the alveolar surface.

A large group of genes encoding for growth factors, cytokines and chemokines were all significantly altered in bleomycin-treated tissue. Glial cell line-derived neurotrophic factor (GDNF) has been shown to promote epithelial cell proliferation in the eye (You *et al.*, 2000). Up-regulation of the GDNF (L15305) gene may stimulate epithelial repair. Granulocyte-macrophage colony-stimulating factor (GM-CSF) was another of the genes classed with this group. Excess phospholipid and protein on the lung can be ablated by increased GM-CSF (U00620), owing to its effect on alveolar macrophages (Trapnell and Whitsett, 2002). It has also been shown to modulate proliferation of the lung epithelium (Huffman Reed *et al.*, 1997). Both these effects of GM-CSF could be related to potential repair mechanisms. Vascular endothelial growth factor (VEGF) plays an important role in regulating vascular permeability in a number of organs (Mura *et al.*, 2004). Elevated levels of VEGF (AF014827) are strongly related to increases in capillary leak (Thickett *et al.*, 2002). In the lung tissue samples, VEGF was over two-fold higher in the damaged tissue, which may have led to increased breakdown of the endothelial/epithelial barriers and increased fluid on the lung surface. Erythropoietin (EPO) is a multifunctional cytokine that has potent tissue-protective activity. These effects are governed in part by the inhibition of apoptosis and restoration of vascular auto-regulation (Brines *et al.*, 2004). Up-regulation of EPO may result in reduced apoptosis and restoration of the

damaged vasculature observed during oedema. FGF was up-regulated at this time point, compared to down-regulation at seven days post-instillation of a single bleomycin dose. The effects of FGF (D64085) have been described previously. The up-regulation of this gene could result in increased proliferation of epithelial and endothelial cells. The most effected of the growth factors was basic FGF (bFGF), with a four-fold up-regulation in gene expression. Increases in bFGF (M22427) could lead to increased endothelial proliferation and differentiation (Yayon and Klagsbrun, 1990). Thus, the effects of FGF and bFGF may also be involved in the potential repair mechanisms.

Within the group of hormones, peptide YY (M17523) was found to be down-regulated in bleomycin-treated tissue taken seven days after a single instillation. In contrast, it was up-regulated in bleomycin-treated tissue from three days after a double dose. Increased levels of peptide YY could lead to increased reabsorption of fluid from the lung, acting as a potential repair mechanism. The hormone vasoactive intestinal peptide (VIP) and its receptor (U09631) are thought to have an influence on a variety of immune responses (Bellinger *et al.*, 1996). The increased inflammatory response is evidenced by the large influx of free cells to the lung. VIP (X02341) is also implicated in liquid secretion (Ballard and Inglis, 2004). Again, the up-regulation of this gene may result in increased liquid on the lung. Preprolactin (AF022935) is a precursor to prolactin, which has been shown to have osmoregulatory effects (Robertson, 1989) and elevated levels may result in increased fluid on the lung surface. However, prolactin has also been implicated in epithelial cell differentiation in the skin (Paus, 1991), which is more likely to form part of the repair mechanisms.

Interleukin 1 (IL-1) mediates a potent pro-inflammatory response, including the activation of neutrophils (Tanabe *et al.*, 2005). The up-regulation of IL-1 (M98820) causes an increase in inflammation, which coincides with the increased number of inflammatory cells in BAL at this time point.

Similar to progressive oedema, a large number of kinases were altered in the bleomycin-treated tissue. Modulation of pro-inflammatory responses is known to be one of the effects of the cAMP-dependant protein kinase (X57986) (Panettieri, 2002). Up-regulation of this gene might cause an increased inflammatory response. Initiation factor-2 Kinase plays an important role in the control of cell growth and survival (Kaempfer, 2003). Activation of this kinase can induce apoptotic cell death (Clemens, 2004). JNK3 (L27128) was altered during both progressive and severe oedema; the effects of JNK 3 were previously described in Section 5.4.1. The two isoforms of protein kinase C (PKC) have a distinct role in the regulation of cell cycle. Over-expression of these genes can attenuate cellular proliferation (Zhou and Hershenson, 2003). Up-regulation of initiation factor-2 kinase, JNK3 and the PKC (X07286, X07287) isoforms could lead to impaired cell growth and increased apoptosis; events which appear to have taken place as evidenced by the large scale destruction of the alveolar architecture.

A number of ras-related genes were differentially expressed in the model for progressive oedema (seven days, single instillation). During this model for severe injury, two different ras-related genes (X06889, X06890) were altered. Changes in expression of these genes may have an effect on endocytosis and exocytosis.

A 14-kDa phospholipase A2 (PLA2) precursor was shown to be significantly altered in bleomycin-treated tissue. This 14-kDa isoform of PLA2 (U07798) is a secretory protein which is involved in signalling pathways involving inflammatory reactions (Niessen *et al.*, 2003). The up-regulation of this gene could result in increased inflammatory responses, which were observed during this study.

The phylogenic tree predictor (Tree Top) was used to identify clusters of genes. There were four large groups, of which two were of particular interest because they were similar to a cluster occurring in the early oedema model (three days after a single bleomycin instillation). Although the specific genes in these clusters varied between the two time points, the behaviour of the

genes as a group was very similar. As such, these clusters, both consisting mainly of ion channels and trafficking proteins, could act as potential markers for mild and severe pulmonary oedema.

5.5 CONCLUSIONS

During progressive oedema (seven days after a single bleomycin dose), a number of changes in gene expression were observed. Whilst a large proportion of these were related to cellular signalling, a number of the changes could be linked to oedema and inflammation. There was also evidence pointing to some potential repair mechanisms, such as reduced apoptosis and increased cellular proliferation.

In the severe oedema model (three days after a double bleomycin dose), a greater number of changes in gene expression were observed. Similar to progressive oedema, a large proportion of these were related to cellular signalling and a number of the changes could also be linked to oedema and inflammatory responses. Contrary to the thymidine uptake assay, which indicated that there was no significant increase in cellular turnover at this time point, some potential repair mechanisms were noted. A number of gene products could be related to reduced apoptosis and/or increased cellular proliferation. These repair mechanisms may be a continuation of processes that were induced earlier during the time course of the bleomycin treatment.

Five genes were consistent across progressive and severe oedema. However, in every case the genes were down-regulated during progressive oedema and up-regulated during severe oedema. Consequently, these genes were not useful as markers for pulmonary oedema.

There was more consistency when comparing the mild oedema model to the severe model. The cluster of ion channels and trafficking proteins were consistently up-regulated during both mild and severe oedema. The relationship between these two stages of injury could be linked to the early

phase of oedema, as both the mild and severe models are three days post dosing (either single or double instillation). Although there were no genes which were considered relevant during all three stages of injury, there were two genes which appeared over two time points. The gene encoding for a Na+/Cl- betaine/GABA transporter appeared during mild and severe oedema. The glucocorticoid receptor gene was consistently altered during both mild and progressive injury. Therefore, these single genes may be the best potential biomarkers of oedematous injury.

CHAPTER 6:

IMMUNOHISTOCHEMICAL ANALYSIS OF LUNG SECTIONS

6.1 INTRODUCTION

The discovery of novel proteins provides new opportunities for development of drug therapies. In particular, secreted and transmembrane proteins have properties that lend themselves to being used as therapeutic agents or targets (Clark *et al.*, 2003). The cysteine-rich secreted protein (CRISP) family is a large group of secreted proteins that function in some invertebrates, insects and plants as venoms and toxins. Several non-venomous family members have previously been described, although the function of these proteins is largely unknown (Smith *et al.*, 2001). One of these proteins is known as cocoacrisp (CC). The function of CC is still under investigation, however the sequence and structure is well defined (Figure 6.1).

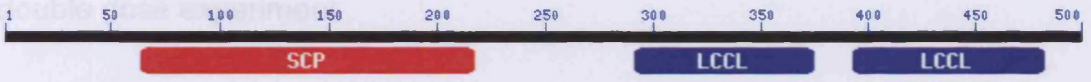

Figure 6.1 *Sequence homology map for cocoacrisp (NCBI) showing SCP module and two LCCL domains.*

Cocoacrisp contains an SCP module which is found in many species of secretory proteins, including the CRISP family (Ookuma *et al.*, 2003). The main characteristic of this protein is the presence of two LCCL domains. The LCCL domain was first identified in *Limulus* factor C from the horse-shoe crab. The key functional aspect of this protein is its sensitivity to lipopolysaccharide (LPS) endotoxin. Binding of LPS to factor C initiates a host defence mechanism, protecting the organism from infection. It is thought that the LCCL domain may be involved in the binding of LPS (Trexler *et al.*, 2000). Another protein known to contain the LCCL domain is the late gestation lung protein, Lgl1. Lgl1 is involved in lung maturation, and like CC it contains two LCCL domains. Increased expression of Lgl1 has been shown to coincide with the production of surfactant (Kaplan *et al.*, 1999). Similarly to factor C, surfactant proteins SP-A and SP-D bind LPS and therefore play an important role in the innate immune response. The increase in Lgl1 could

induce a similar effect as the surfactant components, resulting in protection of the lung from pathogens (Trexler *et al.*, 2000).

Investigations into the function of CC were carried out by Dr. Ilyas Kahn in the laboratory of Prof. Charlie Archer at the Cardiff School of Biosciences. During Dr Kahn's investigations, immunohistochemical analysis of bovine embryos revealed a CC signal in the developing lung. Consequently, it was decided to carry out the same procedures on mature lung. Tissue sections were taken from the rat lung used in the preliminary bleomycin studies. CC was detected in bleomycin tissue both three and seven days after bleomycin dosing, however, no signal was observed after saline instillation. These initial studies indicated that CC may act as a potential marker for early bleomycin-induced pulmonary injury. Further studies were carried out using lung tissue from the double dose experiment.

The following chapter details the procedures and findings from the immunohistochemical detection of cocoacrisp in bleomycin-treated lung tissue sections.

6.2 MATERIALS

6.2.1 MATERIALS AND SUPPLIERS

Supplier:	Material:
Vector Laboratories, Peterborough	Antigen Unmasking Solution (H-3300) RTU Vectastain Universal Quick Kit (PK-7800) Vector NovaRed Substrate Kit for Peroxidase (SK-4800)
In-house antibody production	Cocoacrisp Primary Antibody (rabbit) Control Serum Pre-Bleed (rabbit)
BDH, Dorset	DPX Mountant (36029)
Sigma-Aldrich, Dorset	Tris Buffered Saline (T6664) Tween 20 (P7949)
Leica Microsystems (UK) Ltd, Buckinghamshire	Leica Q550 IW Workstation Leica QWin Image Analysis Software

6.2.2 STOCK SOLUTIONS

Hydrogen Peroxide Solution	0.3% Hydrogen Peroxide Methanol
TBS/Tween	0.1% Tween 20 Tris Buffered Saline (TBS)
Primary Antibody/Serum Control	0.05% Primary Antibody (1°)/Serum Control 1.5% Blocking Serum TBS

6.3 METHODS

6.3.1 PREPARATION OF TISSUE FOR IMMUNOHISTOCHEMISTRY

Animals were treated with a single or double dose of bleomycin or saline and then sacrificed three, seven and twenty-eight days after dosing, as described in Sections 2.3.1-2.3.4. The lungs were inflated and stored in 10% neutral buffered formalin at 4°C for a minimum of 24 hours (Section 3.3.3.1). After this time the lungs were processed for paraffin embedding and sectioning (Section 3.3.3.2-3.3.3.4).

6.3.2 ANTIGEN UNMASKING

Sectioned tissue samples were prepared for the immunoassay by dewaxing as described in Section 3.3.3.4. After dewaxing, antigen unmasking was carried out on the fixed lung tissue sections. The fixation process led to cross-linking within the tissue to such an extent that the specific antigen binding sites were masked. This was due to the length of time the tissue was stored in 10% neutral buffered formalin. Antigen unmasking breaks down some of this cross-linking to expose the antigen for further immunoassay techniques.

Antigen unmasking solution (Vector) was diluted 1 in 100 with distilled water in glass coplin jars. The solution was then heated to boiling point in a microwave. The lung tissue sections were immersed in the boiling solution for two minutes prior to washing in tap water for five minutes.

6.3.3 BLOCKING ENDOGENOUS PEROXIDASE ACTIVITY

In order to quench peroxidase activity endogenous to the tissue, all the lung tissue sections were immersed in 0.3% hydrogen peroxide solution (section 6.2.2) for 30 minutes, followed by a wash in tap water (two minutes).

6.3.4 *IMMUNOHISTOCHEMISTRY*

The immunoassay was carried out using a RTU Vectastain Universal Quick kit (Vector) containing prediluted blocking serum (normal horse serum), prediluted biotinylated pan-specific secondary antibody and ready-to-use streptavidin/peroxidase preformed complex. Tissue sections were washed with TBS/tween solution (section 6.2.2) prior to incubating the sections with blocking serum for 10 minutes. The sections were then incubated with the cocoacrisp primary antibody or serum control (section 6.2.2) at 4°C overnight. The following morning the sections were given two five-minute TBS washes before the secondary antibody was added. The secondary antibody was incubated for 10 minutes before being washed for another five minutes with TBS. The streptavidin/peroxidase complex was added to the sections for five minutes. Another five-minute wash with TBS was carried out prior to addition of the peroxidase substrate, NovaRed (Vector). NovaRed solution was made up according to the kit instructions and incubated on the sections for 15 minutes. Sections were washed in tap water then counter-stained for five minutes with light green stain. Following a 30 second wash in tap water, slides were dehydrated and fixed using DPX mounting medium, described in Section 3.3.4.

6.3.5 *IMAGE ANALYSIS*

Image analysis (IA) was used to capture digitised LM images of saline and bleomycin-treated tissue sections. LM images (x100 magnification) were saved as TIFF files and imported into the Leica Q550IW Image Analysis System (Leica Microsystems, UK), for image processing.

Image processing involved adjustment of the background white levels to ensure all the lung tissue and staining were detected in the TIFF images (Figure 6.2A). Once this parameter was established, IA involved the detection of lung tissue that contained the CC label (shaded blue, Figure 6.2B). The total area (mm^2) of CC label in control versus bleomycin-treated samples was calculated.

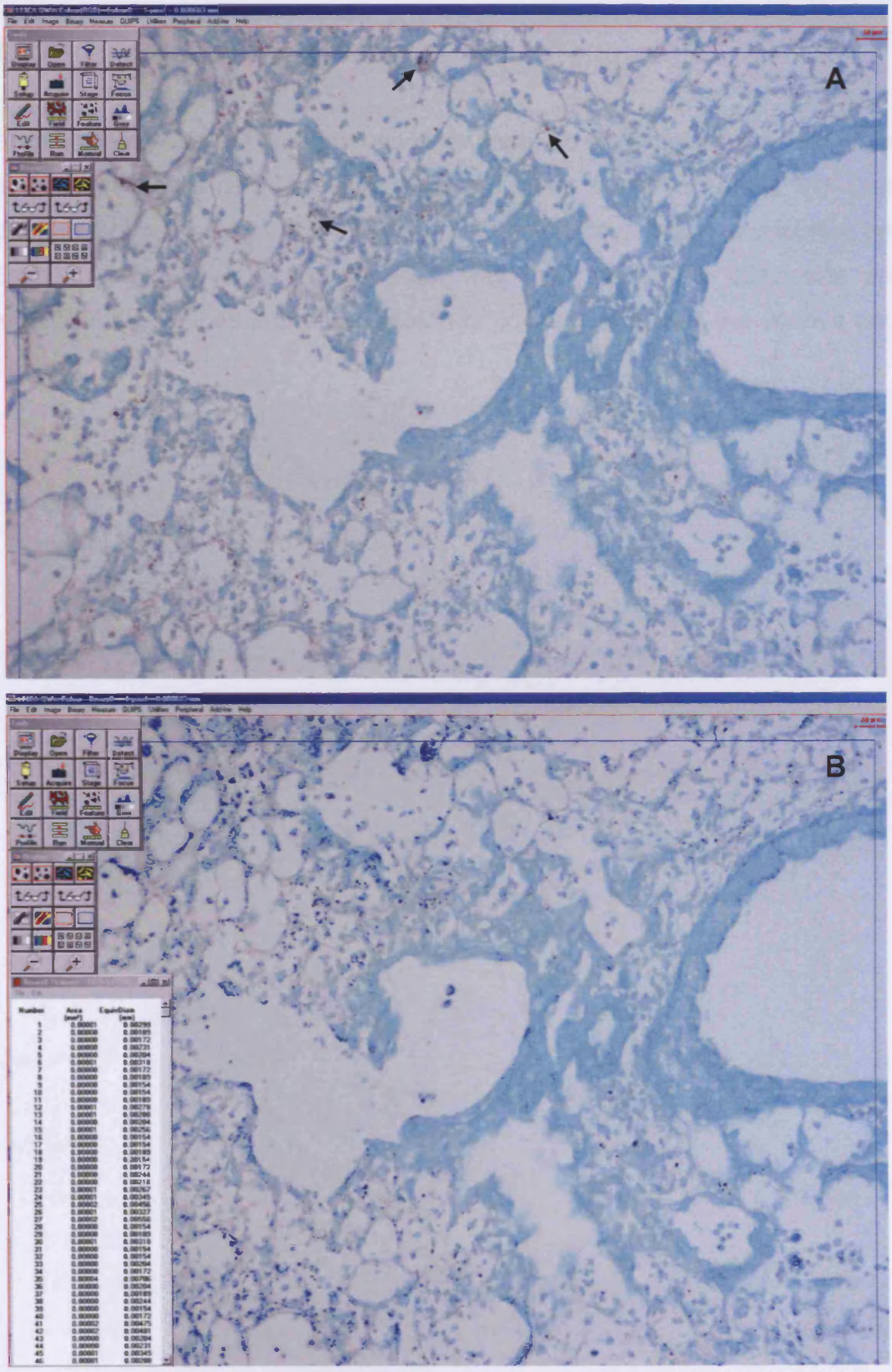

Figure 6.2 *Digitised images of cocoacrisp labelled tissue. A: Raw image showing cocoacrisp labelling as a red/brown colour, indicated by arrows; B: Image converted by image analysis system for colour detection, cocoacrisp label coloured blue.*

6.3.6 *STATISTICAL ANALYSIS*

At each time point, 10 TIFF images were captured of random areas over three lung tissue sections. These images were then quantified using the Qwin analysis software (Leica Microsystems). The resulting data was imported into Excel. A two-tailed Student's t-test was then applied to determine any statistical differences in the expression of cocoacrisp across the various time points.

6.4 RESULTS

6.4.1 LM OF LUNG TISSUE SECTIONS

Microscopic analysis of sections treated with serum control rather than primary antibody was carried out at all time points for both saline and bleomycin-instilled lung tissue. These samples showed no evidence of labelling (Figure 6.3).

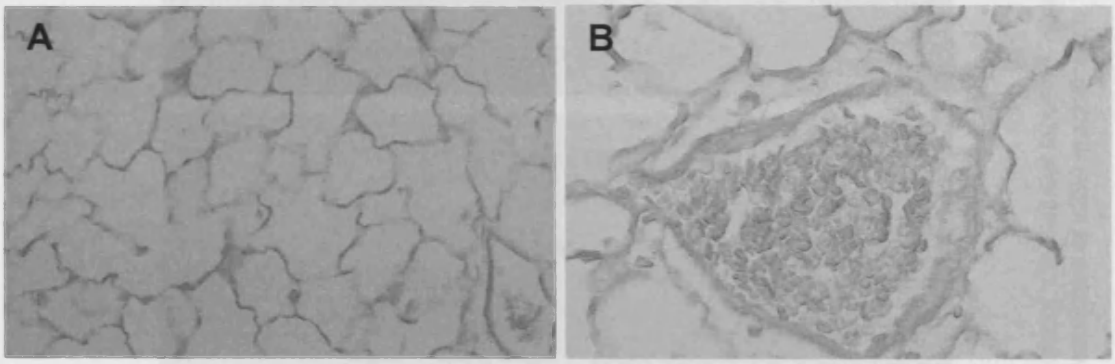

Figure 6.3 *Lung sections three days post-single bleomycin-treatment. Sections incubated with serum control rather than primary antibody. A: Alveolar spaces (x100 magnification), B: Blood vessel (x200 magnification).*

Equivalent analysis was carried out to determine the expression of CC in bleomycin and saline-instilled lung. A very low level of the protein could be detected in all the saline-treated samples, although it was very difficult to determine visually (data not shown). At three and seven days after a single bleomycin dose an increase in CC expression was observed. Examples of these observations are shown in Figure 6.4. Cocoacrisp could be seen mainly lining the surface of the tissue (Figure 6.4A). This occurred primarily in areas of the tissue which appeared more severely effected by the treatment. There was also consistent appearance of CC detected in the blood vessels (Figure 6.4B). The other significant area of CC expression was in regions of the tissue where the lung architecture was largely disorganised (Figure 6.4C).

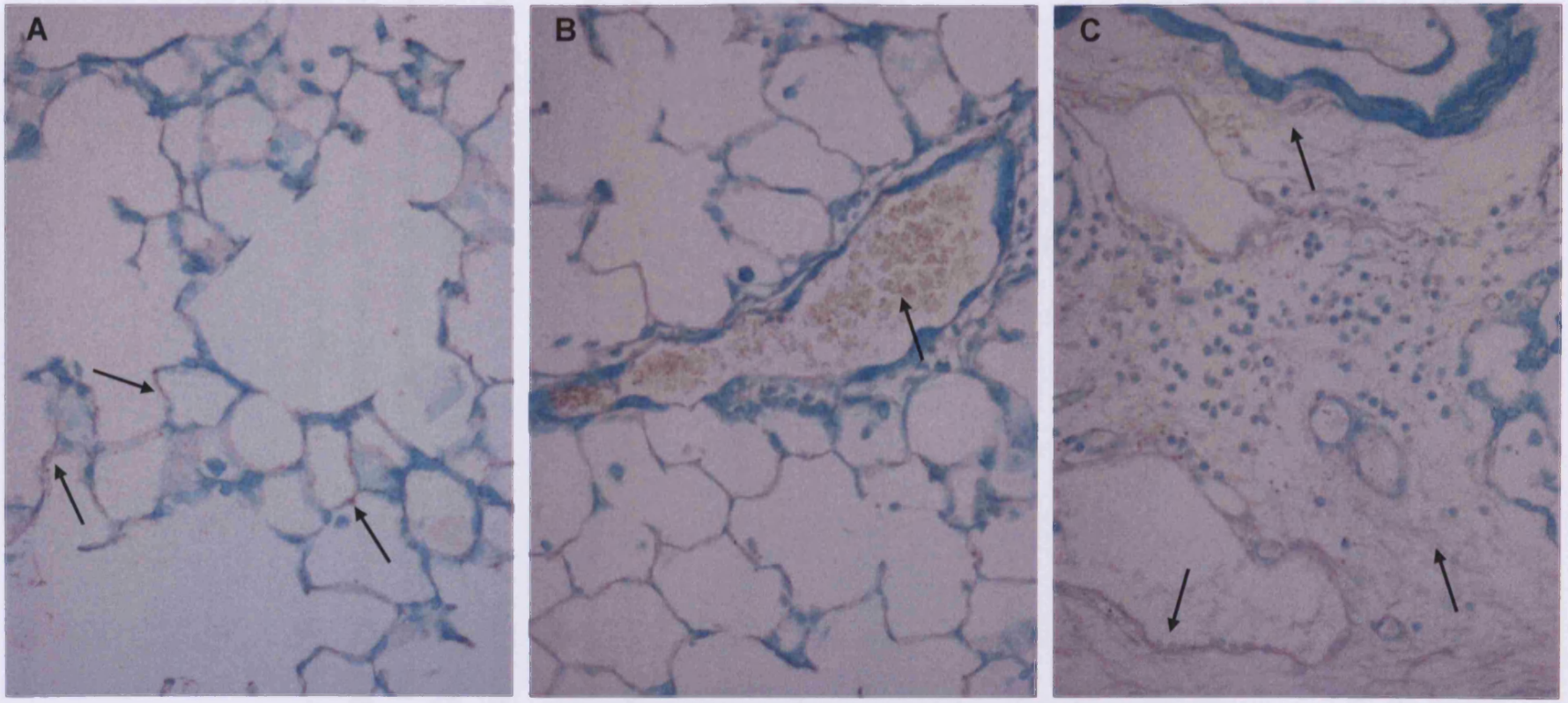

Figure 6.4 *Cocoacrisp expression in lung tissue three days after bleomycin treatment. Cocoacrisp labelling: red/brown colour, indicated by arrows; A: Alveoli, B: Blood vessel, C: Region of disorganised tissue structure. All images shown at x200 magnification.*

6.4.2 *IMAGE ANALYSIS OF LUNG TISSUE SECTIONS*

Quantification of the images shown in Section 6.4.1 allowed further analysis of cocoacrisp expression in the tissue. The area (mm^2) of cocoacrisp label detected in the tissue was used as the value for CC expression. The resulting data is shown in Figure 6.5.

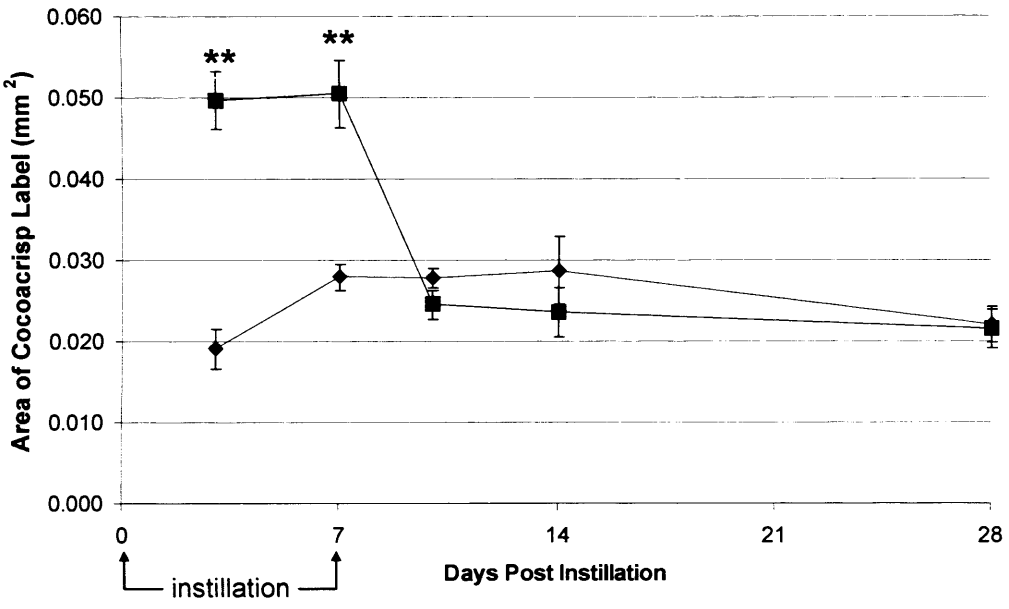

Figure 6.5 *Cocoacrisp expression in lung sections after saline (◆) or bleomycin (■) treatment. Error bars indicate one standard deviation. ** Significant (p≤ 0.001)*

After a single bleomycin instillation the amount of cocoacrisp expression was more than doubled in comparison to saline instillation. At both three and seven days post-instillation the difference in CC expression in lung tissue was statistically significant with a t-test result of $p \leq 0.0003$. After the second instillation, there was no significant difference between saline and bleomycin-instilled tissue.

6.5 DISCUSSION

The cocoacrisp study was carried out to investigate the possibility that this novel secreted protein might act as a marker for early bleomycin-induced injury. During the preliminary investigations Dr. Kahn only found CC expression in bleomycin-treated tissue. No signal was observed in saline-instilled lung. However, during this study, in all saline samples there appeared to be a low level of CC expression. This baseline signal appeared to be matched by the samples treated with a double bleomycin instillation. It was thought that some non-specific hybridisation may have been occurring. However, the lack of signal in the serum control samples confirmed that the cocoacrisp expression observed in the experimental samples was genuine. Cocoacrisp expression appeared to be significantly elevated three and seven days after a single bleomycin instillation; as the injury progressed the amount of CC dropped back down to control levels.

The homology of CC to Lgl1 and other CRISP proteins suggested that it was a secreted extracellular protein. This appeared to be confirmed by the location of CC on the surface of the lung and in the blood vessels. If the similarity in structure between CC and Lgl1 persists to the function of the protein, CC could be involved in the defence of the lung to insult (Trexler *et al.*, 2000). The appearance of CC on the lung surface would seem to support this theory. If this is the case, it is purely an immediate response, as the levels rapidly return to baseline levels.

The Lgl1 protein has also been implicated in the regulation of extracellular matrix (ECM) degradation by modulation of trypsin activity (Kaplan *et al.*, 1999). The breakdown of the ECM, particularly proteoglycans, leads to increased vascular permeability (Miserocchi *et al.*, 2001). This is one of the critical events in the development of pulmonary oedema. Lgl1 causes trypsin inhibition which could result in reduced ECM degradation, and hence, reduced oedema. Again, assuming a similar role for CC as Lgl1, this could mean CC was involved in the protection of the ECM. This theory was supported by the

significant levels of CC in areas of disorganised lung architecture. Similarly, some mammalian CRISP proteins are found loosely associated to sperm and have been indicated in sperm-oocyte fusion (Evans, 2002). As oocytes are surrounded by a matrix containing hyaluronan (a proteoglycan) (Richards, 2005), there is potential that these interactions could be linked to CRISP-related ECM remodelling.

Some CRISPs isolated from snake venom have been shown to function by blocking voltage-gated calcium and/or potassium channels (Yamazaki and Morita, 2004; Guo *et al.*, 2004). This implies yet another potential role for CC in the resistance to developing pulmonary oedema.

An important feature of this secreted protein was its regular appearance in the blood vessels and in the lung lining. If cocoacrisp can be detected in blood or BAL, it has good potential as a biological marker for early bleomycin-induced oedema. The ability to screen blood or lavage samples (rather than tissue samples, requiring a biopsy for gene analysis) increases the possibility of creating screening or diagnostics tools for clinical applications.

6.6 CONCLUSIONS

To summarise, cocoacrisp has many potential mechanisms involving resistance to the development of pulmonary oedema, and the defence of the lung to pathogens. The appearance of elevated levels of CC in the blood and possibly BAL gives it great potential as a clinical marker for early bleomycin-induced lung injury.

CHAPTER 7:

GENERAL DISCUSSION

7.1 OVERVIEW

The primary aim of this study was to identify biomarkers for pulmonary oedema, inflammation and epithelial repair. This would be achieved by using an animal model of lung injury to develop a better understanding of the genetic mechanisms underlying the disease state.

Bleomycins are a family of antibiotic compounds used extensively in cancer chemotherapy. Unfortunately, the repeated use of bleomycin in the treatment of these diseases is known to cause pulmonary toxicity. The lung injury induced by bleomycin ranges from pulmonary oedema, inflammation (cellular infiltration) and type II hyperplasia, to interstitial fibrosis. This progression of injury is reproducibly generated in a variety of experimental animal models. In this study, a single intratracheal instillation of bleomycin was employed. This was expected to induce a model of lung inflammation, oedema and the progressive destruction of normal lung architecture.

An important objective was to use conventional toxicological and histological approaches to characterise the model and to determine the severity of lung injury. Once this had been accomplished, the principal aim was achieved by applying genomics to evaluate the genetic responses of the tissue to various levels of injury.

The purpose of genomics is to gain a better understanding of biochemical mechanisms and cellular pathways at the genetic level. An important element of this is to define global gene expression profiles. Gene arrays have been developed which can simultaneously determine the expression of numerous genes by measuring mRNA abundance. Using these arrays, and by assessing gene expression patterns, it was possible to identify genetic markers of various stages of pulmonary damage and repair.

7.2 CHARACTERISATION OF BLEOMYCIN MODEL

Prior to gene profiling, this model of bleomycin-induced lung injury was characterised. By investigating the biochemical (conventional toxicology) and morphological (histology and TEM) changes in the lung, clear differentiation between models of injury and cellular repair was successfully achieved.

Three days after a single bleomycin dose evidence of focal lung damage and mild oedema could be measured. This progressed into focal areas of intra-alveolar oedema by seven days post-instillation. The most severe oedema was observed three days after the second bleomycin instillation, with large areas of the lung showing complete destruction of the normal architecture. The injury had lessened after seven days but severe interstitial and intra-alveolar oedema remained. Three weeks after the second dose, the levels of lung injury had significantly reduced but remained noticeable. The endpoints of pulmonary injury are outlined below:

Day 3	(single dose)	Mild/early oedema
Day 21	(double dose)	
Day 7	(single dose)	Progressive oedema
Day 7	(double dose)	
Day 3	(double dose)	Severe oedema

Measurement of DNA synthesis and the progressive alteration in the structure of type II cells indicated that that cellular proliferation was induced seven days after bleomycin dosing (acute repair). These repair processes were still functioning three weeks (chronic) after a double bleomycin dose.

Models for mild, progressive and severe oedema were successfully characterised, providing the opportunity to study both the onset and progression of the injury whilst allowing some investigation into epithelial repair mechanisms.

7.3 *IDENTIFICATION OF BIOLOGICAL MARKERS*

Optimisation of the macroarray procedure was successfully achieved, primarily by increasing the purity of the starting material. By improving the RNA isolation techniques the capacity to obtain reproducible results from the macroarray was increased.

To gain a wider understanding of the oedematous reactions, a number of replicates were used at each stage of the injury. The inherent variations in genetic expression were overcome by the design of the normalisation and data analysis methods. A number of different analytical tools were applied to the data, however most proved to be redundant. Two analytical methods were developed to enable analysis of a small number of replicates (range method) and a larger number of replicates (2sd method). These methods were combined with a Student's t-test to give a more statistical element to the analysis. Changes in gene expression predicted by the macroarray were compared to changes quantified by Q-PCR. The data correlated very strongly, indicating that the optimisation of the array procedure and the newly developed analysis methods were successful. These techniques were then applied to the oedema model.

During mild oedema (three days after a single dose) a cluster of five up-regulated ion channels and transporter proteins was identified. All these genes could be linked to the movement of water, which coincided with the progression of oedema. Of the remaining genes a large number appear to be involved in osmoregulation, whilst several more may be involved in inflammation. The majority of the genes altered at this time point appeared to be involved in the control of water balance in the lung and the progression of inflammatory responses.

Almost twice the number of genes were altered during progressive oedema (seven days after a single bleomycin dose). Once more, a large number of ion channels and transporter proteins were identified, many of which could be

linked to water transport. The second largest cluster was made up of kinases, several of which were involved in cell cycle and apoptosis signalling. A number of the remaining genes had potential links to metabolism, cell cycle control and maintenance of water levels. So while a large proportion of these genes were related to cellular signalling, a number of the changes could be linked to oedema and inflammation. There was also evidence pointing to some potential repair mechanisms, such as reduced apoptosis and increased cellular proliferation.

During severe oedema (three days after a double bleomycin dose) an even greater number of changes in gene expression were observed. The majority of differentially expressed genes were encoding for ion channels and transporter genes. Of the remaining genes, a large number could be associated with epithelial and endothelial cell cycle, immune responses and osmoregulation. Thus, during the severe oedema model, whilst some of the genes appeared to be involved in the continuation of repair mechanisms, the majority of genes were involved in regulating lung water content and modulating immune responses.

There were a few consistencies between the different models of oedema. One consistency was denoted by the up-regulation of the cluster of ion channels and trafficking proteins during both mild and severe oedema. This similarity in gene behaviour could be related to the development (onset) of oedema, as in both of these models onset occurs only three days after dosing. This family of genes could potentially act as a marker for the onset of oedema. Two individual genes appeared consistently across two time points. The Na+/Cl- betaine/GABA transporter gene was consistently up-regulated during mild and severe oedema, and the gene encoding for a glucocorticoid receptor gene was similarly altered during both mild and progressive injury. As such, these single genes may be potential markers

The serendipitous discovery of cocoacrisp expression in oedematous tissue could represent the best marker uncovered by this study. This protein may be linked to surfactant production, extracellular matrix remodelling and the

blocking of ion channels. One of the most significant elements of this discovery was that CC was detected on the surface of the lung and in blood vessels. This affords the opportunity to develop clinical screening or diagnostic tools utilising blood or BAL samples.

7.4 CONCLUSIONS

In conclusion, the macroarray analysis of the bleomycin oedema model has provided new transcriptional data on the mechanisms of the events leading to pulmonary oedema. Some potential repair mechanisms have also been highlighted. The main findings from this study are outlined below:

- The use of toxicology and histology was demonstrated as an appropriate technique for quantifying and characterising a model of pulmonary injury.

- A simple and effective method was created for analysing the large amounts of data generated by these high throughput array systems. This form of analysis has been corroborated by the use of the well established molecular biology technique Q-PCR. This method can be used for comparison of groups of data, as in this study. A more clinical application of this technique may be achieved by using it to compare a single patient or unknown sample to an established 'normal' or control data set.

- Implementation of the macroarrays combined with suitable analysis methods successfully provided screening of large numbers of genes to aid in the search for biomarkers.

- A group of genes encoding for ion channels and transporter proteins were found to be consistently altered in the early stages after bleomycin treatment. This family of genes shows good potential to act as markers for early pulmonary oedema.

- Potential genetic markers were identified in the specific genes encoding for the Na+/Cl- betaine/GABA transporter and the glucocorticoid receptor. As well as acting as markers, these genes are prospective targets for treatment.

- Cocoacrisp protein was also identified as a possible biomarker for early bleomycin-induced pulmonary injury. The presence of this protein in BAL and blood render it a potential clinical tool.

7.5 *FUTURE WORK*

The Clontech macroarray was not the most robust of techniques, and better technologies have recently come on the market which may be preferable. For example, the GEArray (Bioscience Corporation, USA) utilises cDNA oligos on a small nylon membrane, and chemiluminescence or fluorescence rather than radiolabelling can be used for detection. As such, the results can be achieved within hours rather than days. These arrays can be used to study a wide range of genes as done in this study, or to study specific pathways (e.g. apoptosis, signal transduction). Application of these new 'pathway' arrays has the potential to generate a more specific understanding of the mechanisms underlying oedema. Or conversely, microarrays could be tailored to specific families of genes and used to broaden the search for markers. The findings of the current study could be used to direct the type of genes on either pathway or microarrays, i.e. ion channels and trafficking proteins, growth factors, chemokines and cytokines, kinases.

The RNA used in this study was extracted from tissue and therefore contains a large number of different cell types. Using laser capture methods it may be possible to select individual cells (e.g. type II cells, macrophages), and carry out gene array analysis on RNA extracted from a single cell type. This could further clarify the specific mechanisms of the progression of oedema, and particularly the repair processes.

It is certainly worth considering further investigations into the function of the ion channels and trafficking proteins with regard to oedema. Perhaps research into the effects of channel blockers might be considered, to prevent the progression of oedema. In addition, more in-depth studies of the specific marker genes Na+/Cl- betaine/GABA transporter and the glucocorticoid receptor should be carried out. This would help to clarify their specific involvement in the onset of oedema and perhaps identify their role as therapeutic targets.

Changes in gene expression are good early indicators of injury, as the first biological responses to insult are at the genetic level. However, a major setback with regard to using these results at the clinical level is the necessity for tissue samples to obtain RNA. In order to obtain a patient sample, a lung biopsy would need to be carried out. This causes particular difficulty in obtaining normal control samples. As such, it would be preferable to identify changes in specific proteins which may be present in blood or even in BAL to act as clinical markers. A major problem with using changes in mRNA level is that it does not necessarily correlate to changes in protein expression and function. Accordingly, it would seem important that the changes in protein expression between normal and oedematous samples are studied. This could involve either specifically targeting gene products identified by this study (Western blotting), or by carrying out further proteomic studies (2D-SDS PAGE) to identify proteins of interest.

Further investigations into the function of cocoacrisp, whether it is present in BAL, and whether it can be detected in blood are important. CC is potentially a very good marker for early oedema and research into its role in the development or resistance to oedema could prove enlightening.

REFERENCES

Adamson, I. Y. R. (1984). Drug-Induced Pulmonary Fibrosis. *Environmental Health Perspectives* **55**, 25-36.

Adamson, I. Y. R. and Bakowska, J. (1999). Relationship of Keratinocyte Growth Factor and Hepatocyte Growth Factor Levels in Rat Lung Lavage Fluid to Epithelial Cell Regeneration after Bleomycin. *American Journal of Pathology* **155**, 949-954.

Ahmed, F. E. (2002). Molecular Techniques for Studying Gene Expression in Carcinogenesis. *Journal of Environmental Science and Health Part C Environmental Carcinogenesis and Ecotoxicology Reviews* **20**, 77-116.

Al-Bazzaz, F. J. (1986). Regulation of Salt and Water Across Airway Mucosa. *Clinics in Chest Medicine* **7**, 259-272.

American_Lung_Association. (2002). The Respiratory System. *www.lungusa.org/learn/resp_sys.html.*

Aso, Y., Yoneda, K. and Kikkawa, Y. (1976). Morphological and Biochemical Study of Pulmonary Changes Induced by Bleomycin in Mice. *Laboratory Investigations* **35**, 558-568.

Azoulay, E., Attalah, H., Yang, K., Herigault, S., Jouault, H., Brun-Buisson, C., Brochard, L., Harf, A., Schlemmer, B. and Delclaux, C. (2003). Exacerbation with Granulocyte Colony-Stimulating Factor of Prior Acute Lung Injury during Neutropenia Recovery in Rats. *Critical Care Medicine* **31**, 157-165.

Bakowska, J. and Adamson, I. Y. R. (1998). Collagenase and Gelatinase Activities in Bronchoalveolar Lavage Fluids During Bleomycin-Induced Lung Injury. *Journal of Pathology* **185**, 319-323.

Balazs, G., Noma, S., Khan, A., Eacobacci, B. S. and Herman, P. G. (1994). Bleomycin-Induced Fibrosis in Pigs: Evaluation with CT. *Radiology* **191**, 269-272.

Balharry, D., Oreffo, V. and Richards, R. J. (2005). Use of Toxicogenomics for Identifying Genetic Markers of Pulmonary Oedema. *Toxicology and Applied Pharmacology* **204**, 101-108.

Ballard, S. T. and Inglis, S. K. (2004). Liquid Secretion Properties of Airway Submucosal Glands. *Journal of Physiology* **556**, 1-10.

Baron, J., Burke, J. P., Guengerich, F. P., Jakoby, W. B. and Voight, J. M. (1988). Sites for Xenobiotic Activation and Detoxication within the Respiratory Tract: Implications for Chemically Induced Toxicity. *Toxicology and Applied Pharmacology* **93**, 493-505.

Barranco, S. C., Luce, J. K., Romsdahl, M. M. and Humphrey, R. M. (1973). Bleomycin as a Possible Synchronizing Agent for Human Tumour Cells *In Vivo*. *Cancer Research* **33**, 882-887.

Bartosiewicz, M., Trounstine, M., Barker, D., Johnston, R. and Buckpitt, A. (2000). Development of a Toxicological Gene Array and Quantitative Assessment of this Technology. *Archives of Biochemistry and Biophysics* **367**, 66-73.

Bellinger, D. L., Lorton, D., Brouxhon, S., Felten, S. and Felten, D. L. (1996). The Significance of Vasoactive Intestinal Polypeptide (VIP) in Immunomodulation. *Advances in Neuroimmunology* **6**, 5-27.

Bennett, M. K., Garcia-Arraras, J. E., Elferink, L. A., Peterson, K., Fleming, A. M., Hazuka, C. D. and Scheler, R. H. (1993). The Syntaxin Family of Vesicular Transport Receptors. *Cell* **74**, 863-873.

Berman, J. S., Beer, D. J., Theodore, A. C., Kornfeld, H., Bernardo, J. and Center, D. M. (1990). Lymphocyte Recruitment to the Lung. *American Review of Respiratory Disease* **142**, 238-257.

BéruBé, K. A., Quinlan, T. R., Fung, H., Magae, J., Vacek, P., Taatjes, D. J. and Mossman, B. T. (1996). Apoptosis is Observed in Mesothelial Cells After Exposure to Crocidolite Asbestos. *American Journal of Respiratory Cell and Molecular Biology* **15**, 141-147.

Bishop, A. E. (2004). Pulmonary Epithelial Stem Cells. *Cell Proliferation* **37**, 89-96.

Black, J. D. (2000). Protein Kinase C-Mediated Regulation of the Cell Cycle. *Frontiers in Bioscience* **5**, 406-423.

Bowden, D. H. (1976). The Pulmonary Macrophage. *Environmental Health Perspectives* **16**, 55-60.

Bowden, D. H. (1984). The Alveolar Macrophage. *Environmental Health Perspectives* **55**, 327-341.

Bradford, M. M. (1976). A Rapid and Sensitive Method for the Quantitation of Microgram Quantities of Protein Utilising the Principle of Protein-Dye Binding. *Analytical Biochemistry* **72**, 248-254.

Breeze, R. G. and Wheeldon, E. B. (1977). The Cells of the Pulmonary Airways. *American Review of Respiratory Disease* **116**, 705-777.

Brent, R. (1999). Functional Genomics: Learning to Think about Gene Expression Data. *Current Biology* **9**, R338-R341.

Brines, M., Grasso, G., Fiordaliso, F., Sfacteria, A., Ghezzi, P., Fratelli, M., Latini, R., Xie, Q., Smart, J., Su-Rick, C. et al. (2004). Erythropoietin Mediates Tissue Protection Through an Erythropoietin and Common β-Subunit Heteroreceptor. *Proceedings of the National Academy of Science, USA* **101**, 14907-14912.

Brown, P. O. and Botstein, D. (1999). Exploring the New World of the Genome with DNA Microarrays. *Nature Genetics Supplement* **21**, 33-37.

Brown, R. F. R., Drawbaugh, R. B. and Marrs, T. C. (1988). An Investigation of Possible Models for the Production of Progressive Pulmonary Fibrosis in the Rat. The Effects of Repeated Intratracheal Instillation of Bleomycin. *Toxicology* **51**, 101-110.

Castranova, V., Rabovsky, J., Tucker, J. H. and Miles, P. R. (1988). The Alveolar Type II Epithelial Cell: A Multifunctional Pneumocyte. *Toxicology and Applied Pharmacology* **93**, 472-83.

Catravas, J. D., Lazo, J. S., Dobuler, K. J., Mills, L. R. and Gillis, C. N. (1983). Pulmonary Endothelial Dysfunction in the Presence or Absence of Interstitial Injury Induced by Intratracheally Injected Bleomycin in Rabbits. *American Review of Respiratory Disease* **128**, 740-746.

Chardin, P. (1988). The *Ras* Superfamily Proteins. *Biochimie* **70**, 865-868.

Chomczynski, P. and Sacchi, N. (1987). Single-Step Method of RNA Isolation by Acid Guanidinium Thiocyanate-Phenol-Chloroform Extraction. *Analytical Biochemistry* **162**, 156-159.

Clark, H. F., Gurney, A. L., Abaya, E., Baker, K., Baldwin, D., Brush, J., Chen, J., Chow, B., Chui, C., Crowley, C. et al. (2003). The Secreted Protein Discovery Initiative (SPDI), a Large-Scale Effort to Identify Novel Human Secreted and Transmembrane Proteins: A Bioinformatics Assessment. *Genome Research* **13**, 2265-2270.

Clemens, M. J. (2004). Targets and Mechanisms for the Regulation of Translation in Malignant Transformation. *Oncogene* **23**, 3180-3188.

Clive, S., Jodrell, D. and Webb, D. (2001). Gastrin-Releasing Peptide is a Potent Vasodilator in Humans. *Clinical Pharmacology and Therapeutics* **69**, 252-259.

Clontech. (2001). Atlas Arrays RT-PCR User Manual PT3270 (PR1X380).

Cunningham, M. J., Liang, S., Fuhrman, S., Seilhamer, J. J. and Somogyi, R. (2000). Gene Expression Microarray Data Analysis for Toxicology Profiling. *Annals of the New York Academy of Sciences* **919**, 52-67.

Cutillo, A. G., Chan, P. H., Ailion, D. C., Watanabe, S., Rao, N. V., Hansen, C. B., Albertine, K. H., Laicher, G. and Durney, C. H. (2002). Characterisation of Bleomycin Lung Injury by Nuclear Magnetic Resonance: Correlation Between NMR Relaxation Times and Lung Water and Collagen Content. *Magnetic Resonance in Medicine* **47**, 246-256.

Dai, C., Price, J. O., Brunner, T. and Krantz, S. B. (1998). Fas Ligand is Present in Human Erythroid Colony-Forming Cells and Interacts with Fas Induced by Interferon γ to Produce Erythroid Cell Apoptosis. *Blood* **91**, 1235-1242.

Daniels, C. B. and Orgeig, S. (2003). Pulmonary Surfactant: The Key to the Evolution of Air Breathing. *News in Physiological Sciences* **18**, 151-157.

Das, N., Gupta, S. and Mazumdar, S. (2001). Direct Observation of Release of Cytochrome *c* from Lipid-Encapsulated Protein by Peroxide and Superoxide: A Possible Mechanism for Drug-Induced Apoptosis. *Biochemica and Biophysical Research Communications* **286**, 311-314.

Dethloff, L. A., Gladen, B. C., Gilmore, L. B. and Hook, G. E. R. (1989). Kinetics of Pulmonary Surfactant Phosphatidylcholine Metabolism in the Lungs of Silica-Treated Rats. *Toxicology and Applied Pharmacology* **98**, 1-11.

Devereux, T. R., Donin, B. A. and Philpot, R. M. (1989). Xenobiotic Metabolism by Isolated Pulmonary Cells. *Pharmacology and Therapeutics* **41**, 243-256.

deVos, S., Hofmann, W. K., Grogan, T. M., Krug, U., Schrage, M., Miller, T. P., Braun, J. G., Wachsman, W., Koeffler, H. P. and Said, J. W. (2003). Gene Expression Profile of Serial Samples of Transformed B-cell Lymphomas. *Laboratory Investigations* **83**, 271-285.

Doelman, C. J. A. and Bast, A. (1990). Oxygen Radicals in Lung Pathology. *Free Radical Biology and Medicine* **9**, 381-400.

Dong, Y., Ganther, H. E., Stewart, C. and Ip, C. (2002). Identification of Molecular Targets Associated with Selenium-Induced Growth Inhibition in Human Breast Cells Using cDNA Microarrays. *Cancer Research* **62**, 708-714.

Dorr, R. T. (1992). Bleomycin Pharmacology: Mechanism of Action and Resistance, and Clinical Pharmacokinetics. *Seminars in Oncology* **19**, 3-8.

Duncan, C. A. (1989). Lung Metabolism of Xenobiotic Compounds. *Clinics in Chest Medicine* **10**, 49-58.

Eisen, M. B., Spellman, P. T., Brown, P. O. and Botstein, D. (1998). Cluster Analysis and Display of Genome-Wide Expression Patterns. *Proceedings of the National Academy of Science, USA* **95**, 14863-14868.

Ekimoto, H., Takahashi, K., Matsuda, A., Takita, T. and Umezawa, H. (1985). Lipid Peroxidation by Bleomycin-Iron Complexes *In Vitro*. *Journal of Antibiotics* **38**, 1077-1082.

El-Salhy, M., Suhr, O. and Danielsson, A. (2002). Peptide YY in Gastrointestinal Disorders. *Peptides* **23**, 397-402.

Evans, J. P. (2002). The Molecular Basis of Sperm-Oocyte Membrane Interactions During Mammalian Fertilisation. *Human Reproduction Update* **8**, 297-311.

Evans, M. J., Johnson, L. V., Stephens, R. and Freeman, G. (1976). Renewal of the Terminal Bronchiolar Epithelium in the Rat Following Exposure to NO_2 or O_3. *Laboratory Investigations* **35**, 246-257.

Ezaki, T., Baluk, P., Thurston, G., La Barbara, A., Woo, C. and McDonald, D. M. (2001). Time Course of Endothelial Cell Proliferation and Microvascular Remodelling in Chronic Inflammation. *American Journal of Pathology* **158**, 2043-2055.

Filderman, A. E., Genovese, L. A. and Lazo, J. S. (1988). Alterations in Pulmonary Protective Enzymes Following Systemic Bleomycin Treatment in Mice. *Biochemical Pharmacology* **37**, 1111-1116.

Folkesson, H. G., Nitenberg, G., Oliver, B. L., Jayr, C., Albertine, K. H. and Matthay, M. A. (1998). Up-regulation of Alveolar Epithelial Fluid Transport after Subacute Lung Injury in Rats from Bleomycin. *American Journal of Physiology - Lung Cellular and Molecular Physiology* **275**, L478-L490.

Foster, D. A. (1993). Intracellular Signalling Mediated by Protein-Tyrosine Kinases: Networking Through Phospholipid Metabolism. *Cellular Signalling* **5**, 389-399.

Frank, L. (1985). Effects of Oxygen on the Newborn. *Federation Proceedings* **44**, 2328-2334.

Gallagher, A. M. and Gottlieb, R. A. (2001). Proliferation, Not Apoptosis, Alters Epithelial Cell Migration in Small Intestine of CFTR Null Mice. *American Journal of Physiology - Gastrointestinal and Liver Physiology* **281**, G681-G687.

Gelderblom, M., Eminel, S., Herdegen, T. and Waetzig, V. (2004). c-Jun N-terminal Kinases (JNKs) and the Cytoskeleton-Functions Beyond Neurodegeneration. *International Journal of Developmental Neuroscience* **22**, 559-564.

Genebee. (2001). TreeTop - Phylogenetic Tree Prediction. *www.genebee.msu.su/services/phtree_reduced.html.*

Gil, J. and Reiss, O. K. (1973). Isolation and Characterisation of Lamellar Bodies and Tubular Myelin from Rat Lung Homogenates. *The Journal of Cell Biology* **58**, 152-171.

Godwin, T. A. (1995). Structure and Function of the Lung. *www.edcentre.med.cornell.edu/CUMC_PathNotes/Respiratory/Respiratory.html.*

Goldstein, A. L. and Badamachian, M. (2004). Thymosins: Chemistry and Biological Properties in Health and Disease. *Expert Opinion on Biological Therapy* **4**, 559-573.

Gonzalez-Rothi, R. J. and Harris, J. O. (1986). Pulmonary Alveolar Proteinosis. Further Evaluation of Abnormal Alveolar Macrophages. *Chest* **90**, 656-661.

Gonzalez, F. J. (2005). Role of Cytochromes P450 in Chemical Toxicity and Oxidative Stress: Studies with CYP2E1. *Mutation Research* **569**, 101-110.

Goodman, B. E., Fleischer, R. S. and Crandall, E. D. (1983). Evidence for Active Na+ Transport by Cultured Monolayers of Pulmonary Alveolar Epithelial Cells. *American Journal of Physiology - Cell Physiology* **245**, C78-C83.

Grattendick, K., Stuart, R., Roberts, E., Lincoln, J., Lefkowitz, S. S., Bollen, A., Moguilevsky, N., Friedman, H. and Lefkowitz, D. (2002). Alveolar Macrophage Activation by Myeloperoxidase: A Model for Exacerbation of Lung Inflammation. *American Journal of Respiratory Cell and Molecular Biology* **26**, 716-722.

Grunfeld, C. and Palladino, M. A. (1990). Tumour Necrosis Factor: Immunologic, Antitumour, Metabolic, and Cardiovascular Activities. *Advances in Internal Medicine* **35**, 45-71.

Guo, M., Teng, M., Niu, L., Liu, Q., Huang, Q. and Hao, Q. (2004). Crystal Structure of Cysteine-Rich Secretory Protein Stecrisp Reveals the Cysteine-Rich Domain has a K+ -Channel Inhibitor-Like Fold. *Journal of Biological Chemistry* **280**, 12405-12412.

Haley, K. J., Sunday, M. E., Osathanondh, R., Du, J., Vathanaprida, C., Karpitsky, V. V., Krause, J. E. and Lilly, C. M. (2001). Developmental Expression of Neurokinin A and Functional Neurokinin-2 Receptors in Lung. *American Journal of Physiology - Lung Cellular and Molecular Physiology* **280**, L1348-L1358.

Hall, A. (1990). The Cellular Functions of Small GTP-Binding Proteins. *Science* **249**, 635-640.

Harkema, J. R., St.George, J., Hyde, D. M., Plopper, C. G. and Mariassy, A. (1991). Epithelial Cells of the Conducting Airways: A Species Comparison. In *Lung Biology in Health and Disease*, vol. 55 (ed. S. G. Farmer and D. W. P. Hay): Marcel Dekker Inc.

Hay, J., Haslam, P. L., Dewar, A., Addis, B., Turner-Warwick, M. and Laurent, G. (1987). Development of Acute Lung Injury after the Combination of Intravenous Bleomycin and Exposure to Hyperoxia in Rats. *Thorax* **42**, 374-382.

Hay, J., Shahzeidi, S. and Laurent, G. (1991). Mechanisms of Bleomycin-Induced Lung Damage. *Archives of Toxicology* **65**, 81-94.

Hook, G. E. R. (1991). Alveolar Proteinosis and Phospholipidoses of the Lungs. *Toxicologic Pathology* **19**, 482-513.

Housley, D. G., Brown, R. F. R., Lindsay, C. and Richards, R. J. (1996). Lung Epithelial Cell Differentiation and Repair. *M.O.D Report*, Cardiff.

Huffman Reed, J. A., Rice, W. R., Zsengeller, Z. K., Wert, S. E., Dranoff, G. and Whitsett, J. A. (1997). GM-CSF Enhances Lung Growth and Causes Alveolar Type II Epithelial Cell Hyperplasia in Transgenic Mice. *American Journal of Physiology - Lung Cellular and Molecular Physiology* **273**, L715-L725.

Iguchi, K., Usami, Y., Hirano, K., Hamatake, M., Shibata, M. and Ishida, R. (1999). Decreased Thymosin β_4 in Apoptosis Induced by a Variety of Antitumor Drugs. *Biochemical Pharmacology* **57**, 1105-1111.

Izbicki, G., Segel, M. J., Christensen, T. G., Conner, M. W. and Breuer, R. (2002). Time Course of Bleomycin-Induced Lung Fibrosis. *International Journal of Experimental Pathology* **83**, 111-119.

Jang, A. S., Lee, J. U., Choi, I. S., Park, K. O., Lee, J. H., Park, S. W. and Park, C. S. (2004). Expression of Nitric Oxide Synthase, Aquaporin 1 and Aquaporin 5 in Rat After Bleomycin Inhalation. *Intensive Care Medicine* **30**, 489-495.

Jeffery, P. K. (2000). Pathological Spectrum of Airway Inflammation. In *Cellular Mechanisms in Airways Inflammation*, (ed. C. P. Page K. H. Banner and D. Spiner): Birkhauser Verlag.

Johnson, M. D., Widdicombe, J. H., Allen, L., Barbry, P. and Dobbs, L. G. (2002). Alveolar Epithleial Type I Cells Contain Transport Proteins and Transport Sodium, Supporting an Active Role or Type I Cells in Regulation of Lung Liquid Homeostasis. *Proceedings of the National Academy of Science, USA* **99**, 1966-1971.

Kadenbach, B., Stroh, A., Huther, F. J., Reimann, A. and Steverding, D. (1991). Evolutionary Aspects of Cytochrome c Oxidase. *Journal of Bioenergetics and Biomembranes* **23**, 321-334.

Kaempfer, R. (2003). RNA Sensors: Novel Regulators of Gene Expression. *EMBO Reports* **4**, 1043-1047.

Kahl, C. R. and Means, A. R. (2003). Regulation of Cell Cycle Progression by Calcium/Calmodulin-Dependent Pathways. *Endocrine Reviews* **24**, 719-736.

Kaminski, N., Allard, J. and Heller, R. A. (2000a). Use of Oligonucleotide Arrays to Analyze Drug Toxicity. *Annals of the New York Academy of Sciences* **919**, 1-8.

Kaminski, N., Allard, J., Pittet, J. F., Zuo, F., Griffiths, M. J. D., Morris, D., Huang, X., Sheppard, D. and Heller, R. A. (2000b). Global Analysis of Gene Expression in Pulmonary Fibrosis Reveals Distinct Programs Regulating Lung Inflammation and Fibrosis. *Proceedings of the National Academy of Science, USA* **97**, 1778-1783.

Kanda, H. and Miura, M. (2004). Regulatory Roles of JNK in Programmed Cell Death. *Journal of Biochemistry* **136**, 1-6.

Kaplan, F., Ledoux, P., Kassamali, F. Q., Gagnon, S., Post, M., Koehler, D., Deimling, J. and Sweezey, N. B. (1999). A Novel Developmentally Regulated Gene in Lung Mesenchyme: Homology to a Tumour-Derived Trypsin Inhibitor. *American Journal of Physiology - Lung Cellular and Molecular Physiology* **276**, L1027-L1036.

Katsuma, S., Nishi, K., Tanigawara, K., Iwaka, H., Shiojima, S., Takagaki, K., Kaminishi, Y., Suzuki, Y., Hirasawa, A., Ohgi, T. et al. (2001). Molecular Monitoring of Bleomycin-Induced Pulmonary Fibrosis by cDNA Microarray-Based Gene Expression Profiling. *Biochemical and Biophysical Research Communications* **288**, 747-751.

Kellogg, D. R. (2003). Wee1-Dependent Mechanisms Required for Coordination of Cell Growth and Cell Division. *Journal of Cell Science* **116**, 4883-4890.

Kim, K. and Malik, A. B. (2003). Protein Transport Across the Lung Epithelial Barrier. *American Journal of Physiology - Lung Cellular and Molecular Physiology* **284**, L247-L259.

Knippschild, U., Gocht, A., Wolff, S., Huber, N., Löhler, J. and Stöter, M. (2005). The Casein Kinase 1 Family: Participation in Multiple Cellular Processes in Eukaryotes. *Cellular Signalling* **17**, 675-689.

Kreda, S. M., Gynn, M. C., Fenstermacher, D. A., Boucher, R. C. and Gabriel, S. E. (2001). Expression and Localisation of Epithelial Aquaporins in the Adult Human Lung. *American Journal of Respiratory Cell and Molecular Biology* **24**, 224-234.

Kuo, Y. C., Tsai, W. J., Wang, J. Y., Chang, S. C., Lin, C. Y. and Shiao, M. S. (2001). Regulation of Bronchoalveolar Lavage Fluids Cell Function by Immunomodulatory Agents from *Cordyceps sinensis*. *Life Sciences* **68**, 1067-1082.

Lach, E., Haddard, E. B. and Gies, J. P. (1993). Contractile Effect of Bombesin on Guinea Pig Lung *In Vitro*: Involvement of Gastrin-Releasing Peptide-Preferring Receptors. *American Journal of Physiology* **264**, L80-L86.

Langenback, E. G., Bergofsky, E. H., Halpern, J. G. and Foster, W. M. (1990). Supramicron-Sized Particle Clearance from Alveoli: Route and Kinetics. *Journal of Applied Physiology* **69**, 1302-1308.

Lazo, J. S., Catravas, J. D. and Gillis, C. N. (1981). Reduction in Rabbit Serum and Pulmonary Angiotensin Converting Enzyme Activity After Subacute Bleomycin Treatment. *Biochemical Pharmacology* **30**, 2577-2584.

Lazo, J. S., Hoyt, D. G., Sebti, S. M. and Pitt, B. R. (1990). Bleomycin: A Pharmacologic Tool in the Study of Pathogenesis of Interstitial Pulmonary Fibrosis. *Pharmacology and Therapeutics* **47**, 347-358.

Lazo, J. S. and Humphreys, C. J. (1983). Lack of Metabolism as the Biochemical Basis of Bleomycin-Induced Pulmonary Toxicity. *Proceedings of the National Academy of Science, USA* **80**, 3064-3068.

Lee, M. T., Kuo, F. C., Whitmore, G. A. and Skiar, J. (2000). Importance of Replication in Microarray Gene Expression Studies: Statistical Methods and Evidence from Repetitive cDNA Hybridisations. *Proceedings of the National Academy of Science, USA* **97**, 9834-9839.

Lee, S. Y. and O'Grady, S. M. (2003). Modulation of Ion Channel Function by P2Y Receptors. *Cell Biochemistry and Biophysics* **39**, 75-88.

Leech, C. J. and Faber, J. E. (1996). Different Alpha-Adrenoceptor Subtypes Mediate Constriction of Arterioles and Venules. *American Journal of Physiology* **270**, H710-H722.

Lehnert, B. E., Valdez, Y. E. and Stewart, C. C. (1986). Translocation of Particles to the Tracheobronchial Lymph Nodes after Lung Deposition: Kinetics and Particle-Cell Relationships. *Experimental Lung Research* **10**, 245-266.

Leipziger, J. (2003). Control of Epithelial Transport via Luminal P2 Receptors. *American Journal of Physiology - Renal Physiology* **284**, F419-F432.

Leong, K. G. and Karsan, A. (2000). Signalling Pathways Mediated by Tumour Necrosis Factor Alpha. *Histology and Histopathology* **15**, 1303-1325.

Lewis, R. W., Harwood, J. L. and Richards, R. J. (1987). The Fate of Instilled Pulmonary Surfactant in Normal and Quartz-Treated Rats. *Biochemical Journal* **243**, 679-685.

Lockhart, D. J. and Winzeler, E. A. (2000). Genomics, Gene Expression and DNA Arrays. *Nature* **405**, 827-836.

Lohmann-Matthes, M. L., Steinmüller, C. and Franke-Ullmann, G. (1994). Pulmonary Macrophages. *European Respiratory Journal* **7**, 1678-1689.

Lum, H. and Malik, A. B. (1994). Regulation of Vascular Endothelial Barrier Function. *American Journal of Physiology - Lung Cellular and Molecular Physiology* **267**, L223-L241.

Lynn, W. S., Bhattacharya, S. N., Passerro, M. P. and Tye, R. (1974). Composition and Function of Pulmonary Surfactant. *Annals of the New York Academy of Sciences* **221**, 209-211.

Mannon, P. and Taylor, I. L. (1994). The Pancreatic Polypeptide Family. In *Gut Peptides: Biochemistry and Physiology*, (ed. J. H. Walsh and G. J. Dockray), pp. 341-370. New York: Raven Press Ltd.

Matalon, S., Lazrak, A., Jain, L. and Eaton, D. C. (2002). Biophysical Properties of Sodium Channels in Lung Alveolar Epithelial Cells. *Journal of Applied Physiology* **93**, 1852-1859.

Mehta, D., Bhattacharya, J., Matthay, M. A. and Malik, A. B. (2004). Integrated Control of Lung Fluid Balance. *American Journal of Physiology - Lung Cellular and Molecular Physiology* **287**, L1081-L1090.

Miller, B. E. and Hook, G. E. R. (1988). Isolation and Characterisation of Hypertrophic Type II Cells from the Lungs of Silica-Treated Rats. *Laboratory Investigations* **58**, 565-575.

Miller, B. E. and Hook, G. E. R. (1990). Hypertrophy and Hyperplasia of Alveolar Type II Cells in Responses to Silica and Other Pulmonary Toxicants. *Environmental Health Perspectives* **85**, 15-24.

Miserocchi, G., Negrini, D., Passi, A. and De Luca, G. (2001). Development of Lung Edema: Interstitial Fluid Dynamics and Molecular Structure. *News in Physiological Sciences* **16**, 66-71.

Mocellin, S., Wang, E., Panelli, M., Pilati, P. and Marincola, F. M. (2004). DNA Array-Based Gene Profiling in Tumour Immunology. *Clinical Cancer Research* **10**, 4597-4606.

Mura, M., dos Santos, C. C., Stewart, D. and Liu, M. (2004). Vascular Endothelial Growth Factor and Related Molecules in Acute Lung Injury. *Journal of Applied Physiology* **97**, 1605-1617.

Murphy, T. J., Thurston, G., Ezaki, T. and McDonald, D. M. (1999). Endothelial Cell Heterogeneity in Venules of Mouse Airways Induced by Polarised Inflammatory Stimulus. *American Journal of Pathology* **155**, 93-103.

Mustelin, T. and Burn, P. (1993). Regulation of *src* Family Tyrosine Kinases in Lymphocytes. *Trends in Biochemical Sciences* **18**, 215-220.

Nadon, R. and Shoemaker, J. (2002). Statistical Issues with Microarrays: Processing and Analysis. *TRENDS in Genetics* **18**, 265-271.

NetDoctor.co.uk. (2002). Medicines: Bleomycin. *www.netdoctor.co.uk/medicines/showpreparation.asp?id=3423.*

Nielsen, S., Chou, C. L., Marples, D., Christensen, E. I., Kishore, B. K. and Knepper, M. A. (1995). Vasopressin Increases Water Permeability of Kidney Collecting Duct by Inducing Translocation of Aquaporin-CD Water Channels to Plasma Membrane. *Proceedings of the National Academy of Science, USA* **92**, 1013-1017.

Niessen, H. W. M., Krinjnen, P. A. J., Visser, C. A., Meijer, C. J. L. M. and Hack, C. E. (2003). Type II Secretory Phospholipase A2 in Cardiovascular Disease: A Mediator in Atherosclerosis and Ischemic Damage to Cardiomyocytes? *Cardiovascular Research* **60**, 68-77.

O'Grady, S. M. and Lee, S. Y. (2003). Chloride and Potassium Channel Function in Alveolar Epithelial Cells. *American Journal of Physiology - Lung Cellular and Molecular Physiology* **284**, L689-L700.

Onodera, T., Nakamura, M., Sato, T. and Akino, T. (1983). Biochemical Characterisation of Pulmonary Washings of Patients with Alveolar Proteinosis, Interstitial Pneumonitis and Alveolar Cell Carcinoma. *Tohoku Journal of Experimental Medicine* **139**, 145-263.

Ookuma, S., Fukuda, M. and Nishida, E. (2003). Identification of a DAF-16 Transcriptional Target Gene, *scl*-1, that Regulates Longevity and Stress Resistance in *Caenorhabditis elegans*. *Current Biology* **13**, 427-431.

Panettieri, R. A. (2002). Airway Smooth Muscle: An Immunomodulatory Cell. *Journal of Allergy and Clinical Immunology* **110**, S269-S274.

Paus, R. (1991). Does Prolactin Play a Role in Skin Biology and Pathology? *Medical Hypotheses* **36**, 33-42.

Peão, M. N. D., Aguas, A. P., DeSa, C. M. and Grande, N. R. (1994). Neoformation of Blood Vessels in Association with Rat Lung Fibrosis Induced by Bleomycin. *The Anatomical Record* **238**, 57-67.

Pennie, W. D. (2000). Use of cDNA Microarrays to Probe and Understand the Toxicological Consequences of Altered Gene Expression. *Toxicology Letters* **112-113**, 473-477.

Petty, C. N. and Lucero, M. T. (1999). Characterisation of Na+ -Dependent Betaine Transporter with Cl- Channel Properties in Squid Motor Neurones. *Journal of Neurophysiology* **81**, 1567-1574.

Pitt, B. R., Lister, G., Fontán, J. J. P. and Davies, P. (1991). Functional Assessment of Pulmonary Capillary Surface Area in the 2-mo-old Lamb. *Journal of Applied Physiology* **70**, 1677-1685.

Postlethwaite, A. E., Smith, G. N., Mainardi, C. L., Seyer, J. M. and Kang, A. H. (1984). Lymphocyte Modulation of Fibroblast Function *In Vitro*: Stimulation and Inhibition of Collagen Production by Different Effector Molecules. *The Journal of Immunology* **132**, 2470-2477.

Promega. (1999). Promega Technical Manual: pGEM-T and pGEM-T Easy Vector Systems.

Qiagen. (2001). RNeasy Mini Handbook.

Quinlan, T. R., BéruBé, K. A., Marsh, J. P., Janssen, Y. M. W., Taishi, P., Leslie, K. O., Hemenway, D., O'Shaughnessy, P. T., Vacek, P. and Mossman, B. T. (1995). Patterns of Inflammation, Cell Proliferation, and Related Gene Expression in Lung After Inhalation of Chrysotile Asbestos. *American Journal of Pathology* **147**, 728-739.

Reynolds, L. and Richards, R. J. (2001). Can Toxicogenomics Provide Information on the Bioreactivity of Diesel Exhaust Particles? *Toxicology* **165**, 145-152.

Richards, J. S. (2005). Ovulation: New Factors that Prepare the Oocyte for Fertilisation. *Molecular and Cellular Endocrinology* **234**, 75-79.

Richards, R. J. and Curtis, C. G. (1984). Biochemical and Cellular Mechanisms of Dust-Induced Lung Fibrosis. *Environmental Health Perspectives* **55**, 393-416.

Richards, R. J., Masek, L. C. and Brown, R. F. R. (1991). Biochemical and Cellular Mechanisms of Pulmonary Fibrosis. *Toxicologic Pathology* **19**, 526-539.

Richardson, D. L., Pepper, D. S. and Kay, A. B. (1976). Chemotaxis for Human Monocytes by Fibrinogen-Derived Peptides. *British Journal of Haematology* **32**, 507-513.

Robertson, M. T. (1989). Prolactin, Human Nutrition and Evolution, and the Relation to Cystic Fibrosis. *Medical Hypotheses* **29**, 87-99.

Roche. (1999). 5-Bromo-2-deoxy-uridine Labelling and Detection Kit II. *(Pack insert).*

Roche. (2000). Cell Proliferation and Viability. *www.roche-applied-science.com/prod_inf/manuals/cell_man/cell_toc.html.*

Rooney, S. A., Young, S. L. and Mendelson, C. R. (1994). Molecular and Cellular Processing of Lung Surfactant. *FASEB Journal* **8**, 957-967.

Rosenfeld, J. L., Knoll, B. J. and Moore, R. H. (2002). Regulation of G-Coupled Receptor Activity by Rab GTPases. *Receptors and Channels* **8**, 87-97.

Sanlioglu, A. D., Aydin, C., Bozuk, H., Terzioglu, E. and Sanlioglu, S. (2004). Fundamental Principles of Tumour Necrosis Factor-Alpha Gene Therapy Approach and Implications for Patients with Lung Carcinoma. *Lung Cancer* **44**, 199-211.

Sato, H., Sagai, M., Suzuki, K. T. and Aoki, Y. (1999). Identification by cDNA Microarray, of A-raf and Proliferating Cell Nuclear Antigen as Genes Induced in Rat Lung by Exposure to Diesel Exhaust. *Research Communications in Molecular Pathology and Pharmacology* **105**, 77-85.

Savani, R. C., Godinez, R. I., Godinez, M. H., Wentz, E., Zaman, A., Cui, Z., Pooler, P. M., Guttentag, S. H., Beers, M. F., Gonzales, L. W. et al. (2001). Respiratory Distress After Intratracheal Bleomycin: Selective Deficiency of Surfactant Proteins B and C. *American Journal of Physiology - Lung Cellular and Molecular Physiology* **281**, L685-L693.

Savani, R. C., Hou, G., Liu, P., Wang, C., Simons, E., Grimm, P. C., Stern, R., Greenberg, A. H., DeLisser, H. M. and Khalil, N. (2000). A Role for Hyaluronan in Macrophage Accumulation and Collagen Deposition After Bleomycin-Induced Lung Injury. *American Journal of Respiratory Cell and Molecular Biology* **23**, 475-484.

Scarpelli, E. M. (1988). Surfactants and the Lining of the Lung. In *John Hopkins Series in Contemporary Medicine and Public Health*, (ed. E. M. Scarpelli). Baltimore and London: The John Hopkins University Press.

Sedgwick, J. B., Menon, I., Gern, J. E. and Busse, W. W. (2002). Effects of Inflammatory Cytokines on the Permeability of Human Lung Microvascular Endothelial Cell Monolayers and Differential Eosinophil Transmigration. *Journal of Allergy and Clinical Immunology* **110**, 752-756.

Selig, W. M., Bloomquist, M. A., Cohen, M. L. and Fleisch, J. H. (1988). Serotonin-Induced Pulmonary Responses in the Perfused Guinea Pig Lung: Evidence for 5HT2 Receptor-mediated Pulmonary Vascular and Airway Smooth Muscle Constriction. *Pulmonary Pharmacology* **1**, 93-99.

Shellito, J., Esparza, C. and Armstrong, C. (1987). Maintenance of the Normal Rat Alveolar Macrophage Cell Population. The Roles of Monocyte Influx and Alveolar Macrophage Proliferation in Situ. *American Review of Respiratory Disease* **135**, 78-82.

Sigma-Molecular-Biology. (1994). Tri-Reagent Technical Bulletin MB-205.

Slonim, D. (2002). From Patterns to Pathways: Gene Expression Data Analysis Comes of Age. *Nature Genetics Supplement* **32**, 502-508.

Smith, D. M., Collins-Racie, L. A., Marigo, V. A., Roberts, D. J., Davis, N. M., Hartmann, C., Schweitzer, R., LaVallie, E. R., Gamer, L., McCoy, J. et al. (2001). Cloning and Expression of a Novel Cysteine-Rich Secreted Protein Family Member Expressed in Thyroid and Pancreatic Mesoderm within the Chicken Embryo. *Mechanisms of Development* **102**, 223-226.

Smith, L. L. and Wyatt, I. (1981). The Accumulation of Putrescine into Slices of Rat Lung and Brain and its Relationship to the Accumulation of Paraquat. *Biochemical Pharmacology* **30**, 1053-1058.

Smith, L. L., Wyatt, I. and Cohen, G. M. (1982). The Accumulation of Diamines and Polyamines into Rat Lung Slices. *Biochemical Pharmacology* **31**, 3029-3033.

Spencer, H. (1985). Pulmonary Oedema and Its Complications and the Effects of Some Toxic Gases and Substances on the Lung. In *Pathology of the Lung*, vol. 2: Pergamon Press Ltd.

Stalheim, L., Ding, Y., Gullapalli, A., Paing, M. M., Wolfe, B. L. and Morris, D. R. (2005). Multiple Independent Functions of Arrestins in the Regulation of Protease-Activated Receptor-2 Signalling and Trafficking. *Molecular Pharmacology* **67**, 78-87.

Starcher, B. C., Kuhn, C. and Overton, J. E. (1978). Increased Elastin and Collagen Content in the Lungs of Hamsters Receiving an Intratracheal Injection of Bleomycin. *American Review of Respiratory Disease* **117**, 299-305.

Stubbe, J. and Kozarich, J. W. (1987). Mechanisms of Bleomycin-Induced DNA Degradation. *Chemical Reviews* **87**, 1107-1136.

Südhoff, T. C. (2004). The Synaptic Vesicle Cycle. *Annual Review of Neuroscience* **27**, 509-547.

Südhoff, T. C., Czernik, A. J., Kao, H. T., Takei, K., Johnston, P. A., Horiuchi, A., Kanazir, S. D., Wagner, M. A., Perin, M. S. and De Camilli, P. (1989). Synapsins: Mosaics of Shared and Individual Domains in a Family of Synaptic Vesicle Phosphoproteins. *Science* **245**, 1474-1480.

Sugita, Y., Fujiwara, Y., Taniguchi, H., Mori, T., Ishii, T., Niwa, H., Okada, Y., Takiguchi, S., Yasuda, T., Yano, M. et al. (2003). Quantitative Molecular Diagnosis of Peritoneal Lavage Fluid for Prediction of Peritoneal Recurrence in Gastric Cancer. *International Journal of Oncology* **23**, 1419-1423.

Swaisgood, C. M., French, E. L., Noga, C., Simon, R. H. and Ploplis, V. A. (2000). The Development of Bleomycin-Induced Pulmonary Fibrosis in Mice Deficient for Components of the Fibrinolytic System. *American Journal of Pathology* **157**, 177-187.

Tallett, A., Chilvers, E. R., Hannah, S., Dransfield, I., Lawson, M. F., Haslett, C. and Sethi, T. (1996). Inhibition of Neuropeptide-Stimulated Tyrosine Phosphorylation and Tyrosine Kinase Activity Stimulates Apoptosis in Small Cell Lung Cancer Cells. *Cancer Research* **56**, 4255-4263.

Tanabe, M., Matsumoto, T., Shibuya, K., Tateda, K., Miyazaki, S., Nakane, A., Iwakura, Y. and Yamaguchi, K. (2005). Compensatory Response of IL-1 Gene Knockout Mice After Pulmonary Infection with *Klebsiella Pneumoniae*. *Journal of Medical Microbiology* **54**, 7-13.

Taupenot, L., Harper, K. L. and O'Connor, D. T. (2003). Mechanisms of Disease: The Chromogranin-Secretogranin Family. *The New England Journal of Medicine* **348**, 1134-1149.

Taylor, A. E. and Gaar, K. A. (1970). Estimation of Equivalent Pore Radii of Pulmonary Capillary and Alveolar Membranes. *American Journal of Physiology* **218**, 1133-1140.

Telford, I. R. and Bridgeman, C. F. (1995). Respiratory System. In *Introduction to Functional Histology*: Harper Collins College Publishers.

Thickett, D. R., Armstrong, L. and Millar, A. B. (2002). A Role for Vascular Endothelial Growth Factor in Acute and Resolving Lung Injury. *American Journal of Respiratory and Critical Care Medicine* **166**, 1332-1337.

Thrall, R. S., McCormick, J. R., Jack, R. M., McReynolds, R. A. and Ward, P. A. (1979). Bleomycin-Induced Pulmonary Fibrosis in the Rat. *American Journal of Pathology* **95**, 117-130.

Trapnell, B. C. and Whitsett, J. A. (2002). GM-CSF Regulates Pulmonary Surfactant Homeostasis and Alveolar Macrophage-Mediated Innate Host Defence. *Annual Review of Physiology* **64**, 775-802.

Treadwell, J. A. and Singh, S. M. (2004). Microarray Analysis of Mouse Brain Gene Expression Following Acute Ethanol Treatment. *Neurochemical Research* **29**, 257-269.

Trexler, M., Bányai, L. and Patthy, L. (2000). The LCCL Module. *European Journal of Biochemistry* **267**, 5751-5757.

Turnage, R. H., Nwariaku, F., Murphy, J., Schulman, C., Wright, K. and Yin, H. (2002). Mechanisms of Pulmonary Microvascular Dysfunction During Severe Burn Injury. *World Journal of Surgery* **26**, 848-853.

Umezawa, H. (1979). Advances in Bleomycin Studies. In *Bleomycin: Chemical, Biochemical and Biological Aspects*, (ed. S. M. Hecht), pp. 24-36. New York: Springer.

Vaandrager, A. B. (2002). Structure and Function of the Heat-Stable Enterotoxin Receptor/Guanylyl Cyclase C. *Molecular and Cellular Biochemistry* **230**, 73-83.

Veldhuizen, R. A. W., Ito, Y., Marcou, J., Yao, L., McCaig, L. and Lewis, J. F. (1997). Effects of Lung Injury on Pulmonary Surfactant Aggregate Conversion *In Vivo* and *In Vitro*. *American Journal of Physiology - Lung Cellular and Molecular Physiology* **272**, L872-L878.

Verkman, A. S. and Mitra, A. K. (2000). Structure and Function of Aquaporin Water Channels. *American Journal of Physiology - Renal Physiology* **278**, F13-F28.

Vig, B. K. and Lewis, R. (1978). Genetic Toxicology of Bleomycin. *Mutation Research* **55**, 121-145.

Walker, S. R., Williams, M. C. and Benson, B. (1986). Immunocytochemical Localisation of the Major Surfactant Apoproteins in Type II Cells, Clara Cells, and Alveolar Macrophages of Rat Lung. *Journal of Histochemistry and Cytochemistry* **34**, 1137-1148.

Walsh, G. M., Sexton, D. W. and Blaylock, M. G. (2003). Corticosteroids, Eosinophils and Bronchial Epithelial Cells: New Insights into the Resolution of Inflammation in Asthma. *Journal of Endocrinology* **178**, 37-43.

Warburton, D. and Bellusci, S. (2004). The Molecular Genetics of Lung Morphogenesis and Injury Repair. *Paediatric Respiratory Reviews* **5**, S283-S287.

Weibel, E. R. (1978). Morphological Basis of Alveolar-Capillary Gas Exchange. *Physiological Reviews* **53**, 419-495.

West, J. B. (1992). Pulmonary Pathophysiology - The Essentials. Baltimore: Williams and Wilkins.

West, J. B. (2000). Vascular Diseases. In *Pulmonary Pathophysiology - The Essentials*, (ed. J. Burnard), pp. 101-113. Baltimore: Lippincott, Williams and Wilkins.

Williams, M. C. (2003). Alveolar Type I Cells: Molecular Phenotype and Development. *Annual Review of Physiology* **65**, 669-695.

Witschi, H. (1976). Proliferation of Type II Alveolar Cells: A Review of Common Responses to Toxic Lung Injury. *Toxicology* **5**, 267-277.

Wolfensohn, S. and Lloyd, M. (1998). Practical Use of Distress Scoring Systems in the Application of Humane Endpoints. In *Handbook of Laboratory Animal Management and Welfare*, pp. 48-53. Oxford: Blackwell Science.

Wright, J. R. and Youmans, D. C. (1993). Pulmonary Surfactant Protein A Stimulates Chemotaxis of Alveolar Macrophage. *American Journal of Physiology - Lung Cellular and Molecular Physiology* **264**, L338-L344.

Wu, J. C., Kozarich, J. W. and Stubbe, J. (1983). The Mechanism of Free Base Formation from DNA by Bleomycin. *The Journal of Biological Chemistry* **258**, 4694-4697.

Wyatt, I., Soames, A. R., Clay, M. F. and Smith, L. L. (1988). The Accumulation and Localisation of Putrescine, Spermidine, Spermine, and Paraquat in the Rat Lung. *In Vitro* and *In Vivo* Studies. *Biochemical Pharmacology* **37**, 1909-1918.

Yamazaki, Y. and Morita, T. (2004). Structure and Function of Snake Venom Cysteine-Rich Secretory Proteins. *Toxicon* **44**, 227-231.

Yanagisawa, M., Kurihara, H., Kimura, S., Tomobe, Y., Kobayashi, M., Mitsui, Y., Yazaki, Y., Goto, K. and Masaki, T. (1988). A Novel Potent Vasoconstrictor Peptide Poduced by Vascular Endothelial Cells. *Nature* **332**, 411-415.

Yano, T., Mason, R. J., Pan, T., Deterding, R. R., Nielsen, L. D. and Shannon, J. M. (2000). KGF Regulates Pulmonary Epithelial Proliferation and Surfactant Protein Gene Expression in Adult Rat Lung. *American Journal of Physiology - Lung Cellular and Molecular Physiology* **279**, L1146-L1158.

Yayon, A. and Klagsbrun, M. (1990). Autocrine Regulation of Cell Growth and Transformation by Basic Fibroblast Growth Factor. *Cancer and Metastasis Reviews* **9**, 191-202.

Yoshikai, Y. and Nishimura, H. (2000). The Role of Interleukin 15 in Mounting an Immune Response Against Microbial Infections. *Microbes and Infection* **2**, 381-389.

You, L., Kruse, F. E. and Völcker, H. E. (2000). Neurotrophic Factors in the Human Cornea. *Investigative Ophthalmology and Visual Science* **41**, 692-702.

Young, L. and Adamson, I. Y. R. (1993). Epithelial-Fibroblast Interactions in Bleomycin-Induced Lung Injury and Repair. *Environmental Health Perspectives* **101**, 56-61.

Young, B. and Heath, J. W. (2000). Respiratory System. In *Wheaters Functional Histology*: Churchill Livingstone.

Zeisberg, M., Shah, A. A. and Kalluri, R. (2005). Bone Morphogenic Protein-7 Induces Mesenchymal to Epithelial Transition in Adult Renal Fibroblasts and Facilitates Regeneration of Injured Kidney. *The Journal of Biological Chemistry* **280**, 8094-8100.

Zhao, Y., Young, S. L. and McIntosh, J. C. (1998). Induction of Tenascin in Rat Lungs Undergoing Bleomycin-Induced Pulmonary Fibrosis. *American Journal of Physiology* **274**, L1049-L1057.

Zhou, L. and Hershenson, M. B. (2003). Mitogenic Signalling Pathways in Airway Smooth Muscle. *Respiratory Physiology and Neurobiology* **137**, 295-308.

APPENDIX

Available online at www.sciencedirect.com

SCIENCE DIRECT

Toxicology and Applied Pharmacology 204 (2005) 101–108

Toxicology and Applied Pharmacology

www.elsevier.com/locate/ytaap

Use of toxicogenomics for identifying genetic markers of pulmonary oedema

Dominique Balharry[a,*], Victor Oreffo[b], Roy Richards[a]

[a]*Cardiff School of Biosciences, Cardiff University, Museum Avenue, Cardiff, CF10 3US, United Kingdom*
[b]*AstraZeneca, Loughborough, Leicestershire, LE11 5RH, United Kingdom*

Received 30 June 2004; accepted 26 August 2004
Available online 11 November 2004

Abstract

This study was undertaken primarily to identify genetic markers of oedema and inflammation. Mild pulmonary injury was induced following the instillation of the oedema-producing agent, bleomycin (0.5 units). Oedema was then confirmed by conventional toxicology (lavage protein levels, free cell counts and lung/body weight ratios) and histology 3 days post-bleomycin instillation.

The expression profile of 1176 mRNA species was determined for bleomycin-exposed lung (Clontech Atlas macroarray, $n = 9$). To obtain pertinent results from these data, it was necessary to develop a simple, effective method for bioinformatic analysis of altered gene expression. Data were $\log_{10}$ transformed followed by global normalisation. Differential gene expression was accepted if: (a) genes were statistically significant ($P \leq 0.05$) from a two-tailed t test; (b) genes were consistently outside a two standard deviation (SD) range from control levels. A combination of these techniques identified 31 mRNA transcripts (approximately 3%) which were significantly altered in bleomycin treated tissue. Of these genes, 26 were down-regulated whilst only five were up-regulated. Two distinct clusters were identified, with 17 genes classified as encoding hormone receptors, and nine as encoding ion channels. Both these clusters were consistently down-regulated.

The magnitude of the changes in gene expression were quantified and confirmed by Q-PCR ($n = 6$), validating the macroarray data and the bioinformatic analysis employed.

In conclusion, this study has developed a suitable macroarray analysis procedure and provides the basis for a better understanding of the gene expression changes occurring during the early phase of drug-induced pulmonary oedema.[1]

Keywords: Pulmonary oedema; Macroarray; Bleomycin; Inflammation

Introduction

The development of pulmonary oedema is caused by a number of factors, including: capillary damage, oxygen and ozone toxicity, clinical intravenous administration of fluids, drug/chemical action and high altitude (Spencer, 1985). It is also a life-threatening complication of a variety of heart and lung diseases (Roguin et al., 2000). As such, it is important that we understand more about the mechanisms of oedema and are able to identify this disease as early as possible.

The primary objective of this study was to investigate differential gene expression at the transcriptional level during the development of pulmonary oedema and inflammation. Comparing compromised and non-compromised samples provided a list of candidate genes involved in the early phase response to pulmonary injury. These genes could provide potential biomarkers for pulmonary oedema.

Bleomycin has been used in a variety of animal models to induce pulmonary injury and ultimately fibrosis (rabbit:

* Corresponding author. Cardiff School of Biosciences, Cardiff University, Museum Avenue, Cardiff, CF10 3US, United Kingdom. Fax: +44 029 20874116.
E-mail address: balharry@cf.ac.uk (D. Balharry).

[1] This work has been presented orally, in part at the British Association for Lung Research Summer Meeting, University of Brighton, 3–5 September, 2003 and in full at the British Toxicology Society Annual Congress, Heriot Watt University, Edinburgh, 21–24 April 2004.

0041-008X/$ - see front matter © 2004 Elsevier Inc. All rights reserved.
doi:10.1016/j.taap.2004.08.022

Catravas et al., 1983; mouse: Aso et al., 1976; hamster: Starcher et al., 1978; Snider et al., 1978; rat: Thrall et al., 1979; and pig: Balazs et al., 1994). In this study, a single intratracheal instillation was used to investigate the earlier stages of pulmonary injury in rats.

Bleomycin initially induces oedema and inflammation, followed by progressive destruction of the normal lung architecture (Shen et al., 1988). The pathological changes in the lung parenchyma following intratracheal instillation of bleomycin are cellular infiltration, pulmonary oedema, changes to type II pneumocytes, changes to alveolar architecture, and following multiple instillation, pulmonary fibrosis (Brown et al., 1988). The lung injury that develops in the initial 48 h following a single intratracheal bleomycin dose (1.5 units) is characterised histologically by perivascular oedema, capillary congestion and alveolar wall thickening (Thrall et al., 1979). The oedema is predominantly interstitial, with minimal intra-alveolar oedema. The inflammatory cell infiltrate in the alveolar walls and spaces has been quantified in hamsters treated with a single intratracheal dose (1 unit). Chandler et al. (1983) found an eight-fold increase in the number of macrophages, monocytes, lymphocytes, and neutrophils 4 days after bleomycin instillation.

The maximum level of cellular infiltrate has been shown to occur 3 days post-bleomycin instillation (Adamson and Bakowska, 1999). Another study used the accumulation of albumin in the interstitial tissues as a measure of vascular permeability. This resulted in an increase in the albumin space, which peaked at 3 days (Hay et al., 1987). These experiments both indicated that oedema consistently occurred 3 days after pulmonary injury.

In the present study, conventional toxicological techniques (lung weight lavage protein free cell numbers) were used to monitor the extent of pulmonary oedema and inflammation (Lee and Richards, 2004).

Experiments were designed to identify early molecular markers for events in pulmonary injury. Recent advances in gene array technology mean it is possible to compare patterns of mRNA expression of many thousands of genes simultaneously. For the majority of genes, changes in mRNA abundance are related to changes in protein concentration (Lockhart and Winzeler, 2000). The degree of mRNA expression is very informative about the state of a cell and the activity of genes.

In order to examine global gene expression in lung tissue, macroarray technology was applied. The Clontech Atlas™ rat cDNA expression macroarray system was used for this study. This was chosen because it is readily available and offers reproducibility to a greater range of laboratories than the more expensive microarray systems. This methodology has been used successfully in previous studies to investigate toxicant effects in the lung (Reynolds and Richards, 2001).

Materials and methods

Experimental model of pulmonary oedema and inflammation

Experiments were performed in accordance with the codes of practice specified by the Home Office (UK), and following approval from the local ethical committee.

Pathogen-free, male Sprague–Dawley rats (Charles River Ltd., UK) weighing 200–250 g were lightly anaesthetised with halothane (Rhone Merieux, UK) and dosed with a single intratracheal (IT) instillation (Reynolds and Richards, 2001). Animals were treated with 0.5 units of bleomycin sulphate (Kyowa Hakko, UK) suspended in 0.5 ml 0.15 M NaCl (n = 9). Sham controls received only 0.5 ml 0.15 M NaCl (n = 9). Animals were closely monitored over the three day period, using a post procedure pain and distress score sheet (Wolfensohn and Lloyd, 1998). Recovery was rapid with no signs of adverse health effects.

Bronchoalveolar lavage (BAL) fluid analysis

Three days post-IT instillation of bleomycin, the animals were anaesthetised with halothane and sacrificed by a lethal intraperitoneal injection (1–2 ml) of Euthatal (Rhone Merieux, UK). The rats were subsequently weighed and cardio-respiratory death confirmed prior to dissection. Lung wet weight (including trachea and bronchi) was measured. Bronchoalveolar lavage (BAL) was performed by cannulation of the trachea followed by four washes with 6–8 ml sterile saline (0.9%). The recovered aliquots were pooled and centrifuged for 20 min (300 × g). The trachea and bronchi were removed and the weight of the lung parenchyma (LP) was calculated. The lobes of the lung were separated, flash frozen in liquid nitrogen and stored at −80 °C for use in gene-profiling studies.

The LP weight measured previously was used to calculate the LP to body mass ratio. During infection, injury or inflammation, an influx of cells and protein will cause an increase in the lung weight, reflected in an elevated LP body mass ratio (Richards and Curtis, 1984).

The increase in concentration of acellular protein in BAL was used as a sensitive marker of oedema resulting from damage to epithelial or endothelial cells (Richards and Curtis, 1984). The total protein concentration of BAL (300 × g) was determined by the Bradford assay (Bradford, 1976). Assays for each animal were performed in triplicate.

Increased cellular infiltrate was used to monitor the level of inflammation. The number of large free cells (LFC) within the BAL fluid was measured using a haemocytometer.

Histology of lungs

In separate experiments, histological specimens were prepared for light microscopy. Lungs were excised 3 days post-IT instillation of saline (n = 3) or bleomycin (n = 3) and inflated with 10% neutral-buffered formalin. The inflated lungs were tied off and immediately immersed in

10% neutral buffered formalin to be processed for paraffin embedding and sectioning. The upper right lobe was embedded in paraffin wax and 5 μm sections were cut on a microtome. Sections were stained with haematoxylin and eosin and analysed by light microscopy.

Macroarray of lung tissue

The Atlas cDNA Rat 1.2 array system (BD Biosciences) was used to assess gene expression. These macroarrays consist of 1185 cDNA sequences (200–600 bp) spotted onto a nylon membrane. These include plasmid and bacteriophage DNAs as negative controls to confirm hybridisation specificity, as well as several housekeeping cDNAs as positive controls.

The macroarray procedure was carried out on saline- (n = 9) and bleomycin- (n = 9) treated tissue in accordance with the BD Atlas cDNA Expression Arrays User Manual. In brief, probe mixtures were synthesised by reverse transcription of each RNA population (isolated using RNeasy mini kit, Qiagen). The resultant ^{32}P-labeled cDNA was then purified and hybridised to separate array membranes overnight. The following day, the membranes were washed with a high stringency solution. The hybridisation pattern was ascertained by phosphorimaging.

Macroarray data analysis

Initial processing of the array data was carried out using Atlas Image 2.0. The ratio and difference thresholds were set to 1 and 1000, respectively to ensure all genes were included in further analysis. The signal-to-background ratio for all arrays was set low at 50%. The resultant report was comprised of all genes on the array and their corresponding adjusted intensity value (total signal minus background).

Normalisation. The raw array data resulting from processing by Atlas Image is not normally distributed. Therefore, prior to further analysis, the raw expression data was $\log_{10}$ transformed. This served to reduce skewness, kurtosis and outliers. Subsequently, each array was normalised by dividing the spot intensity of each gene by the median spot intensity of the whole array. The median value was chosen as the preferred method of normalisation, as the mean value is highly influenced by the extreme behaviour of relatively few genes. This removed the effects of experimental differences and enabled direct comparison between arrays.

Analysis. Post normalisation, a quantitative analysis was carried out. The ratio of adjusted intensities was calculated as a measure of altered gene expression. Ratio was calculated for up-regulated genes by dividing bleomycin gene intensity by sham gene intensity. For down-regulated genes, sham was divided by bleomycin intensity, and a minus sign was placed in front of the resulting ratio. This generated a figure that was representative of fold change in expression. The positive or negative sign indicated up- or down-regulation of the gene. Previous experiments have shown that 75% of genes with a ratio change of 1.5 or more can be confirmed by RT PCR (deVos et al., 2003; Treadwell and Singh, 2004). The lower cut off point for identifying relevant genes was therefore set at a ratio of 1.5.

Numerous statistical techniques are available to make comparisons between groups of data. However, with a relatively low number of experimental replicates, an alternative method of determining significant differences in gene expression, which took into account the intra group variability, was required. The method developed accommodated the limited sample size and included a statistical element to generate a greater level of confidence in the data. This simple analysis technique was developed using the sham-control data to set parameters against which the bleomycin samples were compared. For each gene, the mean adjusted intensity value from each of the nine sham arrays was plotted on a graph ± two standard deviations (SD). The interval was set at two standard deviations because for any given gene, if the data are normally distributed, 95% of the population will fall within ± 2SD from the mean. The mean ± 2SD established the range of normal gene expression against which the oedema samples could be compared. If the mean of all nine of the oedema samples fell outside the two standard deviation limits, the gene was considered relevant for further study (Fig. 1).

This method was compared and contrasted with a two-tailed unpaired Student's t test.

Quantitative PCR (Q-PCR) of selected genes

The macroarray procedure is considered semi-quantitative due to the inherent variations in hybridisation reactions. Therefore, confirmation of the gene expression changes calculated from the macroarray and subsequent analysis was required. To accurately quantify these alterations in genetic expression and to confirm the reproducibility of the data, quantitative PCR (Q-PCR) was used. A

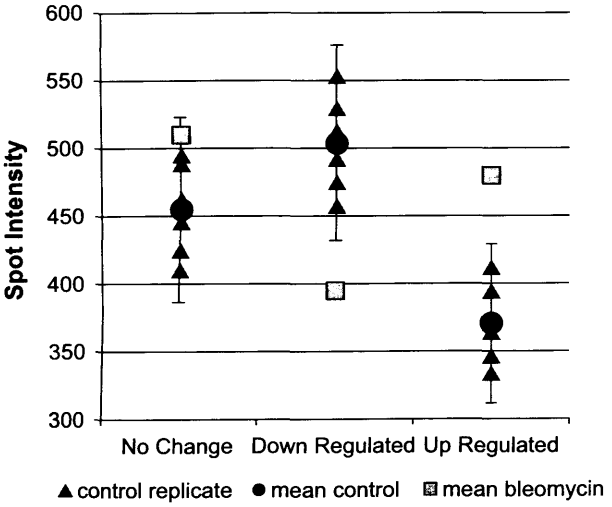

Fig. 1. Gene 1: not significantly different from controls; genes 2 and 3: relevant for further study. Sample of experimental data.

Table 1
Primer sequences for PCR

Primer name		Primer sequence	Primer length	Fragment size
B04d	Forward	TGGCAGACGCTCTTGGGCGAGAG	23	227
B04d	Reverse	CACCACCGGAAAGCCGCTGTACG	23	
D03j	Forward	GGGACCCGTGCCATTGTTTCTGAC	24	279
D03j	Reverse	GGCGTAGATGAAGTTGAAGGTCGCG	25	
D07c	Forward	CGCCGCTCGCGCCTCATGATC	21	190
D07c	Reverse	CGAAGACACCGCTGGTCATCCAG	23	
D09f	Forward	GAAGTTTCGCTCATGGACCTACGAC	25	192
D09f	Reverse	AGTGGTTTGCGACGAATGATGAAGTC	26	
D14i	Forward	AGCTGCTGCTGTGGCACAGTGCAC	24	297
D14i	Reverse	GCAGTTGGCTCAGGCACTTTGTCTG	25	
G43	Forward	CCCTCTGAACCCTAAGGCCAACCG	24	285
G43	Reverse	GTGGTGGTGAAGCTGTAGCCACGC	24	

small sample of genes ($n = 6$) highlighted by the previously described methods was chosen (Table 1). The genes were selected primarily by their biological function, but also according to the analytical method by which they were detected (2SD method, or t test).

The purified PCR product of the gene of interest was ligated into a pGEM-T plasmid vector (Promega). This was than transformed into competent *Escherichia coli* cells (JM109, Promega). Successful transformation was detected by the differing ability of the clones to metabolise X-Gal/IPTG. The plasmids and inserts were isolated from liquid culture using Wizard *Plus* SV Miniprep DNA Purification Systems (Promega). The inserts were sequenced to confirm that the correct product had been achieved.

Real-time PCR was carried out on an Applied Biosystems ABI PRISM 7700 Sequence Detection System. SYBR green (Qiagen) incorporation was used to quantify relative gene expression. A standard curve (10 fg–100 pg) was constructed for each gene from RNA extracted from untreated lung tissue. This was then used as a reference for calculating the RNA expression within the experimental samples.

Results

Bronchoalveolar lavage (BAL) fluid analysis

The following parameters were recorded for each rat: body weight, the lung parenchymal (LP)/body weight ratio, the total surface protein concentration and the large free cell (LFC) count from the lavage sample. The saline-treated ($n = 9$) and bleomycin-treated ($n = 9$) groups were compared for each of the toxicological effects. A two-tailed Student's t test was used to determine the statistical relationship between the two groups, shown in Fig. 2.

The weight gain of the bleomycin treated rats was carefully monitored from the time of the dose to the time of sacrifice. The final difference in weight between the sham group and the bleomycin treated group was only 5%. This indicated that the animals had not reacted adversely to the bleomycin treatment.

An increase in the lung/body weight ratio, protein concentration and the number of large free cells indicates oedema and mild inflammation of the lung. In all these categories, data are significantly different between saline- and bleomycin-treated groups. This clearly indicates that oedema and mild inflammation was occurring in the lungs of the bleomycin treated rats after 3 days.

Histology of lungs

Haematoxylin and eosin staining was carried out on separate tissue sections. This was done as visual confirmation to the basic toxicology described above. The results from 3 days after bleomycin instillation are shown in Fig. 3.

Sham-treated tissue has normal alveolar architecture, with no evidence of swollen septa. In the bleomycin-treated samples, there was evidence of an influx of macrophages after 3 days and widespread thickening of the alveolar interstitium (indicated by arrows).

Macroarray analysis

Following histological and biochemical confirmation of pulmonary oedema, the lung tissue was processed through the macroarray system. The information generated from the macroarray was analysed as described previously. Genes with a consistent difference in expression between saline- and bleomycin-treated tissue were identified by the standard deviation method (Fig. 4). The same data were analysed by a two-tailed t test. The resulting gene lists were limited to genes with a ratio change of over 1.5. The gene lists generated using the two methods of analysis were compared for consistencies. Genes present on the lists from both techniques were considered particularly relevant. A list combining genes from both analysis techniques was compiled and is shown in Table 2.

As well as considering the statistical relevance as determined above, it was important to take into account the biological significance and clustering of the genes.

Of the five up-regulated genes, four are involved in active transport of molecules across membranes and the fifth was a

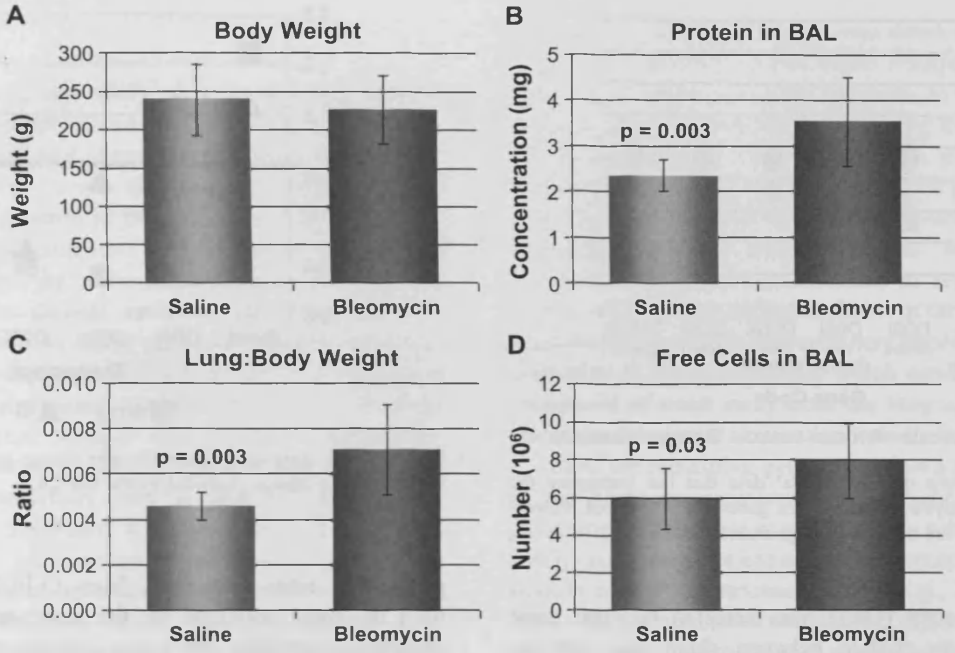

Fig. 2. Graphs showing a comparison between the saline-treated and bleomycin-treated groups. Error bars show standard deviation (n = 9).

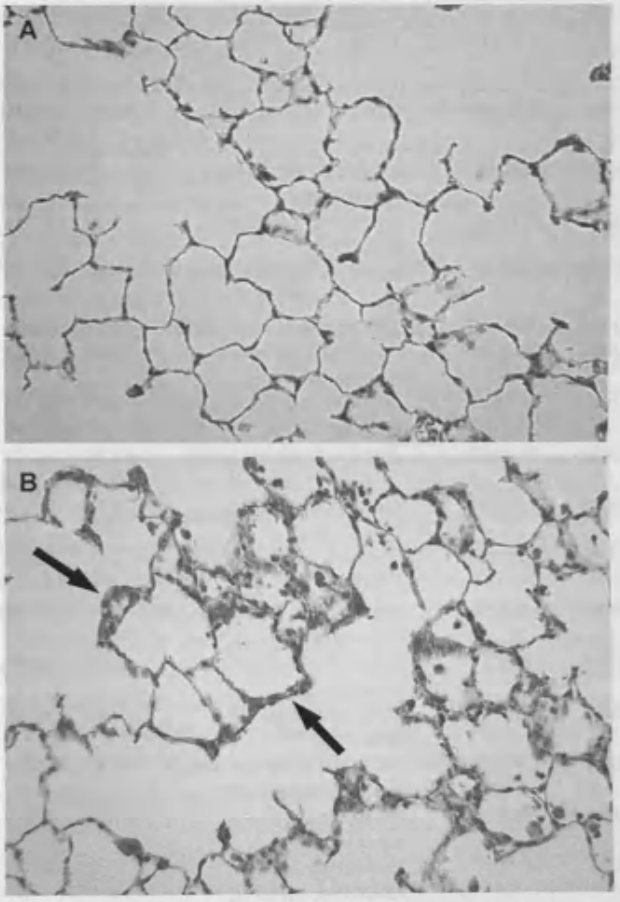

Fig. 3. Photomicrographs of lung sections stained with haematoxylin and eosin (×16 magnification). (A) sham-treated; (B) bleomycin treated. Black arrow: interstitial thickening.

chloride channel. The remaining significantly altered genes belonged to two functional groups, the neurotransmitter receptors/ion transport proteins (seven genes) and hormone receptors/G protein-coupled receptors (18 genes).

Quantitative PCR

Quantitative PCR was carried out to achieve two separate aims. The first was to validate the accuracy of gene expression changes predicted by the array. Secondly, this technique was used to determine the suitability of the mean ± 2SD and *t* test methods of analysis for highlighting relevant gene changes.

Q-PCR was carried out on five of the genes selected by the two analysis methods, and one housekeeping gene. The genes were chosen according to their potential biological significance, as well as the method by which they were highlighted. The genes were: a chloride channel protein (B04d), substance K receptor (D03j), vasopressin receptor (D07c), neuronal acetylcholine receptor beta-2 subunit (D09f), granulocyte colony stimulating factor (D14i) and cytoplasmic β-actin (G43). Genes B04d and D07c may both be involved in water transport and reabsorption, and both were highlighted using the *t* test. Gene D03j has been implicated in bronchoconstriction of large airways and enhancement of vascular permeability. Gene D14i has been shown to significantly increase alveolar cell recruitment and pulmonary oedema (Azoulay et al., 2003). Both D03j and D14i were selected using the standard deviation (SD) method. Gene D09f was chosen because it was one of several genes in a tight cluster, and was the only gene identified by both methods to undergo Q-PCR. The house-

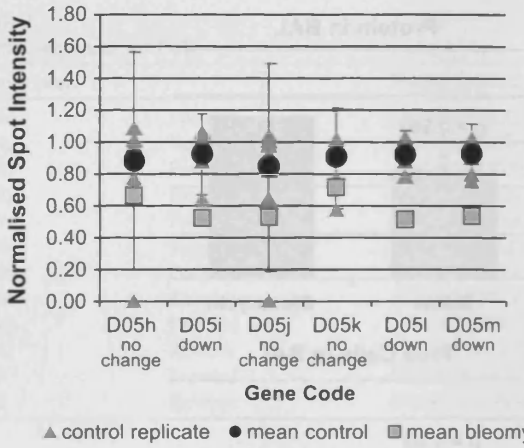

Fig. 4. Shows a sample of experimental data that has undergone the standard deviation analysis method. Three genes are considered relevant (down-regulated), two are not deemed significant.

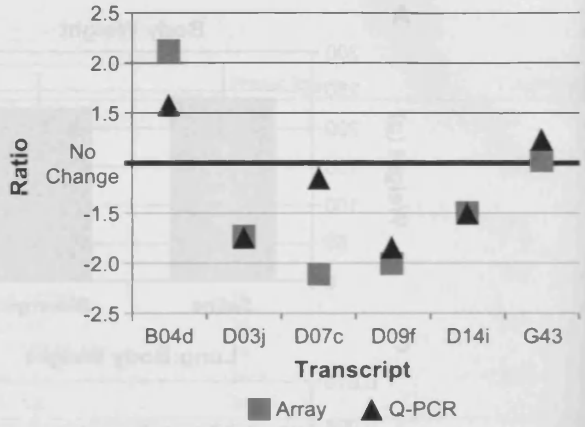

Fig. 5. Shows comparison between ratio change predicted by the macroarray and ratio change predicted by the Q-PCR.

keeping gene, β-actin (G43), was selected because there appeared to be no change between sham and oedema samples.

The concentration of each gene in the samples was determined, and used to calculate a ratio change for each gene. The ratio calculated from Q-PCR was compared with the ratio predicted by the macroarray (Fig. 5). The correlation between the ratios calculated by both techniques was very high. Gene D07c showed a lower level agreement, but both methods consistently indicated down-regulation.

Table 2
Shows all genes identified by the standard deviation and/or *t* test methods

Code	Accession #	Gene	Ratio	*t* test, *P* value	Code	Accession #	Gene	Ratio	*t* test, *P* value
B04d	D50497	chloride channel protein ◆	2.12	0.038	D06k	U40395	*cannabinoid receptor 1, neuronal* ■	−1.70	0.064
B07l	U15098	glutamate transporter ◆	1.66	0.032	D07c	Z11690	*vasopressin/arginine receptor* ■	−2.10	0.038
B07m	U28927	Na+/Cl− betaine/GABA transporter ◆	1.69	0.032	**D07f**	**L10073**	***serotonin receptor 5B*** ■	**−1.74**	**0.049**
B08m	U10096	Na-K-Cl cotransporter ◆	2.15	0.018	D07m	X63574	*somatostatin receptor 3* ■	−1.55	0.064
B09h	L10362	Synaptic vesicle protein 2B ◆	1.83	0.018	**D08e**	**J03933**	***thyroid hormone beta receptor*** ■	**−1.69**	**0.028**
D02j	X62314	*somatostatin receptor 1* ■	−1.65	0.079	D08f	M36074	*mineralocorticoid receptor (MR)* ■	−2.14	0.034
D03j	M31838	*substance K receptor (SKR)* ■	−1.71	0.058	**D08g**	**M14053**	***glucocorticoid receptor*** ■	**−1.84**	**0.029**
D03k	X56661	*gastrin-releasing peptide receptor* ■	−1.51	0.085	D09b	X95579	*GABA-A receptor rho-1 subunit* △	−1.51	0.086
D04g	M34842	*thyroid stimulating hormone receptor* ■	−1.55	0.062	D09e	Z11716	*glutamate receptor 7 (GLUR7)* △	−2.16	0.031
D04n	**L02842**	***follicle stimulating hormone receptor*** ■	**−1.80**	**0.037**	**D09f**	**L31622**	***neuronal ACh receptor β2 subunit*** △	**−1.99**	**0.015**
D05i	**D32045**	***alpha 1B adrenergic receptor*** ■	**−1.76**	**0.045**	D09g	M85035	*glutamate receptor 2 precursor* △	−1.53	0.077
D05l	**L05596**	***Serotonin receptor 1F*** ■	**−1.81**	**0.034**	**D09k**	**X15467**	***GABA-A receptor β-2 subunit*** △	**−2.08**	**0.016**
D05m	**L10072**	***serotonin receptor 5A*** ■	**−1.74**	**0.049**	D09l	L08497	*GABA-A receptor gamma-2 subunit* △	−1.72	0.059
D06d	M88096	*Cholecystokinin receptor* ■	−1.53	0.072	D10g	L08493	*GABA receptor α−4 subunit* △	−1.54	0.079
D06f	M93273	*Somatostatin receptor 2* ■	−1.70	0.060	D14i	U37101	*granulocyte colony stimulating factor* △	−1.51	0.084
D06j	U37058	*Neuromedin B receptor* ■	−1.70	0.060					

Genes in italics were identified as significant by the 2SD method.
Genes in bold italics were identified by both techniques. ◆ Transporter proteins, ■ Hormone receptors, △ Ion channels.

Discussion

The objectives of this study were to develop suitable methods for analysis of macroarray data, and to use these methods to identify potential markers of pulmonary oedema. Conventional toxicology was used to determine the level of oedema and inflammation in the lung. The tissue was then processed for genetic analysis. To gain a more comprehensive understanding of the oedematous reaction, 18 individual rats were used for genetic analysis. This approach was chosen in preference to using replicate samples from one tissue source. Obtaining replicates from different biological samples results in increased random error but the findings have better external validity and broader applicability (Nadon and Shoemaker, 2002). Conventional toxicology methods were successfully used to determine the level of lung injury. The increased lung/body weight ratio and protein levels in bleomycin-treated rats all pointed to oedema. The increase in macrophages indicated a slight inflammation of the lung tissue. As these changes were statistically significant, it suggested that the alterations were caused by the bleomycin dose. These results were supported by the histological data. After 3 days, the damaged interstitium was clearly visible, as was an apparent accumulation of macrophages at focal regions of the lung surface.

After these techniques were used to identify the extent of damage to the lung at 3 days, the tissue was then processed for genetic analysis. The variation in genetic expression was due to inherent differences in animal response to treatment, and day-to-day experimental variations. Initial normalisation of the data was performed to overcome experimental differences. Biological variation was addressed by the number of sample replicates, and the design of the normalisation and data analysis methods.

The standard deviation method is a very stringent analysis technique for determining significant genes from a limited number of sample replicates. Any gene that falls outside the two standard deviation limit is considered to be altered by the treatment to the 0.05 significance level. Therefore, when the mean of all nine genes fell outside this control range (Fig. 1), the gene was considered to be a reliable marker for oedema. Once the control data set has been established, individual samples can easily be assessed against it. As such, this approach has good potential for clinical use.

The *t* test was used to generate more statistical evidence of altered gene expression. This technique is appropriate for use on both small and large sample sets, but cannot be used to compare one individual sample against a control data set.

Some of the genes identified by a combination of these analysis methods are discussed below.

A group of five transporter proteins (symporters and antiporters) were identified as significant. Of these genes, three were chloride channels. These were up-regulated and may be involved in increased movement of water molecules by active transport, an event which would certainly occur in oedema. However, a vasopressin receptor (D07c), which is involved in water reabsorption was down-regulated by over two-fold. Vasopressin controls the resorption of water and regulates the osmotic content of blood. In the kidney, it acts on the renal collecting ducts, increasing the permeability to water (Nielsen et al., 1995). Therefore, in the lung, down-regulation of this gene may reduce cellular permeability. This would lead to increased water on the alveolar surface, which is known to occur during oedema. Mineralocorticoid receptors (D08f) are also involved in regulation of water balance via an effect on ion transport in the epithelium of the renal tubules. A similar response may be observed in the lung. This gene is down-regulated, which could lead to reduced movement of water away from the lung surface. This could again result in water accumulation in the alveolar spaces.

All of the remaining genes were down-regulated. Several of the hormone receptors appear to be involved in the physiological response to oedema. The substance K receptor (D03j) and gastrin-releasing peptide receptor (D03k) affect smooth muscle constriction (Haley et al., 2001, Lach et al., 1993). Down-regulation could affect dilation of the conducting airways of the lung, which should increase the flow of air to the lungs. This would seem appropriate as the air spaces are covered by the oedematous fluid reducing the level of oxygen exchange. More direct links to oedema are unclear. Granulocyte colony-stimulating factor (D14i) mediates the inflammatory response, and is involved in the enhancement of vascular permeability (Sedgwick et al., 2002). Gastrin-releasing peptide receptor (D03k) is implicated in vasodilation (Clive et al., 2001). Conversely, the serotonin receptors (D05l, D05m, D07f) are involved in pulmonary vascular and airway constriction (Selig et al., 1988), effects often observed during the inflammatory process. Alpha 1B adrenergic receptor (D05i) is also implicated in venule constriction (Leech and Faber, 1996). Glucocorticoid receptors (D08g) are thought to be involved with anti-inflammatory responses (Walsh et al., 2003). Down-regulation would result in increased inflammatory responses, as evidenced by the elevated number of free cells in BAL.

Clusters of genes are more reliable as markers for a pathological reaction, as a single anomaly should not affect the successful identification of oedema. Of the 31 significant genes selected by the methods described in this study, five belong to the symporters and antiporters family, all of which were up-regulated. The 18 genes classified as hormone receptors included a cluster of three genes encoding nuclear receptors (D08e, D08f, D08g). These genes are not necessarily directly related to oedema, however, as a cluster they are worth considering further. Similarly, within the group of seven ion channels, three were more tightly clustered (D09e, D09f, D09g).

The changes in gene expression predicted by the macroarray were confirmed by Q-PCR. All of the genes tested showed an extremely high level of correlation, with the exception of D07c. However, even in this case, the genetic response was shown to be down-regulated, which was in agreement with the change predicted by the array. This

indicated that both analysis methods are appropriate for selecting relevant genes.

In conclusion, the preliminary macroarray analysis has provided new transcriptional data on the mechanisms of pulmonary oedema following bleomycin treatment. High numbers of replicates ($n = 9$) imply a good level of trust in the resulting data, and have been confirmed by Q-PCR. New methods have been developed for successful analysis of macroarray data. The *t* test is a well-established, conventional method with recognised statistical significance. The standard deviation method is good for analysing groups of data. It can also be used to compare individual unknown samples against an established control range, which may be more practical in industrial/medical scenarios.

Acknowledgments

The author would like to thank AstraZeneca for funding this study. Also, many thanks to Helen Wise and Keith Sexton for their help establishing the array protocol.

There are no conflicts of interest.

References

Adamson, I.Y.R., Bakowska, J., 1999. Relationship of keratinocyte growth factor and hepatocyte growth factor levels in rat lung lavage fluid to epithelial cell regeneration after bleomycin. Am. J. Pathol. 155, 949–954.

Aso, Y., Yoneda, K., Kikkawa, Y., 1976. Morphologic and biochemical study of pulmonary changes induced by bleomycin in mice. Lab. Invest. 35, 558–568.

Azoulay, E., Attalah, H., Yang, K., Herigault, S., Jouault, H., Brun-Buisson, C., Brochard, L., Harf, A., Schlemmer, B., Delclaux, C., 2003. Exacerbation with granulocyte colony-stimulating factor of prior acute lung injury during neutropenia recovery in rats. Crit. Care Med. 31, 157–165.

Balazs, G., Noma, S., Kahn, A., Eacobacci, T., Herman, P.G., 1994. Bleomycin-induced fibrosis in pigs: evaluation with CT^1. Radiology 191, 269–272.

Bradford, M.M., 1976. A rapid and sensitive method for the quantification of microgram quantities of protein utilising the principle of protein-dye binding. Anal. Biochem. 72, 248–254.

Brown, R.F.R., Drawbaugh, R.B., Marrs, T.C., 1988. An investigation of possible models for the production of progressive pulmonary fibrosis in the rat. The effects of repeated intratracheal instillation of bleomycin. Toxicology 51, 101–110.

Catravas, J.D., Lazo, J.S., Dobuler, K.J., Mills, L.R., Gillis, C.N., 1983. Pulmonary endothelial dysfunction in the presence or absence of interstitial injury induced by intratracheally injected bleomycin. Am. Rev. Respir. Dis. 128, 740–746.

Chandler, D.B., Hyde, D.M., Giri, S.N., 1983. Morphometric estimates of infiltrative cellular changes during development of bleomycin-induced pulmonary fibrosis in hamsters. Am. J. Pathol. 112, 170–177.

Clive, S., Jodrell, D., Webb, D., 2001. Gastrin-releasing peptide is a potent vasodilator in humans. Clin. Pharmacol. Ther. 69, 252–259.

deVos, S., Hofmann, W.K., Grogan, T.M., Krug, U., Schrage, M., Miller, T.P., Braun, J.G., Wachsman, W., Koeffler, H.P., Said, J.W., 2003. Gene expression profile of serial samples of transformed B-cell lymphomas. Lab. Invest. 83, 271–285.

Haley, K.J., Sunday, M.E., Osathanondh, R., Du, J., Vathanaprida, C., Karpitsky, V.V., Krause, J.E., Lilly, C.M., 2001. Developmental expression of neurokinin A and functional neurokinin-2 receptors in lung. Am. J. Physiol., Lung Cell Mol Physiol. 280, L1348–L1358.

Hay, J.G., Haslam, P.L., Dewar, A., Addis, B., Turner-Warwick, M., Laurent, G.J., 1987. Development of acute lung injury after the combination of intravenous bleomycin and exposure to hyperoxia in rats. Thorax 42, 374–382.

Lach, E., Haddard, E.B., Gies, J.P., 1993. Contractile effect of bombesin on guinea pig lung in vitro: involvement of gastrin-releasing peptide-preferring receptors. Am. J. Physiol. 264, L80–L86.

Lee, S.H., Richards, R.J., 2004. Montserrat volcanic ash induces lymph node granuloma and delayed lung inflammation. Toxicology 195, 155–165.

Leech, C.J., Faber, J.E., 1996. Different alpha-adrenoceptor subtypes mediate constriction of arterioles and venules. Am. J. Physiol. 270, H710–H722.

Lockhart, D.J., Winzeler, E.A., 2000. Genomics, gene expression and DNA arrays. Nature 405, 827–836.

Nadon, R., Shoemaker, J., 2002. Statistical issue with microarrays processing and analysis. TRENDS in Genetics 18, 265–271.

Nielsen, S., Chou, C.L., Marples, D., Christensen, E.I., Kishore, B.K., Knepper, M.A., 1995. Vasopressin increases water permeability of kidney collecting duct by inducing translocation of aquaporin-CD water channels to plasma membrane. Proc. Natl. Acad. Sci. U.S.A. 92, 1013–1017.

Reynolds, L.J., Richards, R.J., 2001. Can toxicogenomics provide information on the bioreactivity of diesel exhaust particles? Toxicology 165, 145–152.

Richards, R.J., Curtis, C.G., 1984. Biochemical and cellular mechanisms of dust-induced lung fibrosis. Environ. Health Persp. 55, 393–416.

Roguin, A., Behar, D.B., Ami, H.B., Reisner, S.A., Edelstein, S., Linn, S., Edoute, Y., 2000. Long-term prognosis of acute pulmonary oedema—An ominous outcome. Eur. J. Heart Fail. 2, 137–144.

Sedgwick, J.B., Menon, I., Gern, J.E., Busse, W.W., 2002. Effects of inflammatory cytokines on the permeability of human lung microvascular endothelial cell monolayers and differential eosinophil transmigration. J. Allergy Clin. Immunol. 110, 752–756.

Selig, W.M., Bloomquist, M.A., Cohen, M.L., Fleisch, J.H., 1988. Serotonin-induced pulmonary responses in the perfused guinea pig lung: evidence for 5HT2 receptor-mediated pulmonary vascular and airway smooth muscle constriction. Pulm. Pharmacol. 1, 93–99.

Shen, A.S., Haslett, C., Feldsien, D.C., Henson, P.M., Cherniack, R.M., 1988. The intensity of chronic lung inflammation and fibrosis after bleomycin is directly related to the severity of acute injury. Am. Rev. Respir. Dis. 137, 564–571.

Snider, G.L., Hayes, J.A., Korthy, A.L., 1978. Chronic interstitial pulmonary fibrosis produced in hamsters by endotracheal bleomycin. Am. Rev. Respir. Dis. 117, 1099–1108.

Spencer, H., 1985. Pulmonary Oedema and Its Complications and the Effects of Some Toxic Gases and Substances on the Lung, Pathology of the Lung. Pergamon, New York, pp. 705–731.

Starcher, B.C., Kuhn, C., Overton, J.E., 1978. Increased elastin and collagen content in the lungs of hamsters receiving an intratracheal injection of bleomycin. Am. Rev. Respir. Dis. 117, 299–305.

Thrall, R.S., McCormick, J.R., Jack, R.M., McReynolds, R.A., Ward, P.A., 1979. Bleomycin induced pulmonary fibrosis in the rat. Am. J. Pathol 95, 117–130.

Treadwell, J.A., Singh, S.M., 2004. Microarray analysis of mouse brain gene expression following acute ethanol treatment. Neurochem. Res 29, 257–269.

Walsh, G.M., Sexton, D.W., Blaylock, M.G., 2003. Corticosteroids, eosinophils and bronchial epithelial cells: new insights into the resolution of inflammation in asthma. J. Endocrinol. 178, 37–43.

Wolfensohn, S., Lloyd, M., 1998. Practical use of Distress Scoring Systems in the Application of Humane Endpoints. Handbook of Laboratory Animal Management and Welfare. Blackwell Science, Oxford, pp. 48–53.